Denitrification with pyrite for bioremediation of nitrate contaminated groundwater

Clara Torrentó Aguerri

DENITRIFICATION WITH PYRITE FOR BIOREMEDIATION OF NITRATE CONTAMINATED GROUNDWATER

Clara Torrentó Aguerri

PhD Thesis

Department of Crystallography, Mineralogy and Ore Deposits
University of Barcelona

Supervisors:

Dr. Jordi Cama i Robert
Dr. Albert Soler i Gil
Dr. Jordi Urmeneta Maso

Institute of Environmental Assessment
and Water Research (IDAEA), CSIC

UNIVERSITAT DE BARCELONA

idaea

UNIVERSITY OF BARCELONA

Faculty of Geology
Department of Crystallography, Mineralogy and Ore Deposits

DENITRIFICATION WITH PYRITE FOR BIOREMEDIATION OF NITRATE CONTAMINATED GROUNDWATER

Thesis presented by

Clara Torrentó Aguerri

to obtain the degree of Doctor in Earth Sciences

Work conduced in the Institute of Environmental Assessment and Water Research (IDAEA, CSIC) under the supervision of

Dr. Jordi Cama i Robert
Institute of Environmental Assessment and Water Research (IDAEA), CSIC

Dr. Albert Soler i Gil
Department of Crystallography, Mineralogy and Ore Deposits, University of Barcelona

Dr. Jordi Urmeneta Maso
Department of Microbiology, University of Barcelona

Barcelona, July, 2010

UNIVERSITAT DE BARCELONA

idaea

This thesis has been funded by the Spanish Government with a FPU grant and the projects CICYT-CGL2005-08019-C04-01 (PAPAS: "Procesos de Atenuación natural y remedio pasivo de contaminantes en aguas subterráneas"), CICYT-CGL2008-06373-C03-01 (PAIS: "Ground Water Pollution from Agricultural and Industrial Sources: Contaminant Fate, Natural and Induced Attenuation, and Vulnerability") and TRACE PET 2008-0034 ("Aplicación de técnicas isotópicas para la cuantificación y seguimiento de procesos de desnitrificación de acuíferos") from the Spanish Government and the projects SGR2005-00933 and SGR2009-00103 from the Catalan Government.

Abstract

In the last decades, nitrate pollution has become a major threat to groundwater quality. The consequences include health concerns and environmental impacts. Nitrate contamination is mainly derived from agricultural practices, such as the application of manure as fertilizer. The Osona area (NE Spain) is one of the areas vulnerable to nitrate pollution from agricultural sources. Nitrate is derived from intensive farming activities and the high nitrate content results in a loss of water availability for domestic uses. The most important natural nitrate attenuation process is denitrification. Denitrifying bacteria are generally heterotrophic and use carbon compounds as the electron donor. Nevertheless, a limited number of bacteria are able to carry out chemolithotrophic denitrification, and to utilize inorganic compounds. Several field studies have suggested by means of geochemical and/or isotopic data that denitrification in some aquifers is controlled by pyrite oxidation. However, the feasibility of pyrite-driven denitrification has been questioned several times in laboratory studies. This thesis is concerned with the role of pyrite in denitrification and its potential use as a bioremediation strategy.

Earlier studies showed the occurrence of denitrification processes in a small area located in the northern part of the Osona region and suggested that sulfide oxidation had an important role in natural attenuation. Therefore, the first part of this thesis deals with the characterization of the denitrification processes occurring in the Osona aquifer and their spatial and temporal variations. Denitrification processes linked to pyrite oxidation

were identified in some zones of the studied area by means of multi-isotopic methods integrated with classical hydrogeological methods.

Nitrate removal from groundwater can be accomplished by the enhancement of *in situ* biological denitrification. One such bioremediation strategy is biostimulation, which involves the addition of suitable electron donors and/or energy sources to stimulate indigenous denitrifying microorganisms. The second part of this thesis is devoted to clarify the role of pyrite as electron donor for denitrification and to evaluate the feasibility of a bioremediation strategy based on pyrite addition to stimulate native denitrifying bacteria. Nitrate consumption in experiments amended with pyrite and inoculated with *Thiobacillus denitrificans* demonstrated that this bacterium is able to reduce nitrate using pyrite as the electron donor. The efficiency in nitrate removal and the nitrate reduction rate depended on the initial nitrate concentration, pH and pyrite grain size. High nitrate removal efficiency was attained in long-term flow-through experiments under laboratory conditions similar to those found in slow-moving, nitrate-contaminated groundwater. In addition, biostimulation experiments performed with sediments and groundwater from the Osona aquifer showed that the addition pyrite stimulated the activity of the indigenous microbial community and enhanced the nitrate removal. Furthermore, the long-term efficiency of the process was demonstrated. Hence, biostimulation with pyrite could be considered to remediate nitrate contamination in groundwater in future water management strategies, although further research is needed, especially at field scale.

It is critical for the success of the bioremediation strategy that not only the processes but also the microbial populations and their changes induced by the bioremediation treatment be well understood. The addition of pyrite resulted in an increase in the proportion of denitrifying bacteria and both autotrophic and heterotrophic denitrifiers were stimulated. Bacterial populations closely related to the *Xanthomonadaceae* might probably be the dominant autotrophic denitrifiers that used pyrite as the electron donor in the biostimulated experiments.

The N and O isotopic enrichment factors associated with the pyrite-driven denitrification were computed and used to recalculate the extent of the natural nitrate attenuation in the Osona aquifer. This refinement becomes useful to predict the evolution of the contaminant in the aquifer, and it should be taken into account for potential implementation of induced remediation techniques. The isotopic approach was proved to be an excellent tool to identify and quantify natural denitrification processes in the field, and to monitor the efficacy of bioremediation strategies in the laboratory.

In order to improve the long-term performance of potential bioremediation strategies based on pyrite-driven denitrification, it is necessary to know the contribution of attached and free-phase denitrifying bacteria to this process in aquifers. The last part of this thesis addresses the ability of *T. denitrificans* to grow and colonize pyrite surfaces. In the colonization experiments, attachment onto pyrite surface was required for at lest a small number of the cells in order to accomplish pyrite-driven denitrification. Nevertheless, both attached and planktonic cells probably contributed to the overall denitrification. However, the details of the relative roles of the two phases and the specific mechanisms remain to be addressed.

Resum

A les darreres dècades, la contaminació de nitrat de l'aigua subterrània ha esdevingut un dels principals problemes que afecten la qualitat dels recursos hídrics subterranis. La presència de nitrat a l'aigua subterrània està relacionada, principalment, amb pràctiques agrícoles, com per exemple, l'ús intensiu de purins com a fertilitzant orgànic. La comarca d'Osona (Catalunya) és una de les àrees declarades vulnerables a la contaminació per nitrat d'origen agrícola. El nitrat procedeix principalment de la intensa activitat agrícola i ramadera.

El principal procés d'atenuació natural del nitrat és la desnitrificació. La majoria dels bacteris desnitrificants són heteròtrofs i usen compostos orgànics com a font d'electrons. Tanmateix, també existeixen bacteris desnitrificants autòtrofs que són capaços d'usar compostos inorgànics, com a donants d'electrons. Estudis de camp previs han demostrat a partir de dades geoquímiques i/o isotòpiques que en alguns aqüífers la desnitrificació està controlada per l'oxidació de pirita. Tot i així, hi ha estudis de laboratori que qüestionen la viabilitat de la desnitrificació lligada a l'oxidació de pirita (compost inorgànic donant d'electrons).

En aquesta tesi s'estudia el paper de la pirita en la desnitrificació i la seva possible aplicació com a estratègia de bioremediació d'aigües contaminades amb nitrat. Estudis previs demostraren l'ocurrència de processos de desnitrificació a Osona, en una petita

àrea situada en el sector nord de la zona d'estudi. Els resultats d'aquests estudis suggereixen que l'oxidació de sulfurs hi juga un paper molt important en l'atenuació natural. A la primera part de la tesi s'exposa la caracterització dels processos de desnitrificació que tenen lloc en l'aqüífer d'Osona, així com de les seves variacions temporals i espacials. S'han usat mètodes multi-isotòpics integrats amb mètodes hidrogeològics clàssics, que han servit per identificar l'existència de processos de desnitrificació lligats a l'oxidació de pirita en algunes zones de l'àrea d'estudi.

L'eliminació del nitrat de l'aigua subterrània pot aconseguir-se mitjançant estratègies que incentiven la desnitrificació biològica *in situ*. Una de les estratègies de bioremediació *in situ* és la bioestimulació, que consisteix en afegir donants d'electrons o fonts d'energia apropiades per tal d'estimular l'activitat de bacteris desnitrificants existents en el medi. En la segona part de la tesi s'esbrina el paper de la pirita com a potencial donant d'electrons en els procés de desnitrificació i s'avalua la viabilitat d'una estratègia de bioremediació, basada en l'addició de pirita per estimular l'activitat de bacteris desnitrificants autòctons. Experiments amb pirita i inoculats amb *Thiobacillus denitrificans* han demostrat que aquest bacteri és capaç de reduir el nitrat utilitzant la pirita com a donant d'electrons. A més a més, s'ha determinat que l'eficiència i la velocitat de reducció del nitrat depèn de la seva concentració inicial, del pH i de la mida de gra de la pirita. En experiments de flux continu, de llarga durada que simulen el flux d'aigües subterrània contaminades amb nitrat, s'han aconseguit altes eficiències en l'eliminació del nitrat. A més a més, s'han realitzat experiments de bioestimulación amb pirita usant aigua subterrània i sediments de l'aqüífer d'Osona. Aquests experiments han demostrat que afegint pirita s'aconsegueix d'estimular l'activitat dels bacteris desnitrificants autòctons i, per tant, induir i/o augmentar la desnitrificació. També, s'ha provat l'alta eficiència d'aquest procés a llarg termini. Per tant, l'ús de la pirita podria tenir-se en compte com a estratègia per a l'eliminació de nitrat en properes mesures de gestió dels recursos hídrics. Tanmateix, cal més investigació, i especialment, a escala de camp.

Per aconseguir l'èxit amb la bioremediació cal conèixer amb detall els processos i les poblacions microbiològiques que intervenen en els canvis poblacionals associats al tractament de bioremediació. Els resultats dels experiments de bioestimulació han demostrat que els bacteris desnitrificants autòtrofs dominants en el sistema són probablement poblacions relacionades amb *Xanthomonadaceae*. L'addició de pirita suposa un increment en la proporció de bacteris desnitrificants i produeix l'estimulació tant dels desnitrificants autòtrofs com dels heteròtrofs.

A més a més, s'han calculat els factors d'enriquiment isotòpic de N i O associats al procés de desnitrificació per oxidació de pirita. Aquests factors d'enriquiment s'han usat per recalcular el grau d'atenuació natural del nitrat que té lloc en l'aqüífer d'Osona. Aquest recàlcul pot ser d'utilitat a l'hora de predir l'evolució de la contaminació en l'aqüífer i cal tenir-lo en compte a l'hora d'implementar possibles tècniques de remediació induïda. Per tant, la metodologia isotòpica ha demostrat ser una eina excel·lent per identificar i quantificar processos de desnitrificació natural i per monitoritzar l'eficàcia d'estratègies de bioremediació en el laboratori.

Per millorar el rendiment i la durabilitat de potencials estratègies de bioremediació basades en la desnitrificació i oxidació de pirita és necessari conèixer la contribució relativa dels bacteris desnitrificants planctònics i dels bacteris adherits als sediments. Així, a l'última part de la tesi l'interès s'enfoca en l'avaluació de l'habilitat de *T. denitrificans* en colonitzar i créixer sobre la superfície de la pirita. Els resultats experimentals de colonització suggereixen que per aconseguir la desnitrificació amb pirita com a donant d'electrons, cal que una part dels bacteris s'adhereixi a la superfície de la pirita. No obstant, sembla que ambdós bacteris, adherits i planctònics, contribueixen al procés global. Tanmateix, queda pendent d'examinar el paper específic de cada tipus en la desnitrificació.

Resumen

INTRODUCCIÓN

En las últimas décadas, la contaminación por nitrato del agua subterránea se ha convertido en uno de los principales problemas que afectan a la calidad de los recursos hídricos subterráneos. La presencia de nitrato en el agua subterránea principalmente se debe a pérdidas en pozos negros y redes de saneamiento en mal estado y a prácticas agrícolas, como por ejemplo vertidos de residuos ganaderos o uso intensivo de purines como fertilizantes orgánicos. La concentración máxima de nitratos permitida por la directiva 98/83/EC en aguas destinadas al consumo humano es de 50 mg L^{-1}. Sin embargo, a menudo las aguas de los acuíferos presentan concentraciones más elevadas. La ingestión de altas concentraciones de nitratos puede provocar la enfermedad meta-hemoglobina en niños y bebés (Comly, 1945; Magee y Barnes, 1956). Algunos autores también sugieren que los compuestos nitrogenados pueden actuar como iniciadores de cánceres en humanos (Volkmer et al., 2005; Ward et al., 2005). Además, el nitrato contribuye a los procesos de eutrofización de las aguas superficiales (Rabalais et al., 2009).

La región de Osona es una de las áreas declaradas vulnerables a la contaminación por nitratos de origen agrícola en Cataluña (Decret 283/1998). En esta comarca existen más de 1000 granjas, la mayor parte situadas en un área reducida, con un número de

cabezas de ganado de cerca de 1000000 de porcino, 100000 de bovino y 60000 de ovino. Esta intensa actividad agrícola y ganadera produce grandes cantidades de residuos orgánicos, principalmente purines. Una pequeña parte de los purines es procesada en plantas de tratamiento, y el resto es utilizado en los campos como fertilizante orgánico. Después de décadas de aplicación y a pesar de detallados planes de gestión, en la parte central de Osona (Plana de Vic) la contaminación por nitratos es generalizada, con concentraciones que a menudo se sitúan muy por encima de los 50 mg L^{-1}.

La dinámica hidrogeológica ha permitido determinar tres zonas: la zona 1 comprende la zona de recarga situada al norte del río Ter; la zona 2 comprende la zona de recarga del margen oriental de la Plana al sur del Ter; y la zona 3, que comprende el centro de la Plana de Vic (Fig. 1).

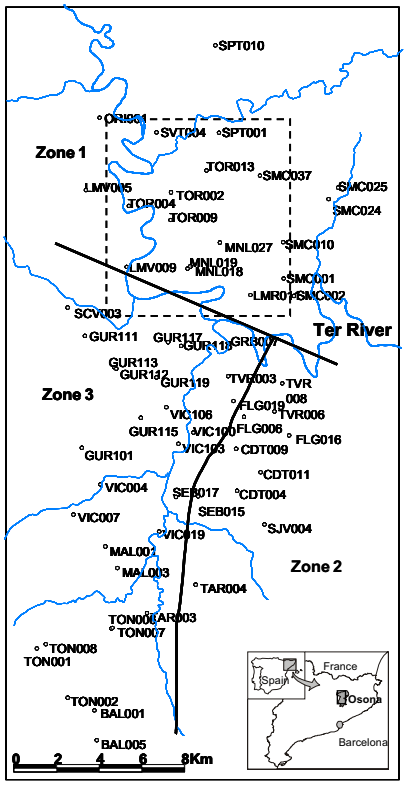

Figura 1. Zona de estudio. Se incluyen los puntos de muestreo y las tres zonas en las que se ha divido. También se incluye el area caracterizada en Vitòria et al. (2008).

Hidrogeológicamente, la zona estudiada está constituida por una serie de acuíferos desarrollados en niveles de carbonatos y de areniscas carbonatadas, donde la porosidad está principalmente desarrollada con la presencia de una importante red de fracturación. En este sistema, los niveles acuíferos se encuentran parcialmente aislados por niveles de marga que actúan como acuitardos. Menció et al. (2010) han identificado dos sistemas de flujo, uno superficial, correspondiente a los acuíferos libres, que reciben las aplicaciones de purines, y uno profundo, semiconfinado, con una menor exposición a la infiltración de nitrógeno en condiciones naturales, pero donde el efecto de las captaciones, y la construcción de los pozos, no entubados, puede generar una infiltración forzada desde los acuíferos superiores, con una elevada concentración en nitratos.

El principal proceso de atenuación natural del nitrato es la desnitrificación, que consiste en la reducción del nitrato a nitrógeno gas mediante la acción de bacterias anaeróbicas facultativas capaces de usar el nitrato como aceptor de electrones (Knowles, 1982). La mayoría de las bacterias desnitrificantes son heterótrofas y usan compuestos orgánicos como fuente de electrones:

$$4NO_3^- + 5C + 2H_2O \rightarrow 2N_2 + 4HCO_3^- + CO_2 \qquad (1)$$

Sin embargo, también existen bacterias desnitrificantes autótrofas, que son capaces de usar compuestos inorgánicos como donadores de electrones. En algunos acuíferos la desnitrificación está controlada por la oxidación de pirita (desnitrificación autótrofa), como se ha demostrado en estudios de campo previos mediante el uso de datos geoquímicos y/o isotópicos (Postma et al., 1991; Aravena y Robertson, 1998; Cravotta, 1998; Pauwels et al., 1998; 2000; 2010; Beller et al., 2004; Schwientek et al., 2008; Zhang et al., 2009a):

$$14NO_3^- + 5FeS_2 + 4H^+ \Rightarrow 7N_2 + 10SO_4^{2-} + 5Fe^{2+} + 2H_2O \qquad (2)$$

Sin embargo, varios estudios de laboratorio han cuestionado la viabilidad de la desnitrificación ligada a la oxidación de pirita (Devlin et al., 2000; Schippers y Jorgensen, 2002; Haaijer et al., 2007).

Las herramientas isotópicas son útiles para identificar la fuente del nitrato, evaluar la evolución del contaminante y predecir procesos de atenuación natural. La composición isotópica del nitrato disuelto se ha usado para identificar la existencia de procesos de desnitrificación en acuíferos contaminados con nitrato (Aravena y Robertson, 1998; Grischek et al., 1998; Mengis et al., 1999; Cey et al., 1999). Durante la desnitrificación, a medida que disminuye la concentración de nitrato se produce un aumento combinado de $\delta^{15}N$ y $\delta^{18}O$ del nitrato residual (Böttcher et al., 1990), con una relación $\varepsilon N/\varepsilon O$ que varía entre 1.3 y 2.1 (Böttcher et al., 1990; Mengis et al., 1999; Cey et al., 1999; DeVito et al., 2000; Fukada et al., 2003).

$$\delta^{15}N_{residual} = \delta^{15}N_{initial} + \varepsilon_N \ln\left(\left[NO_3^-\right]_{residual}/\left[NO_3^-\right]_{initial}\right) \quad (3)$$

$$\delta^{18}O_{residual} = \delta^{18}O_{initial} + \varepsilon_O \ln\left(\left[NO_3^-\right]_{residual}/\left[NO_3^-\right]_{initial}\right) \quad (4)$$

El estudio de la composición isotópica de los solutos implicados en las reacciones de desnitrificación ($\delta^{34}S$ y $\delta^{18}O$ del sulfato disuelto y/o $\delta^{13}C$ del carbono inorgánico disuelto) permite determinar si los procesos que controlan la atenuación natural del nitrato son autótrofos o heterótrofos (Aravena y Robertson, 1998; Pauwels et al., 1998; 2000; 2010; Schwientek et al., 2008). La desnitrificación por oxidación de materia orgánica debería ir acompañada de un aumento en la concentración de HCO_3^- y un descenso en las concentraciones de COT y NO_3^- y en los valores de $\delta^{13}C$. La ocurrencia de procesos de desnitrificación ligados a la oxidación de sulfuros puede identificarse con un aumento en los valores de $\delta^{15}N_{NO3}$ y $\delta^{18}O_{NO3}$ y en la concentración de SO_4^{2-}, acompañado de un

descenso en la concentración de NO_3^-. Vitòria et al. (2009) demostraron la ocurrencia de procesos de desnitrificación en Osona, en una pequeña área situada en el sector norte de la zona de estudio de esta tesis (Fig. 1). A partir de datos multi-isotópicos, estos autores pusieron de manifiesto que la oxidación de sulfuros juega un papel muy importante en la atenuación natural observada en la zona.

Los procesos de atenuación natural normalmente son lentos y por ello se han desarrollado distintas estrategias de eliminación del nitrato. Las técnicas tradicionales (ósmosis inversa, electrodiálisis, intercambio iónico) son relativamente caras y producen desechos con altas concentraciones de nitrato, que deben ser tratados (Soares, 2000). Las estrategias de biorremediación pueden ser una buena alternativa para reducir las concentraciones de nitrato a niveles aceptables. Con estas técnicas se pretende incentivar la desnitrificación biológica que tiene lugar de forma natural en el sistema contaminado. Una de esas estrategias de bioremediación *in situ* es la bioestimulación, que consiste en añadir donadores de electrones o fuentes de energía apropiados para estimular la actividad de bacterias desnitrificantes existentes en el medio (Soares, 2000). En el caso de la desnitrificación heterótrofa, varios compuestos orgánicos han sido evaluados como donadores de electrones, como por ejemplo metanol, etanol, metano, algodón, paja de trigo o sacarosa (Mateju et al., 1992; Soares, 2000; Park and Yoo, 2009). Incentivar la desnitrificación autótrofa tiene varias ventajas respecto a la desnitrificación heterótrofa: no es necesaria una fuente orgánica externa, lo que reduce el coste, y se minimiza además el tratamiento de los residuos y el efecto de taponamiento. Varios compuestos inorgánicos han sido evaluados como donadores de electrones para incentivar la desnitrificación autótrofa: hierro metálico (Choe et al., 2004; Della Rocca et al., 2006; Rodríguez-Maroto et al., 2009), Fe^{2+} (Straub et al., 1996; Benz et al., 1998; Nielsen y Nielsen, 1998; Straub y Buchholz-Cleven, 1998; Devlin et al., 2000; Kappler y Newman, 2004; Weber et al., 2006; Miot et al., 2009) y azufre elemental (Batchelor y Lawrence, 1978; Hashimoto et al., 1987; Zhang y Lampe, 1999; Soares, 2002; Sierra-Alvarez et al., 2007; Moon et al., 2008). Sólo unos pocos estudios han estudiado la desnitrificación autótrofa

por oxidación de pirita u otros sulfuros (Devlin et al., 2000; Schippers y Jorgensen, 2002; Haaijer et al., 2007; Jorgensen et al., 2009). Sólo Jorgensen et al. (2009) consiguieron inducir desnitrificación mediante adición de pirita a sedimentos de un acuífero contaminado con nitratos.

Otra estrategia de biorremediación *in situ* es el bioaumento, que consiste en añadir al sistema organismos capaces de transformar o eliminar el contaminante (Vogel, 1996). Para ello, pueden usarse cultivos puros de bacterias con una capacidad metabólica específica, consorcios enriquecidos a partir de sistemas contaminados o microorganismos modificados genéticamente. Esta estrategia, sin embargo, puede fallar debido principalmente a problemas de adaptación de los organismos añadidos o de competencia biológica entre las bacterias añadidas y las autóctonas (Goldstein et al., 1985; McClure et al., 1991; Vogel, 1996). En la bibliografía existen algunos ejemplos de estudios de laboratorio de desnitrificación inducida mediante estrategias combinadas de bioestimulación y bioaumento (Manconi et al., 2006; Flores et al., 2007; Sánchez et al., 2008; Zhang et al., 2009b).

Para mejorar el rendimiento y la durabilidad de las posibles estrategias de biorremediación basadas en la desnitrificación ligada a la oxidación de pirita, es necesario conocer la contribución relativa de las bacterias desnitrificantes planctónicas y las adheridas a los sedimentos. Estudios previos sugieren que la mayor parte de los microorganismos en los acuíferos se encuentran adheridos a los sedimentos y que esa forma de vida sésil ofrece distintas ventajas en comparación con la forma de vida planctónica (Harvey et al., 1984; Costerton et al., 1995; Bekins et al., 1999; Lehman et al., 2001; Griebler et al., 2002). Sin embargo, existe cierta controversia acerca del papel de ambas fases en los procesos de disolución de minerales (Silverman y Ehrlich, 1964; Silverman, 1967; Schippers y Sand, 1999; Sand et al., 2001; Crundwell, 2003; Leang et al., 2003; Lovley et al., 2004; Gorby et al., 2006; Sand y Gehrke, 2006). Se han propuesto diferentes mecanismos según los cuales las bacterias son capaces de conseguir la

transferencia de electrones entre las células y las fases minerales: (1) mecanismos indirectos, en los que no es necesaria la adhesión de la bacteria al mineral, (2) mecanismos directos, en los que debe existir contacto directo entre la bacteria y el mineral, y (3) combinaciones de ambos tipos de mecanismos. En la bibliografía se han encontrado dos trabajos centrados en evaluar el papel de las poblaciones planctónicas y adheridas en los procesos de desnitrificación, ninguno de ellos basado en bacterias desnitrificantes autótrofas (Teixeira y Oliveira, 2002; Iribar et al., 2008). En ambos estudios, la capacidad desnitrificante es mayor en la población adherida a los sedimentos que en la planctónica. De acuerdo con estos resultados, las estrategias de desnitrificación inducida podrían optimizarse usando sistemas de inmovilización para retener a los microorganismos desnitrificantes (Cassidy et al. 1996), como por ejemplo, células inmovilizadas en una matriz adherente: geles de alginato (Tal et al., 1997; 1999; 2003; Liu et al., 2003) o esferas de alcohol polivinílico (Zhang et al., 2009b).

OBJETIVOS

El principal objetivo de esta tesis es estudiar el papel de la pirita en la desnitrificación y su posible aplicación como estrategia de biorremediación de aguas contaminadas con nitrato.

La primera parte de la tesis (Capítulo 2) se ocupa de la caracterización de los procesos de atenuación natural del nitrato en el acuífero de Osona. Los principales objetivos de esta parte son:

- Confirmar la ocurrencia de procesos de desnitrificación en Osona, en un área más amplia que la estudiada por Vitòria et al. (2009), con objeto de determinar el grado de alcance regional de la desnitrificación. Determinar la existencia de estos procesos de desnitrificación es de vital importancia para predecir y evaluar el estado de las reservas futuras de agua de boca.

- Caracterizar los procesos de desnitrificación y determinar el papel de la oxidación de pirita en los mismos.

- Caracterizar las variaciones temporales y espaciales de los procesos de atenuación natural. Se pretende identificar las zonas donde la desnitrificación es más efectiva y determinar los factores espaciales que controlan la desnitrificación, como por ejemplo las características hidrogeológicas o las tasas de extracción de agua en cada zona. El estudio de la evolución temporal de la desnitrificación puede servir además para predecir la evolución del contaminante y de los procesos de atenuación natural del mismo.

La segunda parte de la tesis (Capítulos 3 y 4) discute el potencial de la desnitrificación mediante la oxidación de pirita como estrategia de bioremediación de aguas subterráneas contaminadas con nitratos. Los principales objetivos de esta parte son:

- Clarificar el papel de la pirita como potencial donador de electrones en los procesos de desnitrificación. Se pretende además determinar si la bacteria autótrofa *Thiobacillus denitrificans* es capaz de reducir nitrato usando pirita como donador de electrones.

- Examinar el efecto del pH, concentración de nitrato y tamaño de grano de la pirita en la eficacia del proceso de desnitrificación.

- Evaluar la viabilidad de una estrategia de biorremediación basada en la adición de pirita para estimular la actividad de bacterias desnitrificantes autóctonas.

- Examinar la capacidad de desnitrificación de los microorganismos presentes en sedimentos y en el agua subterránea del acuífero de Osona.

- Evaluar si la población microbiológica autóctona puede ser estimulada añadiendo pirita (bioestimulación). Determinar también la viabilidad de una estrategia combinada de bioestimulación y bioaumento.

- Evaluar la eficacia, rendimiento a largo plazo y durabilidad del tratamiento bajo condiciones de flujo continuo, que simulan mejor el flujo dinámico del agua subterránea.

- Caracterizar la población desnitrificante autóctona y evaluar cómo le afecta la bioestimulación con pirita, lo que permitirá conocer cuáles son los microorganismos capaces de adaptarse y explotar los hábitats contaminados.

- Calcular los factores de enriquecimiento isotópico de N y O usando material del acuífero de Osona, lo que permitirá cuantificar el grado de atenuación natural que tiene lugar en la zona de estudio.

La última parte de la tesis (Capítulo 5) se centra en el papel de las bacterias planctónicas y las adheridas a los sedimentos en la desnitrificación ligada a la oxidación de pirita. Los objetivos de esta parte son:

- Evaluar la habilidad de *T. denitrificans* de colonizar y crecer sobre la superficie de la pirita. Se pretende además cuantificar la velocidad de colonización y estimar la densidad de bacterias adheridas.

- Determinar si *T. denitrificans* requiere adherirse a la superficie de la pirita para llevar a cabo la desnitrificación por oxidación de pirita.

RESULTADOS Y DISCUSIÓN

En la **primera parte de la tesis** se han usado métodos multi-isotópicos integrados con métodos hidrogeológicos clásicos para caracterizar las aguas subterráneas del área de Osona. La composición isotópica del nitrato disuelto ($\delta^{15}N_{NO3}$, $\delta^{18}O_{NO3}$) ha permitido identificar la existencia de procesos de desnitrificación en las aguas subterráneas de la zona. De acuerdo con los procesos de desnitrificación, en las muestras estudiadas se observa un enriquecimiento en $\delta^{18}O$ y $\delta^{15}N$ del nitrato residual (Fig. 2). La relación $\varepsilon N/\varepsilon O$ es de 1.8, que entra dentro del rango de valores publicados en la bibliografía (entre 1.3 y 2.1, Böttcher et al., 1990; Mengis et al., 1999; Cey et al., 1999; DeVito et al., 2000; Fukada et al., 2003). Aproximadamente un 25% de las muestras pueden considerarse claramente desnitrificadas, con valores de $\delta^{15}N_{NO3} > +15‰$ y valores de $\delta^{18}O_{NO3} > +5‰$.

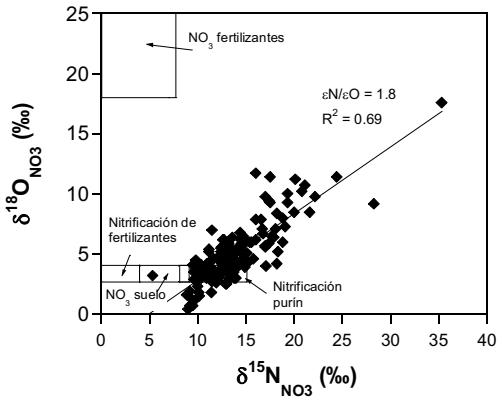

Figura 2. Diagrama $\delta^{15}N_{NO3}$ versus $\delta^{18}O_{NO3}$ de las muestras estudiadas. Se incluye la composición isotópica de las principales fuentes de nitrato (Mengis et al., 2001; Vitòria et al., 2004b; Vitòria et al., 2008).

El uso combinado de datos químicos e isotópicos ($\delta^{15}N_{NO3}$, $\delta^{18}O_{NO3}$, $\delta^{18}O_{SO4}$ y $\delta^{34}S_{SO4}$) ha servido para demostrar que los procesos de atenuación natural están ligados a la oxidación de pirita. En la mayor parte de las muestras con un grado de desnitrificación importante ($\delta^{15}N_{NO3} > +15‰$) la $\delta^{34}S_{SO4}$ presenta valores negativos, coherentes con los valores de las piritas diseminadas en los materiales del acuífero ($\delta^{34}S < -5‰$, Pierre et al.,

1994), confirmando el papel de este mineral en el proceso de desnitrificación. Debido a la litología carbonatada del acuífero, que tampona las concentraciones de HCO_3^- y los valores de $\delta^{13}C$, la desnitrificación por oxidación de la materia orgánica no se ha podido evaluar ni descartar.

Se han identificado las dos zonas del área de estudio donde la desnitrificación es más efectiva (sectores norte y oeste). Los resultados del estudio temporal muestran que en la mayoría de los pozos estudiados existe un equilibrio entre la entrada de nitrato por aplicación de purines y la pérdida de nitrato por procesos de desnitrificación. En cinco muestras se observa un predominio de los procesos de desnitrificación ligados a la oxidación de pirita durante todo el periodo de estudio. La variación con el tiempo de la composición química e isotópica de estas muestras ha servido para calcular los valores de enriquecimiento isotópico de N y O propios del acuífero de Osona (εN entre -4.4‰ y -15.5‰, con un valor promedio de -7.0‰ y εO entre -8.9‰ y -1.9‰, con un valor promedio de -4.6‰).

Usando estos valores, se ha aproximado el grado de desnitrificación natural en el acuífero (valor promedio del 30%), de acuerdo con la siguiente expresión:

$$DEN(\%) = \left[1 - \frac{[NO_3]_{residual}}{[NO_3]_{initial}}\right] \times 100 = \left[1 - e^{\left(\frac{\delta_{(residual)} - \delta_{(initial)}}{\varepsilon}\right)}\right] \times 100 \qquad (5)$$

En la **segunda parte de la tesis**, los experimentos tratados con pirita e inoculados con la bacteria *Thiobacillus denitrificans* han demostrado que esa bacteria es capaz de reducir nitrato usando pirita como donador de electrones. Además, se ha determinado que la eficiencia y la velocidad de reducción de nitrato dependen de la concentración inicial de nitrato, del tamaño de grano de la pirita y del pH, de manera que la reacción es más eficaz a medida que disminuye la concentración de nitrato (de aproximadamente 4

mM a 2.5 y 1 mM) y el tamaño de grano de la pirita (de 50-100 μm a 25-50 μm) (Fig. 3). Valores de pH inferiores a 6 claramente afectan a la actividad bacteriana.

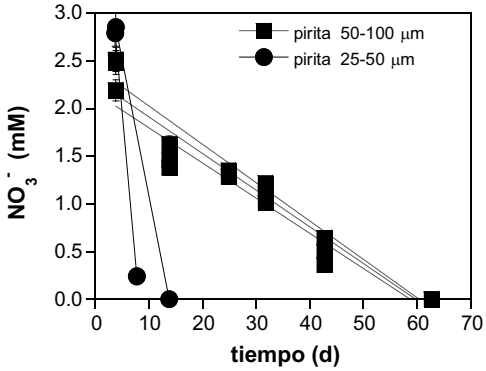

Figura 3. Consumo de nitrato versus tiempo en experimentos batch inoculados con *T. denitrificans*. La velocidad de reducción de nitrato es mayor en los experimentos que contienen pirita de tamaño de grano de 25-50 μm que en los experimentos con pirita 50-100 μm.

En experimentos de flujo continuo de larga duración, que simulan el flujo de aguas subterráneas contaminadas con nitrato, se han conseguido altas eficiencias en la eliminación del nitrato. En el experimento inoculado con *T. denitrificans* y llevado a cabo bajo una carga de nitrato de 0.21 mmol NO_3^- L^{-1} d^{-1} y un tiempo de residencia de 11.5 d, la eliminación total de nitrato se alcanza tras 70 d y se mantiene durante los 200 d de duración de los experimentos (Fig. 4A). Sin embargo, en los experimentos de flujo continuo no inoculados y no esterilizados (carga de nitrato entre 0.11 y 0.50 mmol NO_3^- L^{-1} d^{-1} y tiempos de residencia entre 2.3 y 3.9 d), aunque también se produce reducción de nitrato, ésta es menos efectiva e impredecible, probablemente debido a cambios en la población bacteriana (Fig. 4B). Los resultados de estos experimentos demuestran que las bacterias presentes en las muestras de pirita utilizadas, pese a no ser nativas de un sistema contaminado con nitrato, son capaces de adaptarse a las nuevas condiciones y consumir nitrato, en la mayor parte de los casos sin requerir largos periodos de adaptación. La comunidad desnitrificante que se desarrolla en estos experimentos probablemente es una mezcla entre poblaciones autótrofas, capaces de usar la pirita como

donador de electrones, y poblaciones heterótrofas, que usarían como fuente de carbono la materia orgánica generada tras la muerte y lisis de las células autótrofas.

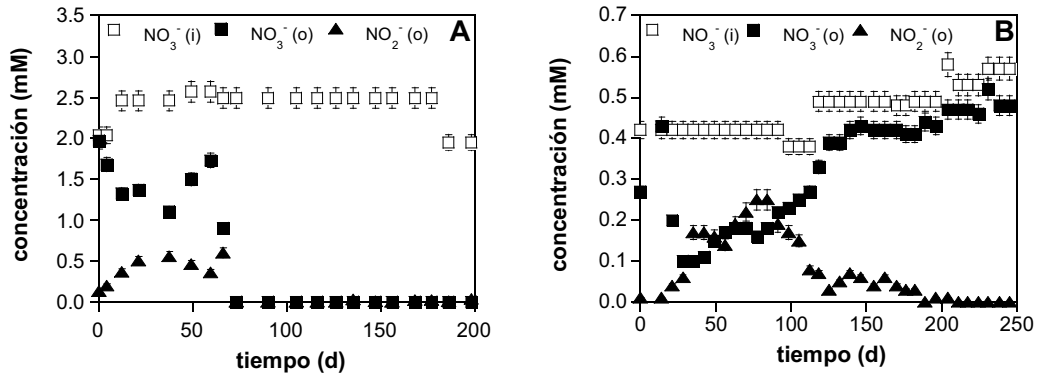

Figura 4. Variación con el tiempo de las concentraciones de nitrato y nitrito en las soluciones de entrada (i) y de salida (o) de: (A) experimento de flujo continuo inoculado con *T. denitrificans*; (B) uno de los experimentos no inoculados y no esterilizados.

Por otro lado, se han calculado los factores de enriquecimiento isotópico de N y O asociados a la desnitrificación por oxidación de pirita mediada por *T. denitrificans* (Fig. 5).

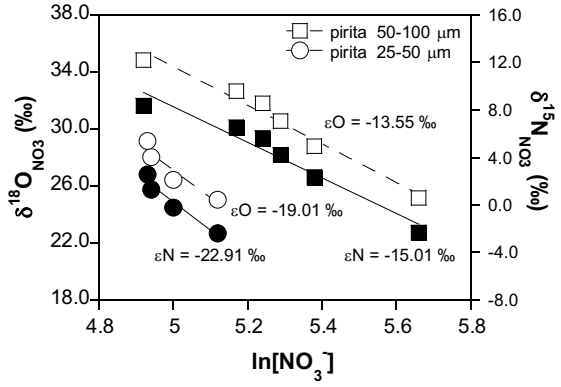

Figura 5. Resultados isotópicos de dos experimentos tratados con pirita e inoculados con *T. denitrificans*. Diagrama $\delta^{15}N$ (símbolos sólidos) y $\delta^{18}O_{NO3}$ (símbolos abiertos) versus $\ln[NO_3^-]$. Los valores de εN y εO se obtienen de la pendiente de las rectas de regresión.

Los valores obtenidos (εN entre -15.0‰ y -22.9‰ y εO entre -13.5‰ y -19.0‰) se encuentran dentro del rango de valores publicados en la bibliografía para otros cultivos puros de bacterias desnitrificantes, ninguno de ellos con bacterias autótrofas (Wellman et al., 1968; Delwiche y Steyn, 1970; Toyoda et al., 2005). Estos valores de εN y εO indican el grado de fraccionamiento isotópico que puede esperarse en acuíferos contaminados con nitrato en los que predominan los procesos de desnitrificación autótrofa.

En esta segunda parte de la tesis también se han realizado experimentos de bioestimulación con pirita usando agua subterránea y sedimentos del acuífero de Osona. Estos experimentos han demostrado que con la aplicación de pirita se consigue estimular la actividad de las bacterias desnitrificantes autóctonas y, por tanto, inducir y/o aumentar la desnitrificación (Fig. 6). En los experimentos blancos (esterilizados) y en los no bioestimulados con pirita, no se produce reducción de nitrato (Fig. 6), lo que indica que no existen cantidades suficientes de donadores de electrones apropiados en el material del acuífero y demuestra que la desnitrificación es un proceso mediado por microorganismos. La población microbiológica autóctona es capaz de reducir nitrato usando pirita como donador de electrones, siendo innecesario el bioaumento con *T. denitrificans*. En las condiciones probadas en los experimentos de bioestimulación/bioaumento, la adición de *T. denitrificans* solamente acelera levemente la velocidad de reducción de nitrato (Fig. 6), lo que sugiere que las bacterias inoculadas no son capaces de competir con las bacterias desnitrificantes autóctonas.

Se ha probado además la alta eficiencia de este proceso a largo plazo. En los experimentos de flujo continuo, la eliminación total del nitrato se produce tras, como mucho, 24 d y se mantiene durante los 180 d de duración de los experimentos (Fig. 7). Estos resultados indican la rápida adaptación de las bacterias nativas del material del acuífero a la adición de pirita. La alta eficiencia del proceso en los experimentos de flujo continuo de larga duración lleva a pensar que la aplicación de pirita puede considerarse como una estrategia de eliminación de nitrato en futuras medidas de gestión de los

recursos hídricos. Sin embargo, es necesaria más investigación, especialmente a escala de campo.

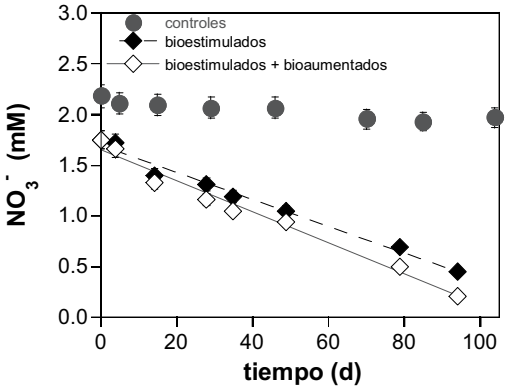

Figura 6. Variación de la concentración de nitrato con el tiempo en los experimentos batch con sedimentos y agua subterránea del acuífero de Osona. Se muestras los resultados de los experimentos controles (sin pirita y/o esterilizados), experimentos bioestimulados (con pirita) y experimentos bioestimulados/bioaumentados (con pirita y *T. denitrificans*).

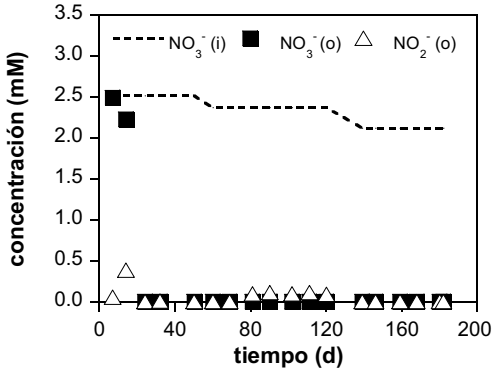

Figura 7. Variación con el tiempo de las concentraciones de nitrato y nitrito en las soluciones de entrada (i) y de salida (o) de uno de los experimentos de flujo continuo con sedimentos y agua subterránea del acuífero y bioestimulado con pirita.

Para conseguir que la biorremediación tenga éxito es necesario conocer con detalle no sólo los procesos, sino también las poblaciones microbiológicas que intervienen y los cambios poblacionales asociados al tratamiento de biorremediación. Para ello se han utilizado técnicas moleculares independientes de cultivo, como la reacción en cadena de la polimerasa (PCR) acoplada a electroforesis en geles con gradiente desnaturalizante

químico (DGGE) o la PCR cuantitativa de los genes *16S rRNA* (población total) y *nosZ* (población desnitrificante). Los resultados de los experimentos de bioestimulación han puesto de manifiesto que las bacterias desnitrificantes autótrofas dominantes en el sistema probablemente son poblaciones relacionadas con la familia *Xanthomonadaceae*. La adición de pirita supone un incremento en la proporción de bacterias desnitrificantes (Fig. 8) y produce la estimulación de tanto desnitrificantes autótrofos como heterótrofos. Los resultados muestran además que *T. denitrificans* no es la bacteria desnitrificante dominante en el sedimento ni en el agua subterránea del acuífero de Osona.

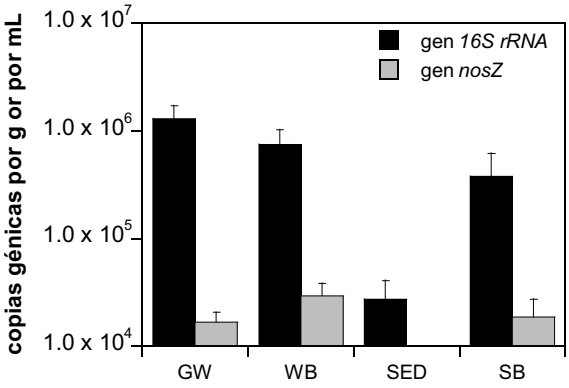

Figura 8. Número de copias de los genes *16S rRNA* y *nosZ* en muestras acuosas (copias génicas mL^{-1}) o en muestras sólidas (copias génicas g^{-1}). GW: agua subterránea original; WB: muestra acuosa al final de uno de los experimentos bioestimulados; SED: sedimento del acuífero original; SB: muestra sólida al final de uno de los experimentos bioestimulados.

Se han calculado además los factores de enriquecimiento isotópico de N y O asociados al proceso de desnitrificación por oxidación de pirita (εN entre -27.6‰ y -25.0‰ y εO entre -21.27‰ y -19.49‰) (Fig. 9). Los valores de εN se encuentran dentro del rango de valores publicados en la bibliografía para experimentos de laboratorio con sedimentos de otros acuíferos (entre -14.6‰ y -34.1‰; Grischek et al., 1998; Sebilo et al., 2003; Tsushima et al., 2006). Los factores de enriquecimiento obtenidos son, sin embargo, más bajos que los publicados en estudios de desnitrificación *in situ* (εN entre -57‰ y -4‰ y εN entre -18.3‰ y -8.0‰; Böttcher et al., 1990; Fustec et al., 1991; Aravena y

Robertson, 1998; Mengis et al., 1999; Pauwels et al., 2000; Fukada et al., 2003; Singleton et al., 2007) y que los obtenidos para el acuífero de Osona en la primera parte de la tesis. Esta divergencia es coherente con la discrepancia general existente entre factores de enriquecimiento calculados en el campo y en el laboratorio, que es debida a la heterogeneidad de los acuíferos.

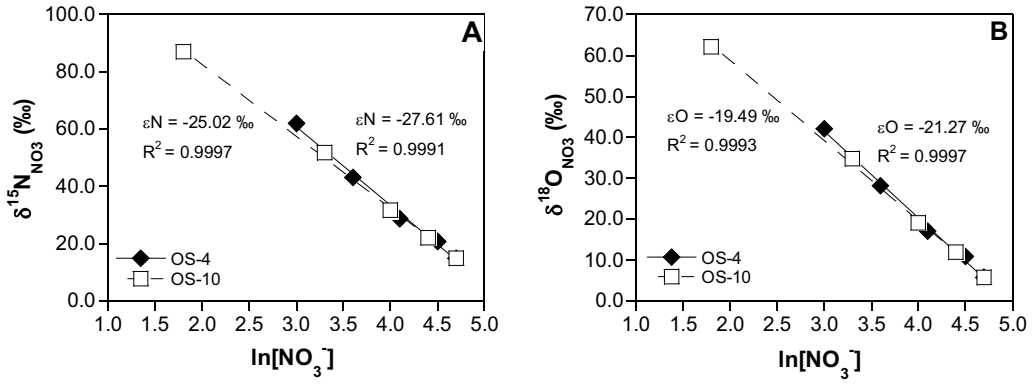

Figura 9. Resultados isotópicos de los experimentos OS-4 (bioestimulado) y OS-10 (bioestimulado/bioaumentado). (A) Diagrama $\delta^{15}N$ versus $\ln[NO_3^-]$; (B) diagrama $\delta^{18}O_{NO3}$ versus $\ln[NO_3^-]$. Los valores de εN y εO se obtienen de la pendiente de las rectas de regresión.

Los factores de enriquecimiento obtenidos en los experimentos con material del acuífero de Osona se han usado para recalcular el grado de atenuación natural del nitrato que está teniendo lugar en el acuífero (valor promedio de 10%) y que había sido sobreestimado en la primera parte de esta tesis. Este recálculo puede ser útil para predecir la evolución de la contaminación en el acuífero y debe ser tenido en cuenta a la hora de implementar posibles técnicas de remediación inducida. Por tanto, la metodología isotópica ha demostrado ser una herramienta excelente para identificar y cuantificar procesos de desnitrificación natural y para monitorizar la eficacia de estrategias de biorremediación en el laboratorio.

En la **tercera parte de la tesis** se han llevado a cabo experimentos de colonización usando fragmentos pulidos de pirita para evaluar la capacidad de *T. denitrificans* de crecer sobre la superficie de la pirita. Tras una semana, pueden observarse células sueltas adheridas a la superficie, así como células en división. Al cabo de tres semanas, se detectan microcolonias, aisladas unas de otras y ocupando aproximadamente el 2% de la superficie de pirita disponible (Fig. 10). La velocidad de colonización de *T. denitrificans* sobre la superficie del mineral es de unas 35 células mm^{-2} h^{-1}. Se estima que alrededor de un 0.3% de las bacterias se adhieren a la superficie de la pirita, mientras que el resto permanecen en solución.

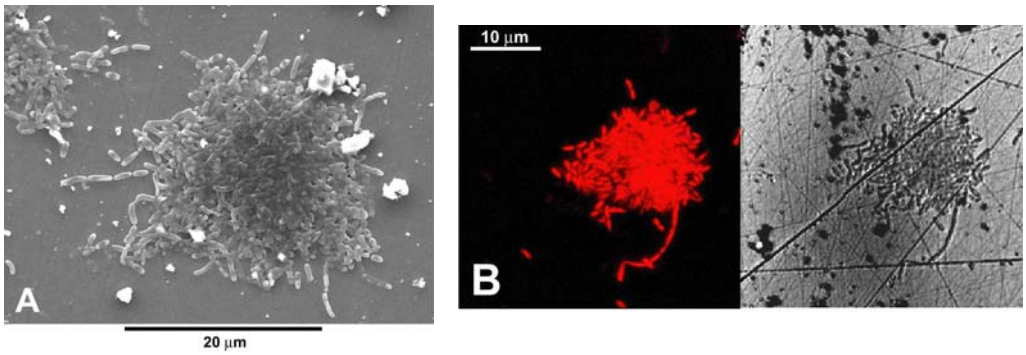

Figura 10. Ejemplos de microcolonias de células de *T. denitrificans* adheridas a la superficie de la pirita tras 3 semanas. (A) Microscopio electrónico de barrido (SEM); (B) Microscopio confocal (CLSM).

El número de bacterias adheridas al mineral aumenta con el tiempo, mientras que el número de bacterias planctónicas se mantiene constante durante las 9 semanas de duración de los experimentos. Esto sugiere que tanto las bacterias planctónicas como las adheridas a la pirita se mantienen metabólicamente activas. Por tanto, los resultados sugieren que, para conseguir desnitrificar usando la pirita como donador de electrones, es necesaria que una parte de las bacterias se adhiera a la superficie de la pirita. No obstante, parece que tanto las bacterias adheridas como las planctónicas contribuyen en el proceso global. Sin embargo, queda pendiente determinar cuál es el papel específico de ambas fases en la desnitrificación. Estos resultados podrían aplicarse a sistemas naturales

para predecir la distribución espacial de las bacterias desnitrificantes en los acuíferos, aunque son necesarios experimentos de colonización *in situ* para determinar si es posible extrapolar estos resultados a acuíferos contaminados con nitrato.

CONCLUSIONES

- Se ha identificado la existencia de procesos de desnitrificación en las aguas subterráneas de Osona mediante el uso combinado de $\delta^{15}N$ y δ^{18} del nitrato disuelto.

- Mediante el uso combinado de datos químicos e isotópicos ($\delta^{15}N_{NO3}$, $\delta^{18}O_{NO3}$, $\delta^{18}O_{SO4}$ y $\delta^{34}S_{SO4}$) se ha puesto de manifiesto que los procesos de atenuación natural están ligados a la oxidación de pirita.

- Se han identificado las dos zonas del área de estudio donde la desnitrificación es más efectiva: en la zona de recarga del norte de la Plana de Vic y en el sector central de la Plana, donde la aplicación de purines es mayor.

- Se han estimado los valores de enriquecimiento isotópico de N y O asociados a la desnitrificación en el acuífero de Osona: εN entre -4.4‰ y -15.5‰ y εO entre -8.9‰ y -1.9‰.

- A partir de los valores de εN y εO obtenidos, se ha aproximado el grado de desnitrificación natural en el acuífero de Osona, que presenta un valor promedio del 30%.

- Se ha demostrado que la bacteria *Thiobacillus denitrificans* es capaz de usar la pirita como donador de electrones en la reducción de nitrato.

- La eficiencia y la velocidad con la que *T. denitrificans* reduce el nitrato dependen de la concentración inicial de nitrato, del tamaño de grano de la pirita y del pH.

- En experimentos de flujo continuo de larga duración estimulados con pirita e inoculados con *T. denitrificans* se han conseguido altas eficiencias en la eliminación de nitrato.

- En los experimentos de flujo continuo no inoculados y no esterilizados, también se produce reducción de nitrato, pero es menos efectiva e impredecible. Las bacterias presentes, pese a no ser nativas de un ambiente contaminado con nitrato, son capaces de reducir el nitrato, probablemente mediante una combinación de desnitrificación autótrofa y heterótrofa.

- Se han calculado los factores de enriquecimiento isotópico de N y O asociados a la desnitrificación por oxidación de pirita mediada por *T. denitrificans*: εN entre -15.0‰ y -22.9‰ y εO entre -13.5‰ y -19.0‰.

- La población desnitrificante nativa de los sedimentos y del agua subterránea del acuífero de Osona puede estimularse añadiendo pirita. La bioestimulación con pirita puede ser por tanto una buena estrategia de desnitrificación inducida.

- Se ha puesto de manifiesto que para inducir la desnitrificación autótrofa en los sedimentos del acuífero no es necesario el bioaumento con *T. denitrificans*. Las bacterias inoculadas son incapaces de competir con las bacterias autóctonas en las condiciones probadas en los experimentos.

- La bioestimulación supone un incremento en la proporción de bacterias desnitrificantes y un cambio en la diversidad de la población microbiana. La

adición de pirita produce la estimulación de desnitrificantes tanto autótrofos como heterótrofos.

- Poblaciones relacionadas con la familia *Xanthomonadaceae* probablemente son las bacterias desnitrificantes autótrofas dominantes en el sistema, capaces de reducir nitrato usando pirita como donador de electrones.

- Los resultados de los experimentos de bioestimulación de flujo continuo muestran que las bacterias autóctonas responden de forma rápida a la adición de pirita, de manera que se alcanza una eliminación total del nitrato en poco tiempo y se mantiene durante los 180 d de duración de los experimentos.

- Se han calculado los factores de enriquecimiento isotópico de N y O para el material del acuífero de Osona: εN entre -27.6‰ y -25.0‰ y εO entre -21.27‰ y -19.49‰.

- Los factores de enriquecimiento obtenidos en los experimentos con material del acuífero de Osona se han usado para recalcular el grado de atenuación natural que está teniendo lugar en el acuífero. Se obtiene un valor promedio del 10%.

- Los resultados de los experimentos de colonización de *T. denitrificans* sobre la superficie de la pirita sugieren que tanto las células adheridas al mineral como las que se mantienen en solución (planctónicas) contribuyen en la desnitrificación.

Los resultados de esta tesis sugieren que la aplicación controlada de pirita podría ser una buena estrategia de bioremediación para mitigar la contaminación en acuíferos contaminados con nitrato. En un acuífero como el de Osona, donde se están produciendo procesos de desnitrificación por oxidación de pirita de forma natural, estimular a la

población microbiológica autóctona añadiendo pirita supondría incentivar a una población que ya está activa y aclimatada a esas condiciones. Son necesarios más estudios, especialmente a escala de campo, para optimizar esta estrategia de biorremediación, evaluar si la alta eficiencia en la eliminación de nitrato obtenida en el laboratorio puede extrapolarse a sistemas naturales y determinar la longevidad del tratamiento. La optimización del tratamiento puede conseguirse buscando las condiciones óptimas que garanticen la supervivencia de las bacterias y el rendimiento del proceso a largo plazo. También debe tenerse en cuenta el origen y la composición química de la pirita, ya que una de las limitaciones de esta desnitrificación inducida podría ser la liberación de metales tóxicos que pueden estar presentes en cantidades traza en la estructura del mineral (As, Ni, etc.).

Agradecimientos

Una vez finalizada esta etapa, me gustaría dar las gracias a todas las personas que lo han hecho posible.

En primer lugar, agradecer a mis directores, el Dr. Jordi Cama, el Dr. Albert Soler y el Dr. Jordi Urmeneta, por darme la oportunidad de realizar esta tesis y por toda la ayuda, apoyo, dedicación y confianza que han depositado en mí durante todos estos años.

También quiero agradecer a la Dra. Neus Otero, quien, aunque no figure como directora, se ha comportado como tal. Gracias por su inestimable ayuda y colaboración.

Muchas gracias a la Dra. Katrina Edwards y al Dr. Gordon Southam por su hospitalidad, ayuda y dedicación prestadas durante mis estancias en la University of Southern California y en la University of Western Ontario. Y también a toda la gente que conocí en Los Angeles y en London por su cálida acogida y ayuda, dentro y fuera del laboratorio: Nina, Jaime, Jason, Roman, Clara, Lewis, Alicia, Nathan y Kebbi, Ian, Lachlan, Kim, Greg, Lyndsay, Celeste, Alex, Charles, Nancy.

Estoy muy agradecida al Dr. Marc Viñas por toda su incalculable ayuda con la parte de los análisis moleculares. Muchas gracias por todos sus consejos, sugerencias y explicaciones.

Agradezco también toda la ayuda prestada por los técnicos de los Serveis Científics Tècnics de la Universidad de Barcelona (Eva Pelegrí, Toni Padró, Maite Romero, Laia Balart, Ana Domínguez, Eva Prats, Javier García, Lorenzo Calvo, Eduard Carbonell, Pilar Teixidor, Pilar Rubio, Rosa María Marimón, Xavier Alcobé, Xavier Llovet, Joan Gámez, Ismael Diez, Gerard Oncins), los del Instituto Jaume Almera/IDAEA (Josep Elvira, Rafa Bartrolí, Mercé Cabañas, Silvia Rico) y los de la Facultad de Geología de la Universidad de Barcelona (Adolf Samper, Vicenç Planella, Montserrat Sibila). Sin ellos, habría sido imposible obtener muchos de los resultados que se presentan en esta tesis. Y también, al personal administrativo del Jaume Almera y del IDAEA, gracias a los cuales todos los trámites han sido mucho más fáciles.

Muchísimas gracias a todos mis compañeros y amigos del Jaume Almera/IDAEA y del Maima. Especialmente a Mapi, Patricia y Esteban, porque ellos entienden toda la emoción que comporta terminar esta tesis. También gracias a todos los demás: Ana, Vanessa, Tobias, Francesco, Manuela, Arantxa, Marco, Jose Luis, Ester, Jordi F., Katrien, María, Carmen, Roger, Jordi P., Massimo, Georgina, Raúl, Carme. Gracias por vuestras sugerencias, ideas y ayuda en el laboratorio y por vuestros ánimos, compañía, cafés, cervezas, terapias de grupo, cenas, juergas y horas de compañía en el laboratorio o en el despacho.

Muchas gracias también al ghetto 'maño' de Barcelona (Sara, Mapi, Fabio, María, Nuria, Ángel, Miriam, Juanmi, Manolo, Cristina, Pili, JP, Vicent, Ivan, Raquel, Laura, Antonio, Esti, Lorena, Ruth, Patricia) por haber estado siempre a mi lado en los buenos y malos momentos. Han sido unos años maravillosos!

Muchísimas gracias a los geólogos de Zaragoza: Clara, Elena, Ana, Nino, Ángela, Juan, Javi, Iván, Alfredo, Enzo, Nacho, Darío, Diego, Miguel y Raúl. Con vosotros empezó todo. Muchas gracias por compartir mis penas y glorias, por vuestra alegría inagotable y por estar siempre ahí cuando os he necesitado.

En último lugar, agradecer también a mi familia por su constante e incondicional apoyo y su cariño. No hace falta decir mucho más. Gracias a mi madre, a Mariona y a Beatriz, porque siempre me habéis apoyado en todas mis decisiones, habéis confiado en mí y habéis estado dispuestas a dejarlo todo para escucharme y ayudarme. Gracias también al resto de la familia. Sin todos vosotros esto no habría sido posible.

Espero que estas pocas palabras (ya sabéis que de palabras no ando normalmente sobrada…) hayan servido para plasmar el agradecimiento y cariño a todos los que habéis colaborado de una forma u otra para hacer realidad esta tesis. Y a todos los que sienten que forman parte de esto y que no he nombrado por olvido. Gracias.

Table of contents

List of figures

List of Tables

Chapter 1

Introduction

Nitrate is one of the most common chemical contaminant in the world's groundwater aquifers (Spalding and Exner, 1993). Widespread pollution of drinking water sources by nitrate is an important environmental problem. In the last decades, nitrate pollution has become a major threat to groundwater quality as the threshold value for drinking water (50 mg L^{-1}, Council Directive 98/83/EC) is being reached in most of the local and regional aquifers in Europe.

A drinking water nitrate concentration in excess of the standard poses a considerable health risk because high nitrate ingestion can cause methemoglobinemia in infants and young children (Comly, 1945; Magee and Barnes, 1956). Ingested nitrate is reduced to nitrite, which binds to hemoglobin to form methemoglobin (MetHb). Methemoglobinemia occurs when elevated levels of MetHb (exceeding about 10%) interfere with the oxygen-carrying capacity of the blood. Infants are particularly susceptible to developing methemoglobinemia for several reasons, including their increased capacity to convert nitrate to nitrite and their lower levels of the enzyme cytochrome b5 reductase, which converts MetHb back to hemoglobin (Ward et al, 2005). Some authors even point out that nitrogen compounds can act as human cancer

promoters (Volkmer et al., 2005; Ward et al., 2005). Furthermore, nitrate can stimulate the growth of aquatic plants, contributing to eutrophication of natural surface water bodies (Rabalais, 2009).

Groundwater contamination by nitrate usually originates from anthropogenic sources, mainly as a result of wastewater discharges and the intensive application of fertilizers and animal manure to agricultural land. The European Nitrate Directive (Council Directive 91/676/EEC) emphasizes the importance of preventing pollution caused by nitrates from agricultural sources. According to this directive, each State member must identify its vulnerable zones - zones draining into water affected by or vulnerable to N pollution - and establish a Codes of Good Agricultural Practice. In Catalonia (NE Spain), nine areas have been declared vulnerable to nitrate pollution from agricultural sources (Decret 283/1998/DOGC). One of the vulnerable areas with the highest nitrate concentration is the Osona area, where nitrate is derived from intensive farming activities. This intensive activity produces considerable amounts of organic animal wastes (more than 10.000 tones N/y), mainly as pig manure. Most of them are spread out on the fields. Even though the local administration regulates and controls the present use and distribution of manure as fertilizer, nitrate pollution in Osona shows the effect of decades of uncontrolled manure application, which has resulted in nitrate contents in groundwater often exceeding 100 mg L^{-1}. This high nitrate content leads to a loss of water availability for domestic uses in an area where precipitation is irregular and scarce and poses a threat to water management.

To improve water management in those areas vulnerable to nitrate pollution, it is essential to understand the processes that control groundwater nitrate content. The most important natural nitrate attenuation process is denitrification, i.e. the reduction of nitrate to dinitrogen gas by anaerobic facultative bacteria that utilize nitrate as the electron acceptor (Knowles, 1982). This process involves the formation of a number of nitrogen intermediates and can be summarized as follows:

$$NO_3^- \rightarrow NO_2^- \rightarrow NO \rightarrow N_2O \rightarrow N_2 \quad (1.1)$$

Bacteria that are capable of denitrification are ubiquitous, and thus denitrification occurs widely throughout terrestrial, freshwater, and marine systems where the following conditions arise simultaneously (Zumft, 1997): (i) nitrate and electron donor availability, (ii) low oxygen concentrations (dissolved oxygen concentrations less than around 1-2 mg L^{-1}, e.g. Korom, 1992; Cey et al., 1999), and (iii) favorable environmental conditions (temperature, pH, other nutrients and trace elements).

Denitrifying bacteria are generally heterotrophic and use a wide range of carbon compounds (sugars, organic acids, amino acids) as the electron donor. Nevertheless, a limited number of bacteria are able to carry out chemolithotrophic denitrification, and to utilize inorganic compounds such as reduced sulfur compounds, hydrogen, ferrous iron or uranium (IV) as electron donors, and inorganic carbon (CO_2 or HCO_3) as the carbon source for cell material synthesis (Straub et al., 1996; Zumft, 1997; Beller, 2005). For example, the bacterium *Paracoccus denitrificans* can denitrify using hydrogen (Smith et al., 1994) and the obligate chemolithoautotrophic bacterium *Thiobacillus denitrificans* is well known for its ability to couple the oxidation of various sulfur and reduced iron compounds to denitrification (Beller et al., 2006).

Under usual aquifer conditions, pyrite is typically expected to be the electron donor. Denitrification by pyrite oxidation is expressed as:

$$14NO_3^- + 5FeS_2 + 4H^+ \Rightarrow 7N_2 + 10SO_4^{2-} + 5Fe^{2+} + 2H_2O \quad (1.2)$$

If the Fe^{2+} produced is oxidized:

$$NO_3^- + 5Fe^{2+} + 6H^+ \Rightarrow \frac{1}{2}N_2 + 5Fe^{3+} + 3H_2O \quad (1.3)$$

an overall reaction where denitrification mediated by pyrite oxidation occurs is expressed as:

$$15NO_3^- + 5FeS_2 + 10H_2O \Rightarrow \frac{15}{2}N_2 + 10SO_4^{2-} + 5Fe(OH)_3 + 5H^+ \qquad (1.4)$$

Several field studies have suggested by means of geochemical and/or isotopic data that denitrification in aquifers is controlled by pyrite oxidation even in the presence of organic matter (Postma et al., 1991; Aravena and Robertson, 1998; Cravotta, 1998; Pauwels et al., 1998; 2000; 2010; Beller et al., 2004; Schwientek et al., 2008; Zhang et al., 2009a). However, the feasibility of pyrite-driven denitrification has been questioned several times in laboratory studies (Devlin et al., 2000; Schippers and Jorgensen, 2002; Haaijer et al., 2007). Only in Jorgensen et al. (2009), has been denitrification coupled to pyrite oxidation satisfactorily accomplished. Nevertheless, little is still known about the kinetics, the limiting factors and the involvement of *T. denitrifican*s-like bacteria in this reaction.

Sources and processes affecting groundwater nitrate can be characterized by means of its isotopic composition ($\delta^{15}N$, $\delta^{18}O$). The N and O isotope fractionation has been qualitatively used to indicate natural bacterially mediated nitrate reduction in contaminated aquifers (Aravena and Robertson, 1998; Grischek et al., 1998; Mengis et al., 1999; Cey et al., 1999). During denitrification, microorganisms prefer the lighter isotopes ^{14}N and ^{16}O leaving the remaining nitrate progressively enriched in ^{15}N and ^{18}O (Böttcher et al., 1990). Therefore, the decrease in nitrate concentration is coupled to an increase in the $\delta^{15}N$ and $\delta^{18}O$ of the residual nitrate with a $\varepsilon N/\varepsilon O$ ratio that ranges from 1.3 (Fukada et al., 2003) to 2.1 (Böttcher et al., 1990). Intermediate enrichment ratios were reported by Mengis et al. (1999), Cey et al. (1999) and DeVito et al. (2000). To determine the relative roles of heterotrophic and autotrophic processes in denitrification, several studies have used the coupled approach of chemical data with the $\delta^{15}N$ and/or $\delta^{18}O$ of dissolved nitrate and the isotopic composition of the ions involved in denitrification reactions, such as, for example, the $\delta^{34}S$ and $\delta^{18}O$ of dissolved sulfate, and/or the $\delta^{13}C$ of dissolved inorganic

carbon (Aravena and Robertson, 1998; Pauwels et al., 1998; 2000; 2010; Schwientek et al., 2008).

Vitòria et al. (2008) showed the occurrence of denitrification processes in a small area located in the northern part of the Osona region and suggested that sulfide oxidation had an important role in natural attenuation. Accordingly, the first objectives of this thesis are to confirm that denitrification takes place in a larger area than that studied by Vitòria et al. (2008), to characterize the denitrification processes that control natural attenuation in the Osona aquifer and to study their spatial and temporal variations. Understanding the processes that control nitrate content and their spatial and temporal trends is of practical significance for the successful application of water-protection strategies. Therefore, the first part of this thesis relays on the characterization of the denitrification processes occurring in the Osona aquifer.

Denitrification in natural systems proceeds very slowly, and it is not significant for lowering nitrate concentrations in aquifers. That is why the removal of nitrate from groundwater and wastewater has attained great significance in recent years as a means of protecting and preserving the environment. The traditional techniques used for lowering nitrate concentration to acceptable levels are ion-exchange, reverse osmosis and electrodialysis. However, the utility of these processes has been limited as they are relatively expensive and they product nitrate concentrated wastes that pose a disposal problem due to the high saline content (Soares, 2000).

Alternatively, enhanced *in situ* biological denitrification can be achieved by adding suitable electron donors and/or energy sources (biostimulation). As regards heterotrophic denitrification, various solids, liquid and gaseous carbon sources have been evaluated, such as wheat straw, cotton, sucrose, methanol, ethanol and methane (Soares, 2000; Park and Yoo, 2009). Denitrification efficiency varies in a wide range between 10% and nearly 100% (Mateju et al., 1992). However, the risk of clogging due to biomass accumulation and gas production is very high. Moreover, the quality of the denitrified water might require post-treatment and disinfection, which increase overall treatment costs.

Compared with conventional heterotrophic denitrification, autotrophic denitrification has two clear advantages: no need for an external organic carbon source, which decreases the cost of the process; and less biomass production, which minimizes the treatment of sludge and the risk of clogging. Much work has been devoted to enhancing denitrification by adding several inorganic electron donors: (1) zero-valent iron (Choe et al., 2004; Della Rocca et al., 2006; Rodríguez-Maroto et al., 2009), (2) ferrous ions in solution (Straub et al., 1996; Benz et al., 1998; Nielsen and Nielsen, 1998; Straub and Buchholz-Cleven, 1998; Devlin et al., 2000; Kappler and Newman, 2004; Weber et al., 2006; Miot et al., 2009), (3) elemental sulfur (Batchelor and Lawrence, 1978; Hashimoto et al., 1987; Zhang and Lampe, 1999; Soares, 2002; Sierra-Alvarez et al., 2007; Moon et al., 2008), and (4) iron bearing materials such as oxides (Weber et al., 2001), silicates (Postma, 1990) and green-rust (Hansen et al, 2001). In comparison, fewer studies have been carried out in nitrate reduction by pyrite and other sulfide minerals (Devlin et al., 2000; Schippers and Jorgensen, 2002; Haaijer et al., 2007; Jorgensen et al., 2009). As stated above, only in Jorgensen et al. (2009) has been denitrification coupled to pyrite oxidation satisfactorily accomplished. The authors showed that the addition of pyrite to the sediment from an aquifer increased nitrate reduction rates.

Another strategy of bioremediation is bioaugmentation, which consists in the addition of microorganisms able to consume, destroy or transform the contaminant. Bioaugmentation is usually performed using microbial strains or mixes of strains that: (1) are isolated from the contaminated site and grown in a medium containing the contaminant, (2) have specific metabolic pathways that are not present in the contaminant site, or (3) are genetically modified. Bioaugmentation provides certain advantages over biostimulation in cases where pollutant toxicity or lack of appropriate microorganisms is important (Vogel, 1996). However, other studies have reported a little effect of bioaugmentation (Stephenson and Stephenson, 1992; Vogel, 1996). Several possible reasons for the failure of bioaugmentation have been proposed, such as problems concerning the adaptation of the inoculated microorganisms, the insufficiency of substrate, the presence of inhibitory substances or inhibitory growth conditions and

competition between the introduced species and the indigenous biomass (Goldstein et al., 1985; McClure et al., 1991; Vogel, 1996). Bioaugmentation can be used in combination with biostimulation to enhance remediation. Few laboratory studies have assessed combined biostimulation/bioaugmentation approaches using autotrophic denitrifying bacteria to enhance denitrification (Manconi et al., 2006; Flores et al., 2007; Sánchez et al., 2008; Zhang et al., 2009b). Flores et al. (2007) and Sánchez et al. (2008) inoculated *Alcaligenes defragrans* and *T. denitrificans* and *Thiomicrospira denitrificans*, respectively, to enriched sludges in order to assess the performance of bioaugmentation for sulfur-oxidizing denitrification processes. In both studies, no advantage of the bioaugmented sludges over the non-bioaugmented ones was observed regarding the efficiency in nitrate removal. Nevertheless, Manconi et al. (2006) showed that inoculation of *T. denitrificans* to an enriched sludge enhanced nitrate removal using thiosulfate as the electron donor. As regards bioaugmentation with encapsulated microorganisms, Zhang et al. (2009b) demonstrated that using polyvinyl alcohol (PVA) beads with immobilized cells of *T. denitrificans* improved efficiency of thiosulfate-based denitrification.

Therefore, one of the main objectives of this thesis is to clarify the role of pyrite as electron donor for denitrification. Once pyrite is confirmed to serve as the electron donor, the further step before applying this strategy in the field is to evaluate the feasibility as bioremediation strategy of adding pyrite to stimulate native denitrifying bacteria and enhance denitrification, at the lab-scale and using sediments and groundwater from the nitrate-contaminated aquifer. In addition to biostimulation adding pyrite, bioaugmentation adding *T. denitrificans* is also evaluated. Accordingly, the second part of this thesis discusses the potential of pyrite as electron donor for denitrification and the capacity of the indigenous bacteria of sediments and groundwater from the Osona aquifer to reduce nitrate using pyrite. Other objective of the second part of the thesis is to determine the composition of the bacterial community of the Osona samples and the impact of the biostimulation and/or bioaugmentation in the populations.

The last part of the thesis is focused on the contribution of attached and free-phase denitrifying bacteria to pyrite-based denitrification in aquifers. Currently, little is known about the mechanisms by which autotrophic denitrifying bacteria can reduce nitrate using pyrite as the electron donor, and whether or not bacteria need to attach to pyrite surfaces. The main objective of this part is to study the ability of *Thiobacillus denitrificans* to grow and colonize pyrite surfaces and to determine if the rate-limiting factor in the pyrite-based denitrification reaction is mass transfer from the solid to the solution or bacterial attachment onto surfaces. This understanding is necessary to improve the performance and longevity of bioremediation processes and to lower their maintenance costs.

1.1 Thesis outline

This thesis is composed of six chapters including the introduction. All the chapters are based on published papers or manuscripts that are currently in preparation for publication or under review by international journals. The thesis is divided into three parts.

Part I (chapter 2) deals with the characterization of the natural nitrate attenuation occurring in groundwater of the Osona aquifer by means of a multi-isotopic approach integrated with the application of classical hydrochemistry data. The objectives of this part are to identify and characterize the denitrification processes occurring in the Osona groundwater, to determine the role of pyrite in the natural attenuation and to study its spatial and temporal variations.

Part II (chapters 3 and 4) discusses the potential of denitrification with pyrite as a bioremediation strategy of nitrate contaminated groundwater. Experiments of chapter 3 are devoted to clarify the role of pyrite as an electron donor in microbial denitrification and to study the kinetics of the reaction. In chapter 4, experiments with material from the Osona aquifer are performed in order to assess if sediments and groundwater from the aquifer have the microbial capacity to denitrify relying on pyrite oxidation and to

evaluate the feasibility of *in situ* bioremediation by biostimulation and/or bioaugmentation. Isotopic and chemical analyses are used to monitor the efficacy of stimulated denitrification. The impact of the biostimulation and/or bioaugmentation in the indigenous microbial community is also evaluated.

Part III (chapter 5) is focused on the characterization of the nature and mechanisms of nitrate reduction using pyrite as the electron donor, being microbially catalyzed. Moreover, the ability of *Thiobacillus denitrificans* to grow and colonize pyrite surface is studied to gain insight of the contribution of attached and free-phase denitrifying bacteria to pyrite-driven denitrification in aquifers.

Chapter 6 provides a summary of the main conclusions of this thesis.

Appendix A includes a short description of the main laboratory methods and protocols used in the experimental work of this thesis. Appendix B contains the bulk dataset of the chemical and isotopic parameters determined for the Osona groundwater samples studied in chapter 2. Appendixes C and D provide the bulk dataset of the experimental results of the experiments presented in chapters 3 and 4, respectively.

Part I:

Natural nitrate attenuation

Chapter 2

Nitrate attenuation in Osona groundwater: multi-isotopic approach

In the last decades, nitrate pollution has become a major threat to groundwater quality as the threshold value for drinking water (50 mg L^{-1}, Council Directive 98/83/EC) is being reached in most of the local and regional aquifers in Europe. The European Groundwater Directive (Council Directive 2006/118/EC) considered nitrate as one of the main contaminants that could hamper the achievement of the goals of the Water Framework Directive (Council Directive 2000/60/EC). High nitrate in drinking water poses a health risk because high nitrate ingestion can cause methemoglobinemia in infants and young children (Comly, 1945; Magee and Barnes, 1956). Some authors even point out that nitrogen compounds can act as human cancer promoters (Volkmer et al., 2005; Ward et al., 2005). Nitrate pollution is linked to the intensive use of synthetic and organic fertilizers, as well as to septic system effluents.

Note: This chapter is based on the article: Otero, N., Torrentó, C., Soler, A., Menció, A. and Mas-Pla, J. (2009) Monitoring groundwater nitrate attenuation in a regional system coupling hydrogeology with multi-isotopic methods: The case of Plana de Vic (Osona, Spain). *Agric, Ecosyst Environ* **133**: 103-113.

In Catalonia, according to the European nitrate directive (Council Directive 91/676/EEC), nine areas have been declared vulnerable to nitrate pollution from agricultural sources (Decret 283/1998/DOGC). One of the vulnerable areas with the highest nitrate concentration is the Osona area, where nitrate is derived from intensive pig farming activities. Even though the local administration regulates and controls the present use and distribution of manure as fertilizer, nitrate pollution in Osona shows the effect of decades of uncontrolled manure application, which has resulted in nitrate contents in groundwater often exceeding 100 mg L^{-1}. This high nitrate content results in a loss of water availability for domestic uses in an area where precipitation is irregular and scarce and poses a threat to water management. To improve water management in those areas vulnerable to nitrate pollution, it is essential to understand the processes that control groundwater nitrate content. In the Osona region, multi-isotopic methods have been applied to identify the sources of nitrate and to determine the existence of denitrification processes (Vitòria et al., 2008).

Stable isotopes of dissolved nitrate are powerful tool to study the denitrification processes. Stable isotopes are usually measured as the ratio between the desired isotope and the most-abundant one, e.g. ^{15}N against ^{14}N. Given that measuring such a small difference cannot be feasibly done in an absolute way, these ratios are almost always established with respect to international standards. As a result, measures are usually expressed in delta notation (Eq. 2.1), where R= $^{15}N/^{14}N$ ratio.

$$\delta^{15}N = \frac{R_{sample} - (R)_{std}}{(R)_{std}} \times 1000 \qquad (2.1)$$

Denitrification, which consists in nitrate reduction to N_2 under anaerobic conditions, is the main natural process to attenuate nitrate pollution in groundwater. During denitrification, as nitrate concentration decreases, residual nitrate becomes enriched in heavy isotopes ^{15}N and ^{18}O with a $\varepsilon N/\varepsilon O$ ratio that ranges from 1.3 (Fukada et al., 2003) to 2.1 (Böttcher et al., 1990). The isotope enrichment factor (ε) is defined in Eq. 2.2:

$$\varepsilon_{product} - \varepsilon_{reac\,tan\,t} = \frac{R_{product}}{R_{reac\,tan\,t}} - 1 \quad (\times 10^3 \text{‰}) \tag{2.2}$$

The approximation $\varepsilon_{product}$- $\varepsilon_{reactant} \approx \delta^{15}N_{product}$- $\delta^{15}N_{reactant}$, can be used for the values of ε and $\delta^{15}N$ usually found in natural abundance studies (Fritz and Fontes, 1980).

The analysis of nitrate for both $\delta^{15}N$ and $\delta^{18}O$ has been useful for the identification of denitrification in groundwater (e.g. Aravena and Robertson, 1998). Moreover, the isotopic composition of dissolved nitrate has also been used to distinguish between dilution and denitrification in groundwater samples in areas where a decrease in nitrate concentration is observed (Grischek et al., 1998; Mengis et al., 1999; Cey et al., 1999).

A further step in the investigation of denitrification processes is to determine the processes governing the reaction. Denitrification refers to the microbiologically mediated process of reduction of nitrate. Two main denitrification reactions have been suggested to occur in aquifers: heterotrophic denitrification by oxidation of organic compounds and autotrophic denitrification by oxidation of inorganic compounds (Rivett et al., 2008). To determine the relative role of heterotrophic and autotrophic processes in denitrification of groundwater, several studies have used the coupled approach of chemical data with the $\delta^{15}N$ and/or $\delta^{18}O$ of dissolved nitrate and the isotopic composition of the ions involved in denitrification reactions, such as, for example, the $\delta^{34}S$ and $\delta^{18}O$ of dissolved sulfate, and/or the $\delta^{13}C$ of dissolved inorganic carbon (Aravena and Robertson, 1998; Pauwels et al., 2000).

Vitòria et al. (2008) showed the occurrence of denitrification processes in a small area located in the northern part of the Osona region and suggested that sulfide oxidation had an important role in natural attenuation. A further step in the investigation of the denitrification processes that take place in this area is the study of their spatial and temporal patterns. Spatial variations can be useful to distinguish the factors that control denitrification processes, such as hydrogeological characteristics of the aquifer or domestic withdrawal rates, in order to identify where measures could be applied to avoid

further deterioration in water quality. Likewise, knowledge of temporal trends in nitrate contents and denitrification processes is also valuable for the successful application of water-protection strategies. Therefore, the main purposes of the present chapter are: (1) to confirm that denitrification takes place in a larger area than that studied by Vitòria et al. (2008), (2) to characterize the denitrification processes that control natural attenuation in this area, and (3) to study their spatial and temporal variations. To this end, groundwater was studied coupling classical hydrochemical data with a comprehensive isotopic characterization of the ions involved in denitrification reactions ($\delta^{15}N_{NO3}$, $\delta^{18}O_{NO3}$, $\delta^{34}S_{SO4}$, $\delta^{18}O_{SO4}$, and $\delta^{13}C_{DIC}$).

2.1 Study area

The Osona region is located to the North of Barcelona, between the Montseny Mountain and the pre-Pyrenees range. This study focuses on its eastern and central part, namely "Plana de Vic", an area of 600 Km^2 belonging to the Ter River basin. Figure 2.1 shows the studied area, which includes the smaller area characterized in Vitòria et al. (2008).

The area has a sub-Mediterranean climate with an annual mean temperature of 13°C and potential evapotranspiration higher than rainfall, making Osona a dry area that mainly relies on groundwater resources to fulfill its agricultural and farming demand. During the studied period (from April 2005 to May 2006), potential evapotranspiration (estimated by Thornthwaite equation) was higher than rainfall except for the time between September 2005 and January 2006. In September 2005, the first significant rainfall event occurred after almost 1 year of a significant drought. Therefore, samples collected in April 2005 and in May 2006 represent groundwater in a dry period and the samples of the October 2005 campaign, groundwater in a wet season.

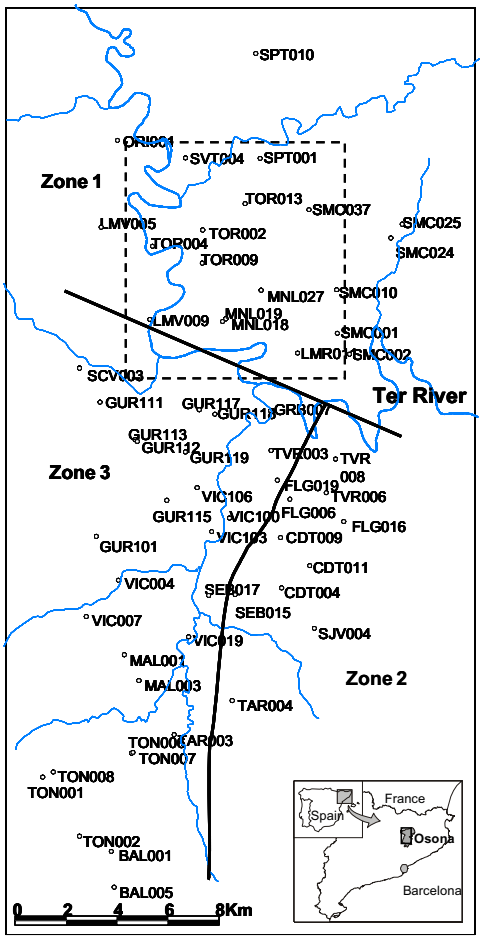

Figure 2.1. Study area, showing sampling sites, and zones. The map includes the area characterized in Vitòria et al. (2008).

From a geological perspective, this hydrogeological system lies on Paleogene sedimentary materials overlying Hercynian crystalline (igneous and metamorphic) rocks (Fig. 2.2a). The stratigraphic sequence primarily consists of carbonate formations, with an alternation of calcareous, marl and carbonate sandstone layers (Fig. 2.2b). These formations show a rather uniform dipping of about 7-10° to the west, with an antiform structure only at the northern limit. Locally, at the south-west of the studied area, a

gypsum marine formation outcrops. Hydrogeologically, the system is made up of a series of confined aquifers located in the carbonate and carbonate-sandstone layers, whose porosity is mainly related to the fracture network. The marl strata act as confining layers, as observed in boreholes and hydrogeological prospecting. Nevertheless, fracture network in those marl layers where the sand content is high allows a vertical leakage between aquifer levels. The main production wells for agricultural demand usually reach depths of more than 100 m, searching for the most productive confined aquifers. Alluvial aquifers are scarce and generally non-productive in the area, except those located at the Ter River terraces.

According to a conceptual flow model of the hydrogeological system in the area (Menció et al., 2010), two main flow systems have been identified: a surficial system, corresponding to unconfined aquifers that are directly affected by manure spreads; and a deep system, corresponding to a semiconfined aquifer that is less vulnerable to direct nitrate leachate under natural conditions. The lack of well casing, unnecessary from a constructive point of view, allows the mixing of waters of distinct qualities within the well, resulting in the extraction of low quality water and, even worse, impoverishing water resources stored in the deeper aquifer layers. Moreover, a downward leakage occurring towards the deeper aquifers because of the fractured nature of the confining units facilitates the entrance of nitrate-rich surficial groundwater and causes a loss of quality resources. Menció et al. (2010) determined three zones in the "Plana de Vic" area, according to its hydrogeological dynamics (Fig. 2.1): Zone 1, located in the northern part of the Ter River and comprising the northern recharge areas; Zone 2, corresponding to the recharge area located at the eastern margin of the "Plana de Vic" to the south of the Ter; and Zone 3, corresponding to the centre of the "Plana de Vic" and the western reliefs, to the south of the Ter. These zones are used in the present study to describe chemical and isotopic features of the studied area and to study temporal and spatial variability of the attenuation processes.

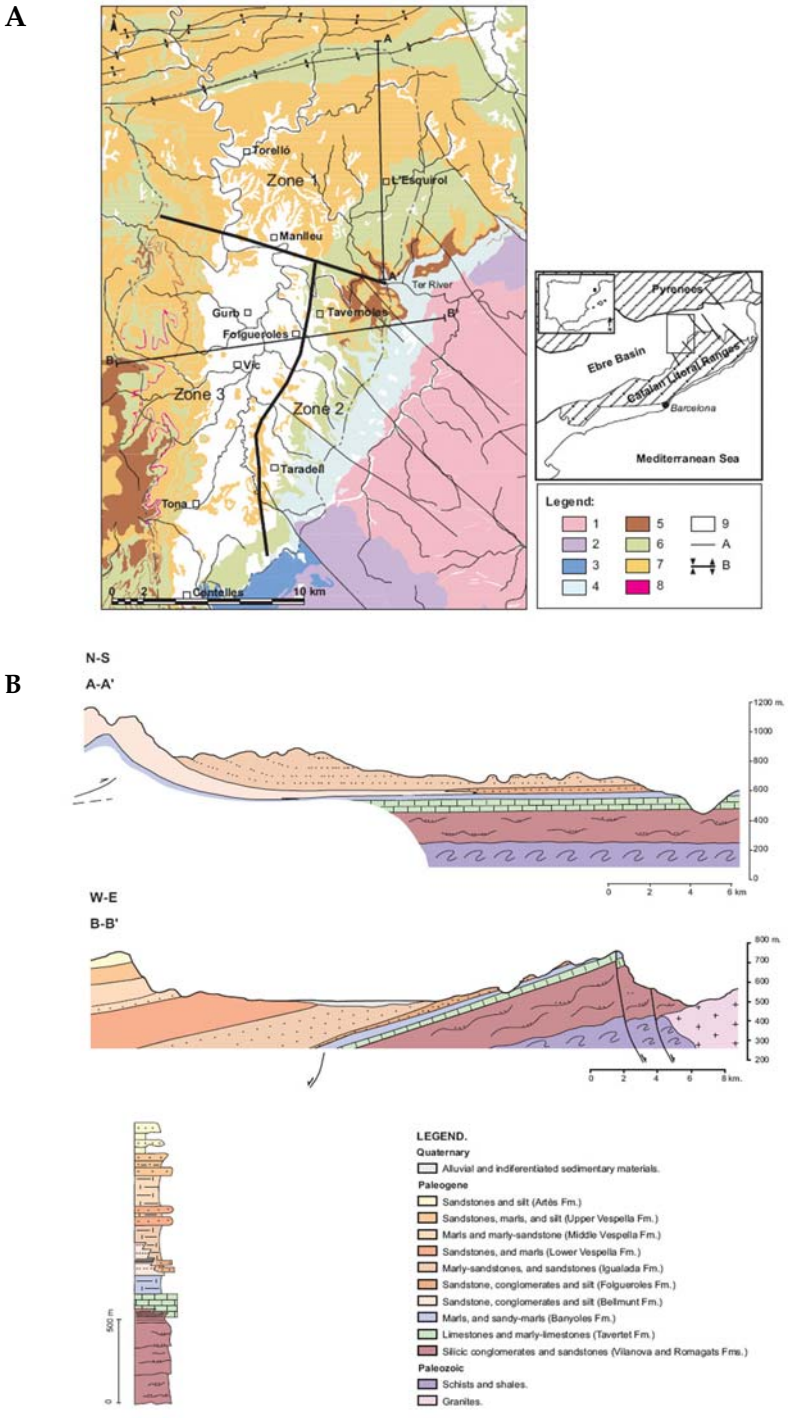

Figure 2.2. (a) Simplified geologic map of the study area (Menció et al., 2010).

Legend: Paleozoic: (1) Igneous rocks, (2) Metamorphic rocks; Mesozoic: (3) Sedimentary rocks; Paleogene: (4) Coarse detritic sandstones and conglomerates (Vilanova and Romagats Fms.), (5) Carbonates (Tavertet Fm.), (6) Sandstone, silt and marl (Bellmunt, Folgueroles and Artès Fms.), (7) Marls and marly sandstones (Banyoles, Igualada, and Vespella Fms.), (8) Evaporitic (gypsum) deposits; Quaternary: (9) Alluvial and other recent undifferentiated formations; (A) Faults, (B) Syncline and anticline folding. (b) Geological cross-sections of the main geological formations in the study area (Menció et al., 2010). See Figure 2.2a for locations.

Osona is classified as vulnerable to nitrate pollution from agricultural sources following the nitrate directive (Council Directive 91/676/EEC). In the "Plana de Vic", nitrate pollution is widespread, with a median concentration above 100 mg L^{-1} over the last six years. As described in detail in Vitòria et al. (2008), huge amounts of pig manure are produced as a result of intensive farming activity. Most of the manure is used as organic fertilizer. Synthetic fertilizers are applied in the areas surrounding villages, as the use of pig manure close to urban areas is forbidden. Regarding non-agricultural sources of nitrate, such as sewage or septic system leakage, the expected contribution is orders of magnitude lower than that for agricultural sources. This is mainly due to the fact that the total population is only 140000 and 93% of the municipalities of the area are connected to sewage treatment plants, with nitrogen elimination treatment. On the other hand, sewage or septic system leakage is unlikely to cause such widespread diffused pollution.

2.2 Methods

Samples for chemical and isotopic characterization were collected in April 2005, October 2005 and May 2006 from 60 pre-existent production wells (Fig. 2.1), except for the May 2006 survey, when only 30 samples were gathered. Physicochemical parameters (pH, temperature, conductivity, dissolved O_2 and Eh) were measured *in situ*, using a flow cell to avoid contact with the atmosphere. The wells were continuously pumped and samples were collected when the Eh values became stabilized. Samples were then stored at 4°C. Chemical parameters (Cl^-, SO_4^{2-}, HCO_3^-, Na^+, Ca^{2+}, Mg^{2+}, K^+, total Fe, total Mn, NO_2^-, NO_3^-, NH_4^+ and TOC) were determined by standard analytical techniques.

The isotopic characterization included the nitrogen and oxygen isotopic composition of dissolved nitrate ($\delta^{15}N_{NO3}$ and $\delta^{18}O_{NO3}$), the sulfur and oxygen isotopic composition of dissolved sulfate ($\delta^{34}S_{SO4}$ and $\delta^{18}O_{SO4}$), and the carbon isotopic composition of dissolved inorganic carbon ($\delta^{13}C_{DIC}$). For the sulfur and oxygen isotopic analysis, the dissolved sulfate was precipitated as $BaSO_4$ by adding $BaCl_2 \cdot 2H_2O$ after acidifying the sample with HCl and boiling it in order to prevent $BaCO_3$ precipitation. For the $\delta^{13}C$ analysis, unfiltered samples were treated with a NaOH-$BaCl_2$ solution to precipitate carbonates, and then filtered at 3 μm. The $\delta^{15}N$ and $\delta^{18}O$ of dissolved nitrate were obtained following the denitrifier method of Sigman et al. (2001) and Casciotti et al. (2002). For the samples of the May 2006 campaign, nitrate analyses were performed using the anion exchange method (Silva et al., 2000, described in detail in Appendix A and in Vitòria et al., 2008). Notation is expressed in terms of δ per mil relative to the international standards: V-SMOW (Vienna Standard Mean Oceanic Water) for $\delta^{18}O$, AIR (Atmospheric N_2) for $\delta^{15}N$, V-CDT (Vienna Canyon Diablo Troillite) for $\delta^{34}S$, and V-PDB (Vienna Peedee Belemnite) for $\delta^{13}C$. The isotope ratios were calculated using international and internal laboratory standards. Reproducibility (≡1σ) of the samples was determined as follows: ±0.3‰ for $\delta^{15}N_{NO3}$; ±0.2‰ for $\delta^{34}S$; ±0.5‰ for both $\delta^{18}O_{NO3}$, and $\delta^{18}O_{SO4}$; and ±0.2‰ for $\delta^{13}C_{DIC}$. Isotopic analyses were prepared at the laboratory of the Mineralogia Aplicada i Medi Ambient research group and analyzed at the Serveis Científic Tècnics of the Universitat de Barcelona, except for the isotopic composition of dissolved nitrates of some samples, which was analyzed at the Woods Hole Oceanographic Institution.

2.3 Results and discussion

Median values of chemical parameters and stable isotopes of dissolved nitrate ($\delta^{15}N_{NO3}$, $\delta^{18}O_{NO3}$), dissolved sulfate ($\delta^{34}S_{SO4}$, $\delta^{18}O_{SO4}$) and dissolved inorganic carbon ($\delta^{13}C_{DIC}$) are summarized in Table 2.1, where groups are distinguished by zone and sampling survey. Bulk dataset is provided in Appendix B.

Table 2.1. Median values of chemical and isotopic data. Groups are distinguished by zone and sampling survey.

	Cond.	DO	Eh	NO_2^-	NH_4^+	NO_3^-	HCO_3^-	Cl^-	SO_4^{2-}	Fe	Mn	$\delta^{13}C_{HCO3}$	$\delta^{34}S_{SO4}$	$\delta^{18}O_{SO4}$	$\delta^{15}N_{NO3}$	$\delta^{18}O_{NO3}$
	µs cm^{-1}	mg L^{-1}	mV	mg L^{-1}	mg L^{-1}	mg L^{-1}	mg L^{-1}	mg L^{-1}	mg L^{-1}	mg L^{-1}	mg L^{-1}	‰	‰	‰	‰	‰
ZONE 1																
April 2005	1114	4.7	361	0.00	0.02	101.5	418.3	54	118	n.d.	n.d.	-12.5	-8.1	4.1	13.9	4.3
October 2005	960	n.d.	380	0.04	0.02	80.9	419.7	53	118	0.10	0.02	-12.3	-9.3	4.2	13.7	5.0
May 2006	914	4.0	417	n.d.	n.d.	125.6	424.6	48	103	0.02	0.02	-11.8	-9.0	4.3	14.8	6.2
ZONE 2																
April 2005	867	5.5	390	0.01	0.02	95.2	369.4	49	67	n.d.	n.d.	-13.2	-0.2	4.7	11.6	3.3
October 2005	848	n.d.	n.d.	0.01	0.02	62.2	380.6	46	74	0.12	0.02	-12.0	-1.0	4.1	11.5	3.4
May 2006	705	6.6	402	n.d.	n.d.	106.7	390.0	32	69	0.02	0.02	-13.7	2.9	4.6	11.5	4.6
ZONE 3																
April 2005	1396	4.3	370	0.01	0.02	141.2	409.4	111	212	n.d.	n.d.	-12.8	-2.8	4.0	13.5	4.3
October 2005	1300	n.d.	375	0.03	0.02	169.6	398.9	109	219	0.08	0.02	-12.4	-4.4	3.8	13.6	3.9
May 2006	1475	4.9	407	n.d.	n.d.	176.2	395.3	122	218	0.02	0.02	-12.1	-1.8	3.1	13.6	5.8

n.d.= not determined

2.3.1 Nitrate sources and evidences of denitrification

Nitrate concentration ranged from 10 to 529 mg L^{-1}, with a median value of 127 mg L^{-1} (*n*=148). The percentage of studied wells with nitrate contents higher than the drinking water threshold of 50 mg L^{-1} was 85% in April 2005, 79% in October 2005 and 81% in May 2006. None of these wells correspond to the drinking water supply network. No clear relation between nitrate content and well depth was observed, due to the mix of waters within the wells as they are uncased production wells. Menció et al. (2010) showed that there is also a downward leakage of nitrate towards the deeper aquifers due to the recharge induced by intensive pumping of the surface aquifer layers, which hinders the interpretation of chemical data.

In the studied area, $\delta^{15}N_{NO3}$ ranged from +5.3‰ to +35.3‰, with a median value of +13.4‰, and the $\delta^{18}O_{NO3}$ ranged between +0.4‰ and +17.6‰, with a median value of +4.5‰ (*n*=147). Isotopic values of the main nitrate sources in the studied area are thoroughly discussed in Vitòria et al. (2008). Most of the Osona samples with higher nitrate concentration showed $\delta^{15}N$ between +9.0‰ and +15‰, in agreement with manure or sewage values (Fig. 2.3a). Coupling nitrogen with oxygen values of dissolved nitrate, most samples are also within the range of manure or sewage-derived nitrate (Fig. 2.3b).

Although the expected contribution from non-agricultural sources of nitrate -sewage or septic system leakage- was much lower than that from agricultural sources, nevertheless, to totally discard the role of sewage in nitrate pollution, the analysis of boron isotopes (Widory et al., 2004; 2005) should be applied in future research. Those samples with nitrate concentration below 100 mg L^{-1} showed higher variability, with $\delta^{15}N$ ranging from +5‰ to +35‰. The value of $\delta^{15}N$ of +5‰ (and $\delta^{18}O_{NO3}$ = +3.2‰), corresponding to a well 200 m deep, showed the lowest NO_3^- and Cl^- concentrations in the studied area (SPT-010). The isotopic composition is in agreement with the isotopic signature of nitrate derived from mineralization of soil organic nitrogen (Heaton, 1986), thus representing a natural end-member.

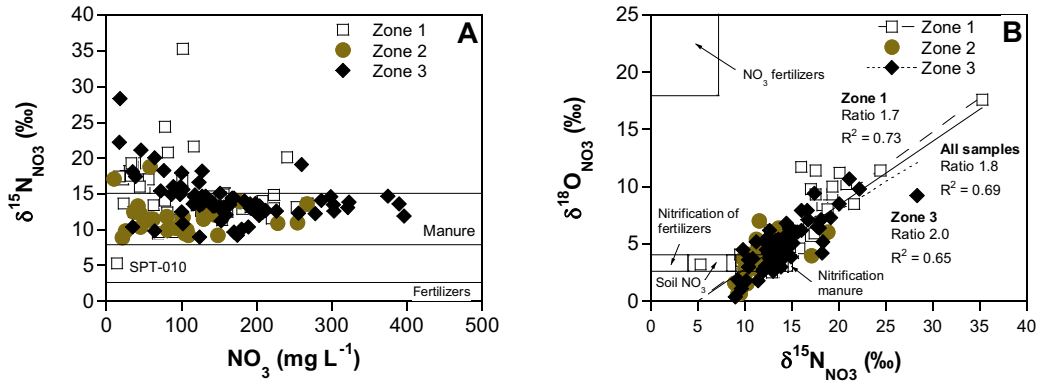

Figure 2.3. (a) Nitrate concentration vs. $\delta^{15}N_{NO3}$ of the studied samples. (b) $\delta^{15}N$ vs. $\delta^{18}O_{NO3}$, together with the isotopic composition of the main nitrate sources in the studied area (Mengis et al., 2001; Vitòria et al., 2004b; Vitòria et al., 2008). Values of $\delta^{18}O$ of nitrate derived from nitrification of NH_4^+ of manure were calculated following experimental expressions of Andersson and Hooper (1983) and Hollocher (1984), using the range of $\delta^{18}O_{H2O}$ of the studied area (from -8‰ to -5.1‰, with a median value of -6.7‰, *n*=149) and $\delta^{18}O_{O2}$ equals to +23.5‰ (Kroopnick and Craig, 1972; Horibe et al., 1973).

The $\delta^{15}N$ values between +15‰ and +35‰ could be explained either by volatilization or by denitrification (Fig. 2.3a), but the observed coupled increase of $\delta^{15}N$ and $\delta^{18}O$ (Fig. 2.3b) suggested that denitrification was taking place, hence discarding volatilization processes. During denitrification, as nitrate concentration decreases, residual nitrate becomes enriched in heavy isotopes ^{15}N and ^{18}O with a εN/εO ratio that ranges from 1.3 (Fukada et al., 2003) to 2.1 (Böttcher et al., 1990). Intermediate enrichment ratios have been reported by Cey et al. (1999), Mengis et al. (1999), DeVito et al. (2000) and Lehmann et al. (2003). In the studied samples, there is a positive correlation (r^2= 0.69) between $\delta^{15}N_{NO3}$ and $\delta^{18}O_{NO3}$, with a slope of 0.56. The observed slope shows that the enrichment for ^{15}N is higher by a factor of 1.8 than for ^{18}O. This value of 1.8 is within the range of reported εN/εO ratios for denitrification in groundwater. Chemical parameters related to redox conditions indicated oxic conditions for most of the studied wells. Eh values varied from 116 mV to 490 mV, with a median value of 378 mV (*n*=123). Measured dissolved oxygen (DO) ranged from 0.8 mg L^{-1} to 16.3 mg L^{-1}, with a median value of 4.9 mg L^{-1} (*n*=90). Manganese was detected in few samples and contents were around 0.05 mg L^{-1}. Fe concentration ranged from 0.02 mg L^{-1} to 1.48 mg L^{-1}, with a median value of 0.08

mg L^{-1} (*n*=71). NO_2^- content varied from 0.01 mg L^{-1} to 3.89 mg L^{-1}, with a median value of 0.03 mg L^{-1} (*n*=66). Nitrite is an intermediate step during denitrification processes (see chapter 1). Although no clear correlation was observed between the nitrite content and ^{15}N or $\delta^{18}O_{NO3}$, the median nitrite concentration for those samples with $\delta^{15}N$> +15‰ was 24.5 μg L^{-1}, whereas the concentration was lower (4.5 μg L^{-1}) for samples with $\delta^{15}N$< +15‰. One requirement for denitrification is anaerobic conditions or restricted oxygen availability (dissolved oxygen concentration less than around 2 mg L^{-1}, e.g. Korom, 1992; Cey et al., 1999). Although in most of the studied wells (85%) dissolved oxygen concentrations were higher than 2 mg L^{-1}, indicating unsuitable conditions for denitrification to occur, isotopic data clearly showed the occurrence of natural attenuation. According to Koba et al. (1997) and Moncaster et al. (2000), denitrification can take place at higher dissolved oxygen concentrations when it occurs in micro-anaerobic environments where dissolved oxygen has been completely removed.

2.3.2 Heterotrophic or autotrophic denitrification?

Denitrification processes take place under reducing environments, usually in the saturated zone. This process is linked either to organic matter oxidation or to sulfide oxidation. The reactions controlling the denitrification process can be revealed, to some extent, by studying chemical data coupled to the isotopic composition of the solutes involved in the reactions: $\delta^{15}N_{NO3}$, $\delta^{18}O_{NO3}$, $\delta^{13}C_{DIC}$, $\delta^{18}O_{H2O}$, $\delta^{34}S_{SO4}$ and $\delta^{18}O_{SO4}$. Denitrification by oxidation of organic matter should result in a decrease of nitrate together with an increase in HCO_3^- concentration. Isotopically speaking, an increase in $\delta^{15}N_{NO3}$ and $\delta^{18}O_{NO3}$ coupled to a decrease in $\delta^{13}C_{DIC}$ is expected (Eq. 2.3).

$$4NO_3^- + 5C + 2H_2O \rightarrow 2N_2 + 4HCO_3^- + CO_2 \qquad (2.3)$$

Pyrite could also act as an oxidant agent, as has been proposed in other aquifers based on geochemical data (Kölle et al., 1983; Böttcher et al., 1990; Postma et al., 1991; Engesgaard and Kipp, 1992; Robertson et al., 1996; Aravena and Robertson, 1998;

Cravotta, 1998; Pauwels et al., 1998; 2000; 2010; Beller et al., 2004; Schwientek et al., 2008; Zhang et al., 2009a). Denitrification by sulfide oxidation takes place in several steps (Eq. 2.4, 2.5 and 2.6):

$$14NO_3^- + 5FeS_2 + 4H^+ \Rightarrow 7N_2 + 10SO_4^{2-} + 5Fe^{2+} + 2H_2O \quad (2.4)$$

$$NO_3^- + 5Fe^{2+} + 6H^+ \Rightarrow \frac{1}{2}N_2 + 5Fe^{3+} + 3H_2O \quad (2.5)$$

$$15NO_3^- + 5FeS_2 + 10H_2O \Rightarrow \frac{15}{2}N_2 + 10SO_4^{2-} + 5Fe(OH)_3 + 5H^+ \quad (2.6)$$

Though it is believed that denitrification by sulfide oxidation cannot occur in carbonated aquifers where pH is higher than 7, nevertheless, if the Fe^{2+} produced is oxidized, following reaction 2.5, a global reaction 2.6 can be written where protons could locally exceed those consumed by carbonate dissolution (Moncaster et al., 2000). If this is the case, denitrification by pyrite oxidation could occur in a carbonate aquifer. Denitrification by sulfide oxidation should result in an increase in SO_4^{2-} concentration coupled to a decrease in NO_3^- concentration. Isotopically, an increase in $\delta^{15}N_{NO3}$ and $\delta^{18}O_{NO3}$ is expected and $\delta^{34}S_{SO4}$ and $\delta^{18}O_{SO4}$ should match with the isotopic composition of sulfates derived from sulfide oxidation.

The $\delta^{34}S$ of the dissolved sulfate ranged from -19.5‰ to +9.3‰, with a median value of -4.4‰ (*n*=149), and the $\delta^{18}O_{SO4}$ varied from -1.1‰ to +9.0 ‰, with a median value of +4.0‰ (*n*=147). Negative sulfur values can be explained by sulfide oxidation. Disseminated pyrite in marls in the area had $\delta^{34}S_{FeS2}$ ranging from -5‰ and -28‰ (Pierre et al., 1994). About 46% of the studied samples showed $\delta^{34}S_{SO4}$ values within this range. As is explained in detail in Vitòria et al. (2008), the $\delta^{18}O$ of sulfates formed via sulfide oxidation must show a relationship with $\delta^{18}O_{H2O}$. Indeed, 83% of the studied samples fall within the experimental area of sulfates derived from sulfide oxidation defined by Van Stempvoort and Krouse (1994) (Fig. 2.4a). Figure 2.4b shows the main sulfate sources in

the area and the studied samples, which plot within an area between sulfate from sulfide oxidation and four positive $\delta^{34}S$ end members: manure sulfate, soil sulfate, fertilizers and evaporites. Due to the absence of major evaporite rock outcrops in the area, the positive sulfur values could be explained in terms of anthropogenic sources linked to agricultural and livestock raising activities (see details in the following section). Only the groundwater recharging in the western reliefs, in the south-western part of Zone 3, could interact with locally outcropping gypsum layers, and thus acquire a different isotopic signature (e.g. samples TON-001, TON-006, TON-007, TON-008, VIC-004 and VIC-007, see Appendix B).

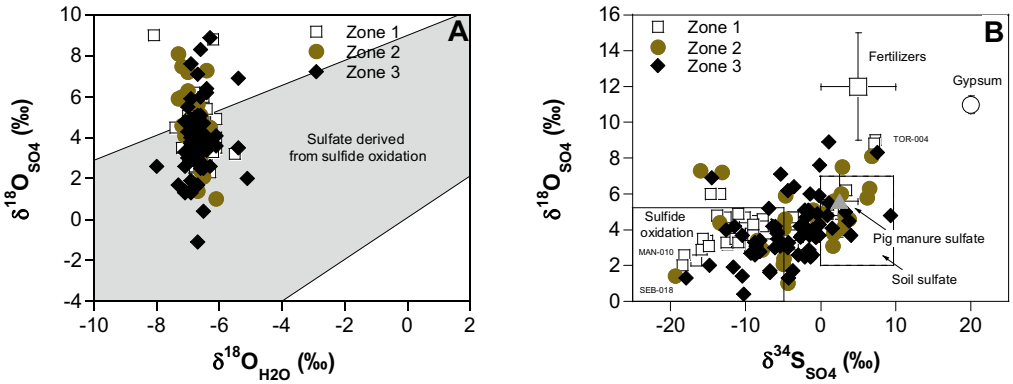

Figure 2.4. (a) $\delta^{18}O_{H2O}$ vs. $\delta^{18}O_{SO4}$ diagram. The experimental area of sulfates derived from sulfide oxidation as defined by Van Stempvoort and Krouse (1994) is shown. (b) $\delta^{34}S_{SO4}$ vs. $\delta^{18}O_{SO4}$. The box represents the sulfates derived from sulfide oxidation. Values for pig manure are taken from Otero et al. (2007) and Cravotta (1997), soil sulfate data from Clark and Fritz (1997), fertilizer data from Vitòria et al. (2004b), and gypsum values from Utrilla et al. (1992).

In a $\delta^{15}N_{NO3}$ vs. $\delta^{34}S_{SO4}$ diagram, samples plot in a mixing line between the isotopic composition of sulfate originated from pyrite oxidation ($\delta^{34}S$ values < -5‰) and the isotopic composition of pig manure ($\delta^{34}S_{SO4}$ values from 0 to +5‰, Otero et al., 2007; and $\delta^{15}N_{NO3}$ values between +8‰ and +15‰, Vitòria et al., 2004a), suggesting a link between pyrite oxidation and denitrification (Fig. 2.5). Moreover, samples with clear denitrification ($\delta^{15}N_{NO3}$ > +15‰) correspond to samples with sulfate from pyrite oxidation, confirming the role of pyrite oxidation in denitrification.

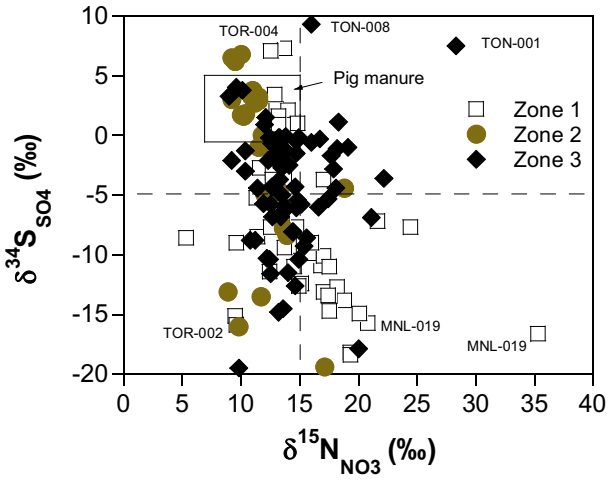

Figure 2.5. $\delta^{15}N_{NO3}$ vs. $\delta^{34}S_{SO4}$ diagram. The box represents the isotopic composition of pig manure (Vitòria et al., 2004a; Otero et al., 2007). Samples of Osona groundwater plot in a mixing line between the isotopic composition of sulfate originated from pyrite oxidation (with $\delta^{34}S$ values < -5‰) and the isotopic composition of pig manure sulfate. Moreover, samples with clear denitrification (with $\delta^{15}N_{NO3}$ > +15‰) correspond to samples with sulfate from pyrite oxidation.

To evaluate the relative role of organic matter oxidation in the natural nitrate attenuation, nitrate isotopes were studied coupled to $\delta^{13}C_{DIC}$ and bicarbonate concentrations. In the studied area, due to the aquifer lithology, which consists mainly of carbonate formations, groundwater has a high natural bicarbonate concentration (up to 576 mg L^{-1}, with a median value of 407 mg L^{-1}) that could buffer the isotopic composition of $\delta^{13}C_{DIC}$. Measured $\delta^{13}C_{DIC}$ varied from -15.5‰ to -9.2‰, with a median value of -12.5‰ (*n*=146), except for two samples with higher values (GRB-118 with -7.6‰, and SVT-004 with -6.9‰ and -7.4‰). These values are in agreement with the known range of $\delta^{13}C_{DIC}$ for groundwater (-16‰ to -11‰, Vogel and Ehhalt, 1963). No clear trend was detected between carbon concentration and isotopic composition (Fig. 2.6), making it difficult to study the role of organic matter oxidation in the denitrification processes.

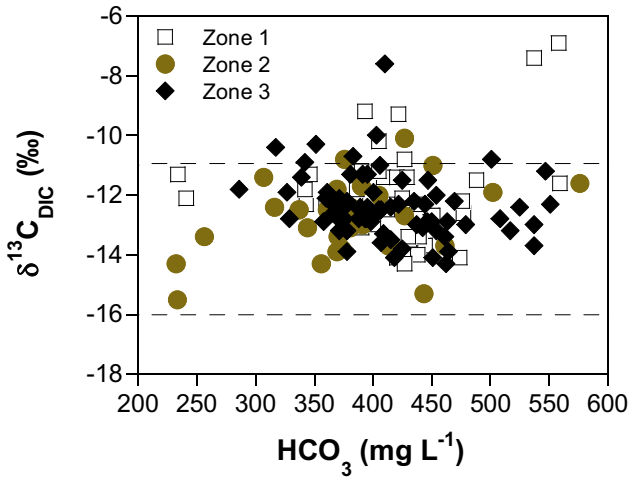

Figure 2.6. HCO_3^- concentration vs. $\delta^{13}C$ of the studied samples. The usual range of $\delta^{13}C_{DIC}$ in groundwater (Vogel and Ehhalt, 1963) is also represented (dotted lines).

2.3.3 Spatial variations of denitrification processes

The highest nitrate contents were detected in Zone 3, where the main crop fields are located and, consequently, where manure application is higher. In the recharge areas (Zones 1 and 2), manure application is less intensive, resulting in lower nitrate concentration in groundwater. The evidence of denitrification and the reactions involved in the denitrification processes were studied for each area, coupling chemical with isotopic data.

In a $\delta^{15}N$ vs. $\delta^{18}O_{NO3}$ diagram (Fig. 2.3b), samples of Zone 1 follow a $\varepsilon N/\varepsilon O$ ratio of 1.7 (r^2=0.73), indicating that denitrification is taking place. About 33% of the samples (16 samples) can be considered clearly denitrified ($\delta^{15}N$ > +15‰ and $\delta^{18}O$ > +5‰). In the $\delta^{34}S$ vs. $\delta^{18}O_{SO4}$ diagram (Fig. 2.4b), all samples, except TOR-004, are in a mixing line between manure sulfate and sulfate from sulfide oxidation, demonstrating the role of pyrite in denitrification. TOR-004 can be explained by a ternary mix between sulfate from gypsum, sulfate from fertilizers and sulfate from pig manure. Moreover, in a $\delta^{15}N_{NO3}$ vs. $\delta^{34}S_{SO4}$

diagram (Fig. 2.5), all the samples considered as clearly denitrified ($\delta^{15}N > +15‰$) had low $\delta^{34}S$ (ranging from -3.7‰ to -18.4‰), confirming that denitrification took place through pyrite oxidation. Negative $\delta^{34}S$ did not necessarily imply high $\delta^{15}N$ since sulfide oxidation could take place by consuming the O_2, and not be related to denitrification (e.g. sample TOR-002). No clear relation was observed between HCO_3^- and either $\delta^{15}N_{NO3}$ or $\delta^{18}O_{NO3}$ (data not shown), making it difficult to study the role of organic matter oxidation in denitrification.

In Zone 2, there was a linear correlation between $\delta^{15}N$ and $\delta^{18}O_{NO3}$, pointing out the occurrence of denitrification processes (Fig. 2.3b), except for sample SJV-004 that had higher $\delta^{18}O_{NO3}$ values. However, only two samples (SEB-015 and SEB-018) can be considered clearly denitrified ($\delta^{15}N_{NO3} > +15‰$ and $\delta^{18}O_{NO3} > +5‰$). Therefore, in this zone denitrification processes are not widespread and only local points show clear signs of denitrification.

In the samples of Zone 3, $\delta^{15}N_{NO3}$ showed a positive correlation ($r^2 = 0.65$) with $\delta^{18}O_{NO3}$, with a slope of 0.51, giving a $\varepsilon N/\varepsilon O$ ratio of 2.0, indicating the occurrence of denitrification processes (Fig. 2.3b). About 24% of these samples can be considered to be clearly denitrified ($\delta^{15}N_{NO3} > +15‰$ and $\delta^{18}O_{NO3} > +5‰$). In denitrification processes, a linear relationship is expected when plotting $\delta^{15}N$ or $\delta^{18}O_{NO3}$ vs. ln $[NO_3^-]$ (Mariotti et al., 1981; Böttcher et al., 1990; Fukada et al., 2003). In the studied case, due to the continuous nitrate inputs, the initial concentration and isotopic composition of percolated water in the recharge areas could differ depending on volatilization processes and rates of application. However, by using the NO_3^-/Cl^- ratio the effects of continuous nitrogen inputs could be averted. A positive correlation is observed between ln (NO_3^-/Cl^-) and both $\delta^{15}N$ (Fig. 2.7a) and $\delta^{18}O_{NO3}$ (data not shown), with correlation coefficients of 0.44 and 0.41, respectively, confirming the occurrence of denitrification processes.

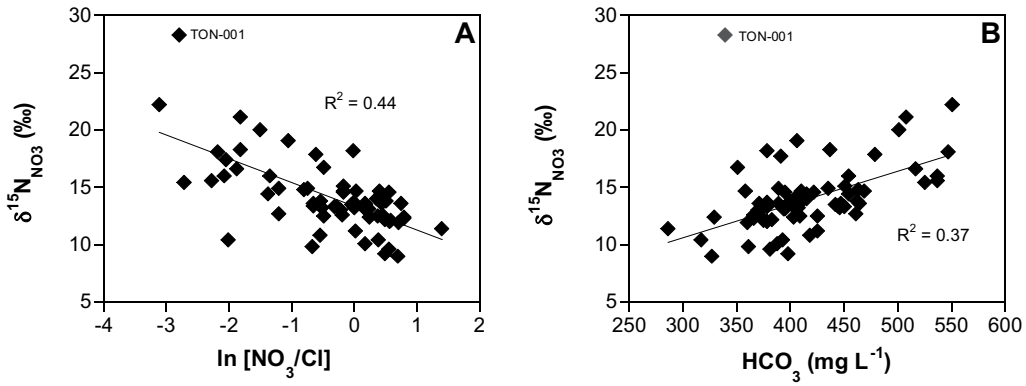

Figure 2.7. Samples from Zone 3. (a) ln (NO_3^-/Cl^-) vs. $\delta^{15}N_{NO3}$. (b) HCO_3^- concentration vs. $\delta^{15}N_{NO3}$.

In a $\delta^{15}N_{NO3}$ vs. $\delta^{34}S_{SO4}$ diagram (Fig. 2.5), several of the samples of the Zone 3 considered to be clearly denitrified ($\delta^{15}N$ > +15‰) had low $\delta^{34}S$ values, indicating a link between sulfide oxidation and denitrification. The sulfur isotopic signal of those samples clearly denitrified, but with $\delta^{34}S_{SO4}$ higher than -5‰, can be explained by the influence of the gypsum sulfate signature, as is confirmed in Fig. 2.4b, where samples from Zone 3 fall in the mixing field between sulfate from sulfide oxidation, sulfate from pig manure and sulfate from gypsum. The role of organic matter oxidation could neither be confirmed nor discarded. A positive trend between HCO_3- concentration and both $\delta^{15}N_{NO3}$ (r^2=0.37; Fig. 2.7b) and $\delta^{18}O_{NO3}$ (r^2=0.38; data not shown) was observed, except for TON-001, suggesting an increase in HCO_3^- concentration due to denitrification by organic matter oxidation. On the other hand, a negative trend between $\delta^{34}S$ and the HCO_3^- concentration was also detected (data not shown). Aravena and Robertson (1998) proposed that if denitrification by pyrite oxidation occurs, the acidity generated in the reaction tends to dissolve carbonates producing an increase in HCO_3^- concentration. Therefore, the HCO_3^- increase could also be related to pyrite oxidation. As there was no clear correlation between $\delta^{13}C_{DIC}$ and the HCO_3^- concentration (data not shown), the two hypotheses are thus possible.

2.3.4 Temporal variability of denitrification processes

To study the temporal evolution of denitrification processes, multipiezometer wells and/or wells located along a groundwater flow line have been used (Mariotti et al., 1988; Böttcher et al., 1990; Postma et al., 1991; Aravena et al., 1993; Aravena and Robertson, 1998).

Considering that in the studied area production wells do not coincide with a specific groundwater flow direction and that the lack of well casing causes the simultaneous exploitation of different aquifer layers, the temporal evolution of denitrification processes in the Osona area was studied using the temporal variations of chemical and isotopic composition of each individual well. Moreover, it is necessary to take into account that the isotopic and chemical composition of a sample reflects the balance between the entry of new nitrate, and the occurrence of denitrification and mixing processes.

No significant changes in $\delta^{15}N_{NO3}$ values along the studied period were observed in 75% of the studied samples. However, in some of the samples it was possible to identify temporal changes in the isotopic and chemical compositions. Taking into account these temporal variations, four groups were distinguished:

- 40% of the samples showed no significant changes in nitrate concentration or isotopic composition.

- 32% of the samples showed a significant increase in nitrate concentration but with no changes in the isotopic composition. This means additional nitrate inputs in the system, with a similar isotopic composition, thus producing no changes in the groundwater isotopic values. All of these samples had $\delta^{15}N_{NO3}$ in the range of manure nitrate (from +10‰ to +15‰).

- Samples MNL0-19, SMC-010, GRB-106, TON-001, TON-008, VIC-103 and VIC-004 increased their nitrate content between April 2005 and May 2006, although $\delta^{15}N$ of

dissolved nitrate decreased (see Appendix B). Starting values in April 2005 were in the range of denitrification ($\delta^{15}N_{NO3}$ > +15‰). A decrease in $\delta^{15}N_{NO3}$ indicated that the entry of new nitrate was more important than the reduction of nitrate by denitrification processes.

- Samples LMV-005, ORI-001, MAL-001, SEB-015 and SEB-017 showed a $\delta^{15}N_{NO3}$ and $\delta^{18}O_{NO3}$ increase, coupled to a decrease in the $\delta^{34}S$ of dissolved sulfate between April 2005 and October 2005 (see Appendix B). Moreover, these samples had $\delta^{15}N_{NO3}$ and $\delta^{18}O_{NO3}$ values indicating clear denitrification. Denitrification processes related to pyrite oxidation predominated, causing a decrease in the nitrate content and an increase in the concentration of dissolved sulfate.

2.3.5 Estimation of the enrichment factors related to denitrification

The denitrification reaction describes a Rayleigh distillation process (Eq. 2.7 and 2.8), where ε is the isotopic enrichment factor that depends on the aquifer materials and characteristics (Mariotti et al., 1981).

$$\delta^{15}N_{residual} = \delta^{15}N_{initial} + \varepsilon_N \ln\left(\left[NO_3^-\right]_{residual}/\left[NO_3^-\right]_{initial}\right) \quad (2.7)$$

$$\delta^{18}O_{residual} = \delta^{18}O_{initial} + \varepsilon_O \ln\left(\left[NO_3^-\right]_{residual}/\left[NO_3^-\right]_{initial}\right) \quad (2.8)$$

According to these equations, the $\delta^{15}N$ and $\delta^{18}O$ of the dissolved nitrate increase proportionately to the logarithm of the residual nitrate fraction. An estimation of the enrichment factors was performed using Eq. 2.7 and 2.8 in those samples in which, between April 2005 and October 2005, denitrification processes related to pyrite oxidation predominated, causing increases in both $\delta^{15}N$ and $\delta^{18}O$ of nitrate and in dissolved sulfate concentration, and decreases in $\delta^{34}S_{SO4}$ and in nitrate content (LMV-005, ORI-001, MAL-001, SEB-015 and SEB-017). The estimated enrichment factors are detailed in Table 2.2. The enrichment factors for nitrogen (between -4.4‰ and -15.5‰, with a median value of -7.0‰) fall well within the range of values reported for denitrification in groundwater

(-4.0‰ for Pauwels et al., 2000; -4.7‰ for Mariotti et al., 1988; -10.0‰ for Spalding and Parrott, 1994; -15.9‰ for Böttcher et al., 1990; and -30.0‰ for Vogel et al., 1981). Only three values of εO have been found in the literature: -8.0‰ (Böttcher et al., 1990), -9.8‰ (Fukada et al., 2003), and -18.3‰ (Mengis et al., 1999). The εO values estimated for the Osona aquifer range between -8.9‰ and -1.9‰, with a median value of -4.6‰. The εN/εO ratio ranges between 0.9 and 2.3, which is also in agreement with literature values: from 1.3 (Fukada et al., 2003) to 2.1 (Böttcher et al., 1990).

Sample	$\delta^{15}N_{NO3}$ (‰)		$\delta^{18}O_{NO3}$ (‰)		NO_3 (mg L^{-1})		εN (‰)	εO (‰)
	April 2005	October 2005	April 2005	October 2005	April 2005	October 2005		
LMV005	21.6	24.4	8.5	11.4	116.0	77.7	-7.0	-7.4
MAL001	14.8	21.1	6.3	10.7	118.4	46.0	-6.7	-4.6
SEB015	13.9	18.8	3.9	6.0	178.4	58.5	-4.4	-1.9
SEB017	13.2	20.0	4.5	8.5	156.2	64.4	-7.7	-4.5
ORI001	13.4	17.0	3.6	5.6	63.0	50.0	-15.5	-8.9

Table 2.2. Estimation of the enrichment factors for N and O associated with the natural denitrification processes.

Once the enrichment factor in a determined area is well characterized, the percentage of denitrification can be estimated on the basis of isotopic characterization (Eq. 2.9), using either εN or εO, or both.

$$DEN(\%) = \left[1 - \frac{[NO_3]_{residual}}{[NO_3]_{initial}}\right] \times 100 = \left[1 - e^{\left(\frac{\delta_{(residual)} - \delta_{(initial)}}{\varepsilon}\right)}\right] \times 100 \qquad (2.9)$$

In the studied area, using the median values of the obtained enrichment factors for nitrogen and oxygen (-7.0‰ and -4.6‰, respectively, *n*=5), a rough estimation of the degree of attenuation can be calculated, following Eq. 2.9. An initial isotopic composition of $\delta^{15}N_{NO3}$ = +15‰ and $\delta^{18}O_{NO3}$ = +5‰ was assumed and the isotopic data of the studied wells was used as the composition of the residual nitrate. In that way, 75% of the samples had isotopic values in the range of manure. These samples were not considered to be clearly denitrified and, consequently, were discarded for the calculations.

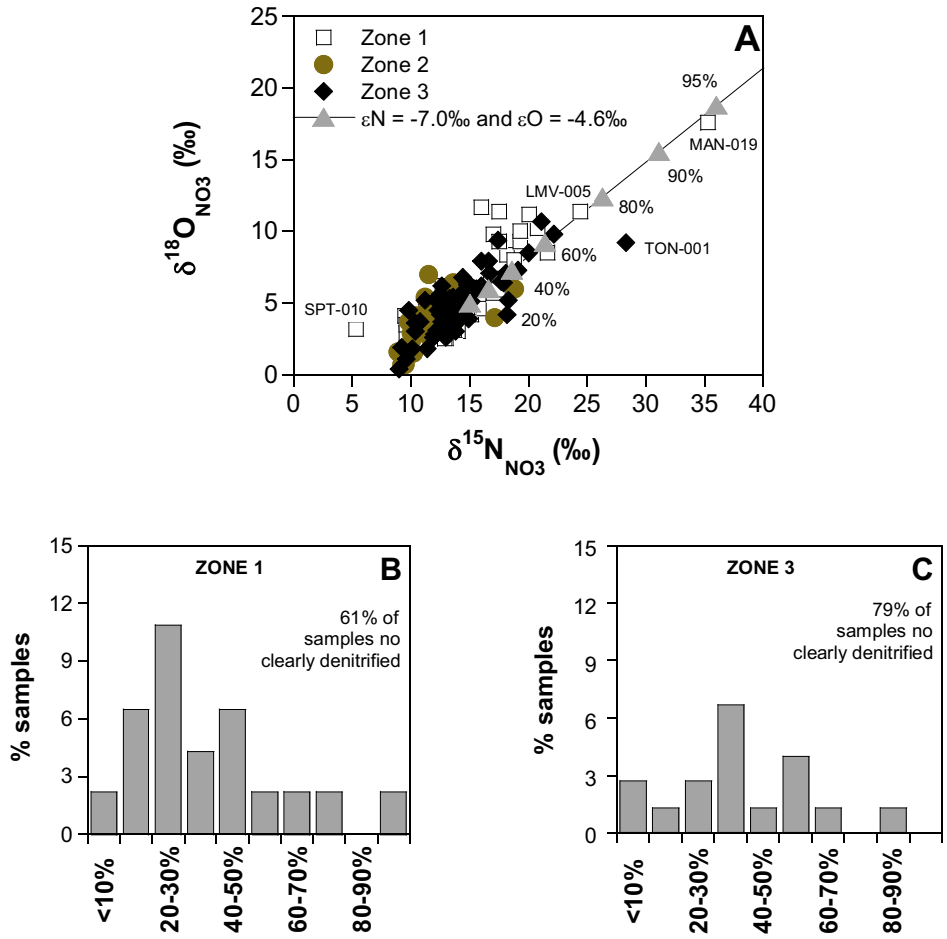

Figure 2.8. (a) Estimation of the percentage of natural denitrification taking place in the studied area, quantified in terms of the estimated isotope enrichment factors (median values of calculated εO and εN are used). Histograms of the percentage of denitrification, calculated using the εN, of samples from Zone 1 (b) and Zone 3 (c).

Based on both εN and εO, the natural attenuation in the remaining 25% of the studied samples varied between 0 and 60%, except for three samples (TON-001, MNL-019, and LMV-005) with denitrification higher than 75% (Fig. 2.8a). Using the estimated enrichment factor for nitrogen, in those samples considered clearly denitrified, the median denitrification (Eq. 2.9) was found to be 33% (n=38), and using εO, the median percentage of denitrification was found to be 25% (n=60). Figures 2.8b and 2.8c show the

histograms of the percentages of denitrification, calculated using the εN of samples from Zones 1 and 3, respectively.

Obtaining real enrichment factors of the aquifer in further laboratory experiments will allow us to quantify a more realistic degree of natural attenuation of nitrate contaminated groundwater in the studied area.

2.4 Conclusions

A multi-isotopic approach has successfully traced the sources of contamination and the processes affecting nitrate attenuation in groundwater in an area such as Osona, with complex and/or poorly studied hydrodynamics, where sampling relies on production wells and with a lack of an adequate infrastructure to monitor the fate of contaminants. Previous results obtained in a smaller area were confirmed, that is, that nitrate pollution in the Osona area is mainly derived from the application of pig manure as organic fertilizer and that the use of synthetic fertilizers has a minimum contribution. The occurrence of denitrification processes in groundwater was linked to pyrite oxidation, as demonstrated by coupling nitrate with sulfate isotopic data.

The relative roles of organic matter and pyrite in natural nitrate attenuation are different according to the distinct hydrogeological settings of the studied area. In that way, in Zone 1 denitrification by sulfide oxidation occurred in one third of the studied samples. In Zone 2, most of the $\delta^{15}N_{NO3}$ and $\delta^{18}O_{NO3}$ values were within the field of manure, and the occurrence of denitrification processes was limited to two samples. In Zone 3, denitrification by sulfide oxidation took place in 24% of the samples and, although some relationships suggested that the oxidation of organic matter could also contribute to denitrification, its role is still unclear.

About 25% of the samples showed a clear denitrification trend throughout the period under study. The nitrogen and oxygen isotopic enrichment factors were estimated using observed temporal variations of nitrate concentration and isotopic composition (εN= -7.0‰ and εO= -4.6‰). An approximation to the extent of natural attenuation was calculated, showing a median value between 25% and 33%, although further laboratory work will be required to obtain more realistic enrichment factors for the aquifer. Further work should focus on the study of the kinetics of denitrification by pyrite oxidation. It should also evaluate the potential of the addition of pyrite as a bioremediation strategy and point out distinct areas in which these bioremediation actions could be used to improve groundwater quality.

Part II:

Denitrification with pyrite as bioremediation strategy

Chapter 3

Denitrification of groundwater with pyrite and *Thiobacillus denitrificans*

Groundwater contamination by nitrate usually originates from anthropogenic sources, mainly as a result of wastewater discharges and the intensive application of fertilizers and animal manure to agricultural land. It is not unusual for groundwater nitrate concentration to exceed the nominal limit of 50 mg L^{-1} set by the 98/83/EC European Union Council Directive.

Nitrate removal is necessary to prevent public-health and environmental impacts. The most significant natural attenuation process is denitrification, i.e. the reduction of nitrate to dinitrogen gas by anaerobic facultative bacteria (and a few archaea) that utilize nitrate as the electron acceptor (Knowles, 1982; Zumft, 1997).

Note: This chapter is based on the article: Torrentó, C., Cama, J., Urmeneta, J., Otero, N. and Soler, A. Denitrification of groundwater with pyrite and *Thiobacillus denitrificans* (submitted to *Chemical Geology*)

Bacteria that are capable of denitrification are ubiquitous with the result that denitrification occurs throughout terrestrial, freshwater, and marine systems where the following conditions arise simultaneously: (1) nitrate and electron donor availability, (2) low oxygen concentrations (dissolved oxygen concentrations less than around 1-2 mg L^{-1}, e.g. Korom, 1992; Cey et al., 1999), and (3) favorable environmental conditions (temperature, pH, other nutrients and trace elements). Denitrifying bacteria are generally heterotrophic and use organic matter as the electron donor. Nevertheless, a limited number of bacteria are capable of carrying out chemolithotrophic denitrification and of using inorganic compounds such as reduced sulfur compounds, hydrogen, ferrous iron or uranium (IV) as electron donors, and inorganic carbon (CO_2 or HCO_3) as the carbon source for cell material synthesis (Straub et al., 1996; Zumft, 1997; Beller, 2005). The obligate chemolithoautotrophic bacterium *Thiobacillus denitrificans* is well known for its ability to couple the oxidation of various sulfur and reduced iron compounds to denitrification (Beller et al., 2006).

Results of chapter 2 and results of other field studies suggest that the occurrence of natural denitrification in some aquifers is coupled to oxidation of pyrite based on geochemical and/or isotopic data (Postma et al., 1991; Le Bideau and Dudoignon, 1996; Aravena and Robertson, 1998; Cravotta, 1998; Pauwels et al., 1998; 2000; 2010; Beller et al., 2004; Schwientek et al., 2008; Zhang et al., 2009a).

Denitrification by pyrite oxidation is expressed as:

$$14NO_3^- + 5FeS_2 + 4H^+ \Rightarrow 7N_2 + 10SO_4^{2-} + 5Fe^{2+} + 2H_2O \qquad (3.1)$$

If the Fe^{2+} produced is oxidized:

$$NO_3^- + 5Fe^{2+} + 6H^+ \Rightarrow \frac{1}{2}N_2 + 5Fe^{3+} + 3H_2O \qquad (3.2)$$

an overall reaction where denitrification mediated by pyrite oxidation occurs is expressed as:

$$15NO_3^- + 5FeS_2 + 10H_2O \Rightarrow \frac{15}{2}N_2 + 10SO_4^{2-} + 5Fe(OH)_3 + 5H^+ \qquad (3.3)$$

Our interest is to characterize this pyrite-driven denitrification reaction and assess its feasibility. Although much work has been devoted to enhancing autotrophic denitrification by adding several inorganic electron donors, such as zero-valent iron, ferrous ions, elemental sulfur, and iron bearing materials (Postma, 1990; Straub et al., 1996; Benz et al., 1998; Hansen et al., 2001; Weber et al., 2001; Soares, 2002; Choe et al., 2004; Sierra-Alvarez et al., 2007), fewer studies have been carried out in nitrate reduction by pyrite and other sulfide minerals (Devlin et al., 2000; Schippers and Jorgensen, 2002; Haaijer et al., 2007; Jorgensen et al., 2009). In these studies, the role of pyrite as electron donor has been questioned, and only in Jorgensen et al. (2009) has been denitrification coupled to pyrite oxidation satisfactorily accomplished. These authors performed pyrite-amended batch experiments with sediment from a sandy aquifer and demonstrated that addition of pyrite increased nitrate reduction rates. However, little is still known about the kinetics, the limiting factors and the involvement of *T. denitrificans*-like bacteria in this reaction.

Therefore, the first goal of this chapter is to determine, clarify and quantify the role of pyrite as an electron donor in the bacterial mediated denitrification process in order to assess its feasibility for nitrate remediation in contaminated groundwater.

In addition, N and O isotope fractionation has been qualitatively used to indicate natural bacterially mediated nitrate reduction in contaminated aquifers (see chapter 2). However, to quantify field denitrification, the enrichment factor (ε) must be determined with reasonable accuracy. N and O enrichment factors have been determined in groundwater field studies (see chapter 2, e.g. Böttcher et al., 1990; Mengis et al., 1999; Fukada et al., 2003) and in laboratory pure culture experiments with denitrifying cultures

(Wellman et al., 1968; Delwiche and Steyn, 1970; Barford et al., 1999). The latter studies are extremely useful because they provide a basis for the interpretation of field data, highlighting the magnitude of fractionation that could occur in different groups of microorganisms under specific biogeochemical conditions. These laboratory estimations of N and O isotope fractionation have been performed with pure cultures of heterotrophic denitrifying bacteria. To our knowledge, isotope fractionation during autotrophic denitrification in laboratory cultures has not been reported to date.

Therefore, the second goal of this chapter is to characterize nitrogen and oxygen isotope fractionation for pyrite-driven denitrification by *T. denitrificans* in order to evaluate the magnitude of the isotopic fractionation expected in nitrate-contaminated aquifers.

To this end, two types of experiments with powdered pyrite were performed: (1) batch experiments inoculated with pure culture of *T. denitrificans* to study the overall reaction and determine isotope fractionation and (2) long-term flow-through experiments to characterize the denitrification process under conditions simulating a natural aquifer environment.

3.1 Experimental section

3.1.1 Pyrite characterization and preparation

Samples of pyrite were from Navajún (batch experiments) and from Cerdanya (flow-through experiments). Powder X-ray diffraction of the samples was determined using a Bruker D5005 diffractometer with Cu Kα radiation over a 2θ range from 0 to 60 degrees with a scan speed of 0.025°/18 s. The X-ray patterns confirmed the samples to be pyrite.

Pyrite samples were crushed and sieved to obtain two particle sizes, one ranging from 25 to 50 μm and the other from 50 to 100 μm. The samples used in two blank (TD-blank-21 and TD-blank-22, Table 3.1) and in two pyrite-amended batch experiments (TD-

13 and TD-14, Table 3.2) were washed with 6 M HCl solution for 5 min and then rinsed with Milli-Q pure water three times before the start of the experiments to remove microparticles and possible iron and sulfur impurities on the pyrite surface. Specific surface areas were determined by the BET gas adsorption method with a Micromeritics ASAP 2000 surface area analyzer, using 5-point N_2 adsorption isotherms (Brunauer et al., 1938). Initial surface areas for 25-50 μm particles were 0.59±0.06 $m^2\ g^{-1}$ for the Navajún pyrite and 0.88±0.09 $m^2\ g^{-1}$ for the Cerdanya pyrite. Surface areas for 50-100 μm particles were 0.43±0.04 $m^2\ g^{-1}$ and 0.62±0.06 $m^2\ g^{-1}$, respectively. After the experiments, BET specific surface area of reacted samples was also measured (see Tables 3.1-3.4).

Pyrite powders for use in batch and inoculated flow-through experiments were sterilized by autoclaving at 121°C for 15 min previously to use in the experiments.

X-ray Photoelectron spectra (XPS) of initial and reacted samples were recorded with a Physical Electronics (PHI) 5500 spectrometer using a monochromatic X-ray source with an Al Kα line of 1486.6 eV energy, and operated at 350 W. The energy scale was calibrated using the $3d_{5/2}$ line for Ag with a width of 0.8 eV and a binding energy of 368.3 eV. All binding energies were corrected by adjusting the C1s peak (corresponding to contamination from hydrocarbons) to a binding energy of 284.6 eV. Atomic concentrations of iron and sulfur were determined from the XPS areas subsequent to the Shirley background subtraction divided by atomic sensitivity factors (Wagner, 1983).

3.1.2 Culture preparation

Thiobacillus denitrificans (strain 12475 from German Collection of Microorganisms and Cell Cultures, DSMZ) was cultured with thiosulfate in an anaerobic (pH 6.8) nutrient medium specially designed for *T. denitrificans*, following Beller (2005). The medium consists of a mixed solution of $Na_2S_2O_3{\cdot}5H_2O$ (20 mM), NH_4Cl (18.7 mM), KNO_3 (20 mM), KH_2PO_4 (14.7 mM), $NaHCO_3$ (30 mM), $MgSO_4{\cdot}7H_2O$ (3.25 mM), $FeSO_4{\cdot}7H2O$ (0.08 mM), $CaCl_2{\cdot}2H_2O$ (0.05 mM) and sterile vitamin, trace element and selenate-tungstate solutions (stock solutions 1, 4, 6, 7 and 8 of Widdel and Bak, 1992). Cultures were maintained under

anaerobic conditions at 30°C and unshaken. Thereafter, the culture was harvested by centrifugation, washed, and resuspended in a sterile saline solution (Ringer 1/4 solution) immediately before the start of the experiments.

3.1.3 Experimental set-up

All the experiments were performed under anaerobic conditions in a sterilized and anaerobic glove box with a nominal gas composition of 90% N_2 and 10% CO_2 at 28±2 °C. Experimental oxygen partial pressure in the glove box was maintained between 0.1 and 0.3% O_2(g), being continuously monitored by an oxygen partial pressure detector with an accuracy of ±0.1% O_2(g). Input solutions were introduced into the glove box at least 12 h before the start of the experiments to allow equilibration with the anaerobic atmosphere and were sparged with N_2 for 15 min before the start of the experiments. The solutions to be autoclaved were degassed before the sterilization. All the experiments were set up with nitrate as the electron acceptor and pyrite as the sole electron donor. Pyrite was added in stoichiometric excess with respect to added nitrate.

Three types of batch experiments were performed: control experiments (Table 3.1), *T. denitrificans*-inoculated experiments amended with pyrite (Table 3.2), and experiments designed to calculate isotope fractionation (Table 3.3).

Two groups of independent control experiments were performed (Table 3.1): (1) pyrite-free experiments (both inoculated and non-inoculated), and (2) blank experiments with pyrite.

Pyrite-amended batch experiments were performed to confirm the occurrence of pyrite-driven nitrate reduction and to evaluate the nitrate removal rate by *T. denitrificans* (Table 3.2.). Two groups of experiments were conducted with two different sizes of pyrite particles (25-50 and 50-100 μm). Each group included three different initial cell densities (approx. 10^5, 10^7 or 10^8 cells mL^{-1}). For each cell density, three different initial nitrate concentrations (approx. 1, 2.5 or 4 mM) were used. Each experiment performed with

approximately 10^8 cells mL^{-1} was repeated 3-4 times in order to assess the reproducibility of the results (Table 3.2).

experiment	inoculum	grain size	initial nitrate	final nitrate (1)	final BET	sulfate produced (2)
	cells mL^{-1}	μm	mM	mM	m^2 g^{-1}	mM
Pyrite-free experiments						
TD-control-10	~10^7	-	4.46	4.50	-	-
TD-control-9	~10^7	-	4.37	4.31	-	-
TD-control-15	~10^7	-	4.31	4.29	-	-
TD-control-11	~10^5	-	4.58	4.57	-	-
TD-control-12	~10^5	-	4.57	4.31	-	-
TD-control-16	~10^7	-	3.76	3.34	-	-
TD-control-17	-	-	5.14	4.98	-	-
TD-control-13	-	-	4.75	4.84	-	-
TD-control-14	-	-	4.75	4.83	-	-
TD-control-18	-	-	4.40	4.19	-	-
TD-control-7	-	-	4.24	4.21	-	-
TD-control-8	-	-	3.78	4.09	-	-
Blank experiments						
TD-blank17	-	50-100	5.08	5.15	0.61	0.25
TD-blank23	-	50-100	4.97	5.02	0.27	0.69
TD-blank16	-	50-100	4.92	5.16	0.40	3.17
TD-blank24	-	50-100	4.54	4.54	0.22	0.53
TD-blank8	-	50-100	4.31	4.36	0.79	1.45
TD-blank10	-	50-100	2.90	2.69	0.53	1.38
TD-blank11	-	50-100	2.71	2.74	0.91	1.95
TD-blank12	-	50-100	2.71	2.79	0.52	2.00
TD-blank9	-	50-100	2.58	2.75	0.55	1.25
TD-blank13	-	50-100	1.08	0.94	0.64	3.26
TD-blank22 (3)	-	25-50	5.15	5.12	1.89	0.43
TD-blank21 (3)	-	25-50	5.06	5.08	0.78	0.25
TD-blank19	-	25-50	5.04	5.05	1.05	0.56
TD-blank18	-	25-50	3.52	3.62	1.10	0.82
TD-blank15	-	25-50	1.52	1.43	1.46	4.93
TD-blank14	-	25-50	0.99	1.08	1.85	0.70

(1) After 60 d in pyrite-free experiments and in blank experiments with 50-100 μm pyrite and after 14 d in blank experiments with 25-50 μm pyrite

(2) From time 0 to 60 d (50-100 μm pyrite) or from 0 to 14 d (25-50 μm pyrite)

(3) Pyrite samples were previously washed with 6M HCl

Table 3.1. Experimental conditions and results of the control batch experiments.

variable	exp.	initial nitrate	final nitrate [1]	final BET	overall NO_3^- removal [1]	NO_3^- reduction rate		sulfate produced [3]	NO_3/SO_4 ratio [4]
		mM	mM	$m^2\ g^{-1}$	%	mmol NO_3^- $kg^{-1}\ d^{-1}$	σ_{rate} [2]	mM	
50-100 μm									
~10^8 cells mL^{-1}									
~4 mM NO_3^-	**TD-1a**	3.89	1.26	0.65	68	0.18	0.06	6.75	0.4
	TD-1b	3.89	1.49	0.67	62	0.22	0.02	1.97	1.2
	TD-1c	3.76	0.90	0.81	76	0.25	0.02	1.73	1.7
	mean ± SD	3.85±0.08	1.22±0.30	0.71±0.09	69±7	0.22±0.03		3.48±2.83	1.1±0.7
~2.5 mM NO_3^-	**TD-2a**	2.51	0.00	0.47	100	0.20	0.02	2.79	0.9
	TD-2b	2.48	0.00	0.79	100	0.19	0.03	2.94	0.8
	TD-2c	2.18	0.00	0.66	100	0.18	0.02	2.43	0.9
	mean ± SD	2.39±0.18	0.00	0.64±0.17	100	0.19±0.01		2.72±0.26	0.9±0.0
~1 mM NO_3^-	**TD-3a**	0.94	0.00	0.64	100	0.47 [5]	-	0.81	1.2
	TD-3b	0.80	0.00	0.72	100	0.40 [5]	-	1.88	0.4
	TD-3c	0.90	0.00	0.56	100	0.45 [5]	-	2.18	0.4
	TD-3d	0.69	0.00	0.74	100	0.35 [5]	-	2.05	0.3
	mean ± SD	0.83±0.11	0.00	0.67±0.09	100	0.42±0.06		1.73±0.62	0.6±0.4
~10^7 cells mL^{-1}									
~4 mM NO_3^-	**TD-4**	4.38	1.17 [6]	1.15	73 [6]	0.76	0.15	1.89	1.7
	TD-5	3.82	2.50	0.53	35	0.12	0.02	2.84	0.5
~1 mM NO_3^-	**TD-6**	1.06	0.00	1.12	100	1.23 [5]	-	1.19	0.9
	TD-7	0.66	0.00	1.04	100	0.81 [5]	-	0.41	1.6
~10^5 cells mL^{-1}									
~4 mM NO_3^-	**TD-8**	4.44	3.64 [6]	0.45	19 [6]	0.09	0.02	0.95	0.8
	TD-9	3.71	2.09	0.45	44	0.38	0.11	4.24	0.4
25-50 μm									
~10^8 cells mL^{-1}									
~4 mM NO_3^-	**TD-10**	4.76	0.00	1.27	100	2.28 [5]	-	3.98	1.2
~2.5 mM NO_3^-	**TD-11**	2.85	0.00	1.34	100	1.43 [5]	-	2.76	1.0
~10^7 cells mL^{-1}									
~4 mM NO_3^-	**TD-12**	4.29	2.15	0.56	50	1.06	0.08	1.24	1.7
	TD-13 [7]	3.94	0.88	1.02	78	1.40	0.13	1.52	2.0
	TD-14 [7]	3.72	0.00	0.90	100	2.50	0.22	3.68	1.0
	TD-15	3.32	0.00	0.34	100	3.50	0.69	3.06	1.2
~2.5 mM NO_3^-	**TD-16**	2.79	0.00	0.36	100	3.16 [5]	-	2.13	1.3
~10^5 cells mL^{-1}									
~4 mM NO_3^-	**TD-17**	3.79	0.55	0.33	86	1.71	0.28	2.56	1.3
	TD-18	3.52	0.00	1.59	100	2.09	0.55	2.67	1.3

(1) After 60 d in experiments with 50-100 μm pyrite and after 14 d in experiments with 25-50 μm pyrite

(2) Standard deviation of the linear regression of nitrate concentration over time (Fig. 3.1)

(3) From 0 to 60 d (50-100 μm pyrite) or from 0 to 14 d (25-50 μm pyrite)

(4) Ratio between nitrate reduced and sulfate produced

(5) Apparent nitrate reduction rates. Complete nitrate removal was detected at first sampling

(6) After 25 d in experiment TD-4 and after 42 d in experiment TD-8

(7) Pyrite samples were previously washed with 6M HCl

Table 3.2. Experimental conditions and results of the pyrite-amended batch experiments inoculated with *T. denitrificans*.

50 mL polypropylene bottles were filled with 25 mL of pH 6.8-7.0 modified medium with the desired concentration of nitrate and sterilized pyrite powder with the desired grain size was added (5 g). The modified medium used in the batch experiments was the *T. denitrificans* nutrient medium without thiosulfate and iron, replacing sulfate salts by chloride salts: NH_4Cl (18.7 mM), KH_2PO_4 (14.7 mM), $NaHCO_3$ (30 mM), $MgCl_2{\cdot}6H_2O$ (3.25 mM) and $CaCl_2{\cdot}2H_2O$ (0.05 mM) and adding the desired NO_3^- concentration as KNO_3. Under these conditions, pyrite will be the only electron donor available for the cells.

Preliminary experiments showed that the initial pyrite-solution interaction caused a decrease in pH to below 6. This was likely due to dissolution of surface grinding-resulted microparticles and possible surficial S-impurities. This pH drop considerably diminished bacterial activity. Denitrification efficiency is very sensitive to pH and an optimum pH range for most denitrifying bacteria is 7-8 (Knowles, 1982). Therefore, after 24-42 h, the supernatant was eliminated and replaced by the fresh input solution. After 48 h, aqueous samples corresponding to time 0 were collected and flasks were inoculated with 1 mL of cell solution with the desired cell density.

To ensure that the possible presence of microparticles and/or oxidation products on the pyrite surface has no significant effect on the rate and efficiency of the reaction, two pyrite-amended experiments were performed with HCl-washed pyrite (TD-13 and TD-14, Table 3.2).

In the experiments designed to characterize nitrogen and oxygen isotope fractionation associated with the process (Table 3.3), the procedure was the same but using 250 mL glass Witeg bottles with 100 mL of solution and 20 g of pyrite; 4 mL of culture were inoculated into each flask.

Batch experiments were run for 14 d (25-50 μm pyrite) or for 60 d (50-100 μm pyrite and pyrite-free experiments), and aqueous samples were periodically taken using sterile syringes. The number of samples was limited to maintain the solid-solution ratio at < 30% of the initial value. Preliminary experiments helped to determine the duration of the

experiments and the frequency of aqueous sampling according to the rate of nitrate consumption.

exp.	grain size	initial nitrate	final nitrate (1)	final BET	overall NO_3^- removal (1)	NO_3^- reduction rate		sulfate produced (3)	NO_3/SO_4 ratio (3)
	μm	mM	mM	$m^2\ g^{-1}$	%	mmol NO_3^- $kg^{-1}\ d^{-1}$	σ_{rate} (2)	mM	
TD-20	50-100	4.61	2.20	0.31	52	0.19	0.03	0.87	2.8
TD-21	25-50	2.71	2.22	0.48	18	0.19	0.04	1.84	0.3

(1) After 60 d in experiment TD-20 and after 14 d in experiment TD-21
(2) Standard deviation of the linear regression of nitrate concentration over time (Fig. 3.1)
(3) From 0 to 60 d (TD-20) or from 0 to 14 d (TD-21)
(3) Ratio between nitrate reduced and sulfate produced

Table 3.3. Experimental conditions and results of the two pyrite-amended batch experiments inoculated with approximately 10^7 cells mL^{-1} *T. denitrificans* culture focusing in calculate isotope fractionation.

Flow-through experiments were performed to closely mimic aquifer conditions. By means of a peristaltic pump, input solutions were circulated through 50 mL polyethylene reactors in which 50-100 μm powdered pyrite (approx. 1 g) was placed. Three types of flow-through experiments were performed: inoculated, blank and non-inoculated (Table 3.4).

The *T. denitrificans* inoculated experiment was carried out to quantify the denitrification activity and to evaluate long-term behavior in pure cultures. Solution was circulated through the reactor after 15 d of inoculation (6.6×10^7 cells mL^{-1}), with a flow rate of approx. 0.003 mL min^{-1}, yielding a hydraulic retention time (HRT) of 11.6 d. Reactors, tubing, pyrite powder and solutions were sterilized before use in the sterilized blank and inoculated experiments.

The non-inoculated experiments, with non-sterilized pyrite powder, were performed to stimulate activity of indigenous bacteria. The flow rate ranged between 0.009 and 0.014 mL min^{-1}, yielding HRT of 2.3-3.9 d. These non-inoculated experiments were replicated to ensure the reproducibility of the results (Table 3.4).

Table 3.4. Experimental conditions and results of blank, inoculated and non-inoculated flow-through experiments.

experiment	nitrate input	HRT	nitrate loading rate	output pH	final BET	mass	max. nitrate reduced	max. nitrate removal	NO_3 reduction rate	S (s.s.)	Fe (s.s.)	NO_3/SO_4 ratio (1) (2)	% NO_3^- reduced due to py oxidation (2) (3)	comments
	mM	d	mmol NO_3^- L^{-1} d^{-1}		m^2 g^{-1}	g	mM	%	mmol NO_3^- kg^{-1} d^{-1}	µmol L^{-1}				
Blank experiment														
BLANK-PYR-1	0.43	3.1	0.14	7.2	0.50	0.79	-	-	-	1.58	b.d. l.	-		
Inoculated experiment														
IN-PYR-1	2.46	11.6	0.21	7.0	0.77	10.00	2.46	100	0.54	2.178	b.d. l.	24	6-10	Complete nitrate removal at 70 d. Lasted until the end (200 d)
Non-inoculated experiments														
NON-PYR-1	0.42	3.2	0.13	4.5	0.44	1.00	0.10	23	1.31	2.35	1.50	18	8-14	Maximum nitrate removal at 50 d. Nitrate reduction stopped at 75 d
NON-PYR-2	0.31	2.7	0.11	7.0	0.40	0.99	0.24	78	4.03	2.67	b.d. l.	40	5-7	Maximum nitrate removal at 175 d. Nitrate reduction stopped at 230 d. Nitrate removal restarted at 240 d and 94% of reduction at the end (370 d)
NON-PYR-3a	0.42	3.1	0.13	7.0	0.48	1.00	0.32	77	3.88	2.25	b.d. l.	18	12-17	Maximum nitrate removal at 35 d. Nitrate reduction stopped at 230 d
NON-PYR-3b	0.43	3.9	0.11	7.0	0.53	1.00	0.32	75	3.30	4.62	b.d. l.	23	10-14	Maximum nitrate removal at 40 d. Nitrate reduction stopped at 120 d
NON-PYR-3c	0.42	3.5	0.12	7.5	0.49	1.00	0.29	69	3.00	1.29	b.d. l.	17	14-18	Maximum nitrate removal at 40 d. Nitrate reduction stopped at 140 d. Nitrate removal restarted at 160 d and 60% at the end (250 d)
NON-PYR-3d	0.43	3.9	0.11	7.5	0.51	1.00	0.21	49	2.38	2.34	b.d. l.	10	18-28	Maximum nitrate removal at 20 d. Nitrate reduction stopped at 75 d. Nitrate removal restarted at 120 d and 60% at the end (240 d)
NON-PYR-3e	0.40	2.3	0.17	6.7	0.53	0.80	0.18	42	3.34	3.87	b.d. l.	59	4-5	Initial stage of 50 d with 1.1 mM NO_3^- input. Maximum nitrate removal at 85 d. Nitrate reduction stopped at 110 d
NON-PYR-3f	0.44	2.5	0.18	7.5	0.34	1.00	0.28	57	5.68	1.32	b.d. l.	>150	1-2	Initial stage of 65 d with pH 3 HCl input solution. Max. nitrate removal at 195 d. Nitrate reduction did not cease. 60% of reduction at the end (365 d)
NON-PYR-4a	0.46	3.4	0.14	7.3	0.50	0.99	0.26	51	2.57	2.00	b.d. l.	>150	1-2	Lag of 80 d before nitrate reduction started. Maximum nitrate removal at 160 d. Nitrate reduction did not cease
NON-PYR-4b	0.48	2.7	0.18	7.0	0.31	0.99	0.26	55	3.68	1.33	b.d. l.	>150	1	Initial stage of 200 d with 1.0 mM NO_3^- input. Maximum nitrate removal at 330 d. Nitrate reduction did not cease. 98% of reduction at the end (380 d)
NON-PYR-4c	0.49	2.9	0.17	7.4	0.29	1.00	0.40	81	4.85	1.56	b.d. l.	>150	1-2	Maximum nitrate removal at 160 d. Nitrate reduction did not cease
NON-PYR-4d	0.50	3.2	0.16	7.7	0.32	1.00	0.12	28	1.62	2.15	b.d. l.	>150		Initial stage of 65 d with 1.0 mM NO_3^- input. Maximum nitrate removal at 165 d. Nitrate reduction did not cease. 83% of reduction at the end (240 d)
NON-PYR-4e	0.53	2.7	0.20	7.4	4.68	0.79	0.32	66	5.42	4.62	b.d. l.	>150	1-3	Maximum nitrate removal at 130 d. Nitrate reduction did not cease. 98% of reduction at the end (335 d)
NON-PYR-5a	0.86	3.5	0.25	7.2	0.64	1.01	0.48	49	3.81	1.84	b.d. l.	79	2-4	Lag of 90 d before nitrate reduction started. Maximum nitrate removal at 195 d. Nitrate reduction did not cease
NON-PYR-5b	0.88	3.5	0.25	7.3	0.41	1.01	0.43	41	3.78	3.45	b.d. l.	77	2-4	Lag of 100 d before nitrate reduction started. Maximum nitrate removal at 195 d. Nitrate reduction did not cease
NON-PYR-6a	1.29	3.9	0.33	7.5	0.62	1.00	0.38	29	2.57	2.20	b.d. l.	86	3-4	Maximum nitrate removal at 90 d. Nitrate reduction stopped at 160 d
NON-PYR-6b	1.30	3.9	0.34	7.2	0.60	1.00	0.32	24	3.89	3.11	b.d. l.	43	5-7	Maximum nitrate removal at 85 d. Nitrate reduction stopped at 105 d
NON-PYR-7	1.72	3.5	0.50	7.0	0.34	1.00	0.31	18	4.45	3.36	b.d. l.	57	3-5	Maximum nitrate removal at 90 d. Nitrate reduction stopped at 120 d

b.d.l. = below detection limit (3.12 µmol L^{-1} S; 0.36 µmol L^{-1} Fe)

HRT= hydraulic retention time

s.s. = steady state

(1) Ratio between measured nitrate reduced and sulfate produced

(2) At time of maximum nitrate removal

(3) Based on the amount of nitrate reduced, sulfate and nitrite produced and the stoichiometry of the reactions Eq. 3.3-3.6

Input solutions in the blank and non-inoculated experiments consisted in $NaNO_3$ solutions with nitrate concentration between 0.1 and 2.6 mM, yielding nitrate loading rates from 0.11 to 0.50 mmol NO_3^- L^{-1} d^{-1}. In the inoculated experiment, the modified medium solution (see before) with 2.5 mM KNO_3 was used (nitrate loading rate of 0.21 mmol NO_3^- L^{-1} d^{-1}). In the two solutions, no other electron donor was added to ensure that pyrite was the only electron donor available for cells. In order to guarantee an optimal pH, pH of influent solutions was between 6.5 and 8. Nevertheless, one of the non-inoculated experiments (NON-PYR-1, Table 3.4) was carried out at pH 4.5 to confirm the fatal effect of pH on nitrate reduction.

Experimental runs lasted between 200 and 375 d and output solutions were collected periodically.

3.1.4 Analytical methods

Aliquots of aqueous samples were filtered through 0.22 μm syringe filters to measure pH, concentrations of cations, anions and, in some samples, $\delta^{15}N$ and $\delta^{18}O$ of dissolved nitrate. Samples were preserved in nitric acid to measure concentrations of total Fe, total S, Mg, Ca, Na, Cl, P, and K by inductively coupled plasma-atomic emission spectrometry (ICP-AES, Thermo Jarrel-Ash with CID detector and a Perkin Elmer Optima 3200 RL). The accuracy on the measurement of Mg, Ca, Na, Cl, P and K was estimated to be around 3%, whereas the accuracy on the measurement of Fe and S was estimated to be 25%, with detection limits of 0.36 and 3.12 μmol L^{-1}, respectively. Anion concentrations (nitrate, nitrite, chloride, and sulfate) were determined by High Performance Liquid Chromatography (HPLC), using an IC-Pack Anion column and borate/gluconate eluent with 12% of HPLC grade acetonitrile. The error associated with the measurements was estimated to be 5% for nitrate, chloride and sulfate and 10% for nitrite. The HPLC measurements for sulfate concentrations were concordant within ±5% with the sulfate concentrations calculated from ICP sulfur elemental data, assuming that concentrations of non-sulfate sulfur species (sulfides and sulfites) were negligible. Samples for

ammonium analysis were preserved acidified to pH<2 with H_2SO_4. Ammonium concentrations were measured using an Orion ammonium ion selective electrode with an analytical uncertainty of 10% and a detection limit of 0.01 mM. pH was measured with a calibrated Crison pH Meter at room temperature (22±2 °C). The pH error was 0.02 pH units.

Samples for N and O isotopes of nitrate were preserved in KOH (pH 11) solution and frozen prior to analysis. The $\delta^{15}N$ and $\delta^{18}O$ of dissolved nitrate were obtained following the denitrifier method (Sigman et al., 2001; Casciotti et al., 2002). Notation is expressed in terms of δ per mil relative to the international standards: V-SMOW (Vienna Standard Mean Oceanic Water) for $\delta^{18}O$, and AIR (Atmospheric N_2) for $\delta^{15}N$. The isotope ratios were calculated using international and internal laboratory standards and results had an accuracy of 0.2 ‰ for $\delta^{15}N$ and 0.5 ‰ for $\delta^{18}O$ of nitrate. Isotopic analyses were performed at the Woods Hole Oceanographic Institution.

3.2 Results and discussion

3.2.1 Nitrate reduction

In the control batch experiments, nitrate concentrations remained unchanged up to 60 d (Table 3.1).

Table 3.2 shows the experimental conditions and the results of the pyrite-amended, *T. denitrificans*-inoculated batch experiments. Specific data for each experiment are shown in Appendix C. Only in these experiments consumption of nitrate over time was observed (Fig. 3.1). The time needed to consume nitrate was dependent on the pyrite grain size and on the initial nitrate concentration. In most of the experiments with 25-50 μm pyrite, nitrate content was mostly consumed within 14 d (Fig. 3.1a). In cultures amended with 50-100 μm pyrite, the time needed to consume most nitrate was longer and decreased by lowering the initial nitrate concentration. With an initial concentration of approx. 4 mM NO_3^-, 35 to 80% of the nitrate content was consumed after 60 d; with

approx. 2.5 mM NO_3^-, nitrate was completely consumed within 60 d; and with approx. 1 mM of NO_3^-, complete consumption of nitrate occurred within 14 d (Fig. 3.1b). Figure 3.1c shows two examples of batch experiments carried out with 50-100 μm pyrite.

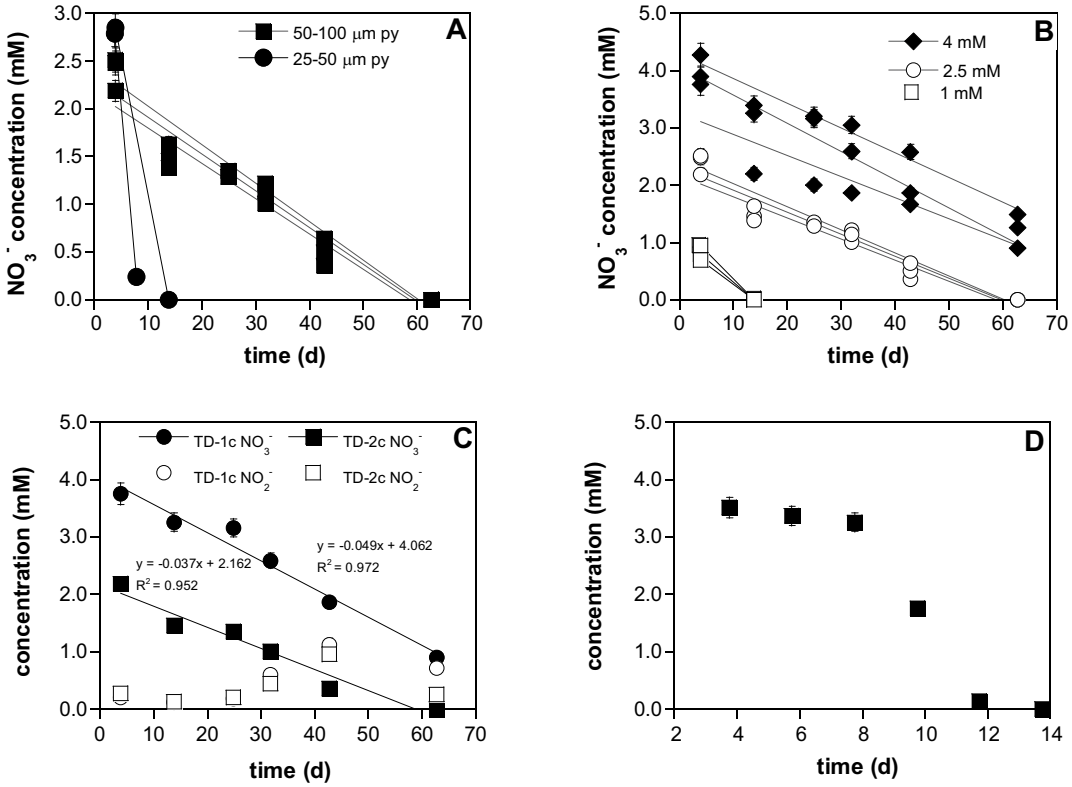

Figure 3.1. Variation of nitrate concentration over time in representative pyrite-amended batch experiments inoculated with *T. denitrificans*. (a) Consumption of nitrate over time in the experiments performed with approx. 2.5 mM NO_3^- solution; (b) Consumption of nitrate over time in the experiments amended with 50-100 μm pyrite and inoculated with approx. 10^8 cells mL^{-1}; (c) NO_3^- and NO_2^- concentration vs. time of experiments TD-1c and TD-2c; Solid lines represent the fitting of measured NO_3^- concentration versus time used to compute zero-order nitrate reduction rates. Determination coefficients (R^2) were ≥ 0.9 except in 2 experiments; (d) Variation of nitrate in the experiment TD-9, with cell density of approximately 10^5 cells mL^{-1}.

An initial stage of 7 d during which nitrate concentration barely decreased was observed with a low initial cell density (~10^5 cells mL^{-1}). An example is given in the Figure 3.1d. This occurred because a longer adaptation time was necessary for bacteria to grow into a population large enough to bring about a detectable change in nitrate

concentration. Nevertheless, the final percentages of reduced nitrate tended to resemble those of experiments with higher initial cell density (Table 3.2).

As regards the flow-through experiments, Table 3.4 shows the conditions and the results of the blank, inoculated and non-inoculated flow-through experiments. Specific data for each experiment are shown in Appendix C. Nitrate reduction occurred in all the non-inoculated and the inoculated experiments, but not in the blank experiment. In the *T. denitrificans*-inoculated experiment (with a nitrate loading rate of 0.21 mmol NO_3^- L^{-1} d^{-1}), partial nitrate removal occurred for 70 d (Fig. 3.2a). Subsequently, complete nitrate removal was achieved and lasted until the end of the experiment (200 d), indicating a high long-term efficiency of *T. denitrificans* in nitrate removal using pyrite as the electron donor under the study conditions.

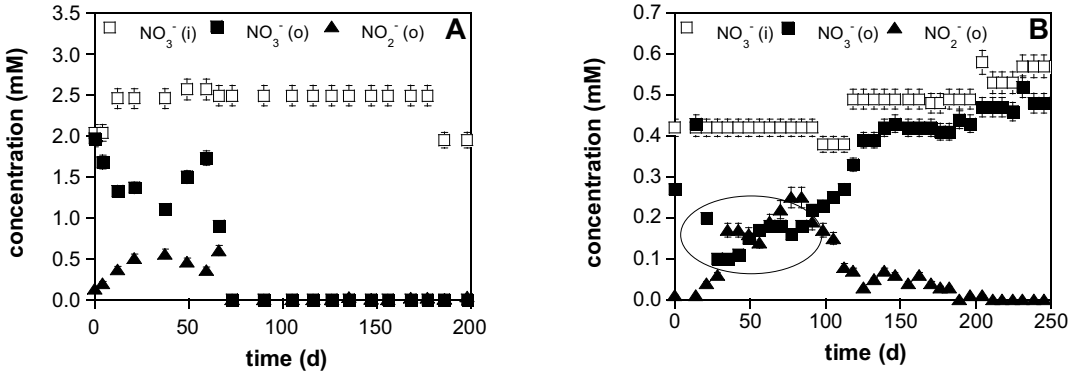

Figure 3.2. Variation of NO_3^- and NO_2^- concentration vs. time in input (i) and output (o) solutions of two representative flow-through experiments. See Table 3.4. (a) Experiment inoculated with *T. denitrificans* culture (IN-PYR-1); (b) One non-inoculated experiment (NON-PYR-3a). The ellipse shows the nitrate concentration values used to calculate nitrate reduction rate (see Eq. 3.7).

Figure 3.2b shows the consumption of nitrate in one representative non-inoculated flow-through experiment. In these experiments, a maximum nitrate reduction was achieved after 50-200 d (Table 3.4). Thereafter, nitrate content remained fairly constant until nitrate reduction slowed down to stop (e.g. NON-PYR-3a, Fig. 3.2b). Nonetheless, in some experiments after an apparent cessation of nitrate reduction, reduction restarted and high nitrate removal efficiency (60-94%) was finally attained (e.g. NON-PYR-2, Fig.

3.3a). In three experiments, a lag of approximately 80-100 d was observed before nitrate reduction started (e.g. NON-PYR-4a, Fig. 3.3b). In other experiments, nitrate reduction apparently did not cease during the duration of the tests (e.g. NON-PYR-4c, Fig. 3.3c). These behaviors could be attributed to changes in the microbial population over the course of the runs.

At pH 4.5 (NON-PYR-1), nitrate reduction was less effective than that observed in experiments carried out at pH 6.5-8, confirming the marked decrease in microbial activity due to acid pH (Table 3.4).

In the non-inoculated experiments, nitrate reduction efficiency was dependent on the nitrate loading rate. As is shown in the Table 3.4, when the nitrate loading rate ranged between 0.11 and 0.25 mmol NO_3^- L^{-1} d^{-1}, nitrate reduction was effective (overall nitrate removal of 40-80%), lasting up to 150-350 d. In contrast, with high nitrate loading rates (0.33-0.50 mmol NO_3^- L^{-1} d^{-1}), nitrate reduction efficiency was lower (overall nitrate removal lower than 30%), lasting only 20-70 d (e.g. NON-PYR-6b, Fig. 3.3d). It should be noted that, although efficiency in nitrate removal was different, the maximum amount of nitrate removed was similar in the two cases (between 0.12 and 0.48 mM for lower nitrate loading rates and 0.31-0.38 mM for higher ones). Therefore, a maximum nitrate removal of 0.48 mM was attained, regardless of the input concentration of nitrate.

Nitrate reduction to diatomic nitrogen gas occurs in four steps, nitrite being one of the intermediate products. The basic nitrate reduction pathway is represented as $NO_3^- \rightarrow NO_2^- \rightarrow NO \rightarrow N_2O \rightarrow N_2$.

In most of the batch experiments nitrite reduction took place rapidly and the final products were N-gaseous compounds (i.e. NO, N_2O or N_2). Furthermore, no significant changes in the ammonium concentration were detected over time, ruling out dissimilatory nitrate reduction to ammonium (Korom, 1992). Beller et al. (2006) showed that *T. denitrificans* has all the necessary genes encoding the four essential enzymes that catalyze denitrification. Our results confirm that these bacteria are able to reduce, at least,

nitrate and nitrite. However, transient nitrite accumulation was evident in 6 batch experiments (TD-1a, TD-1b, TD-1c, TD-2a, TD-2b and TD-2c). Two examples are shown in Figure 3.1c. Peak nitrite concentrations were observed after 43 d, accounting for 15-35% of the initial nitrate concentration. Thereafter, nitrite concentration decreased.

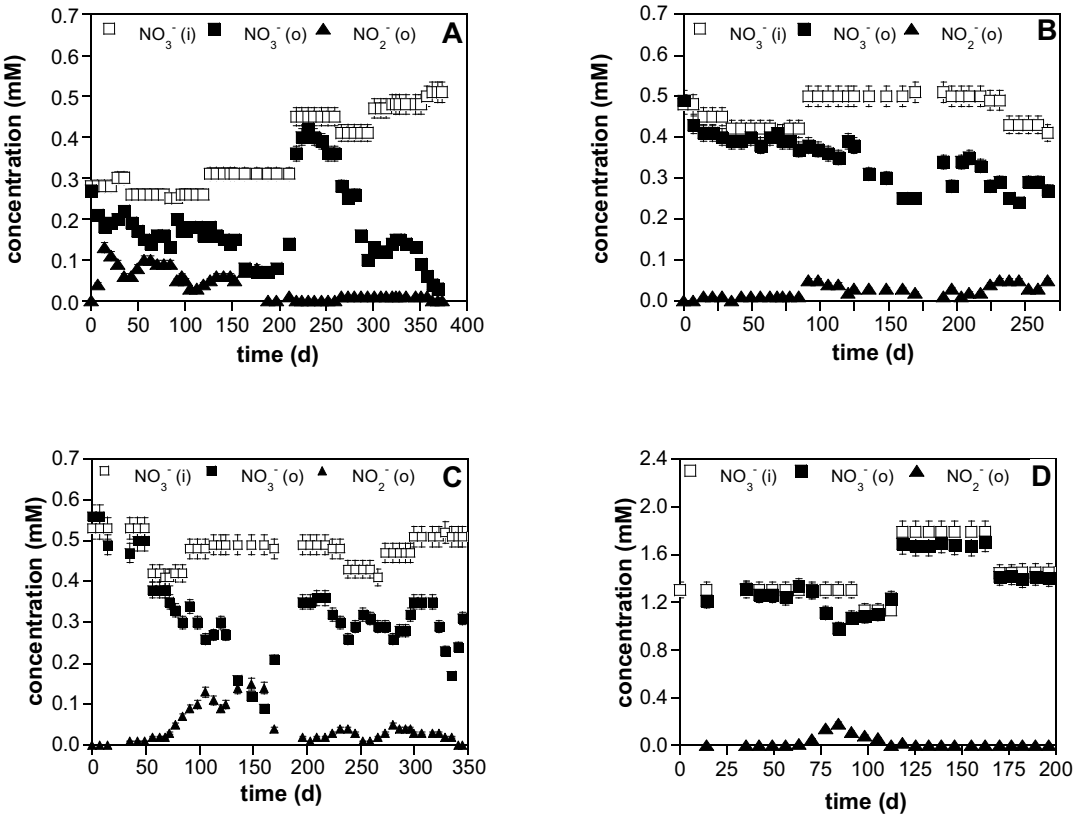

Figure 3.3. Variation of nitrate and nitrite concentration over time in input (i) and output (o) solutions of four representative non-inoculated flow-through experiments. See Table 3.4. (A) Experiment NON-PYR-2. Nitrate reduction apparently ceased after 230 d, but 10 d later, it restarted and about 94% nitrate removal efficiency was achieved at the end (370 d). (B) Experiment NON-PYR-4a. In contrast to other non-inoculated experiments, a lag of approx. 80 d was observed before nitrate reduction started. (C) Experiment NON-PYR-4c. Nitrate reduction started at 50 d and did not cease during the duration of the run (350 d). (D) Experiment NON-PYR-6b, performed with high nitrate loading rate (0.34 mmol NO_3^- L^{-1} d^{-1}). In contrast to the experiments with lower nitrate loading rate, nitrate removal was less effective and lasted only 30 d.

Nitrite was also present in some output solutions in the flow-through experiments. In the inoculated experiment, nitrite accumulated during the first 70 d, after which a

complete nitrate removal was attained (Fig. 3.2a). In most of the non-inoculated flow-through experiments, nitrate reduction consisted of two stages. In the first stage, reduction products were nitrite and N-gaseous compounds, and in the second stage, only nitrite was produced before the denitrification ceased. An example is given in the Figure 3.4. The figure depicts variation of the influent nitrate concentration (0.40 mM NO_3^-) and the sum of nitrate and nitrite concentrations of the output solution as a function of time in one representative experiment. Nitrate reduction took place from the beginning, lasting 120 d. In the first 70 d, nitrate was reduced to nitrite, which in turn, reduced to some gaseous compound. Thereafter, between 70 and 120 d, nitrate reduced to nitrite, and nitrite was not reduced. After 120 d, nitrate reduction ceased. As occurred in the batch experiments, dissimilatory nitrate reduction to ammonium could be excluded because ammonium concentrations in the output solutions were always below the detection limit.

In both the batch and flow-through experiments, nitrite accumulation resulted from incomplete reduction of nitrate. Since pyrite was the sole electron donor and was placed in excess to avoid electron donor limitation, nitrite accumulation could be due to the competition between nitrate and nitrite reductases for the available electron donor. In this regard, high nitrate content has been found to inhibit nitrite reduction, inducing nitrite accumulation (Betlach and Tiedje, 1981; Blaszczyk, 1993; Thomsen et al., 1994; Van Rijn et al., 1996).

In summary, nitrate removal efficiency diminished as a result of an increase in nitrate concentration (i.e. nitrate loading rate) and in pyrite grain size, and as a result of a decrease in pH. A 100% efficiency in nitrate removal was achieved in the presence of *T. denitrificans*. Under non-sterilized, non-inoculated conditions, nitrate removal efficiency was lower, probably because of changes in the microbial population. Nitrite reduction yielded N-gaseous compounds although transient nitrite accumulation occurred in the open-system experiments.

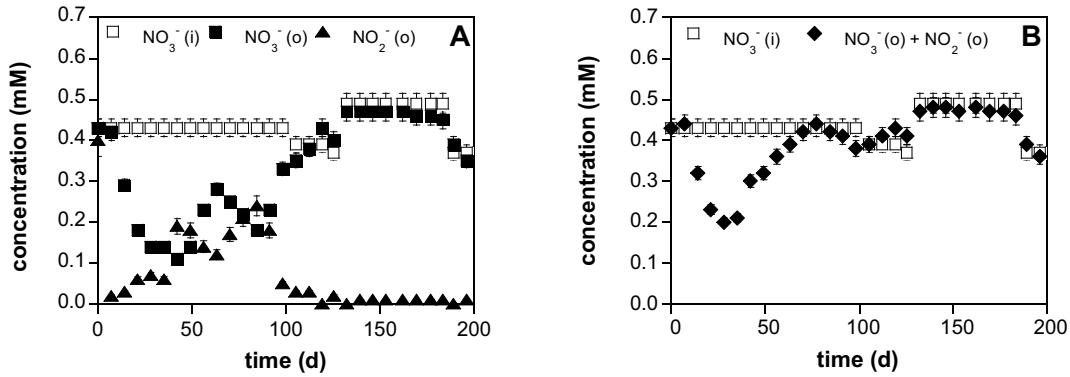

Figure 3.4. Variation of nitrate and nitrite concentration over time in input (i) and output (o) solutions of one of the non-inoculated flow through-experiments (NON-PYR-3b). (a) Evolution of nitrate and nitrite concentrations. (b) Evolution of the sum of nitrate and nitrite concentrations in the output solutions.

3.2.2 Stoichiometry of the pyrite-driven denitrification process

In both batch and flow-through experiments, pyrite dissolution was confirmed by S release. In the batch experiments, an initial high S release was followed by a gradual S increase (Fig. 3.5a). This gradual S release started after time 0 and occurred simultaneously to the reduction of nitrate in the inoculated experiments. The gradual increase in S concentration was also observed in the blank experiments and it was in general lower than in the inoculated experiments (Fig. 3.5a). This suggests that part of the S released in the inoculated experiments could be attributed to pyrite oxidation by traces of dissolved oxygen as observed in the blank experiments. Iron concentrations in all the batch experiments were below the detection limit, given that reacting pH ranged between 6.5 and 7.5.

In the flow-through experiments, output S concentrations were higher at the start of the experiments, subsequently decreasing until a steady state was attained (Fig. 3.5b). High concentrations at the start of the experiments were probably due to dissolution of an outer layer of the reacting mineral or to dissolution of microparticles (Lasaga, 1998).

Iron concentrations were below the detection limit in all the flow-through experiments, except in the first samples (from 0 to 10-50 d), when pH was below 5.5.

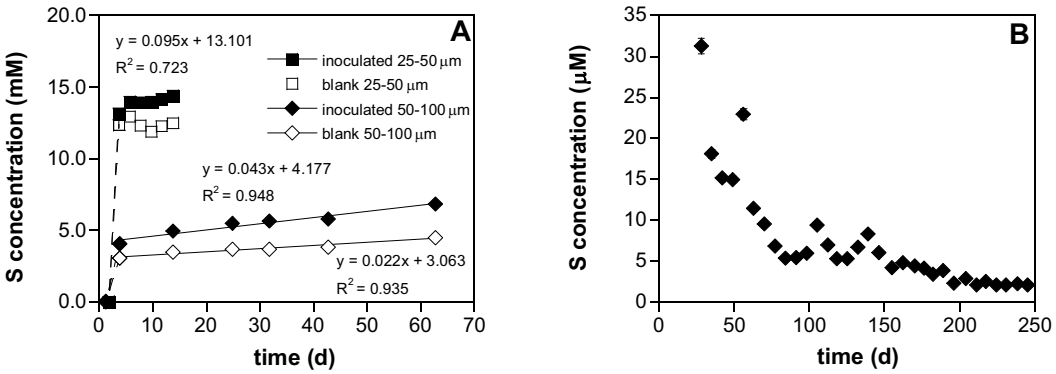

Figure 3.5. Variation of S concentration over time in batch and flow-through experiments. (a) S concentration vs. time in representative blank and inoculated pyrite-amended experiments. Solid lines represent the fitting of measured and S concentration versus time used to compute zero-order S production rates, r_s. (b) S concentration vs. time in one representative flow-through experiment. In this experiment, steady state was considered to be attained after 195 d.

Therefore, the results of both batch and flow-through experiments show that nitrate reduction occurred concurrently with the release of sulfate in the sterilized pyrite-amended experiments inoculated with *T. denitrificans* and in the non-inoculated experiments with non-sterilized pyrite, which showed inherent activity of indigenous bacteria. Under sterile conditions or under the conditions of not adding pyrite, nitrate reduction did not occur. This indicates that nitrate reduction was coupled with pyrite dissolution and was mediated by bacteria. Iron concentration was below detection limit, suggesting that most of the Fe^{2+} resulting from pyrite oxidation was oxidized to Fe^{3+} and precipitated. As stated above, ammonium production could be excluded. Accordingly, the overall reaction can be expressed as Eq. 3.3.

If nitrate reduction was coupled to pyrite dissolution via Eq. 3.3, the measured molar ratio of nitrate consumed to sulfate produced should be close to the stoichiometric ratio of this reaction, which is 1.5. However, in some experiments transient nitrite

accumulation occurred, and therefore, the expected nitrate/sulfate ratio was calculated based on the amount of nitrite accumulated according to the following reaction:

$$15NO_3^- + 2FeS_2 + 7H_2O \Rightarrow 15NO_2^- + 4SO_4^{2-} + 2Fe(OH)_3 + 8H^+ \quad (3.4)$$

where nitrate/sulfate ratio is 3.75.

In most of the experiments, the final products of the overall reaction were gaseous N-compounds (i.e. NO, N_2O, N_2). If the product was NO or N_2O, the nitrate/sulfate ratio should be 2.5 (Eq. 3.5) and 1.9 (Eq. 3.6), respectively:

$$15NO_3^- + 3FeS_2 + 3H_2O + 3H^+ \Rightarrow 15NO + 6SO_4^{2-} + 3Fe(OH)_3 \quad (3.5)$$

$$15NO_3^- + 4FeS_2 + \frac{13}{2}H_2O \Rightarrow \frac{15}{2}N_2O + 8SO_4^{2-} + 4Fe(OH)_3 + H^+ \quad (3.6)$$

In the inoculated pyrite-amended batch experiments, the nitrate/sulfate ratio was calculated using sulfate released after time 0 given that nitrate reduction started after this time. The ratio ranged from 0.4 to 2.0, being in most experiments lower than the possible stoichiometric ratios (Table 3.2). Nevertheless, the ratio was 1.5 within a 15% error in seven experiments. The low nitrate/sulfate ratio indicates an excess of sulfate, which, as stated above, could be explained by additional oxidation of pyrite by traces of dissolved oxygen as observed in the blank experiments. In fact, the excess of sulfate produced in the inoculated experiments (assuming that the reaction occurs via Eq. 3.3) ranged from 0.2 to 5.0 mM, in agreement with sulfate produced in the blank experiments (between 0.2 and 4.9 mM).

It is important to note that in the experiments in which pyrite was previously washed with HCl, the molar nitrate/sulfate ratio was similar to that measured in the rest of the experiments, as occurred with the efficiency and rate of nitrate removal (Table 3.2).

This suggests that the presence of possible microparticles and/or impurities on the pyrite surface had no significant effect on the overall process.

In the non-inoculated flow-through experiments, the measured nitrate/sulfate ratio at the time of maximum nitrate removal was significantly higher than the possible stoichiometric ratios (values higher than 10, Table 3.4). In fact, the percentage of nitrate reduction due to pyrite dissolution was calculated to be 1-30% (Table 3.4). Moreover, this percentage could be lower since an amount of sulfate was released from dissolution of pyrite by traces of dissolved oxygen, as occurred in the blank flow-through experiments.

On the one hand, as pyrite powder and solutions were not previously autoclaved, a mixture of both autotrophic and heterotrophic denitrifying bacteria could have enhanced the denitrifying activity not linked to pyrite oxidation. Dead and lysed cells of the autotrophic bacteria could have acted as the carbon source for the heterotrophic bacteria since organic compounds were not provided (Koenig et al., 2005).

On the other hand, some deficit in aqueous S could be partially attributed to passivation of the pyrite surface owing to precipitation of iron (hydr)oxide solid phases. XPS examination showed an enrichment of Fe onto the pyrite surface since surface Fe/S ratios increased from 0.50 to up to 0.77 (Table 3.5.), which is consistent with the absence of iron in solution. Furthermore, PHREEQC calculations showed that the output solutions were supersaturated with respect to several iron oxy-hydroxides, such as goethite, ferrihydrite and $Fe(OH)_3$. Solution saturation indexes with respect to solid phases ($SI = \log(IAP/K_S)$, where SI is the saturation index, IAP is the ion activity product and K_S is the solid solubility product), and aqueous speciation of solutions were calculated using the code PHREEQC (Parkhurst, 1995) and the MINTEQ database. Although aqueous iron was depleted, calculations were run by using a low iron concentration (1×10^{-3} mM).

Sample	Fe	S	Fe/S
	at. %		
initial	33.5	66.5	0.50
NON-PYR-6b	39.1	60.9	0.64
NON-PYR-3b	43.6	56.4	0.77
IN-PYR-1	58.8	41.2	1.42

Table 3.5. Results obtained from X-ray Photoelectron Spectroscopy (XPS) determinations on the initial and reacted pyrite samples of some flow-through experiments. Surface stoichiometry is represented by molar ratios. Atomic concentrations of Fe and S in the pyrite surfaces were estimated by normalizing out the remaining elements (oxygen and adventitious carbon).

In the inoculated flow-through experiment, the measured nitrate/sulfate ratio was also high (Table 3.4). An iron coating may account for one part of the S deficit. XPS confirmed iron enrichment on the surfaces (Table 3.5) and, according to the PHREEQC calculations, output solutions were supersaturated with respect to iron oxy-hydroxides. However, it has been not possible to account for this discrepancy between the high amount of removed nitrate and the small concentration of released S. One plausible reason could be heterotrophic contamination since aseptic conditions can be difficult to maintain in long-term, continuous-flow experiments inoculated with a pure culture (Claus and Kutzner, 1985).

Figure 3.6 shows the surface of the pyrite retrieved from one non-inoculated flow-through experiment after 250 d. The pyrite surface is mainly covered by a biofilm (Fig. 3.6a). In detail, groups of cells are observed embedded in an organic matrix (Fig. 3.6b).

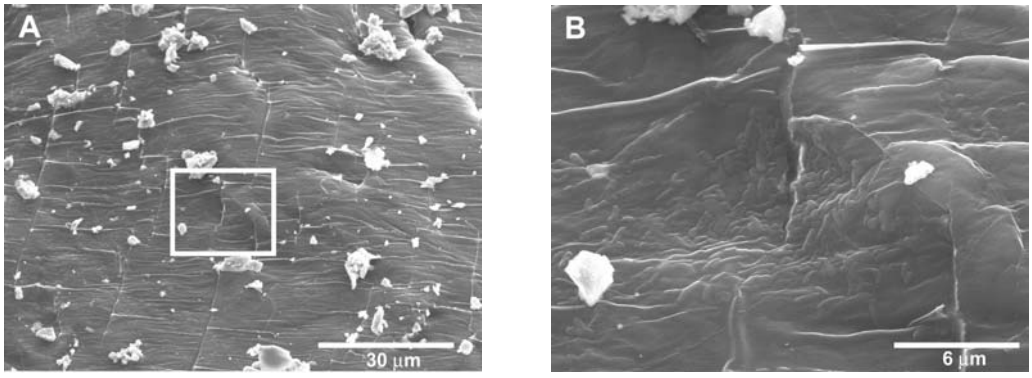

Figure 3.6. SEM images of pyrite surfaces at the end of the NON-PYR-4 non-inoculated flow-through experiment. (a) Pyrite surface covered by a biofilm. The box is magnified in (b); (b) Magnification image showing attached cells surrounded by organic material.

3.2.3 Nitrate reduction rates

In batch experiments, nitrate reduction rates were computed assuming zero-order kinetics and using linear regression to fit the remaining nitrate concentrations vs. time (Fig. 3.1). Computed nitrate reduction rates ranged between 0.09 to 3.50 mmol NO_3^- kg_{py}^{-1} d^{-1}, with $\sigma_{rate} \leq 20\%$ of rate in most cases (Table 3.2).

The nitrate reduction rates were higher in the experiments with 25-50 μm pyrite (2.12±0.83 mmol NO_3^- kg_{py}^{-1} d^{-1}) than in the 50-100 μm ones (0.39±0.31 mmol NO_3^- kg_{py}^{-1} d^{-1}). With initial nitrate concentration of approx. 1 mM, the nitrate reduction rate was higher than the rates with approx. 2.5 and 4 mM NO_3^- (0.62±0.34, 0.19±0.01 and 0.28±0.23 mmol NO_3^- kg_{py}^{-1} d^{-1}, respectively). The variability in average rates of the experiments with similar initial conditions (Table 3.2) could be attributed to different microbial activity (especially in those experiments with low cell density) and/or certain degree of heterogeneity in the range of grain size of the pyrite powders, which has been demonstrated to significantly modify nitrate reduction rates and nitrate removal efficiency.

Rate dependence on pyrite grain size implies that the reduction rate depends on exposed pyrite surface area. The larger the surface area, the higher the rate. A large surface area could enhance mass transfer from solid surfaces to solution and/or bacterial attachment to the surface of pyrite grains. Further experiments are necessary to ascertain whether the rate-limiting factor in the overall process is mass transfer or bacterial adhesion.

In the flow-through experiments, the pyrite-mass normalized nitrate reduction rate, R_{NO3} (mol g^{-1} s^{-1}) was calculated from the maximum consumption of nitrate according to the expression:

$$R_{NO3} = \frac{q\,(C_{NO3} - C^{0}_{NO3})}{m} \qquad (3.7)$$

where q is the flow rate (L s^{-1}) of the solution through the reactor, C_{NO3} and C^{0}_{NO3} are the concentrations (mol m^{-3}) of nitrate in the output and input solutions, respectively, and m is the pyrite mass (g).

In the non-inoculated experiments, computed nitrate reduction rates ranged between 1.62 and 5.42 mmol NO_3^- kg_{py}^{-1} d^{-1} (Table 3.4). Lower nitrate reduction rate was computed in the experiment performed at pH 4.5 (1.31 mmol NO_3^- kg_{py}^{-1} d^{-1}, Table 3.4). The nitrate loading rate faintly affected nitrate reduction rates, although, as discussed above, nitrate reduction efficiency was higher in experiments with low nitrate loading rates (0.11-0.25 mmol NO_3^- L^{-1} d^{-1}). The nitrate reduction rate obtained in the inoculated experiment was 0.54 mmol NO_3^- kg_{py}^{-1} d^{-1}, which was lower than in the non-inoculated experiments although nitrate removal efficiency was higher in the former.

Hence, the results indicate that nitrate reduction rates increased by decreasing grain size and initial nitrate concentration. The nitrate reduction rates were lower in the inoculated flow-through experiment than in the non-inoculated ones, although efficiency in nitrate removal was higher in the former.

3.2.4 N and O isotope fractionation

During denitrification, as nitrate concentration is decreased, residual nitrate becomes enriched in heavy isotopes ^{15}N and ^{18}O. When denitrification is treated as a single-step and unidirectional reaction in a closed system, the change in the isotopic composition of nitrate can be modeled using a Rayleigh-distillation type fractionation model (Mariotti et al., 1981):

$$\delta^{15}N_{residual} = \delta^{15}N_{initial} + \varepsilon_N \ln f \quad (3.8)$$

$$\delta^{18}O_{residual} = \delta^{18}O_{initial} + \varepsilon_O \ln f \quad (3.9)$$

where f is the unreacted portion of nitrate (residual nitrate concentration divided by the initial nitrate concentration), δ(residual) and δ(initial) are the nitrogen or oxygen isotopic compositions (‰) of the residual and initial nitrate, respectively, and ε (‰) is the isotopic enrichment factor. Accordingly, $\delta^{15}N$ and $\delta^{18}O$ of dissolved nitrate increase in proportion to the natural logarithm of the residual nitrate fraction.

Analysis of $\delta^{15}N$ and $\delta^{18}O$ of dissolved nitrate was carried out in two pyrite-amended batch experiments with 50-100 μm (TD-20) and 25-50 μm (TD-21) size fractions of pyrite (Table 3.3). The initial values of $\delta^{15}N_{NO3}$ and $\delta^{18}O_{NO3}$ were -2.3‰ and +25.1‰, respectively, and both values increased over the experimental runs. In the 50-100 μm pyrite experiment, after 60 d, $\delta^{15}N_{NO3}$ and $\delta^{18}O_{NO3}$ increased to +8.4‰ and +34.9‰, respectively, with 52% reduction of initial nitrate. In the experiment with 25-50 μm pyrite, after 16 d, $\delta^{15}N_{NO3}$ and $\delta^{18}O_{NO3}$ increased to +2.6‰ and +29.2‰, respectively, with 18% reduction of initial nitrate. Bulk dataset for both experiments is shown in Appendix C. Figure 3.7a depicts $\delta^{15}N$ and $\delta^{18}O$ of the remaining nitrate vs. ln $[NO_3^-]$ in both experiments. In the 50-100 μm pyrite experiment, the values of εN and εO were -15.0‰ and -13.5‰, respectively, based on the slope of the regression lines. In the experiment

with 25-50 μm pyrite, the values of εN and εO were -22.9‰ and -19.0‰, respectively. In both experiments, there is a positive correlation ($r^2 > 0.99$) between $\delta^{15}N_{NO3}$ and $\delta^{18}O_{NO3}$, with slopes of 0.89 and 0.85, yielding εN/εO ratios of 1.13 and 1.18 (Fig. 3.7b).

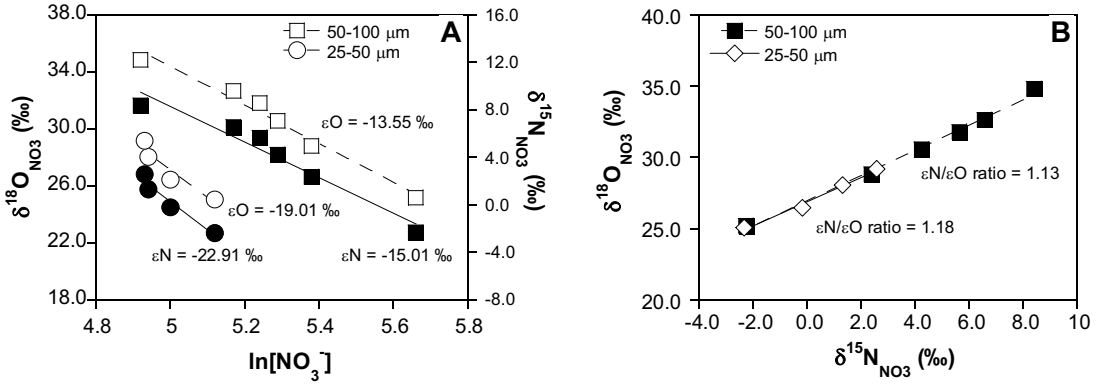

Figure 3.7. Isotopic results of the two pyrite-amended batch experiments inoculated with *T. denitrificans* and focusing in calculate isotope fractionation: TD-21 (with 25-50 μm pyrite) and TD-20 (50-100 μm pyrite). (a) $\delta^{15}N$ (filled symbols) and $\delta^{18}O_{NO3}$ (open symbols) vs. ln[NO_3^-]. Values of εN and εO were obtained from the slope of the regression lines; (b) $\delta^{18}O$ vs. $\delta^{15}N_{NO3}$. Determination coefficients (R^2) ranged from 0.889 to 0.993 in both figures.

To our knowledge, isotope fractionation during autotrophic denitrification in laboratory cultures has not been reported to date. Therefore, the ε ranges obtained in this study using *T. denitrificans* culture were compared with those reported in experiments with heterotrophic denitrifying strains under different growth conditions (Table 3.6). However, it should be noted that the NO_3/SO_4 ratio of the TD-20 experiment (2.8) was significantly higher than the stoichiometric ones, suggesting the possible occurrence of heterotrophic contamination (Table 3.3). In this case, εN and εO could be associated with a mixture of heterotrophic and autotrophic denitrification. These values cannot therefore be unequivocally assigned to the denitrifying activity of *T. denitrificans.*

The εN values obtained in this study (-15.0‰ and -22.9‰) fall well within the range of values reported in the literature for nitrate reduction by heterotrophic denitrifying cultures (from -13.4‰ to -30.0‰, Wellman et al., 1968; Delwiche and Steyn, 1970; Table 3.6).

Nonetheless, the values of εO (-13.5‰ and -19.0‰) were lower than those reported by Toyoda et al. (2005) during the production of N_2O in acetylated experiments with 10 or 100 mM NO_3^- by two heterotrophic denitrifying pure cultures (-3‰ to +32‰; Table 3.6). According to these authors, two isotope effects with opposite $\delta^{18}O$ shifts may arise during nitrate reduction to nitrous oxide. Either (1) preferential reduction of the lighter molecules, which yields negative values of εO, such as those obtained in the present study, or (2) preferential elimination of ^{16}O over ^{18}O, which yields a positive shift that results in an apparent 'inverse isotope effect' with positive values of O fractionation (Casciotti et al., 2002; Toyoda et al., 2005).

Earlier studies with pure cultures of denitrifying bacteria have not determined the εN/εO ratio. The ratio obtained in this study (1.15±0.04) is comparable to ratios obtained from *in situ* studies of denitrification in groundwater, which range from 0.9 to 2.3 (chapter 2 and references within).

The N and O enrichment factors give an idea of the magnitude of the isotopic fractionation that could be expected at field sites dominated by autotrophic denitrification based on pyrite oxidation, such as the Osona aquifer (see chapter 2). However, it should be noted that there is some uncertainty about assigning the isotopic fractionation to denitrification performed exclusively by autotrophic denitrifying bacteria. Further laboratory experiments with aquifer material are needed in order to obtain enrichment factors that are characteristic for the specific aquifer.

3.3 Conclusions

Laboratory experiments were performed to study the feasibility of pyrite-driven denitrification of nitrate-contaminated groundwater. Batch experiments were used to evaluate the ability of *T. denitrificans* to reduce nitrate using pyrite and to determine associated N and O isotopic fractionation. Flow-through experiments were performed to simulate dynamic groundwater flow environment.

Table 3.6. Estimation of the enrichment factors for ^{15}N and ^{18}O in laboratory experiments with pure denitrifying cultures reported in the literature.

Species	System	εN (‰)	εO (‰)	εN / εO	Reference	Notes
Heterotrophic denitrifying bacteria						
Paracoccus denitrificans	$NO_3^- \rightarrow N_2O$	-28.6 ± 1.9	n.d.	n.d.	Barford et al. (1999)	steady-state reactor, acetate as electron donor, 30 mM NO_3^-
Paracoccus denitrificans	$N_2O \rightarrow N_2$	-12.9 ± 5.8	n.d.	n.d.		
Pseudomonas denitrificans	$NO_3^- \rightarrow N_2$	-13.4 to -20.8	n.d.	n.d.	Delwiche and Steyn (1970)	batch, glucose as electron donor
Psedumonas stutzeri	$NO_3^- \rightarrow N_2$	-20 to -30	n.d.	n.d.	Wellman at al. (1968)	batch, 0.01 to 0.03 mM NO_3^-
Pseudomonas chlororaphis	$NO_3^- \rightarrow N_2O$	-12.7	n.d.	n.d.	Sutka et al. (2006)	batch, citrate as electron donor, 10 mM NO_3^-
Pseudomonas aureofaciens	$NO_3^- \rightarrow N_2O$	-36.7	n.d.	n.d.		
Pseudomonas fluorescens	$NO_3^- \rightarrow N_2O$	−39 to −31 (1)	+13 to +32 (1)	n.d.	Toyoda et al. (2005)	batch, citrate as electron donor, acetylated, 10 to 100 mM NO_3^-
	$NO_3^- \rightarrow N_2O$	−22 to −17 (1)	-3 to -11 (1)	n.d.		
Paracoccus denitrificans	$NO_3^- \rightarrow N_2O$	−22 to −10 (1)	+4 to +23 (1)	n.d.		
Psedumonas stutzeri	$NO_2^- \rightarrow N_2$?	-5 to -20	n.d.	n.d.	Bryan et al. (1983)	batch, succinate as electron donor, 0.07 to 2.2 mM NO_2^-
Psedumonas stutzeri	$NO_2^- \rightarrow N_2O$	-9.9 to -19.6	n.d.	n.d.	Shearer and Kohl (1988)	batch, succinate as electron donor, 0.1 to 2.3 mM NO_2^-
Autotrophic denitrifying bacteria						
Thiobacillus denitrificans	$NO_3^- \rightarrow N_2$?	-22.9 (2)	-19.0 (2)	1.2	this study (TD-21)	batch, 25-50 μm pyrite as electron donor, 2.7 mM NO_3^-
Thiobacillus denitrificans	$NO_3^- \rightarrow N_2$?	-15.0 (2)	-13.5 (2)	1.2	this study (TD-20)	batch, 50-100 μm pyrite as electron donor, 4.6 mM NO_3^-

(1) εN (or εO) was calculated as the difference between $\delta^{15}N_{N2O}$ (or $\delta^{18}O_{N2O}$) and $\delta^{15}N_{NO3}$ (or $\delta^{18}O_{NO3}$)
(2) see text for details

Inoculated experiments demonstrated that *T. denitrificans* is able to reduce nitrate using pyrite as the electron donor. Nitrate reduction rate was dependent on pyrite grain size, nitrate concentration and pH. The results indicated that the extent and the rate of denitrification increased as the size of pyrite particles decreased. Moreover, 100% nitrate removal efficiency was achieved in long-term inoculated experiments at experimental conditions that simulate typical conditions of slow-moving, nitrate-contaminated groundwater. Furthermore, inoculated batch experiments permitted to calculate N and O isotopic enrichment factors for pyrite-driven denitrification by *T. denitrificans*. To our knowledge, this is the first study determining N and O isotope fractionation during denitrification by pure cultures of autotrophic denitrifying bacteria. These values indicated the magnitude of the isotope fractionation that occurs in nitrate-contaminated aquifers dominated by autotrophic denitrification.

Nitrate reduction also occurred under non-sterilized, non-inoculated conditions, but nitrate removal efficiencies were lower and unpredictable denitrification stages were observed. Nevertheless, in three experiments performed at low nitrate loading rate, almost 100% of nitrate removal was attained at the end (375 d). These results suggest that bacteria other than inoculated *T. denitrificans* were able to remove nitrate using pyrite at some stage. Furthermore, it should be noted that, although the bacterial community present in the non-inoculated experiments was not native to a nitrate contaminated aquifer, it was able to adapt to the new conditions and as a result reduce nitrate, probably by a combination of both autotrophic and heterotrophic denitrification.

Hence, the addition of pyrite to enhance the activity of denitrifying bacteria could be considered for future water management strategies to remove nitrate at the concentrations commonly found in contaminated agricultural groundwater (up to 5 mM, see chapter 2). Future experiments using sediments from nitrate-contaminated aquifers should address denitrification enhancement by addition of pyrite to stimulate indigenous denitrifying bacteria.

Chapter 4

Bioremediation of nitrate contaminated groundwater (Osona aquifer) by stimulation of denitrification

Nitrate, which is one of the most common contaminants in groundwater, is introduced into the subsurface by industrial and agricultural activities and wastewater discharges. A high nitrate concentration in drinking water poses a considerable health risk (Ward et al., 2005). Moreover, a high nitrate level in surface waters constitutes a serious threat to aquatic ecosystems owing to the increase of algae growth, which contributes to eutrophication (Rabalais, 2009).

Denitrification occurs naturally when certain bacteria use nitrate as the terminal electron acceptor in their respiratory process in the absence of oxygen.

Note: This chapter is based on the article: Torrentó, C., Urmeneta, J., Otero, N., Soler, A., Viñas, M. and Cama, J. Biostimulation with pyrite to enhance denitrification in sediments and groundwater from a nitrate contaminated aquifer (submitted to *Water Research*)

This process consists of a sequence of enzymatic reactions leading to the production of dinitrogen gas (Knowles, 1982). Most of the denitrifying bacteria are heterotrophic and use organic compounds as electron donors. Nevertheless, other denitrifying bacteria are autotrophic and use inorganic compounds as electron donors (Straub et al., 1996; Zumft, 1997; Beller, 2005). Given the ubiquity of denitrifying bacteria in nature, the process takes place naturally in aquifers, soils and seawater when the necessary environmental conditions arise simultaneously.

The Osona area (NE Spain) is affected by widespread groundwater nitrate contamination derived from the excessive application of pig manure as fertilizer. Natural attenuation of nitrate pollution has been reported in some zones of this area (see chapter 2). The multi-isotopic study of the groundwater of the Osona aquifer presented in chapter 2 demonstrated that denitrification processes are related to pyrite oxidation. Other field studies have also suggested that pyrite oxidation regulates denitrification in aquifers even in the presence of organic carbon. In some field studies, low organic content, a decrease in nitrate and an increase in sulfate were used together as the evidence for denitrification coupled to pyrite oxidation (Postma et al., 1991; Beller et al., 2004; Zhang et al., 2009a). Other authors found clear indication for autotrophic denitrification by means of isotopic data, coupling the isotopic composition of nitrate and sulfate (Aravena and Robertson, 1998; Pauwels et al., 1998; 2000; 2010; Schwientek et al., 2008). The results of chapter 2 also allowed us to calculate the percentage of denitrification in the Osona aquifer, which had a median value of 30%. Despite naturally occurring attenuation, nitrate contents in the Osona area largely exceeded the drinking water threshold in most wells.

Denitrification in natural systems proceeds very slowly and it is not very effective in lowering nitrate concentrations in aquifers. This is why several technologies have been developed for removing nitrate (Mateju et al., 1992; Della Rocca et al., 2007). One of these strategies of remediation is stimulation of natural denitrification, utilizing the indigenous populations of denitrifying bacteria. Biostimulation of denitrification processes consists in

the provision of suitable electron donor and/or energy sources to promote nitrate remediation and has proved to be cost-effective for *in situ* and *ex situ* groundwater treatments, adding inorganic or organic electron donors (Soares, 2000). Another strategy of bioremediation is bioaugmentation, which consists in the addition of previously adapted microorganisms to enhance a specific biological activity (Vogel, 1996). Combined biostimulation/bioaugmentation strategies have been used to enhance denitrification in laboratory studies with the addition of pure cultures of denitrifying bacteria (Sánchez et al., 2008), acclimated bacterial communities enriched from contaminated sites (Flores et al., 2007) or encapsulated microorganisms (Tal et al., 1999; Zhang et al., 2009b).

In an aquifer such as the Osona aquifer, in which pyrite-driven denitrification processes are established, stimulation of the denitrifying community has the advantage of promoting an active and acclimated microbial population. Therefore, the feasibility of enhancing natural denitrification by means of biostimulation and combined biostimulation/bioaugmentation must be evaluated. Experimental results of chapter 3 showed that pyrite can serve as the electron donor source to support biological denitrification. In order to enhance *in situ* biological denitrification at field scale, the capacity of native microorganisms to carry out pyrite-driven denitrification must be examined in laboratory experiments with on-site samples. The impact of biostimulation and/or bioaugmentation on the indigenous bacterial community must also be studied. Furthermore, a detailed isotopic characterization of denitrification experiments at laboratory scale is necessary to obtain the enrichment factors that will allow us to better approximate the degree of natural denitrification in the Osona aquifer, as well as to assess the efficacy of the induced attenuation. Moreover, an understanding of the structure of the indigenous bacterial community is warranted to gain insight into the progress of natural attenuation and to further improve bioremediation processes.

Therefore, the aims of the present chapter are:

(1) To examine the biological capacity of the aquifer material to induce pyrite-driven nitrate reduction. This is necessary to evaluate the possibility of implementing *in*

situ bioremediation by adding pyrite to stimulate activity of the indigenous bacteria. In addition to biostimulation, the feasibility of a combined biostimulation/bioaugmentation approach must also be evaluated.

(2) To characterize the denitrifying populations in the Osona aquifer material and to evaluate changes in their composition and diversity during the biostimulated and/or bioaugmented nitrate reduction processes.

(3) To calculate N and O isotope fractionation associated with denitrification in the Osona aquifer in order to quantify the natural occurring nitrate attenuation and provide a tool to assess the efficacy of induced attenuation in future studies at field scale.

To this end, batch and flow-through experiments using saturated material and groundwater from the Osona aquifer were stimulated with pyrite and were performed in an anoxic atmosphere of N_2 and CO_2 (90%/10%). The pyrite-amended experiments designed to assess the feasibility of combined biostimulation/bioaugmentation were inoculated with autotrophic denitrifying bacteria (*Thiobacillus denitrificans*). These bacteria are well known for their ability to couple denitrification to the oxidation of various S- and Fe(II)-containing electron donors (Beller et al., 2006), such as pyrite (chapter 3).

4.1 Experimental methodology

4.1.1 Study site

The Osona area is an area that is classified as vulnerable to nitrate pollution from agricultural sources following the European Nitrate Directive (Council Directive 91/676/EEC). Considerable amounts of pig manure are produced as a result of intensive farming and most of this manure is used as organic fertilizer, leading to widespread groundwater nitrate contamination (see chapter 2). Hydrogeologically, the system is made up of a series of confined aquifers located in carbonate and carbonate-sandstone layers, whose porosity is mainly related to the fracture network (Menció et al., 2010).

These formations are interbedded in marl layers that act as confining strata. The presence of disseminated pyrite in these formations should be noted (Urquiola, 1994). Owing to the fact that the most productive confined aquifers are at deep depth, the main production wells for agriculture and farm demand usually reach depths of more than 100 m. Although deep aquifers are less vulnerable to direct nitrate leachate in natural conditions, groundwater pumping induces a vertical leakage between aquifer levels throughout the fracture network, facilitating the entry of nitrate-rich superficial groundwater. Furthermore, the lack of well casing results in a mix of water of different levels within the wells, which gives rise to the extraction of low quality water (see chapter 2).

4.1.2 Material and characterization

A core hole (Roda de Ter, Osona region) was drilled to a depth of 12 m, about 3 m below the groundwater table, and material was sampled with a core barrel. After removing the core from the barrel, the samples were immediately preserved at 4°C in autoclaved glass flasks with a CO_2 atmosphere generated by a BBL® disposable gas generator envelope.

In the laboratory, the core was aseptically processed under anaerobic conditions. The core was broken using sterilized instruments to obtain unaltered fragments. Therefore, core fragments were crushed and some portions were placed into sterilized containers in an anaerobic atmosphere until used in the experiments.

Powder X-ray diffraction (XRD) of the core samples was performed using a Bruker D5005 diffractometer with Cu $K\alpha$ radiation over a 2θ range from 0 to 60 degrees, with a scan speed of 0.025°/18 s. Rietveld analyses revealed that the sample was mainly composed of calcite (27.2 wt%), muscovite (26.2 wt%) and quartz (23.1 wt%) with small amounts of albite (10.3 wt%), dolomite (7.7 wt%), sudoite (4.9 wt%) and pyrite (0.6 wt%).

Groundwater samples were collected from a well close to the drilling site in sterilized glass bottles filled completely to avoid air in the bottle headspace and stored at

4°C until used. Aseptic sampling techniques and sterile sample containers were used to prevent contamination of groundwater with non-native bacteria. The pH of the water was 6.84 and the water was classified as bicarbonate-calcium type in accordance with the lithology of the aquifer. Groundwater had an elevated nitrate concentration (107 mg L^{-1}) and nitrite was below the detection limit (0.01 mg L^{-1}).

Pyrite fragments were from Navajún (Logroño, NE Spain). Fragments were crushed and sieved to obtain a size particle that ranged from 50 to 100 μm. The XRD pattern confirmed samples to be pyrite. The chemical composition of pyrite was determined by electron microprobe analysis (EMPA) using a Cameca SX-50. The pyrite atomic composition (at. %) was 66.46±0.37 of S and 33.34±0.21 of Fe based on 20 points. Impurities of Ni were detected (0.07±0.05 at. %) and Co, Cu, Zn, As and Pb were below detection limits (Table 4.1). Before the start of the experiments, powdered pyrite was sterilized by autoclaving at 121°C for 15 min.

	Si	S	Fe	Co	Ni	Cu	Zn	As	Pb
at. %	0.022	66.46	33.34	0.012	0.070	0.001	0.008	0.000	0.006
sd	0.008	0.367	0.212	0.023	0.054	0.003	0.006	0.000	0.008
detection limit	0.006	0.047	0.078	0.020	0.027	0.025	0.029	0.020	0.186

Table 4.1. Chemical composition of the pyrite used in the experiments.

Thiobacillus denitrificans (strain 12475 from German Collection of Microorganisms and Cell Cultures, DSMZ) was cultured with thiosulfate in an anaerobic (pH 6.8) nutrient medium specially designed for *T. denitrificans*, following Beller (2005). The medium consisted of a mixed solution of $Na_2S_2O_3 \cdot 5H_2O$ (20 mM), NH_4Cl (18.7 mM), KNO_3 (20 mM), KH_2PO_4 (14.7 mM), $NaHCO_3$ (30 mM), $MgSO_4 \cdot 7H_2O$ (3.25 mM), $FeSO_4 \cdot 7H_2O$ (0.08 mM), $CaCl_2 \cdot 2H_2O$ (0.05 mM) and sterile vitamin, trace element and selenate-tungstate solutions (stock solutions 1, 4, 6, 7 and 8 of Widdel and Bak, 1992). The cultures were maintained unshaken under anaerobic conditions at 30°C. Thereafter, the culture was harvested by centrifugation and washed and resuspended in a sterile saline solution (Ringer 1/4 solution) immediately before the start of the experiments.

4.1.3 Experimental set-up

All the experiments were performed in an anaerobic glove box with a nominal gas composition of 90% N_2 and 10% CO_2 at 28±2 °C. The oxygen partial pressure in the glove box was maintained between 0.1 and 0.3% O_2(g) and was continuously monitored by an oxygen partial pressure detector with an accuracy of ±0.1% O_2(g). Table 4.2 shows the experimental conditions of both batch and flow-through experiments.

4.1.3.1 Batch experiments

Three types of batch experiments were performed in sterilized 250 mL crystal Witeg bottles: a blank experiment, pyrite-free control experiments and pyrite-amended experiments (Table 4.2). All the batch experiments were run in duplicate with the exception of the blank experiment. The blank experiment was carried out to evaluate potential pure chemical nitrate reduction. The objective of the pyrite-free control experiments was to assess potential heterotrophic denitrification. Biostimulation was evaluated by adding pyrite as the electron donor and combined biostimulation/bioaugmentation was evaluated by adding pyrite and pure culture of *T. denitrificans*. In these experiments, pyrite was added in stoichiometric excess with respect to the initial nitrate concentration.

The blank experiment was carried out adding 8 g of autoclaved core fragments and 2 g of sterilized powdered pyrite to 250 mL of autoclaved groundwater (OS-13). In the pyrite-free control experiments, 10 g of core fragments were added to 250 mL of groundwater (experiments OS-1 and OS-2). Two replicate control experiments were carried out using previously autoclaved aquifer sediment and groundwater (experiments OS-11 and OS-12).

In the pyrite-amended experiments, 8 g of core fragments and 2 g of sterilized powdered pyrite were added to 250 mL of groundwater (biostimulated experiments OS-3 and OS-4). Furthermore, two replicate experiments were inoculated with 8 mL of the *T. denitrificans* cell solution (biostimulated/bioaugmented experiments OS-9 and OS-10).

Table 4.2. Experimental conditions of batch and flow-through experiments.

Experiment	Experimental conditions	flow rate	HRT
		mL min^{-1}	d
BATCH EXPERIMENTS			
Blank experiment			
OS-13	8 g autoclaved core fragments, 250 mL autoclaved groundwater, 2 g sterilized pyrite	-	-
Control experiments			
OS-1 and OS-2	10 g core fragments, 250 mL groundwater	-	-
OS-11 and OS-12	10 g autoclaved core fragments, 250 mL autoclaved groundwater	-	-
Pyrite-amended experiments			
Biostimulated experiments			
OS-3 and OS-4	8 g core fragments, 250 mL groundwater, 2 g sterilized pyrite	-	-
OS-7 and OS-8	8 g autoclaved core fragments, 250 mL groundwater, 2 g sterilized pyrite	-	-
Biostimulated/bioaugmented experiments			
OS-9 and OS-10	8 g core fragments, 250 mL groundwater, 2 g sterilized pyrite, 8 mL *T. denitrificans* culture (6.6×10^{7} cells mL^{-1})	-	-
T. denitrificans experiments			
OS-15 and OS-16	8 g autoclaved core fragments, 250 mL autoclaved groundwater, 2 g sterilized pyrite, 8 mL *T. denitrificans* culture (1.2×10^{8} cells mL^{-1})	-	-
FLOW-THROUGH EXPERIMENTS			
OS-17	8 g core fragments, 2 g sterilized pyrite. Input solution: groundwater	0.003	12.3
OS-18	8 g core fragments, 2 g sterilized pyrite. Input solution: sterilized 2.5 mM NO_3^- solution	0.004	9.1
OS-31	Solid material from experiment OS-3. Input solution: groundwater	0.003	12.8
OS-41	Solid material from experiment OS-4. Input solution: sterilized 2.5 mM NO_3^- solution	0.003	11.8
OS-71	Solid material from experiment OS-7. Input solution: groundwater	0.003	13.7
OS-81	Solid material from experiment OS-8. Input solution: sterilized 2.5 mM NO_3^- solution	0.004	8.0
OS-91	Solid material from experiment OS-9. Input solution: groundwater	0.003	13.2
OS-101	Solid material from experiment OS-10. Input solution: sterilized 2.5 mM NO_3^- solution	0.004	8.2

HRT = hydraulic retention time

In addition, two *T. denitrificans*-inoculated experiments were carried out with previously autoclaved core fragments, pyrite and groundwater to determine the denitrifying activity of *T. denitrificans* in the absence of the indigenous bacterial community (*T. denitrificans* experiments OS-15 and OS-16). Moreover, two more pyrite-amended non-inoculated experiments were performed with intact groundwater and with aquifer sediment previously autoclaved (biostimulated experiments OS-7 and OS-8). The purpose of these experiments was to assess relative contributions of solid-attached and free-living indigenous bacteria to denitrification.

Bottles were manually stirred and aqueous samples were collected at appropriate intervals using sterile syringes. The number of samples was limited to keep the solid-solution ratio at <30% of the initial value. Preliminary experiments helped to determine the frequency of sampling. All experiments lasted 100 d.

Nitrate reduction rates were computed assuming zero-order kinetics and using linear regression to fit data of nitrate concentration vs. time. The same procedure was used to calculate sulfate production rates. Nitrate reduction and sulfate production rates were further normalized to the total mass of substrate.

4.1.3.2 Flow-through experiments

Flow-through experiments were performed using polyethylene reactors of 50 mL. Input solution was circulated through the reactor by a peristaltic pump. Reactors operated in an up-flow mode with a flow rate of 0.003-0.004 mL min^{-1}, which corresponds to a hydraulic retention time (HRT) of approximately 8-14 d (Table 4.2). Experimental runs lasted 180 d, output solutions were collected periodically and chemical analyses were performed.

Two flow-through experiments were carried out to study the feasibility and long-term efficiency of bioremediation using pyrite to stimulate aquifer indigenous bacteria. Intact core fragments (8 g) and sterilized powdered pyrite (2 g) were placed into the reactors. Input solution consisted of either groundwater from the aquifer (experiment OS-

17) or a sterilized modified medium solution with 2.5 mM NO_3^- (experiment OS-18). The modified medium solution was composed of 18.7 mM NH_4Cl, 14.7 mM KH_2PO_4, 30 mM $NaHCO_3$, 3.25 mM $MgCl_2 \cdot 6H_2O$, 0.05 mM $CaCl_2 \cdot 2H_2O$ and 2.5 mM KNO_3. The solution was sparged with N_2 for 15 min before sterilization. These two flow-through experiments stimulate aquifer conditions better than the batch experiments.

Other flow-through experiments were carried out using the final solid material retrieved from the previous pyrite-amended batch experiments in order to evaluate the pyrite-driven denitrifying long-term capacity of the bacterial consortium enriched therein. The input solution consisted of either groundwater from the aquifer (experiments OS-31, OS-71 and OS-91) or the modified medium solution with 2.5 mM NO_3^- (experiments OS-41, OS-81 and OS-101).

4.1.4 Chemical and isotopic analyses

Initial groundwater and collected aqueous samples were analyzed to determine cation and anion concentrations, $\delta^{15}N$ and $\delta^{18}O$ of dissolved nitrate, alkalinity and pH. Sample aliquots were filtered through 0.22 μm syringe filters. For cation analyses, samples were acidified with 1% nitric acid and concentrations of total Fe, total S, Mg, Ca, Na, P, and K were measured by inductively coupled plasma-atomic emission spectrometry (ICP-AES). The uncertainty in the measurement of Mg, Ca, Na, S and K was estimated to be around 5%, with detection limits of 2.06, 2.50, 4.35, 3.12 and 2.56 μmol L^{-1}, respectively. The accuracy of the Fe and P measurements was estimated to be around 20% since Fe and P concentrations were close to detection limits (0.36 and 3.23 μmol L^{-1}, respectively) in most samples. Concentrations of nitrate, nitrite, chloride, and sulfate were determined by High Performance Liquid Chromatography (HPLC) using an IC-Pack Anion column and borate/gluconate eluent with 12% of HPLC grade acetonitrile. The error associated with the measurements was estimated to be 5% for nitrate, chloride and sulfate and 10% for nitrite. The sulfate concentrations measured by HPLC and those calculated from ICP sulfur elemental data were concordant within 5%, assuming that concentrations of non-

sulfate sulfur species (sulfides and sulfites) were negligible. Samples for ammonium analysis were preserved acidified to pH<2 with H_2SO_4. Ammonium concentrations were measured using an Orion ammonium ion selective electrode with an analytical uncertainty of 10% and a detection limit of 0.01 mM. pH was measured with a calibrated Crison pH Meter at room temperature (22±2 °C). The pH error was 0.02 pH units. Alkalinity in unfiltered samples was measured by titration using an Aquamerck® alkalinity test kit, with a detection limit of 0.1 meq L^{-1}.

Samples for N and O isotopes of nitrate were preserved with KOH (pH 11) and frozen prior to analysis. The $\delta^{15}N$ and $\delta^{18}O$ of dissolved nitrate were obtained following the denitrifier method (Sigman et al., 2001; Casciotti et al., 2002). Notation is expressed in terms of δ per mil relative to the international standards: V-SMOW (Vienna Standard Mean Oceanic Water) for $\delta^{18}O$ and AIR (Atmospheric N_2) for $\delta^{15}N$. The isotope ratios were calculated using international and internal laboratory standards and the results had an accuracy of 0.2 ‰ for $\delta^{15}N$ and 0.5 ‰ for $\delta^{18}O$ of nitrate. Isotopic analyses were performed at the Woods Hole Oceanographic Institution.

4.1.5 Microbial community analysis

The composition of denitrifying microbial community in aquifer groundwater, core samples, and in aqueous and solid phases retrieved at the end of one biostimulated (OS-4) and one biostimulated/bioaugmented (OS-10) batch experiment was analyzed by denaturing gradient gel electrophoresis (DGGE) of the gene *nosZ*. The total bacterial community was analyzed by DGGE using the *16S rRNA* gene as molecular marker. Selected DGGE bands were excised and sequenced. Moreover, *16S rRNA* and *nosZ* gene copy numbers were quantified by quantitative polymerase chain reaction (qPCR). Molecular analyses were performed at the GIRO Technological Centre.

4.1.5.1 DNA extraction

To extract total DNA from initial groundwater and from aqueous samples of batch experiments, the samples were concentrated by filtering through 0.22-µm cellulose

acetate filters (200 mL of groundwater or 50 mL of aqueous samples). Sediment (0.25 g approximately) was collected from the aquifer and at the end of the batch experiments for subsequent DNA extraction. Samples were stored at -20°C prior to analysis.

Total DNA from the frozen solid samples and from the frozen filters was extracted in duplicate using a bead beating protocol by means of the commercial PowerSoil™ DNA Isolation Kit (Mo-Bio) following the manufacturer's instructions. No further purification was required to prevent PCR inhibition.

4.1.5.2 Amplification by PCR

The V3-V5 variable regions of the *16S rRNA* gene were amplified using the 16S-F341-GC and 16S-R907 primers (Yu and Morrison, 2004). Table 4.3 shows the primers used. The F341-GC primer included a GC clamp at the 5′ end (5′-CGCCCGCCGCGCCCCGCGCCCGTCCCGCCGCCCCCGCCCG-3′). Fragments of the *nosZ* gene were amplified using the primers *NosZ*-F (Kloos et al., 2001) and *NosZ*1622R-GC (Throbäck et al., 2004). The 22R-GC primer included a GC clamp at the 5′ end (5′-GGCGGCGCGCCGCCCGCCCCGCCCCCGTCGCCC-3′). All PCR reactions were performed in a Mastercycler (Eppendorff). Each reaction mixture (50 μL) contained 1.25 U of Takara Ex Taq DNA polymerase (Takara Bio Inc.), 25 mM TAPS (pH 9.3), 50 mM KCl, 2 mM $MgCl_2$, 200 μM each deoxynucleoside triphosphate, 0.5 μM each primer and 100 ng of template DNA quantified using a Low DNA Mass Ladder (Gibco BRL) and Nanodrop (ND-1000, Nanodrop Technologies).

The PCR profile consisted in an initial denaturation at 94°C for 5 min followed by 30 cycles of the following steps: one denaturation step at 94°C for 1 min, one annealing step at 55°C /53°C (*16S rRNA*/*nosZ*, respectively) for 1 min and one elongation step at 72°C for 45 s. The last step involved an extension at 72°C for 10 min (Table 4.4). Amplicons were purified prior to the DGGE analysis using the DNA purification system Wizard® Plus SV (Promega Corporation).

Primer	Position [1]	Gene target	Number of bases	5´→ 3´ sequence	PCR / sequencing program	Hybridization temperature	Reference
16S-F341-GC [2]	341-357	*16S rRNA*	17-47	CCT ACG GGA GGC AGC AG	I/IV	55 ºC	Yu and Morrison (2004)
16S-R907	907–926	*16S rRNA*	20	CCG TCA ATT CCT TTR AGT TT	I/II/IV	55 ºC	Yu and Morrison (2004)
NosZ-F	1169–1188	*nosZ*	20	CGY TGT TCM TCG ACA GCC AG	III	53 ºC	Kloos et al. (2001)
NosZ 1622R-GC [3]	1603–1622	*nosZ*	20	CGS ACC TTS TTG CCS TYG CG	III	53 ºC	Throbäck et al. (2004)

(1) The numbers for positions of *nosZ* primers are the numbers of bases for the beginning of *nosZ* gene in *Pseudomonas aeruginosa* DSM 50071, whereas the numbers used for the position of *16S rRNA* primers are the numbers in the corresponding *Escherichia coli* sequence

(2) GC clamp sequence: 5'- CGC CCG CCG CGC CCC GCG CCC GTC CCG CCG CCC CCG CCC G

(3) GC clamp sequence: 5'-GGC GGC GCG CCG CCC GCC CCG CCC CCG TCG CCC

Table 4.3. Sequences of the primers used in the PCR assays.

Program	Polymerase activation	Denaturation	Annealing	Elongation	Number of cycles	Extension
I. PCR *16S rRNA*-DGGE	94 ºC 5 min	94 ºC 1 min	55 ºC 1 min	72 ºC 45 s	30	72 ºC 10 min
II. Sequencing *16S rRNA*	96 ºC 1 min	96 ºC 10 s	55 ºC 5 s	60 ºC 4 min	25	-
III. PCR *nosZ*-DGGE	94 ºC 5 min	94 ºC 1 min	53 ºC 1 min	72 ºC 45 s	30	72 ºC 10 min
IV. Reamplification DGGE bands	-	94 ºC 30 s	55 ºC 30 s	72 ºC 45 s	30	72 ºC 5 min

Table 4.4. PCR and sequencing programs.

4.1.5.3 Denaturing Gradient Gel Electrophoresis (DGGE)

Approximately 800 ng of purified PCR products quantified using Nanodrop (ND-1000) were loaded onto 8% (w/v) polyacrylamide gels (0.75 mm thick to obtain a better resolution), with denaturing gradients ranging from 30 to 70% (100% denaturant contains 7M urea and 40% (w/v) formamide). The DGGE analyses were performed in a 1×TAE buffer solution (40 mM Tris, 20 mM sodium acetate, 1 mM EDTA, pH 7.4) using a DGGE-4001 System (CBS Scientific Company) at 100V and 60°C for 16 h.

4.1.5.4 Analysis of DGGE images

The DGGE gels were stained for 45 min in a 1×TAE buffer solution containing SybrGold (Molecular Probes, Inc.) and then scanned under blue light by means of a Blue-converter plate (UVP) and a UV Transilluminator (GeneFlash Synoptics Ltd). DGGE

bands were processed using the Gene Tools software v. 4.0 (SynGene Synoptics) and corrected manually. After normalization of the gels, bands with relative peak area intensity exceeding 2% were set aside for further analyses.

4.1.5.5 Sequencing and phylogenetic analysis of DGGE bands

Selected DGGE bands were removed with a sterile razor blade, resuspended in 50 μL sterilized MilliQ water and stored at 4°C overnight. A 1:100 dilution of supernatant was used to reamplify the 16SrRNA DGGE bands with the primers 16S-F341-GC and 16S-R907. Reamplification conditions consisted in 30 cycles of the following steps: one denaturation step at 94°C for 30 s, one annealing step at 55°C for 30 s and one elongation step at 72°C for 45 s. The last step involved an extension at 72°C for 5 min. (Table 4.4).

Finally, band amplicons were sequenced using the primer 16R907 without GC-clamp. Sequencing conditions consisted in an initial denaturation step at 96°C for 1 min, followed by 25 cycles of one denaturation step at 96°C for 10 s, one annealing step at 55°C for 5 s and one elongation step at 60°C for 4 min. (Table 4.4). Sequencing was accomplished using the ABI Prism Big Dye Terminator cycle-sequencing reaction kit version 3.1 (Perkin-Elmer Applied Biosystems) and an ABI 3700 DNA sequencer (PE Applied Biosystems) following the manufacturer's instructions. Sequences were edited and assembled using a version 7.0.9.0 of the BioEdit software (Hall, 1999) and were inspected for the presence of ambiguous base assignments. The sequences were then subjected to the Check Chimera program of the Ribosomal Database Project (Maidak et al., 2000) and aligned against GenBank database by using the alignment tool comparison software BLASTn and RDP search (Altschul et al., 1990; Maidak et al., 2000).

The *16S rRNA* gene nucleotide sequences determined in the present study were deposited into the GenBank database under accession numbers HM765437-HM765449.

4.1.5.6 Quantitative PCR assays

Two independent real-time qPCR reactions were performed for each gene (*16S rRNA* and *nosZ*), for each duplicate genomic DNA extraction. qPCR assays were run on a

MX3000P Real Time PCR equipment (Stratagene) using a reaction volume of 25 μl by using SYBR® Green I qPCR Master Mix (Stratagene). Amplification of products was obtained by using the primers 519F/907R each of them at 200nM for *16S rRNA* gene (Lane, 1991) and *nosZ*1F/*nosZ*1R each of them at 200 nM for *nosZ* gene (Kandeler et al., 2006) (Table 4.5).

Primer	Position [(1)]	Gene target	5´→ 3´ sequence	Reference
519F	519-536	*16S rRNA*	GCCAGCAGCCGCGGTAAT	Lane (1991)
907R	907-926	*16S rRNA*	CCGTCAATTCCTTTGAGTTT	Lane (1991)
nosZ 1F	1184-1203	*nosZ*	WCSYTGTTCMTCGACAGCCAG	Kandeler et al. (2006)
nosZ 1R	1443-1421	*nosZ*	ATGTCGATCARCTGVKCRTTYTC	Kandeler et al. (2006)

(1) The numbers for positions of *nosZ* primers are the numbers of bases for the beginning of *nosZ* gene in *Pseudomonas aeruginosa* DSM 50071, whereas the numbers used for the position of *16S rRNA* primers are the numbers in the corresponding *Escherichia coli* sequence

Table 4.5. Sequences of the primers used in the qPCR assays.

Thermal cycling conditions for the *nosZ*1 primers were as follows: an initial cycle at 95°C for 10 min followed by 40 cycles of 95°C for 30 s, 62°C for 1 min and 80°C for 15 s (fluorescence acquisition step). The thermocycling steps of the qPCR for *16S rRNA* amplification included an initial cycle at 95°C for 10 min and 40 cycles of 95°C for 30 s, 50°C for 30 s, 72°C for 45 s and 80°C for 15 s (fluorescence acquisition step). Product size and purity were confirmed by both melting-curve analysis (Mx3000P real-time PCR instrument software, version 4.0) and gel electrophoresis. Serial dilutions of total DNA extracts from sediment/water samples were quantified and compared to check for the potential presence of PCR inhibitors.

To perform calibration curves, standards were prepared with serial dilutions of a given amount of environmental clone-plasmids containing PCR amplicons of the *16S rRNA* or the *nosZ* gene. Standard curves obtained from both genes showed a linear range between 10^1 and 10^8 gene copies reaction^{-1}, with slopes ranging from -3.3 to -3.5 (Fig. 4.1). The calculated PCR efficiencies for *16S rRNA* and *nosZ* assays were 96 and 97%, respectively.

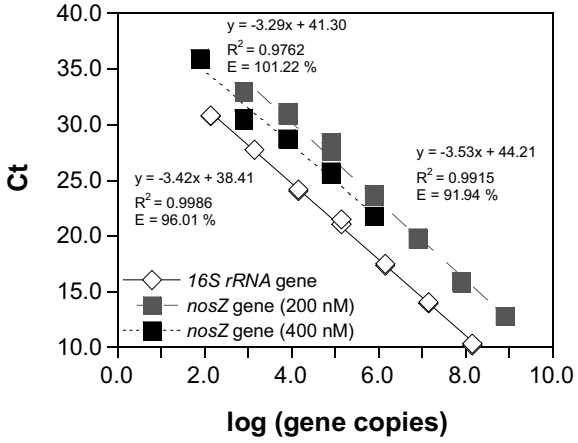

Figure 4.1. Standard curves of the *16S rRNA* and *nosZ* assays obtained by plotting the gene copy numbers of the plasmids versus the cycle number required to elevate the fluorescence signal above the threshold. The PCR efficiencies (E) of the assays are shown.

4.2 Results

4.2.1 Blank and control batch experiments

Figure 4.2 and Table 4.6 show the results of the batch experiments. Specific data for each treatment are shown in Appendix D.

In the blank experiment (OS-13), chemically-driven nitrate reduction did not occur (Fig. 4.2a), and sulfate was released to solution (Fig. 4.2b). In the pyrite-free control experiments (OS-1, OS-2, OS-11 and OS-12), no significant nitrate reduction occurred (Fig. 4.2a) and no significant changes in alkalinity were observed. These results indicate a low background level of electron acceptor needed for nitrate reduction in the aquifer material. Between 0.1 and 0.2 mM sulfate was produced in these pyrite-free experiments (Table 4.6 and Fig. 4.2b), showing the dissolution of the scarce pyrite present in the marl core fragments.

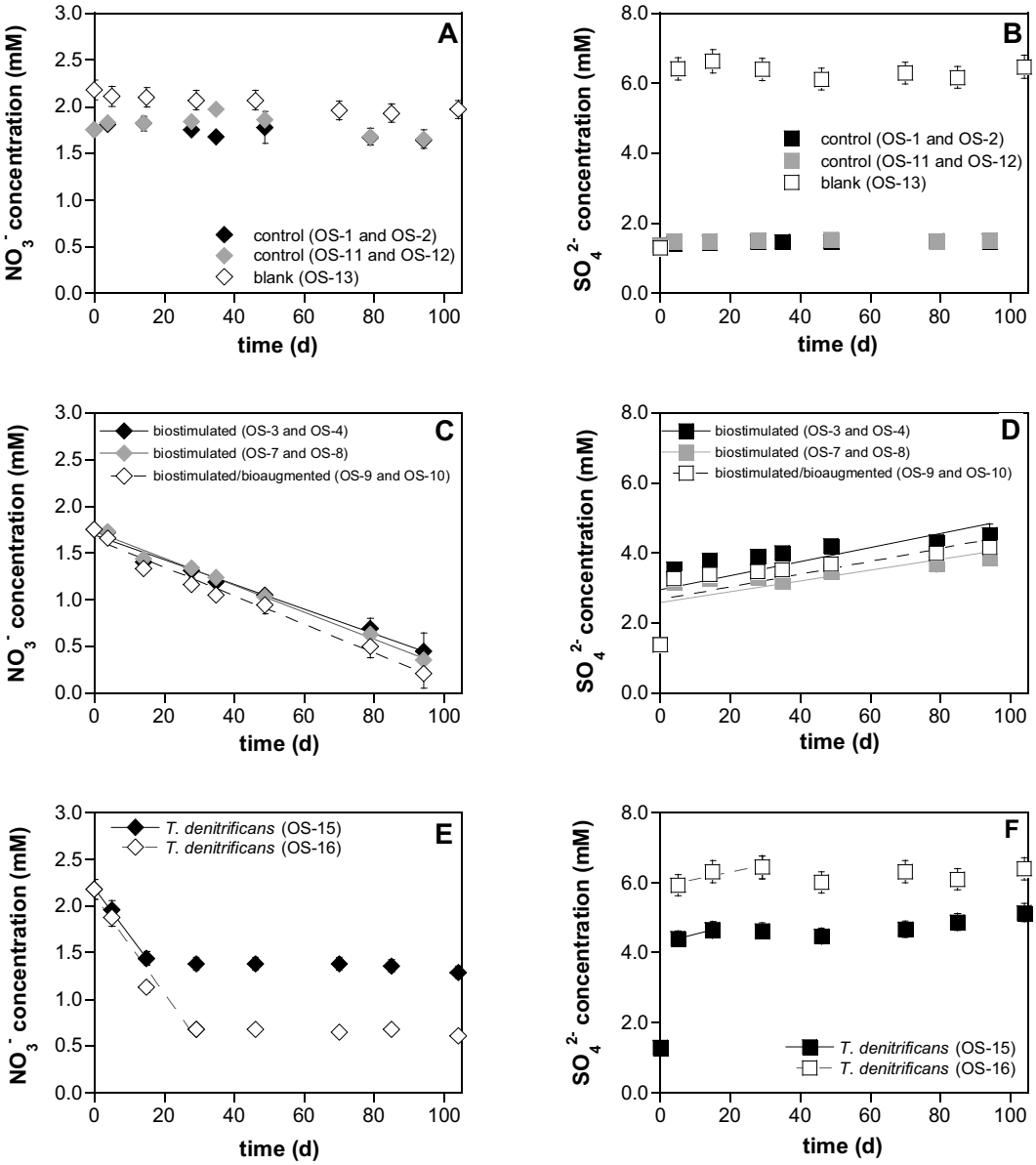

Figure 4.2. Variation of nitrate and sulfate concentration over time in batch experiments. (a) Variation of nitrate concentration vs. time in the blank and control experiments; (b) Variation of sulfate concentration vs. time in the blank and control experiments; (c and e) Consumption of nitrate over time in the pyrite-amended experiments; (d and f) Production of sulfate over time in the pyrite-amended experiments. Lines represent the fit of measured nitrate and sulfate concentration versus time used to compute zero-order nitrate reduction and sulfate production rates, respectively (see Table 4.6).

Table 4.6. Results of blank, control and pyrite-amended batch experiments.

Exp.	*T. denitrificans* inoculum	Nitrate reduction rate (1)			Nitrate reduced	Sulfate produced (0 - 4 d)	Sulfate produced (4 d - end)	Sulfate production rate (2)			NO_3 reduction rate / SO_4 production rate	% of NO_3 reduction related to pyrite oxidation (3)
	cells mL^{-1}	mmol NO_3^- L^{-1} d^{-1}	µmol NO_3^- kg^{-1} d^{-1}	R^2	mM	mM	mM	mmol SO_4^{2-} L^{-1} d^{-1}	µmol SO_4^{2-} kg^{-1} d^{-1}	R^2		
Blank experiment												
OS-13	-	-	-	-	-	5.06	-	-	-	-	-	-
Control experiments												
OS-1	-	-	-	-	-	0.04	-	-	-	-	-	-
OS-2	-	-	-	-	-	0.06	-	-	-	-	-	-
OS-11	-	-	-	-	-	0.04	-	-	-	-	-	-
OS-12	-	-	-	-	-	0.20	-	-	-	-	-	-
Pyrite-amended experiments												
Biostimulated experiments												
OS-3	-	0.012	303	0.970	1.17	2.31	0.63	0.007	180	0.944	1.7	89
OS-4	-	0.014	360	0.989	1.43	2.02	1.34	0.012	311	0.914	1.2	130
OS-7	-	0.014	353	0.993	1.37	1.66	0.70	0.007	174	0.947	2.0	74
OS-8	-	0.015	368	0.992	1.42	1.95	0.69	0.008	189	0.992	1.9	77
mean±sd		0.014±0.001	346±29		1.35±0.12	1.99±0.27	0.84±0.33	0.009±0.003	214±65		1.7±0.4	92±26
Biostimulated/bioaugmented experiments												
OS-9	6.6×10^7	0.014	350	0.971	1.43	1.88	0.81	0.009	216	0.992	1.6	93
OS-10	6.6×10^7	0.017	416	0.987	1.65	1.91	0.97	0.011	273	0.989	1.5	99
mean±sd		0.015±0.002	383±47		1.54±0.16	1.90±0.02	0.89±0.12	0.010±0.002	245±40		1.6±0.1	96±4
T. denitrificans experiments												
OS-15	1.2×10^8	0.051	1268	0.998	0.75	3.04	0.24	0.024	590	-	2.1	70
OS-16	1.2×10^8	0.053	1314	0.960	1.50	4.56	0.51	0.021	514	0.868	2.6	59
mean±sd		0.052±0.001	1291±32		1.12±0.53	3.80±1.07	0.37±0.20	0.022±0.002	552±54		2.4±0.3	64±8

(1) In the OS-15 and OS-16 experiments, nitrate reduction rates were calculated during the first 15 and 29 d, respectively. Afterwards, nitrate reduction stopped (see text)

(2) Sulfate production rate was calculated from 4 d to the end of the experiments, except for the OS-15 and OS-16 experiments, in which it was calculated from 4 d to 15 and 29 d, respectively (see text)

(3) The percentage of nitrate reduction related to pyrite oxidation was calculated comparing the obtained ratio of nitrate reduction rate to sulfate production rate with the stoichiometry of the overall reaction (Eq. 4.3)

4.2.2 Pyrite-amended batch experiments

In the batch experiments where activity of indigenous aquifer bacteria was stimulated by adding pyrite (biostimulated experiments OS-3 and OS-4), initial nitrate concentration of 1.75 mmol L^{-1} decreased to less than 0.60 mmol L^{-1} within 94 days (Fig. 4.2c). Ammonium concentration was below the detection limit (0.01 mmol L^{-1}). No transient nitrite accumulation occurred and sulfate was released to solution (Fig. 4.2d). Total iron concentration was below the detection limit (0.36 μmol L^{-1}). This suggests that ferrous iron was also involved in nitrate reduction, being oxidized to ferric iron and precipitated (solution pH ranged 6.8-7.2). The average nitrate reduction rate was 332±40 μmol NO_3^- kg^{-1} d^{-1} (Table 4.6).

In the biostimulated experiments performed with intact groundwater and with aquifer solid material previously autoclaved (biostimulated experiments OS-7 and OS-8), both nitrate reduction and sulfate release occurred (Fig. 4.2c and 4.2d). The decrease in nitrate concentration and the release of sulfate were similar to those of biostimulated experiments amended with pyrite using non-sterilized core fragments and groundwater (OS-3 and OS-4). The average nitrate reduction rate was also similar to that of the OS-3 and OS-4 experiments (361±11 μmol NO_3^- kg^{-1} d^{-1}, Table 4.6).

In the pyrite-amended batch experiments with the indigenous community and inoculated with the *T. denitrificans* culture (biostimulated/bioaugmented experiments OS-9 and OS-10), the variation of nitrate and sulfate concentrations was similar to that in the biostimulated experiments (Fig. 4.2c and 4.2d). Concentration of nitrite, ammonium and iron was below the detection limits as in the biostimulated experiments. The average nitrate reduction rate was 383±47 μmol NO_3^- kg^{-1} d^{-1}, which is slightly higher than the rate obtained in the biostimulated experiments (Table 4.6).

In the pyrite-amended batch experiments inoculated with *T. denitrificans* and using previously autoclaved aquifer material and groundwater (*T. denitrificans* experiments OS-15 and OS-16), nitrate reduction and sulfate release also occurred (Fig. 4.2e and 4.2f).

However, after 15 d in the OS-15 experiment and after 29 d in the OS-16 experiment, nitrate reduction ceased with about 65% and 30% of the initial nitrate remaining in solution, respectively. The cessation of nitrate reduction was attributed to the decrease in pH to 6.2, which was low enough to affect activity of denitrifying bacteria (see chapter 3; Knowles, 1982). In the remaining experiments, pH was always higher than 6.5. In the OS-15 and OS-16 experiments, concentration of iron was also below the detection limit. Transient nitrite accumulation occurred during the first 45 d. Nevertheless, nitrite was completely removed after 70 d. The averaged nitrate reduction rate (1291±32 μmol NO_3^- kg^{-1} d^{-1}) was about a factor of 3 higher than those for the experiments with only indigenous bacteria (biostimulated experiments OS-3, OS-4, OS-7 and OS-8) and for the experiments with both indigenous and inoculated bacteria (biostimulated/bioaugmented experiments OS-9 and OS-10).

Regardless of the behavior of the nitrate, a significant amount of sulfate was produced during the first 4 d (between 1.6 and 4.6 mM, Table 4.6, Fig. 4.2d and 4.2f). Approximately 5 mM sulfate was also released in the blank experiment during the first 4 d (Table 4.6 and Fig. 4.2b). This release of sulfate could be attributed to pyrite oxidation by an oxidant other than nitrate (e.g. traces of dissolved oxygen). The sulfate production rates were calculated using changes in sulfate concentration measured after 4 d (Table 4.6). In the OS-15 and OS-16 experiments, the sulfate production rate was calculated only from 4 d to 15 and 29 d, respectively, because nitrate reduction occurred only during this period (Fig. 4.2e and 4.2f).

The ratio between the nitrate removal rate and the sulfate production rate (NO_3/SO_4) was calculated for each pyrite-amended batch experiment (Table 4.6). Denitrification coupled to pyrite oxidation is expressed as the following reaction, assuming a negligible accumulation of intermediate N-gaseous products of the reaction (e.g. NO and N_2O):

$$14NO_3^- + 5FeS_2 + 4H^+ \Rightarrow 7N_2 + 10SO_4^{2-} + 5Fe^{2+} + 2H_2O \quad (4.1)$$

If the Fe^{2+} produced is oxidized:

$$NO_3^- + 5Fe^{2+} + 6H^+ \Rightarrow \frac{1}{2}N_2 + 5Fe^{3+} + 3H_2O \quad (4.2)$$

an overall reaction is expressed as:

$$15NO_3^- + 5FeS_2 + 10H_2O \Rightarrow \frac{15}{2}N_2 + 5Fe(OH)_3 + 10SO_4^{2-} + 5H^+ \quad (4.3)$$

The measured NO_3/SO_4 ratio was compared with the stoichiometric molar ratio of the overall reaction (Eq. 4.3), which equals 1.5.

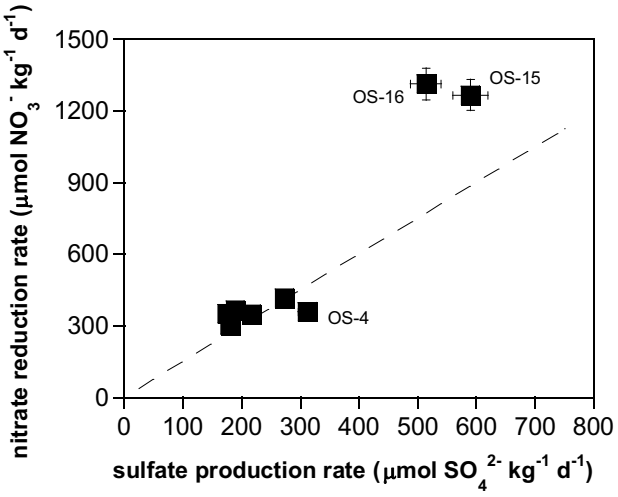

Figure 4.3. Sulfate production rate vs. nitrate reduction rate in the pyrite-amended batch experiments. Straight line shows the expected NO_3/SO_4 ratio of 1.5, following stoichiometry of Eq. 4.3.

In one experiment (OS-4), the NO_3/SO_4 ratio was 1.2, which is somewhat lower than the stoichiometric ratio. This was probably due to an excess of sulfate (0.38 mM) that resulted from pyrite dissolution by traces of dissolved oxygen. Nonetheless, in most of

the experiments with indigenous bacteria (biostimulated and biostimulated/bioaugmented experiments), the NO_3/SO_4 ratios ranged between 1.5 and 2.0, suggesting that between 74 and 99% of nitrate reduction was ascribed to pyrite oxidation (Table 4.6 and Fig. 4.3). Furthermore, in the experiments with only inoculated bacteria (*T. denitrificans* experiments OS-15 and OS-16), the ratio was 2.2 and 2.6, indicating that pyrite oxidation accounted for 59% and 70% of the nitrate reduction, respectively (Table 4.6). The residual fraction of nitrate reduced could be attributed to heterotrophic denitrification.

4.2.3 Flow-through experiments

The performance of two representative flow-through experiments as a function of time is illustrated in Figures 4.4 and 4.5. Specific data for each flow-through experiment are shown in Appendix D.

Nitrate reduction and sulfate release occurred in the two pyrite-amended flow-through experiments performed with intact core fragments (OS-17 and OS-18, Fig. 4.4). In the experiment in which groundwater was used as the input solution (OS-17), complete nitrate removal was achieved after 14 d and lasted until the end of the experiment (150 d) (Fig. 4.4a). In the experiment with the sterilized 2.5 mM NO_3^- modified medium used as the influent (OS-18), complete nitrate removal was attained after 24 d and lasted for the 180-d test period (Fig. 4.4c). In both experiments, nitrite was not detected in the effluent solutions except in the first samples where nitrate consumption was incomplete. Figures 4.4b and 4.4d show that the output S concentration was higher at the start of the experiments, subsequently decreasing until a steady state was attained. This high concentration at the beginning of the experiments was probably due to the dissolution of an outer layer of the pyrite grains or to the dissolution of microparticles attached to pyrite surfaces (Lasaga, 1998).

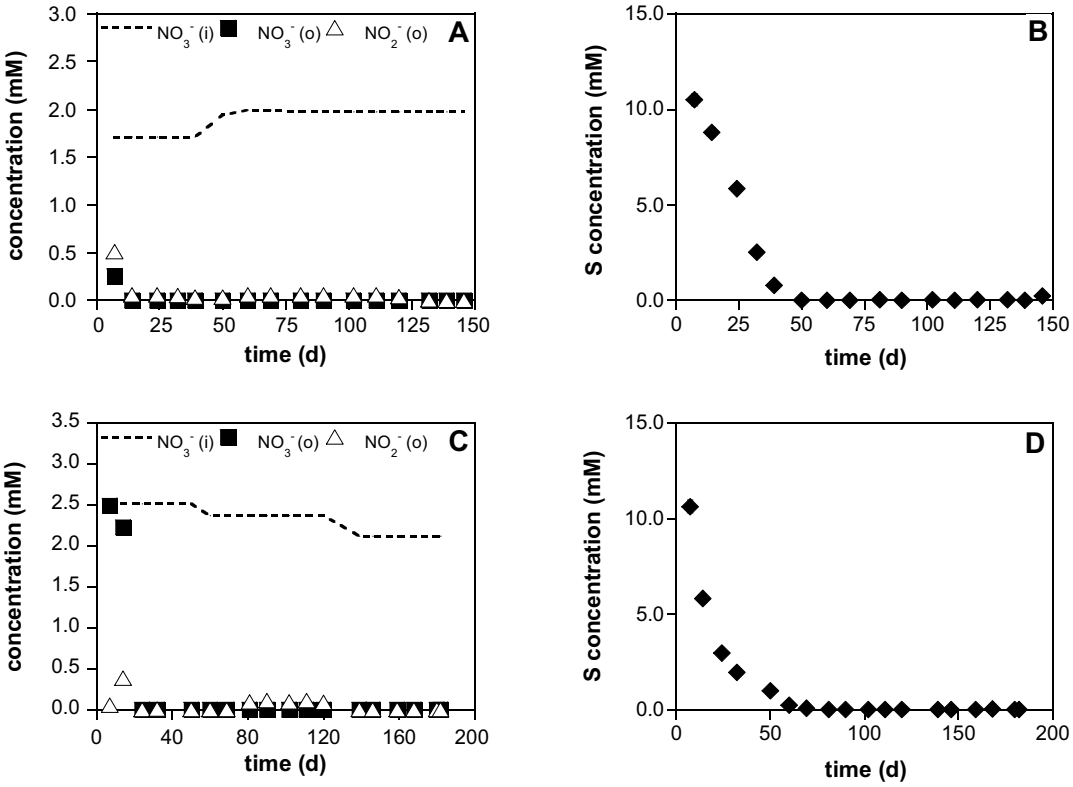

Figure 4.4. Variation of nitrate, nitrite and S concentration over time in the pyrite-amended flow-through experiments performed with intact aquifer solid material. Consumption of nitrate (a) and production of S (b) over time in the OS-17 experiment, with groundwater as the input solution; consumption of nitrate (c) and production of S (d) over time in the OS-18 experiment, with the sterilized 2.5 mM NO_3^- solution as the influent. i: input solution; o: output solution.

Figure 4.5 shows that nitrate reduction and sulfate release also occurred in the flow-through experiments performed using the pyrite and aquifer material with attached biomass of autotrophically acclimated culture retrieved from previous batch experiments. In most of these experiments, complete nitrate removal was achieved after 14 d (Fig. 4.5a and 4.5c). However, complete nitrate removal was attained after 7 d in the OS-91 and OS-101 experiments, which were carried using the material retrieved from the OS-9 and OS-10 batch experiments, which were initially inoculated with *T. denitrificans* (see Appendix D). In all these experiments, nitrite was only detected in the first sample, and S concentration decreased over time until a steady state was achieved (Fig. 4.5b and 4.5d).

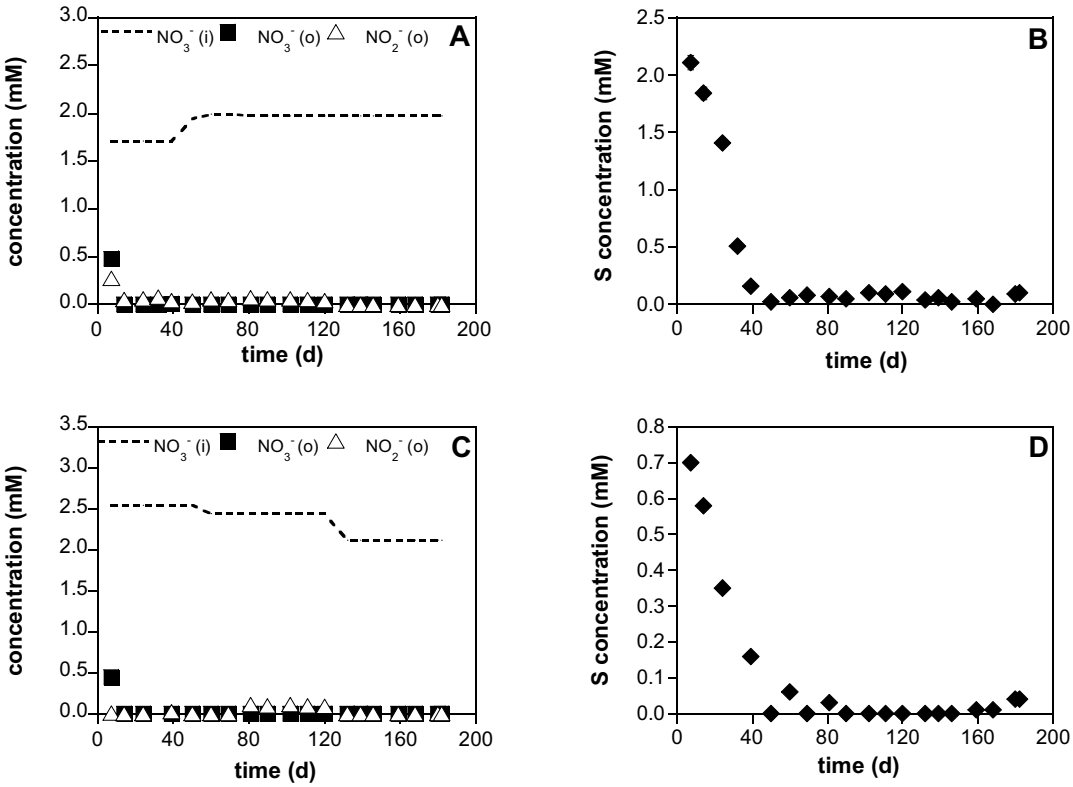

Figure 4.5. Variation of nitrate, nitrite and S concentration over time in two of the flow-through experiments performed with final solid material retrieved from the previous batch experiments. Consumption of nitrate (a) and production of S (b) over time in the OS-31 experiment, with final solid material resulted from the previous OS-3 batch experiment and using groundwater as the input solution. Consumption of nitrate (c) and production of S (d) over time in the OS-41 experiment, with final solid material retrieved from the previous OS-4 batch experiment and using the sterilized 2.5 mM NO_3^- solution as the input solution. i: input solution; o: output solution.

Considering the amounts of nitrate reduced and sulfate produced in the flow-through experiments, between 50 and 99% of the denitrification should be attributed to heterotrophic denitrifying bacteria in line with the stoichiometry of the overall pyrite-driven denitrification reaction (Eq. 4.3).

4.2.4 Isotopic fractionation

During denitrification, as nitrate decreases, residual nitrate becomes enriched in the heavy isotopes ^{15}N and ^{18}O. The denitrification reaction describes a Rayleigh distillation

process (Eq. 4.4 and 4.5), where ε is the isotopic enrichment factor that depends on the aquifer materials and characteristics (Mariotti et al., 1981):

$$\delta^{15}N_{residual} = \delta^{15}N_{initial} + \varepsilon_N \ln f \quad (4.4)$$

$$\delta^{18}O_{residual} = \delta^{18}O_{initial} + \varepsilon_O \ln f \quad (4.5)$$

where f is the unreacted portion of nitrate (residual nitrate concentration divided by initial nitrate concentration), and $\delta_{residual}$ and $\delta_{initial}$ are the nitrogen or oxygen isotopic compositions (‰) of the residual and initial nitrate, respectively.

The N and O isotopic enrichment factors in two pyrite-amended batch experiments (biostimulated experiment OS-4 and biostimulated/bioaugmented experiment OS-10) were calculated from the slope of the regression lines that fit data of nitrate concentration vs. $\delta^{15}N$ or $\delta^{18}O_{NO3}$, respectively.

The nitrogen isotopic enrichment factor (εN) was calculated as -27.61‰ and -25.02‰ for the OS-4 and OS-10 experiments, respectively (Fig. 4.6a). The oxygen isotopic enrichment factor (εO) was -21.27‰ and -19.49‰, respectively (Fig. 4.6b) and the εN/εO ratios were 1.30 and 1.28, respectively (Fig. 4.7).

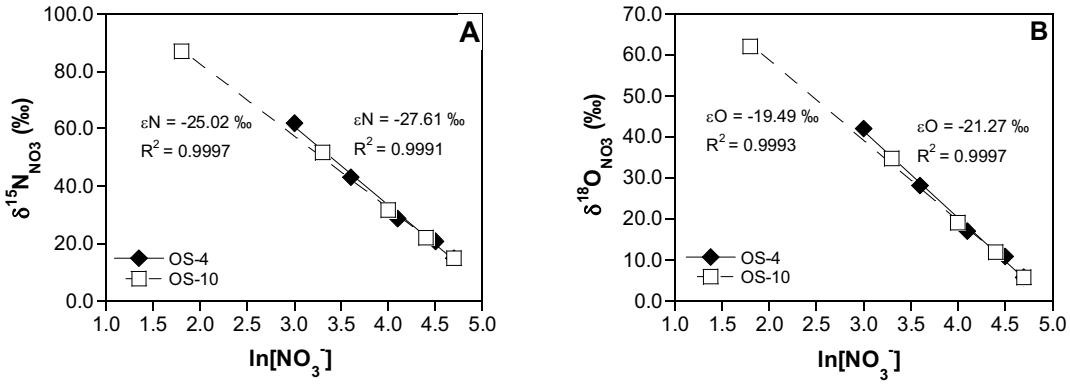

Figure 4.6. Isotopic results of the OS-4 (biostimulated) and the OS-10 (biostimulated/bioaugmented) pyrite-amended batch experiments. (a) $\delta^{15}N$ vs. $\ln[NO_3^-]$; (b) $\delta^{18}O_{NO3}$ vs. $\ln[NO_3^-]$. Values of εN and εO were obtained from the slope of the regression lines.

Table 4.7. Estimated isotopic enrichment factors (εN and εO) and εN/εO ratios obtained in this study and reported in the literature for *in situ* natural denitrification in aquifers and for denitrification in laboratory experiments with sediments from aquifers.

εN (‰)	εO (‰)	εN / εO	Reference	Notes
In situ studies				
-22.9	n.d.	2.1	Aravena and Robertson (1998)	septic sands, multilevel wells
-15.9	-8.0	2.1	Bottcher et al. (1990)	gravelly sand, multilevel wells along a groundwater flux line
-4.7 to -5	n.d.	n.d.	Mariotti et al. (1988)	chalk, wells located along a groundwater flux line
-27.6	-18.3	1.5	Mengis et al. (1999)	riparian zone, wells located along a groundwater flux line
-30±6	n.d.	n.d.	Vogel et al. (1981)	confined aquifer in Kalahari
-9.6	n.d.	n.d.	Spalding and Exner (1993)	multilevel wells
-10	n.d.	n.d.	Spalding and Parrot (1994)	multilevel wells located along a groundwater flux line
-11 to -16	n.d.	n.d.	Bates and Spalding (1998)	
-16	n.d.	n.d.	Bates et al. (1998)	
-4	n.d.	n.d.	Pauwels et al. (2000)	schist, multilevel wells sampled at different time
-13.62	-9.8	1.3	Fukada et al. (2003)	sand and gravel, wells located along a groundwater flux line
-7 to -57	n.d.	n.d.	Singleton et al. (2007)	multilevel wells
-13.9	n.d.	n.d.	Smith et al. (1991)	sand and gravel, multilevel wells
-8.38	n.d.	n.d.	Clément et al. (2003)	riparian zone, wells located along a groundwater flux line
-4 to -5.2	n.d.	n.d.	Fustec et al. (1991)	shallow alluvial groundwater, multilevel wells
n.d.	n.d.	1.7	Cey et al. (1999)	multilevel wells
n.d.	n.d.	1.8	Devito et al. (2000)	sand
-17.9	n.d.	n.d.	Tsushima et al. (2002)	sand and gravel, multilevel wells
-4.4 to -15.5	-1.9 to -8.9	0.9 to 2.3	Chapter 2	carbonate and carbonate-sandstone, confined aquifer (Osona aquifer)
Laboratory studies				
-32.9 to -34.1	n.d.	n.d.	Tsushima et al. (2006)	sediment + groundwater with adjusted NO_3^- concentration, column experiments
-14.6	n.d.	n.d.	Grischek et al. (1998)	aquifer material + river water, column experiments. Sand, silt and gravel aquifer
-17.8	n.d.	n.d.	Sebilo et al. (2003)	rich muddy river bottom sediments, stirred batch experiments
-27.6	-21.3	1.30	this study, OS-4	Osona aquifer sediment + groundwater + pyrite, batch experiment
-25.0	-19.5	1.28	this study, OS-10	Osona aquifer sediment + groundwater + pyrite + *T. denitrificans* culture, batch experiment

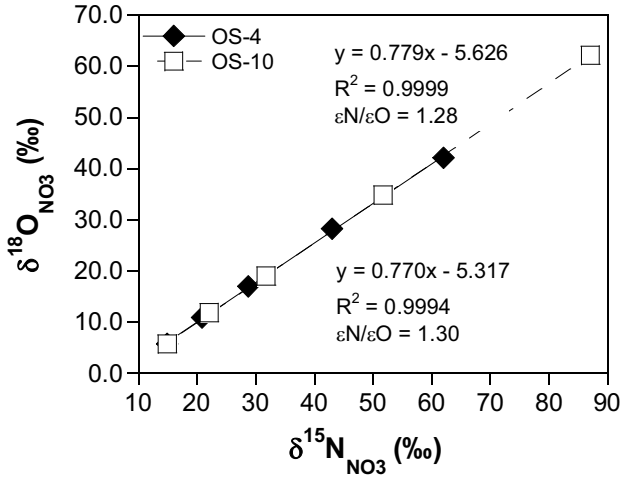

Figure 4.7. $\delta^{18}O$ vs. $\delta^{15}N_{NO3}$ of the OS-4 (biostimulated) and OS-10 (biostimulated/bioaugmented) pyrite-amended batch experiments.

The values of εN are within the range of denitrification enrichment factors attained from laboratory experiments with material from other aquifers (-14.6‰ to -34.1‰; Grischek et al., 1998; Sebilo et al., 2003; Tsushima et al., 2006; Table 4.7).

To our knowledge, the O isotopic enrichment factors associated with denitrification and hence the εN/εO ratios, have not been determined in the laboratory using aquifer sediments. The isotopic enrichment factors and the εN/εO ratios were therefore compared with those estimated for natural groundwater denitrification (Table 4.7). In these *in situ* studies, the εN ranged from -57‰ (Singleton et al., 2007) to -4‰ (Fustec et al., 1991) and only three values of εO have been found: -8.0‰ (Böttcher et al., 1990), -9.8‰ (Fukada et al., 2003), and -18.3‰ (Mengis et al., 1999). The enrichment factors calculated in the present experiments are in general higher than the ones reported in field studies, including the values estimated in chapter 2 for the Osona aquifer (Table 4.7). This difference is consistent with the commonly found discrepancy between enrichment factors for *in situ* studies and those for laboratory experiments. This divergence is attributed to the heterogeneity of aquifers, diversity of microbial communities, variations in temperature, variable presence of electron donors, dispersion effect in the transport of

nitrate and the occurrence in groundwater of other nitrate sinks (Mariotti et al., 1988; Kawanishi et al., 1993).

The εN/εO ratios obtained in the present study are in agreement with reported ratios from *in situ* groundwater studies (Table 4.7) that range from 1.3 (Fukada et al., 2003) to 2.1 (Böttcher et al., 1990; Aravena and Robertson, 1998) and with those estimated in chapter 2 for the Osona aquifer (between 0.9 and 2.3, Table 4.7). Furthermore, the ratios are very close to the εN/εO ratio of 1.15 for pyrite-driven denitrification obtained in the laboratory experiments with pure cultures of *T. denitrificans* of chapter 3.

4.2.5 PCR-DGGE analysis of microbial community

The effects of the two bioremediation treatments on the aquifer bacterial community were analyzed by DGGE by using initial and final samples from the OS-4 (biostimulated) and the OS-10 (biostimulated/bioaugmented) experiments. Based on the visual comparison of the *16S rRNA*-based DGGE patterns before and after the experiments, both treatments produced changes in the composition of the dominant bacterial populations (Fig. 4.8).

The DGGE banding pattern of original groundwater (lanes GW) was compared with patterns of final aqueous samples from the two treatments (lanes WB and WBB). The original groundwater showed 5 faint bands (B2 to B6). Addition of pyrite or addition of pyrite and *T. denitrificans* resulted in the disappearance of these bands and in the appearance of novel predominant bands. A number of bands were common to the final aqueous samples of the two treatments (e.g. B10 and B25, B11 and B29, B13 and B30). However, other bands were unique to the biostimulated treatment (B14, B15 and B16) and to the biostimulated/bioaugmented experiment (B26-27 and B28).

Selected bands were excised and sequenced and the taxonomic assignment of each excised band was performed. Table 4.8 shows the closest relatives of the excised *16S rRNA* DGGE bands. The sequence analysis of the B10 and B25 bands indicated a 97% similarity with the *16S rRNA* gene of *Sediminibacterium sp*., grouped with the *Bacteroidetes*

phylum. The B11 and B29 bands were closely related to an unclassified *β-proteobacteria* (96% similarity), which belongs to the *Methylophilaceae* family. The B30 band was similar (98% similarity) to an unclassified *γ-proteobacteria*, which is closely related to the *Xanthomonadaceae* family.

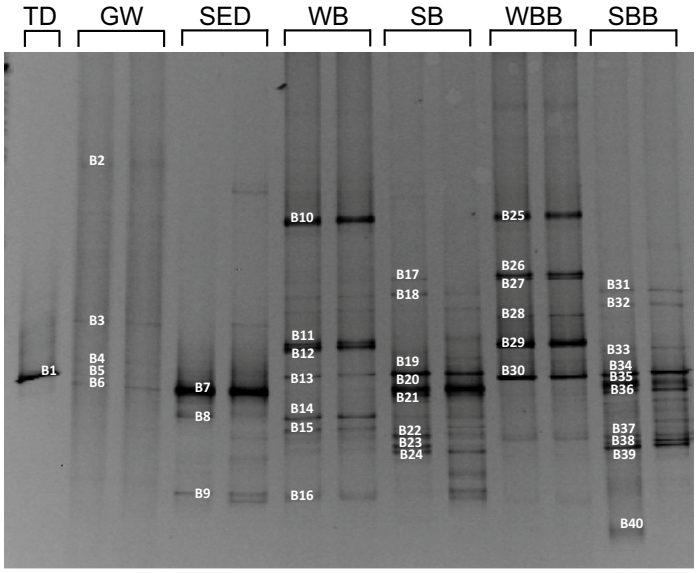

Figure 4.8. DGGE profiles of PCR-amplified *16S rRNA* genes (V3-V5 hypervariable region) from the studied samples. TD: *T. denitrificans* strain; GW: original aquifer groundwater; SED: original aquifer sediment; WB: aqueous sample at the end of the OS-4 biostimulated experiment; SB: solid sample at the end of the OS-4 biostimulated experiment; WBB: aqueous sample at the end of the OS-10 biostimulated/bioaugmented experiment; SBB: solid sample at the end of the OS-10 biostimulated/bioaugmented experiment. The DGGE analyses were reproducible since no variations were observed between the patterns obtained from duplicate DNA extractions.

The original aquifer sediment showed three intense bands, of which B7 band was the strongest (Fig. 4.8, lanes SED). The B20-B21 and B35-B36 bands from the solid sample retrieved at the end of the experiments (lanes SB and SBB) were in the same position as the B7 band from the initial aquifer sediment. The *16S rRNA* gene from these bands (B7, B20 and B21) was identical to that of *Sphingomonas sp*., within the *α-proteobacteria* class. At the end of the experiments, most of the bands of the solid samples (lanes SB and SBB) were shared by the two treatments (e.g. B19 and B34, B20-21 and B35-36, B22 and B37, B23 and B38, B24 and B39). The B19 and B34 bands were in the same position as the B30

band from the final aqueous samples and were also identified as unclassified γ-*proteobacteria*, which are closely related to the *Xanthomonadaceae* family. The *16S rRNA* sequence for the B39 band was consistent (99% similarity) with that found in an uncultured *Sideroxydans*, which belongs to the *β*-class of the *Proteobacteria*. The most important difference between the *16S rRNA*-based DGGE profiles of the two treatments was the appearance of the B40 band in the biostimulated/bioaugmented experiment (lanes SBB). This band had a 99% sequence similarity to an uncultured *Methanogenium sp.*, grouped within the *Euryarchaeota* phylum.

DGGE band	GenBank accession number	Longitude (pb)	Closest organism in GenBank database (accession number)	% Similarity (1)	Phylogenetic group (2)
B1	HM765437	526	*Thiobacillus denitrificans* (AJ243144) (3)	100	*Hydrogenophilaceae (β)*
B7=B20=B21	HM765438/ HM765443	499/526	*Sphingomonas sp*. (AF385529)	100	*Sphingomonadaceae (α)*
B10=B25	HM765439/ HM765444	541/543	*Sediminibacterium sp*. (AB470450)	97	*Chitinophagaceae (B)*
B11=B12=B29	HM765440/ HM765441/ HM765445	547/548/521	Unclassified *β-proteobacteria* (AF351570)	96	*Methylophilaceae (β)*
B19	HM765442	552	Unclassified *γ-proteobacteria* (FJ485034)	95	*Xanthomonadaceae (γ)*
B30=B34	HM765446/ HM765447	490	Unclassified *γ-proteobacteria* (FJ485034)	98	*Xanthomonadaceae (γ)*
B39	HM765448	511	Uncultured *Siderooxidans*	99	*Rhodocyclaceae/Gallionellaceae (β)*
B40	HM765449	487	Uncultured *Methanogenium sp*. (GU247798.1)	99	*Methanomicrobiaceae (E)*

(1) Sequences were aligned against the GenBank database with the BLAST search alignment tool (Altschul et al., 1990) and matched with the closest relative from the GenBank database.

(2) Sequences were matched to phylogenetic groups by using the RDP Naive Bayesian Classifier (Wang et al., 2007); *α*, *β*, *γ*, *B* and *E* represent *α-proteobacteria*, *β-proteobacteria*, *γ-proteobacteria*, *Bacteroidetes* and *Euryarchaeota*, respectively.

(3) The phylogenetic affiliation of the band B1 confirms that the DSMZ 12475 strain used in the combined biostimulated/bioaugmented *experiments was Thiobacillus denitrificans* (100% similarity)

Table 4.8. Sequence analysis of selected bands from the *16S rRNA*-based DGGE gel.

Figure 4.9 shows the *nosZ*-based DGGE profiles of the studied samples. These profiles consisted of many low-intensity bands, indicating the low densities of a variety of denitrifying bacteria genotypes. The DGGE profiles before and after the treatments showed that the addition of pyrite caused changes in the denitrifying community.

The groundwater sample (lanes GW) probably consisted of numerous populations in similar proportions, thus resulting in a smear of bands, which makes it difficult to identify individual populations. After the experiments, few faint bands were observed in

aqueous samples of both experiments (lanes WB and WBB). Only one partial *nosZ* sequence was successfully amplified (band 15), although it could not be clearly assigned to any phylogenetic family.

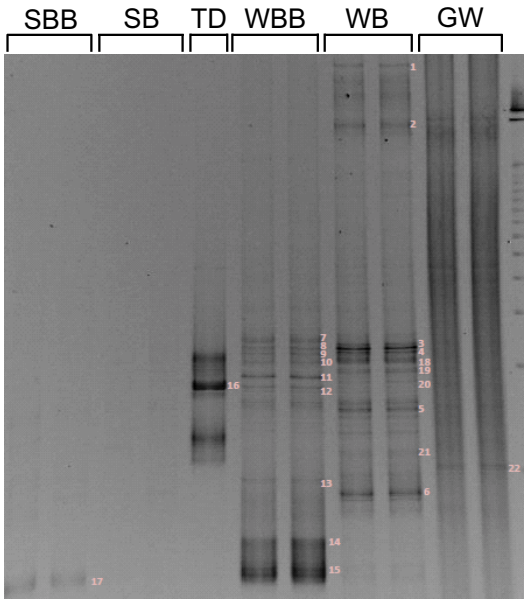

Figure 4.9. DGGE profiles of PCR-amplified *nosZ* fragments from the studied samples. SBB: solid sample at the end of the OS-10 biostimulated/bioaugmented experiment; SB: solid sample at the end of the OS-4 biostimulated experiment; TD: *T. denitrificans* strain; WBB: aqueous sample at the end of the OS-10 biostimulated/bioaugmented experiment; WB: aqueous sample at the end of the OS-4 biostimulated experiment; GW: original aquifer groundwater. The DGGE analyses were reproducible since no variations were observed between the patterns obtained from duplicate DNA extractions.

4.2.6 Quantification of *16S rRNA* and *nosZ* genes

qPCR assays were used to determine the copy number of *16S rRNA* and *nosZ* genes in the initial and final samples of the OS-4 biostimulated experiment (Table 4.9 and Fig. 4.10). The addition of pyrite led to a significant increase in the number of *16S rRNA* copies in the solid samples, but not in the aqueous samples. Nevertheless, an increase in the number of *nosZ* copies was observed in both the sediment and the solution. The number of *nosZ* gene copies in the initial aquifer sediment was below the detection limit (approx. 10^3 *nosZ* copies g^{-1}). It should be noted that *16S rRNA* gene numbers from

environmental samples cannot be converted to cell numbers as the exact number of copies of the *16S rRNA* gene in any given bacterial species varies, ranging from 1 to 13 (Fogel et al., 1999). In contrast to *16S rDNA*, only single copies per genome have been found for the denitrifying genes to date (Philippot, 2002). One exception is the narG gene, which can be present in up to three copies (Philippot, 2002). Therefore, the number of denitrifying organisms is expected to be close to the gene copy number obtained by qPCR.

sample	Gene copy number per mL or g		ratio *nosZ*/*16S* (%)
	16S rRNA	*nosZ*	
GW	$1.30 \pm 0.40 \times 10^6$	$1.66 \pm 0.39 \times 10^4$	1.34 ± 0.46
WB	$7.45 \pm 2.73 \times 10^5$	$2.95 \pm 0.89 \times 10^4$	3.83 ± 0.88
SED	$2.72 \pm 1.34 \times 10^4$	n.d.	n.d.
SB	$3.76 \pm 2.41 \times 10^5$	$1.87 \pm 0.86 \times 10^4$	7.29 ± 3.37

n.d. = not determined

Table 4.9. Gene copy number for the *16S rRNA* and *nosZ* genes in aqueous samples (gene copies mL^{-1}) or in solid samples (gene copies g^{-1}) determined by qPCR. GW: original aquifer groundwater; WB: aqueous sample at the end of the OS-4 biostimulated experiment; SED: original aquifer sediment; SB: solid sample at the end of the OS-4 biostimulated experiment.

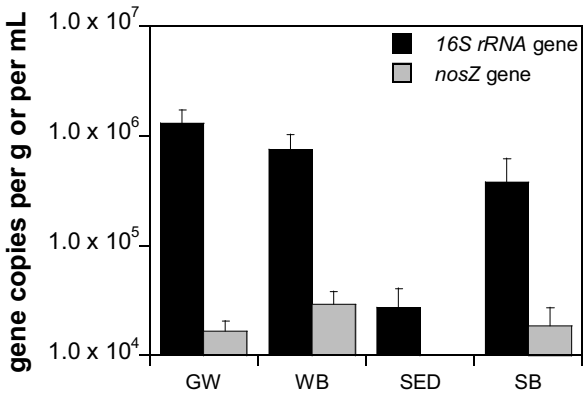

Figure 4.10. *16S rRNA* and *nosZ* genes copy numbers in aqueous samples (gene copies mL^{-1}) or in sediment (gene copies g^{-1}). GW: original aquifer groundwater; WB: aqueous sample at the end of the OS-4 biostimulated experiment; SED: original aquifer sediment; SB: solid sample at the end of the OS-4 biostimulated experiment. Error bars indicate standard errors of qPCR of the two replicate DNA extractions.

The ratio of the *nosZ* to *16S rRNA* genes was determined to evaluate the relative abundance of denitrifiers compared to total bacteria (Table 4.9). Such a calculation was possible for two reasons: a similar amount of DNA was used (same DNA dilution without PCR inhibition for both genes) and similar PCR efficiencies were obtained in the *16S rRNA* and *nosZ* assays. The percentage of *nosZ* to *16S rRNA* genes in the initial groundwater sample was 1.3±0.5%, which is within the range of those reported by Henry et al. (2006; 2008), Kandeler et al. (2006), Chon et al. (2010) and Djigal et al. (2010) for environmental samples (0.1-4%). The relative abundance of the *nosZ* gene in aqueous and solid samples increased from 1.34±0.46% before the experiment to 3.83±0.88% and 7.29±3.37%, respectively, after biostimulation (Table 4.9).

4.3 Discussion

4.3.1 Enhancement of denitrification by biostimulation and response of microbial community

In the blank and pyrite-free batch experiments, insignificant nitrate reduction was observed, indicating the lack of appropriate electron donors in the aquifer material and the involvement of bacteria in the denitrification processes. Nitrate reduction was enhanced in the biostimulated experiments through the addition of pyrite. This suggests that denitrifying bacteria capable of reducing nitrate using pyrite as the electron donor were present in the aquifer material and that the addition of pyrite was required to activate these autochthonous bacteria. The proportion of the *nosZ* gene significantly increased after biostimulation in both aqueous and solid samples (from 1.3±0.5% to 3.8±0.9 and 7.3±3.4%, respectively). It may be assumed that the proportion of denitrifying bacteria increased, indicating that pyrite was used as the electron donor in accordance with the nitrate consumption.

The DGGE fingerprint patterns showed that the composition of the bacterial community in both the sediment and groundwater were highly affected by biostimulation. Sequencing of selected bands indicated that the populations belonged to a

wide phylogenetic range, including members of the classes *α-*, *β-* and *γ-proteobacteria* and the phylum *Bacteroidetes*. *γ-proteobacteria* closely related to the *Xanthomonadaceae* family, detected both in water and sediment system, might presumably be a good candidate for the nitrate reduction using pyrite as the electron acceptor. Furthermore, *Sphingomonas* (*α-proteobacteria*), methylotrophic bacteria (family *Methylophilaceae* of the *β-proteobacteria* class) and members of the *Bacteroidetes* (family *Chitinophagaceae*) probably constituted a less dominant proportion of the autochthonous denitrifiers. In fact, in earlier studies, species belonging or closely related to these groups have been reported as denitrifying bacteria (Finkmann et al., 2000; Ginige et al., 2004; North et al., 2004; Osaka et al., 2006; Akob et al., 2007; Cardenas et al., 2008; Fernández et al., 2008; Sahu et al., 2009; Sun et al., 2009). Accordingly, it is reasonable to assume that these groups were responsible for denitrification in the present experiments. To sum up, members belonging to the *Sphingomonas*, *Bacteroidetes* and *Methylophilaceae* could be affiliated with heterotrophic known denitrifying microorganisms. Since organic carbon sources were not provided externally, the dead and lysed cells of the autotrophic bacteria probably acted as the carbon source for the heterotrophic bacteria (Koenig et al., 2005; Fernández et al., 2008). Given that no heterotrophic denitrification occurred in the pyrite-free experiments, the addition of pyrite to groundwater and sediment from the Osona aquifer stimulated both autotrophic and heterotrophic denitrifying bacteria. Accordingly, between 1 and 26% of the nitrate reduction must be attributed to heterotrophic bacteria so that the ratios between the nitrate removal rate and the sulfate production rate are consistent with the stoichiometry of the overall reaction (Table 4.6).

Surprisingly, although known denitrifying bacteria were detected among predominant *16S rRNA* gene-based DGGE bands, no *16S rRNA T. denitrificans* were detected in initial or final samples of the biostimulated and biostimulated/bioaugmented treatments despite the fact that this bacterium is one of the most well known autotrophic denitrifier (Beller et al., 2006) and despite the fact that it has been shown to denitrify using pyrite as the electron donor (see chapter 3). This would suggest that this bacterium was not the dominant denitrifier in the aquifer and that added *T. denitrificans* were unable

to compete with the indigenous bacteria for the electron acceptor and/or electron donor in the biostimulated/bioaugmented experiments, which is in agreement with the chemical results. In the *nosZ* DGGE (Fig. 4.9), although the bands were not successfully reamplified or sequenced, a very faint band (band 12, lanes WBB) that was in the same position as the band for the *T. denitrificans* strain (band 16, lane TD) was detected in the final aqueous samples of the combined biostimulated/bioaugmented treatment. Although inoculation with *T. denitrificans* slightly accelerated nitrate reduction, bioaugmentation (at the inoculum density tested in the present experiments) was thus not necessary to enhance denitrification. Even, the *16S rRNA* DGGE profile of the biostimulated/bioaugmented experiment (Fig. 4.8, lanes SBB) showed the presence of methanogenic archaea (band B40), which were not clearly observed after the biostimulation treatment. This would suggest that there was an excess of organic matter, probably related to the biomass inoculated. Fermentation of such organic matter could take place, generating hydrogen, which could be used by the methanogenic microbial populations as the electron donor.

After biostimulation, the increase in the proportion of denitrifying bacteria was significantly higher in the sediment-attached community than in the free-living one. Nevertheless, in the biostimulated experiments that used autoclaved core samples (OS-7 and OS-8), the nitrate reduction rate was similar to that obtained in the experiments that used intact core samples (OS-3 and OS-4). Planktonic denitrifiers existing in the aquifer groundwater were therefore able to adapt to the new conditions and use pyrite as the electron donor even in the absence of intact sediment-attached bacteria. This assumption is concordant with the fact that *Xanthomonadaceae*-like bacteria, which were probably the dominant denitrifiers in the system, were detected in both solid and aqueous phases. The main phylogenetic difference between the bacterial communities of aqueous and solid samples was the presence of *Sphingomonas* in the solid samples, whereas the presence of *Bacteroidetes* and methylotrophic *β-proteobacteria* was only detected in the aqueous samples.

The nitrate reduction rates obtained in the present batch experiments using the Osona aquifer material and biostimulated with pyrite (346±29 μmol NO_3^- kg^{-1} d^{-1}) were approximately 25 times higher than the rates obtained by Jorgensen et al. (2009) in pyrite-amended experiments using sediments from the anoxic zone of a sandy aquifer (14±0.2 μmol NO_3^- kg^{-1} d^{-1}). After comparing experimental conditions in Jorgensen et al. (2009) with those in the present study, pyrite grain size, solid:liquid ratio and pH could account for this discrepancy in rates. The results of chapter 3 demonstrated that the size of pyrite particles significantly influenced nitrate removal rates and efficiency in pyrite-driven denitrification experiments with pure cultures of *T. denitrificans*. The nitrate reduction rates calculated in the experiments with pyrite grains from 25 to 50 μm were approximately 5 times higher than the rates in the experiments with 50-100 μm pyrite under the study conditions (see chapter 3). Therefore, the higher rates obtained in the present experiments were higher with respect to those obtained by Jorgensen et al. (2009) could be in part attributed to the larger pyrite grain size used by these authors (45-200 μm). Furthermore, the pH of the initial solution in Jorgensen et al. (2009) (approx. 5.5) was lower than pH of the Osona groundwater (6.84). A pH lower than 6 has been found to affect activity of denitrifying bacteria (see chapter 3; Knowles, 1982) and therefore, lower rates in Jorgensen et al. (2009) could be in part attributed to lower pH values. Another important difference in the experimental conditions, which could also influence the nitrate reduction rate, was the solid:liquid ratio. In our experiments, 10 g of substrate (8 g of core fragments and 2 g of pyrite) were added to 250 mL of groundwater. However, Jorgensen et al. (2009) added 101 g of substrate (100 g of saturated material and 1 g of pyrite) to 475 mL of a nitrate-containing solution. In addition to these discrepancies in the experimental parameters, the divergences in nitrate reduction rates could be also due to differences in the capacity of the indigenous bacterial communities to respond to the addition of pyrite and to accomplish pyrite-driven nitrate reduction.

4.3.2 Long-term performance

In the flow-through experiments, complete nitrate removal commenced in the early stages of the experiments (less than 24 d) and lasted for the 180-d experimental period. This demonstrates the rapid response of the indigenous bacterial community to adapt to the new conditions and efficiently reduce nitrate. This result agrees with the high nitrate removal efficiency reported in chapter 3 for a long-term flow-through pyrite-amended experiment inoculated with *T. denitrificans*. In the present experiments, however, a shorter adaptation time was required for bacteria to accomplish complete nitrate removal, thus providing evidence of the rapid adaptation of the native bacterial community to the addition of pyrite.

The results demonstrated the long-term efficiency of biostimulation through addition of pyrite. This strategy could therefore be used in the field for the remediation of nitrate at the concentrations typically found in contaminated groundwater.

4.3.3 Recalculation of the extent of natural attenuation in the Osona aquifer

In most of the *in situ* groundwater studies, the N and/or O isotopic enrichment factors have been calculated using chemical and isotopic composition of groundwater sampled in multilevel wells and/or in wells located along groundwater flux lines (Table 4.7). However, owing to the lack of well casing and to the fact that sampling wells did not coincide with specific groundwater flow directions, in chapter 2 the εN and εO for the Osona aquifer were estimated using temporal variations of nitrate concentration and $\delta^{15}N_{NO3}$ and $\delta^{18}O_{NO3}$ of a few wells in which denitrification was prevalent during the period under study. The estimated enrichment factor for nitrogen ranged between -4.4‰ and -15.5‰ with a median value of -7.0‰ and the εO ranged from -8.9‰ to -1.9‰ with a median value of -4.6‰.

Based on the *in situ* calculated εN and εO, a roughly estimation of the degree of natural attenuation was performed in chapter 2. The median percentage of denitrification was about 30%. To improve this estimation, the percentage of natural nitrate attenuation was quantified in accordance with the following expression and using the εN and/or εO found in the present experiments with the Osona aquifer material:

$$DEN(\%) = \left[1 - \frac{[NO_3]_{residual}}{[NO_3]_{initial}}\right] \times 100 = \left[1 - e^{\left(\frac{\delta_{(residual)} - \delta_{(initial)}}{\varepsilon}\right)}\right] \times 100 \qquad (4.6)$$

The initial $\delta^{15}N_{NO3}$ and $\delta^{18}O_{NO3}$ values equal +15‰ and +5‰, respectively, which correspond to the isotopic composition of pig manure (see chapter 2). Based on both the average εN= -26.3‰ and εO= -20.4‰, the degree of denitrification varied between 0 and 30%, except for sample MNL-019 that was higher than 50% (Fig. 4.11). The median percentage of denitrification was 10% (*n*=39) using εN= -26.3‰ and 7% (*n*=56) using εO= -20.4‰.

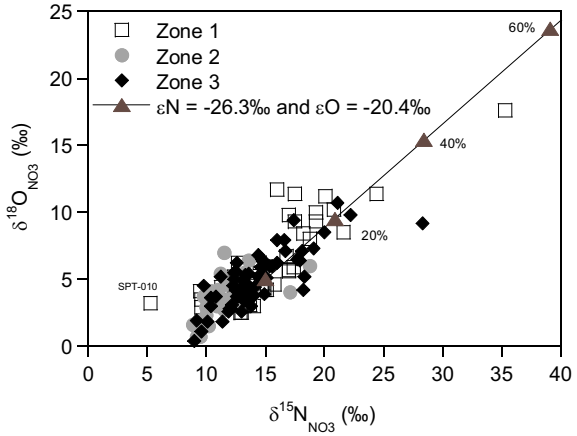

Figure 4.11. $\delta^{15}N$ vs. $\delta^{18}O_{NO3}$ of Osona groundwater used to estimate the percentage of natural denitrification quantified in terms of the isotope enrichment factors obtained in the present experiments (median values are used: εN= -26.3‰ and εO= -20.4‰). The ranges of denitrification percentages calculated using these εN and εO values are shown.

It should be noted that since the isotopic enrichment factors used in the previous calculation were obtained from laboratory experiments and since they are in general higher than those for *in situ* studies, a percentage of natural nitrate attenuation of at least about 10% is estimated for the Osona aquifer.

4.3 Conclusions

The potential for removing nitrate from contaminated groundwater by stimulating the activity of indigenous nitrate-reducing pyrite-oxidizing microorganisms was evaluated in anaerobic experiments using groundwater and sediment collected from the Osona aquifer.

In the batch experiments, the addition of pyrite stimulated nitrate removal in the presence of the indigenous microbial community and also by adding a *T. denitrificans* culture. Most initial nitrate was consumed without nitrite accumulation, yielding a nitrate reduction rate of 358±10 μmol NO_3^- kg^{-1} d^{-1}. Nitrate was removed concurrently with the release of sulfate, confirming the link between nitrate reduction and pyrite oxidation. At least 60% of reduced nitrate was in fact attributed to denitrification coupled to pyrite oxidation, the residual fraction being attributed to heterotrophic denitrification. Indigenous micro-organisms in the aquifer material promoted denitrification under the developed conditions. Inoculation of pure culture of *T. denitrificans* was not necessary.

Quantification of the relative proportions of *nosZ* and *16S rRNA* genes demonstrated that the addition of pyrite increased the proportion of denitrifying bacteria, which was higher in the sediment-attached population than in the planktonic population. Furthermore, the results of the *16S rRNA*- and *nosZ*-based DGGE showed that the composition of the bacterial community underwent a change after biostimulation. Not only autotrophic but also heterotrophic denitrifying bacteria were stimulated through pyrite addition, which is consistent with the balance of the nitrate reduction and sulfate production rates. Bacterial populations closely related to *Xanthomonadaceae* might

probably be a good candidate as the dominant autotrophic denitrifiers that used pyrite as the electron donor.

The evolutions of nitrate concentration, $\delta^{15}N$ and $\delta^{18}O_{NO3}$ in the pyrite-amended experiments were consistent with denitrification. The N and O isotopic enrichment factors (-26.32±1.84‰ and -20.38±1.26‰, respectively) were used to recalculate the extent of natural attenuation of nitrate in the Osona aquifer, previously estimated in chapter 2. The median percentage of denitrification was around 10%, instead of the value of 30% overestimated in chapter 2 using enrichment factors roughly calculated in the field. This refinement could be useful in predicting the evolution of the nitrate contamination in the aquifer and it should be taken into account for potential implementation of induced remediation techniques.

In the flow-through experiments, complete nitrate removal lasted for the 180-d test period. These results demonstrated the long-term capacity of naturally occurring denitrifying bacteria and the bacterial consortium previously enriched in the batch experiments to reduce nitrate using pyrite as the electron donor.

Therefore, controlled addition of pyrite to stimulate the activity of indigenous denitrifying bacteria could be considered to remediate nitrate contamination in groundwater in future water management strategies. However, a serious limitation of this bioremediation strategy could be the release of toxic metals resulting from pyrite oxidation, e.g. As and Ni could be present in minor amounts in the pyrite structure. Thus, care should be taken with the source and characterization of the pyrite for its use as amendment. Further field-scale pilot plant studies are needed to ascertain whether the high nitrate removal efficiency obtained in the present laboratory experiments could be prolonged under field conditions.

Part III:

Growth of *Thiobacillus denitrificans* on pyrite surface

Chapter 5

Attachment and growth of *Thiobacillus denitrificans* on pyrite surfaces

Earlier studies on the distribution of microorganisms in the subsurface have shown that most of the bacterial biomass in aquifers is attached to solid material and only a small fraction is free-living in solution (Harvey et al., 1984; Bekins et al., 1999; Lehman et al., 2001; Griebler et al., 2002). According to these authors, the ratios of attached to suspended cells depend on the mineralogy and particle size of the sediments and on the nutrient availability. Furthermore, most of the attached cells are associated with smaller grain-sized fractions. It is common knowledge that bacteria attached to surfaces in aquatic environments are more active than free-living bacteria although the experimental results are often contradictory (Paerl, 1985; Van Loosdrecht et al., 1990). Moreover, physiological studies of single bacterial populations have demonstrated substantial differences between cells in attached and unattached states in terms of cell size, reproductive rate, enzyme activity and exopolymer production (Van Loosdrecht et al., 1990).

Note: This chapter is based on the article: Torrentó, C., Urmeneta, J., Edwards, K. and Cama, J. Characterization of attachment and growth of *Thiobacillus denitrificans* on pyrite surfaces. In preparation

These discrepancies may be due to different environmental conditions at the solid-liquid interface, when compare with the bulk liquid (e.g. pH, Eh, and nutrients concentration). Accordingly, Marshall and Goodman (1994) suggested that external factors could alter the expression of certain genes and could therefore modify the overall physiological characteristics of the bacteria adhering to a surface.

Attached bacteria occur on surfaces as dispersed monolayers, microcolonies, or three-dimensional biofilms (Costerton et al., 1995). Biofilms consist of a series of discrete columnar biomass structures embedded in a self-produced extracellular matrix and surrounded by numerous pores and channels through which water flows (Costerton et al., 1995). Attachment has a number of advantages in groundwater, including a predictable nutrient flux and access to solid phase nutrients (Dunne, 2002). It has also been reported that bacteria colonizing a surface as a biofilm can be much more resistant to toxic molecules (e.g. antimicrobial agents and heavy metals) than their planktonic counterparts (Teitzel and Parsek 2003; Stewart, 1994).

Currently, there are few data on the relative contributions of attached and planktonic bacteria to denitrification in aquifers. Iribar et al. (2008) studied the denitrification capability of sediment-attached and free-living bacteria in an alluvial aquifer and found that bacterial densities and denitrifying capability were greater in sediment than in groundwater. Furthermore, the bacterial composition of sediment-attached consortium differed from that of the groundwater free-living consortium. Teixeira and Oliveira (2002) compared the activity of cells of the heterotrophic denitrifying bacterium *Alcaligenes denitrificans* grown in suspension with that of cells grown on a solid surface. Their results showed that nitrate consumption was significantly higher for the cells in biofilm form than for the planktonic cells.

Autotrophic denitrification linked to pyrite oxidation has been shown to occur in aquifers (see chapter 2) and in laboratory studies using both the indigenous bacteria of a nitrate-contaminated aquifer (see chapter 4) and pure cultures of an autotrophic denitrifying bacterium, *Thiobacillus denitrificans* (see chapter 3). However, there are few

data on the nature of the reaction and on the mechanisms by which denitrifying bacteria reduce nitrate using pyrite as the electron donor. Moreover, whether or not denitrifying bacteria need to colonize the pyrite surface in order to achieve pyrite-driven denitrification remains unclear. The results of chapter 3 showed that *T. denitrificans* started to consume nitrate using pyrite as the electron without an apparent lag phase. This suggests that either bacteria did not require immediate colonization of pyrite surfaces or that bacteria colonized pyrite surfaces rapidly. The nitrate reduction rate was found to be dependent on the exposed surface area of the pyrite grains (see chapter 3). A high pyrite surface area could lead to a better transfer from solid to liquid phases, resulting in a high pyrite dissolution rate, which suggests that the dissolution of pyrite and the release of dissolved Fe and S-compounds are a prerequisite for nitrate reduction. This indicates that free-living bacteria would play a major role in pyrite-driven denitrification. However, a high pyrite surface area could also lead to an increase in bacterial growth and colonization on the pyrite surface, highlighting the role of attached bacteria. In chapter 4, after biostimulation with pyrite in experiments performed with sediments and groundwater from a nitrate-contaminated aquifer, the proportion of denitrifying bacteria increased in both the sediment-attached and the free-living communities, although the increment was higher in the former.

To date, research into microbial attachment to mineral surfaces has dealt mainly with iron-oxidizing bacteria on pyrite (Solari et al., 1992; Ohmura et al., 1993; Crundwell, 1996; Edwards et al., 1998; Fowler et al., 2001; Sand et al., 2001; Mielke et al., 2003; Harneit et al., 2006; Balci et al., 2007; Pisapia et al., 2008) and few studies have assessed adhesion of iron-reducing bacteria to iron (oxy)(hydr)oxides (Neal et al., 2003; Roberts et al., 2006; Zhang et al., 2010). The means by which bacteria accomplish electron transfer to/from solid-phase minerals has been the subject of scientific debate, and different pathways have been proposed: (1) the enzymatic pathway, in which adhesion of bacteria to the solid is necessary (Silverman and Ehrlich, 1964; Leang et al., 2003; Lovley et al., 2004; Gorby et al., 2006); and (2) the indirect pathways, in which electron transfer occurs by means of shuttle compounds (Silverman, 1967; Sand et al., 2001; Crundwell, 2003; Lovley

et al., 2004). The indirect mechanisms avoid the need for direct contact between cells and mineral. An indirect contact mechanism has also been proposed as a pathway for pyrite oxidation by acidophilic iron-oxidizing bacteria (Schippers and Sand, 1999; Sand et al., 2001; Crundwell, 2003; Sand and Gehrke, 2006). In this case, attached bacteria oxidize ferrous ions to ferric ions within a biofilm made up of bacteria and exo-polymeric material (EPS), and the ferric ions generated within this layer oxidize the sulfide mineral. Thus, bacteria play an important catalytic role in regenerating the oxidant, and also in concentrating the ferric ions in the exo-polymeric layer where the chemical processes take place. Currently, the most accepted pathway for pyrite oxidation by iron-oxidizing bacteria is a combination of the indirect non-contact and the indirect contact mechanisms (Edwards et al., 1998; Pisapia et al., 2008) with the result that both attached and free-living bacteria contribute to pyrite dissolution. However, direct attachment of iron-reducing bacteria is still accepted as the predominant mechanism for accessing Fe(III) minerals in environmental settings (Lovley et al., 2004).

The present chapter focuses on the ability of *T. denitrificans* to colonize pyrite surfaces. The results could help us to better understand the mechanism of the nitrate-dependent pyrite oxidation reaction, and to determine whether *T. denitrificans* requires attachment to the pyrite surface. Given that quantitative measurements of the adhesion of denitrifying bacteria onto minerals are lacking in the literature, it is necessary to quantify cell attachment density and colonization kinetics of *T. denitrificans* onto pyrite surfaces. The results could provide a useful insight into the contribution of attached and free-phase denitrifying bacteria to pyrite-driven denitrification in aquifers. This could improve the long-term performance of bioremediation processes and lower the maintenance costs.

To this end, colonization batch experiments using pyrite slabs were performed under anaerobic conditions.

5.1 Materials and methods

5.1.1 Pyrite preparation

Pyrite was purchased from Wards Scientific. Single whole crystals of pyrite were used to prepare thin polished slabs of 1 mm of thickness (prepared by Spectrum Petrographics, Inc., Vancouver, Canada). A slow-speed saw was used to cut 3 mm length and width blocks from the glued slabs. This procedure allowed the individual blocks to be removed from the glass slide (approximately 3 × 3 × 1 mm blocks, 30 mm^2 surface area and 0.2-0.4 mg each). The blocks were then washed individually with acetone and ethanol (Edwards et al., 2000). Three blocks were used in each experiment. The blocks were sterilized by autoclaving at 121°C for 15 min before the start of the experiments.

5.1.2 Culture preparation

Thiobacillus denitrificans (strain 12475 from the German Collection of Microorganisms and Cell Cultures, DSMZ) was cultured in an anaerobic (pH 6.8) nutrient medium specially designed for *T. denitrificans*, following Beller (2005). The medium consisted of a mixed solution of $Na_2S_2O_3 \cdot 5H_2O$ (20 mM), NH_4Cl (18.7 mM), KNO_3 (20 mM), KH_2PO_4 (14.7 mM), $NaHCO_3$ (30 mM), $MgSO_4 \cdot 7H_2O$ (3.25 mM), $FeSO_4 \cdot 7H_2O$ (0.08 mM), $CaCl_2 \cdot 2H_2O$ (0.05 mM) and sterile vitamin, trace element and selenate-tungstate solutions (stock solutions 1, 4, 6, 7 and 8 of Widdel and Bak, 1992).

Cultures were maintained under anaerobic conditions at 30°C and unshaken by 5-weekly sub-culturing. Thereafter, the culture was harvested by centrifugation and washed and resuspended in a sterile saline solution (Ringer 1/4 solution) immediately before the start of the experiments.

5.1.3 Colonization experiments

Colonization and growth on pyrite surfaces were studied over a 9-week period. Three polished pyrite blocks were placed into 100 mL glass bottles and 48 mL of modified

medium were added to the bottles containing minerals. 2 mL of cell solution (2.0×10^8 cells mL^{-1}) were inoculated into each flask.

The modified medium consisted of the *T. denitrificans* nutrient medium without thiosulfate and the sulfate salts being replaced by chloride salts. Thus, the solution consisted of: NH_4Cl (18.7 mM), KNO_3 (16.1 mM), KH_2PO_4 (14.7 mM), $NaHCO_3$ (30 mM), $MgCl_2 \cdot 6H_2O$ (3.25 mM) and $CaCl_2 \cdot 2H_2O$ (0.05 mM). This modified medium ensured that pyrite was the only electron donor available for the cells.

In the control experiments, modified medium (50 mL) was added to the bottles containing the pyrite blocks and no culture was added.

The colonization experiments were performed under anaerobic conditions, in an anaerobic glove box with a nominal gas composition of 90% N_2 and 10% CO_2 at 28±2 °C. The oxygen partial pressure in the glove box was maintained between 0.1 and 0.3% O_2(g) and was continuously monitored by an oxygen partial pressure detector with an accuracy of ±0.1% O_2(g).

5.1.4 Aqueous samples

The bottles were periodically stirred by hand and aliquots of 3 mL were sampled once a week using sterile syringes.

An aliquot was used to determine the density and viability of the bacterial cell population in suspension as described below. Thereafter, samples were filtered through 0.22 μm syringe filters and part of each filtered sample was preserved for cation analyses by acidifying with nitric acid. Concentrations of cations (total Fe, total S, Mg, Ca, Na, P, and K) were measured by inductively coupled plasma-atomic emission spectrometry (ICP-AES). The uncertainty in the measurement of Mg, Ca, Na, K and P was estimated to be around 5% with detection limits of 2.1, 2.5, 4.4, 2.6 and 3.2 μmol L^{-1}, respectively. The accuracy of the Fe and S measurements was estimated to be around 20% since Fe and S concentrations were closed to the detection limits (0.4 and 3.1 μmol L^{-1}, respectively) in

most samples. The remaining part of each filtered sample was used for anion analysis and pH measurement. Concentrations of nitrate, nitrite, chloride, and sulfate were determined by High Performance Liquid Chromatography (HPLC), using a IC-Pack Anion column and borate/gluconate eluent with 12% of HPLC grade acetonitrile. The error was estimated to be 5% for nitrate, chloride and sulfate and 10% for nitrite. Samples for ammonium analysis were acidified to pH<2 with H_2SO_4. Ammonium concentrations were measured using an Orion ammonium ion selective electrode with an analytical uncertainty of 10% and a detection limit of 0.01 mM. pH was measured with a calibrated Crison pH Meter at room temperature (22 ± 2 °C). The pH error was 0.02 pH units.

Bacterial enumeration was performed by epifluorescent direct counting. Samples were diluted with 0.2-μm-pore-size filtered double distilled water to achieve a final liquid volume of 10 mL, which was added to a black polycarbonate membrane filter (Isopore filters, 0.2-μm pore size, Millipore) placed in the filter tower apparatus support. 100 μL of a 10 μg mL^{-1} DAPI (49-6-diamidino-2-phenylindole dihydrochloride, Sigma-Aldrich) solution were added to the sample in the filter apparatus and the sample and the stain were allowed to stand for 5 min. Thereafter, the stained sample was filtered at a vacuum of less than 200 mbar to avoid cell breakage, lysis, and penetration. The total number of cells was enumerated by direct counts of DAPI-stained cells on a light microscope using epifluorescent illumination and suitable optical filters. The number of cells was counted within squares of an ocular grid at ×1000. Counts were obtained from randomly located fields covering a wide area of the filter and a minimum number of 200 cells were counted per filter.

The LIVE/DEAD® BacLight™ bacterial viability kits (Molecular Probes) were used to differentiate between viable cells and dead cell. These kits contain green-fluorescent nucleic acid stain SYTO® 9 and red-fluorescent nucleic acid stain Propidium Iodide (PI). When used alone, the SYTO® 9 stain generally labels all bacteria that have both intact and damaged membranes. In contrast, PI stain penetrates only those bacteria with damaged membranes, causing a reduction in the SYTO® 9 stain fluorescence when both

dyes are present. For this reason, bacteria with intact cell membranes (viable cells) stain green fluorescence, whereas bacteria with damaged membranes (dead cells) stain red fluorescence.

5.1.5 Solid samples

Once a week, two experiments were sacrificed and the pyrite blocks were taken out of the solution with sterilized forceps and rinsed with a pH 7.1 sterile phosphate buffer.

Initial pyrite blocks and slabs retrieved after 1, 2, 3 and 4 weeks were observed by confocal laser scanning microscopy (CLSM) to quantify cell attachment onto pyrite surface. The slabs were fixed in paraformaldehyde (3% in the pH 7.1 phosphate buffer solution) at 4°C overnight. Thereafter, the slabs were stained with DAPI. After staining, the slides were mounted and examined with a Leica TCS SPE laser scanning confocal microscope. The images were captured with LAS AF software and the cells attached onto surfaces were counted using ImageJ software. Averages were obtained from 10 to 20 images (80.09 × 80.09 μm) depending on cell density and colonization heterogeneity. In each image, the apparent statistical surface covered by bacteria was calculated as the ratio of the number of pixels corresponding to bacteria with respect to the total number of pixels. The number of surface-attached cells was estimated assuming that a single cell had a relative surface coverage of 1 μm^2 (each *T. denitrificans* cell can be regarded as a rod that is 0.5 by 1-3 μm; Kelly and Harrison, 1989). The standard deviation between counts made for separate images was calculated. Other DAPI-stained slabs were observed on a light microscope using epifluorescent illumination and suitable optical filters.

Initial pyrite slabs and those retrieved after 1, 2, 3, 4, 5, 7 and 9 weeks were also examined with scanning electron microscopy (SEM) to study the distribution of cells on the pyrite surface and to observe surface features. The blocks were fixed with 2.5% glutaraldehyde in the pH 7.1 phosphate buffer solution (at 4°C, overnight) to maintain the cell structure and to secure the attached cells to the pyrite surface. Subsequently, the slabs were washed with the phosphate buffer and dehydrated sequentially in graded

ethanol solutions (25, 50, 75, and twice in 100% EtOH – 10 min each). After dehydration, the slabs were chemically dried by soaking them twice in hexamethyldisilazane (HMDS) for 5 min. Next, the slabs were air dried in a fume hood for at least 2 h. Thereafter, the slabs were mounted on stubs and gold palladium coated. The samples were examined by scanning electron microscopy (Leica Stereoscan S360 Cambridge Electron Microscopy) and energy-dispersive microanalysis (EDS; INCA Energy 200) using a beam potential of 15 kV.

5.2 Results and discussion

5.2.1 Chemical results

No changes in nitrate, sulfate, iron and ammonium concentrations nor in pH were detected during the duration of the runs (8 to 65 d) in the inoculated and the control experiments (data not shown). Therefore, nitrate reduction did not occur or was too insignificant to be detected under the experimental conditions.

In chapter 3, *T. denitrificans* was shown to reduce nitrate using pyrite as the electron donor. Nitrate reduction was markedly influenced by the pyrite surface area. The fact that nitrate reduction was undetected in the present experiments could be attributed to the small surface area of the pyrite slabs. Pyrite slabs were used instead of crushed pyrite that has a higher surface area since it was necessary to determine the ability of *T. denitrificans* to colonize pyrite surfaces. The use of polished thin sections facilitates imaging using SEM and CLSM because of their flat surfaces.

5.2.2 Pyrite surface colonization

Figures 5.1 and 5.2 show SEM and CLSM images of the surfaces of the pyrite slabs before and after the colonization experiments.

After 1 week, the SEM (Fig. 5.1b and 5.1c) and the CLSM images (Fig. 5.2b and 5.2c) showed single rod attached cells that started to colonize the pyrite surface. Polishing scratches on the surface may be distinguished. Single attached cells and cells in division are observed in both 1-week and 2-week old samples (Fig. 5.1d-e and 5.2d-f), which reveals direct microbial growth on the pyrite surface. The localization of attached cells on pyrite surfaces was random and no preferential orientation was observed. Nevertheless, in the 7-week old DAPI-stained slabs examined with the light microscope, groups of cells were observed preferentially attached to surface features, such as grooves and microcracks (data not shown).

When attached cells start growing and multiplying, newly formed cells remain attached to each other and microcolonies or biofilms may develop. In 3-week old samples microcolonies in addition to actively dividing single cells were detected on the pyrite surface by SEM (Fig. 5.1f-h) and by CLSM (Fig. 5.2g-i). The images reveal both multilayer microcolonies and simpler groups of cells in which organic films contribute to the cohesion of the cells.

After 4 weeks, small areas of the pyrite surface were covered by the microcolonies embedded in organic substances (Fig. 5.1i-j and 5.2j-l), obstructing the detection of individual cells by SEM. These organic films that cover small areas of the pyrite surface are also observed by SEM in the 5-week old samples (Fig. 5.1k-l).

After 9 weeks, SEM images showed that the pyrite surface areas covered by organic films are more extended (Fig. 5.1m-n). EDS analysis on the covered and uncovered pyrite surfaces (Fig. 5.1n) reveals differences in their elemental compositions. The uncovered pyrite remains as it is, whereas in the covered pyrite the signals of S and Fe are reduced and the signals of C and O are increased (data not shown). Accordingly with SEM observations, 9-weel old samples observed with the light microscopy showed large areas of the pyrite surface covered by organic films (data not shown). The development of a uniform and continuous biofilm was not observed during the 9-week period. Single cells and cells in division were still observed after 9 weeks (Fig. 5.1n).

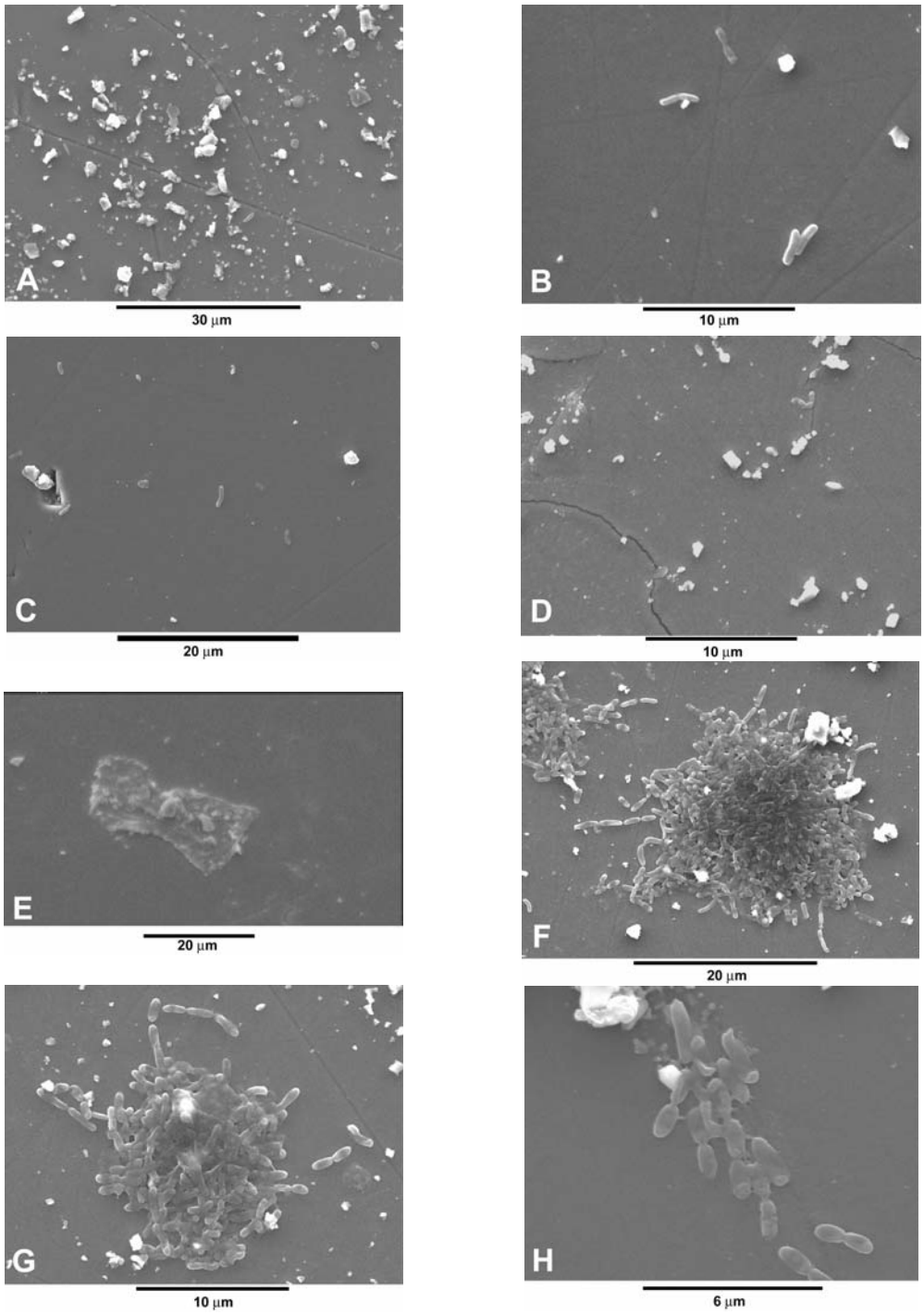
A
30 μm
B
10 μm
C
20 μm
D
10 μm
E
20 μm
F
20 μm
G
10 μm
H
6 μm

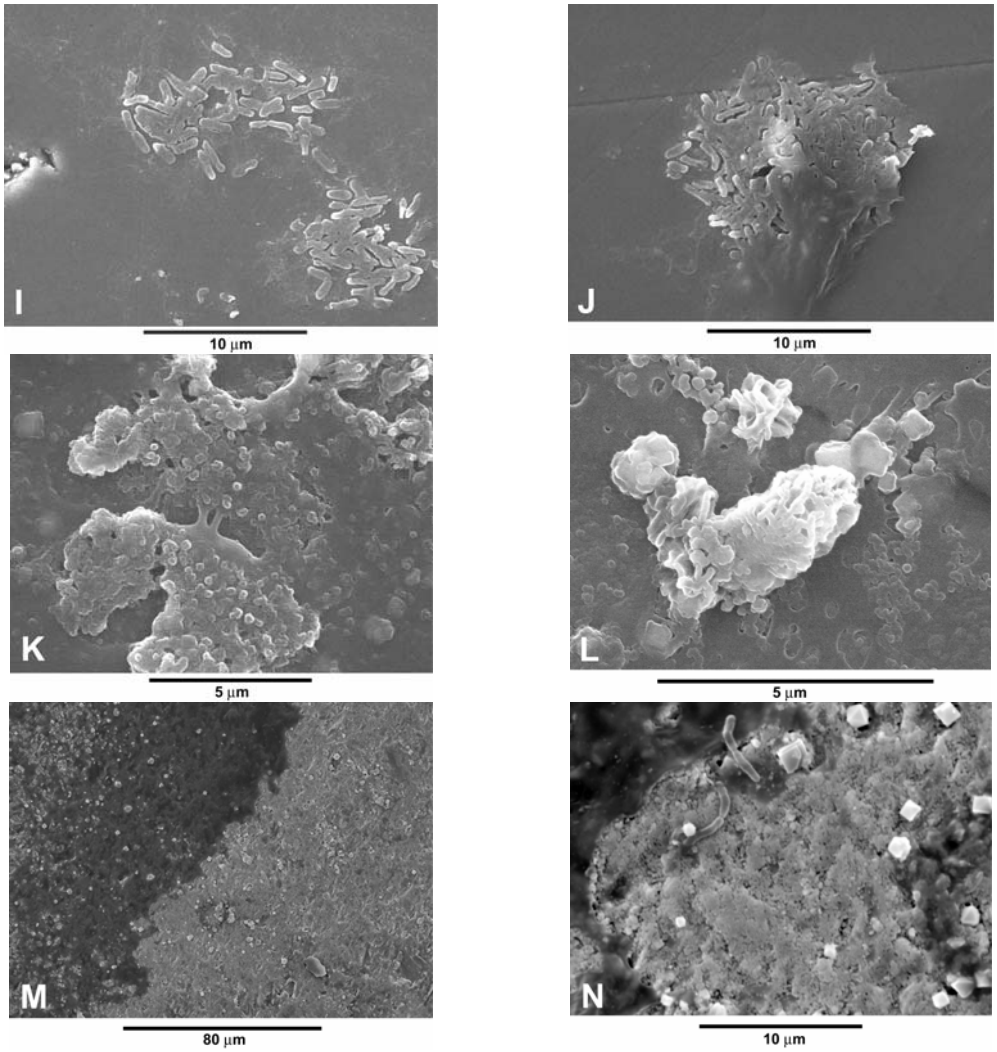

Figure 5.1. SEM images of the initial pyrite surface (A) and after 1 week (B and C), 2 weeks (D and E), 3 weeks (F, G and H), 4 weeks (I and J), 5 weeks (K and L) and 9 weeks (M and N) of the start of the experiments. After 1 and 2 weeks, single attached cells are clearly discernable. After 3 and 4 weeks, microcolonies developed. The coherent action of an organic film is visible in the contact areas between the cells. After 9 weeks, organic films covering larger areas of the pyrite surface are observed. Scale bars are shown.

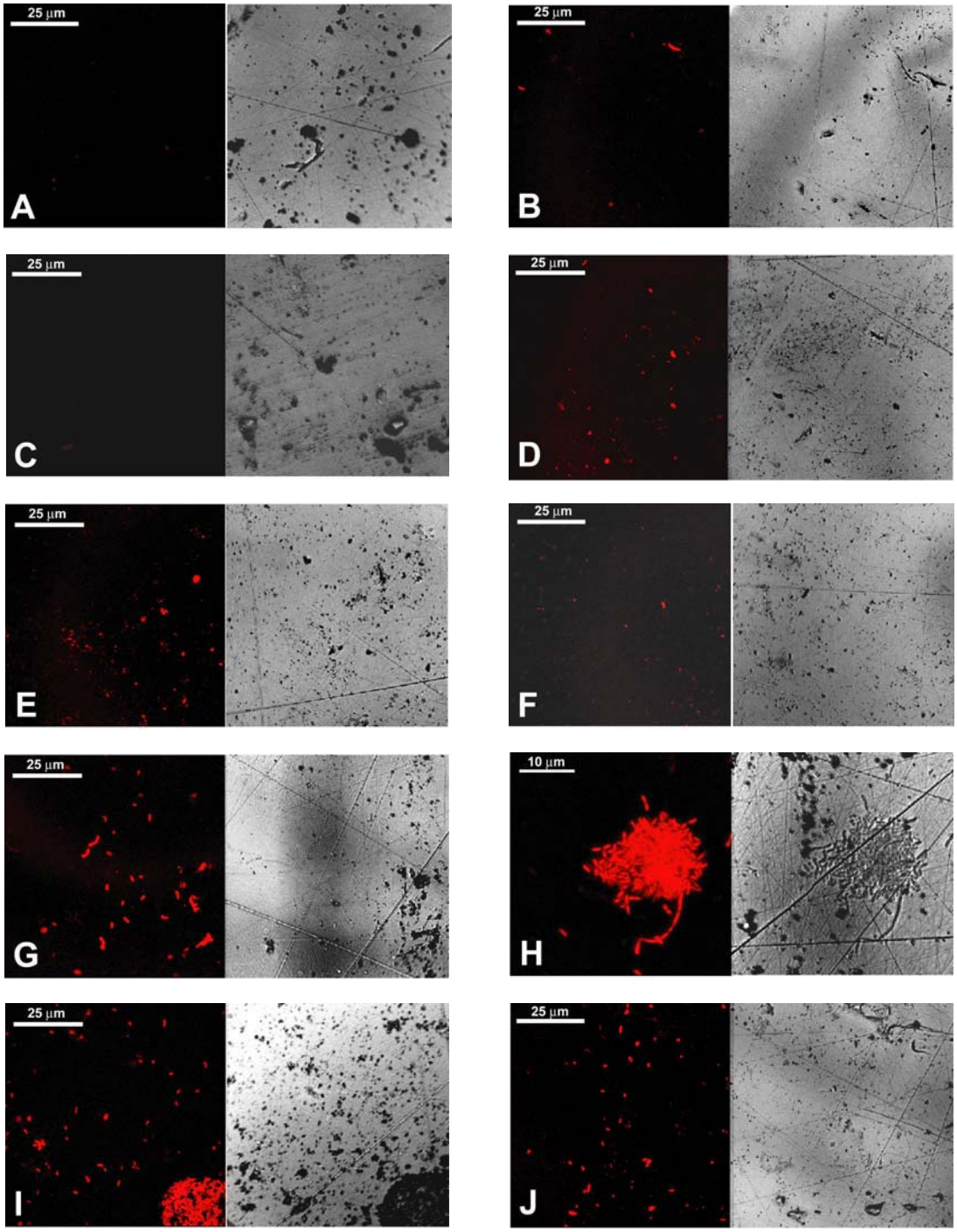
25 µm
A
25 µm
B
25 µm
C
25 µm
D
25 µm
E
25 µm
F
25 µm
G
10 µm
H
25 µm
I
25 µm
J

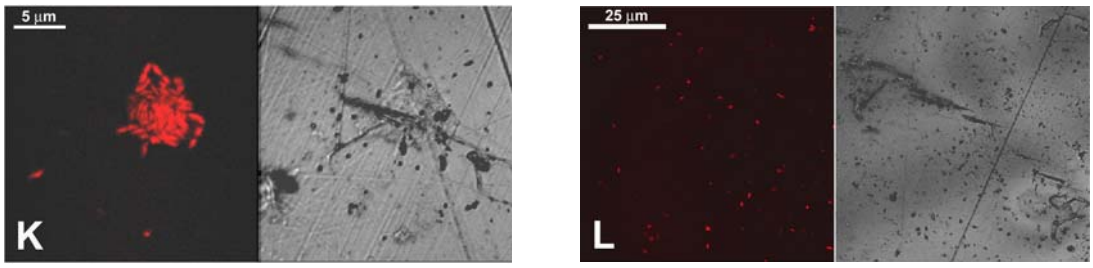

Figure 5.2. Organisms adhering to the surface of pyrite slabs before the start of the experiments (A) and after 1 week (B and C), 2 weeks (D, E and F), 3 weeks (G, H and I) and 4 weeks (J, K and L) of the start of the experiments. Cells shown on the left are stained with DAPI and imaged in a CLSM. Images to the right of each fluorescent image correspond to the same site in transmitted light. Scale bars are shown.

5.2.3 Colonization rate

Colonization rate of *T. denitrificans* onto pyrite surface was estimated by measuring the density of cells attached to pyrite surfaces over time. The density of adhered cells was determined by image analysis of the CLSM images of 1, 2 and 3 weeks following the start of the experiments (Table 5.1). It should be noted that microcolonies are three-dimensional structures. As a result, the way in which the number of attached cells was determined using image analyses of the two-dimensional CLSM pictures could lead to an underestimation of the adhered cell density. Since three-dimensional microcolonies were observed in the 3-week old samples (Fig. 5.1f), the number of attached cells calculated for these samples should be considered as an underestimation. Hence, this method was not used to determine the density of attached cells in older samples.

The number of attached cells increased slowly over time (Table 5.1). This increase could be due either to the attachment of bacteria growing in solution or to the growth and division of the attached bacteria. Although the latter possibility is supported by SEM images (Fig. 5.1), which show attached cells in division and the formation of microcolonies, both processes probably occurred. Most likely, microcolonies were set up by the division of attached cells and by the attachment of planktonic bacteria. Bacteria in

suspension can use either flagella or pili to move along the surface until other bacteria are encountered and microcolonies are formed or enlarged.

	time (d)	% apparent statistical coverage area	cells mm^{-2} on surface (1)
1 week	8	0.06	5.55×10^2
2 weeks	15	0.21	2.07×10^3
3 weeks	22	2.01	$2.01 \times 10^{4\ (2)}$
4 weeks	27	0.87	n.d.

(1) Based on that the relative surface coverage of one *T. denitrificans* cell is 1 μm^2
(2) The calculated value probably is underestimated (see text)
n.d. = not determined (see text)

Table 5.1. Average cell coverage on pyrite surface after 1, 2, 3 and 4 weeks of the start of the experiments. Attached cells were estimated counting from CLSM images and assuming that the relative surface coverage of one cell is 1 μm^2. After 3 weeks, the calculated density of attached cells must be considered as an underestimation, because three-dimensional microcolonies were detected by SEM. As three-dimensional microcolonies were repeatedly observed in the 4 week-old samples, the adhered cell density was not calculated.

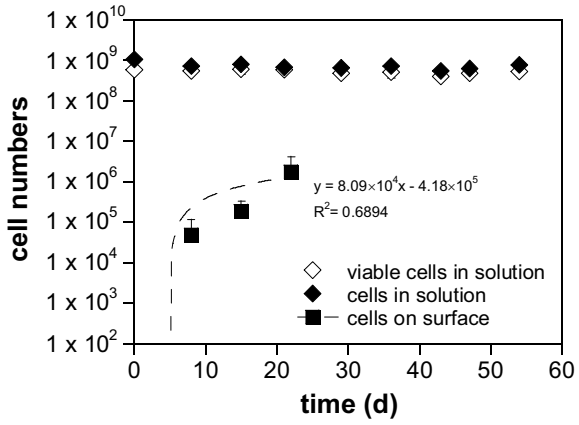

Figure 5.3. Cell number in solution and adhering to the pyrite surface over time. The number of viable and total cells in solution was obtained from LIVE/DEAD and DAPI counts of aqueous samples obtained after 1, 2, 3, 4, 5, 6, 7, 8 and 9 weeks and based on 50 mL volume. Attached cells were estimated by using CLSM images of the surface of the pyrite slabs retrieved from the experiments after 1, 2 and 3 weeks and based on 30 mm^2 available surface. The number of attached cells after 3 weeks was probably underestimated since three-dimensional microcolonies were detected by SEM. Surface colonization rate was estimated from the regression of the data.

Surface colonization rate was found to be 34.9±17.6 cells mm^{-2} h^{-1} for the 3-week period (Fig. 5.3).

Observations with the light microscopy of 7-week old samples stained with DAPI suggest that the density of attached cells was of the same order as that after 3 weeks (data not shown). This suggests that attachment onto the pyrite surface became saturated. Further longer experiments are warranted to corroborate this assumption.

5.2.4 Coverage area

After 3 weeks, the surface cell density was 2.01×10^{4} cells mm^{-2} (0.02 cells μm^{-2}), which is equivalent to one cell every 50 μm^{2} of pyrite surface area.

The area covered by attached *T. denitrificans* cells after 3 weeks was approximately 2% of the total pyrite surface available (Table 5.1).

5.2.5 Viability of cells in solution and percentage of attached cells

Table 5.2 shows the number of *T. denitrificans* cells in solution, including viable and dead cells, in the 9-week experimental period. As shown in Fig. 5.3, the number of cells in solution remained almost constant over time. High viability was observed over this experimental period. Therefore, planktonic cells survived over time although their growth and multiplication were too slow to cause a detectable increase in their number. The percentage of viable cells with respect to total cells in solution tended to decrease slightly over time, suggesting attachments to the pyrite surface or cell death. After 9 weeks, attached single cells and cells in division in addition to mature colonies were observed on the pyrite surface by SEM (Fig. 5.1n), indicating that new attachment of free-living cells occurred over time.

Using the calculated densities of both attached and planktonic cells about 0.3% of total cells were estimated to be attached to the pyrite surface after 3 weeks. After 9 weeks, this percentage is expected to be of the same order as after 3 weeks since light microscopy

observations suggest that the density of attached cells did not increase more after 3 weeks and since the density of planktonic cells remained almost constant over time.

sample	time	cells in solution	viable cells	dead cells	% of viability
	d		$\times 10^7$ cells mL^{-1}		
initial	0	2.12	1.16	0.96	54.7
1 week	8	1.45 ± 0.24	1.08 ± 0.17	0.37 ± 0.10	74.3
2 weeks	15	1.57 ± 0.25	1.19 ± 0.29	0.37 ± 0.08	76.1
3 weeks	21	1.35 ± 0.23	1.16 ± 0.15	0.19 ± 0.08	85.8
4 weeks	29	1.30 ± 0.15	0.94 ± 0.06	0.36 ± 0.01	72.6
5 weeks	36	1.45 ± 0.22	1.03 ± 0.31	0.43 ± 0.01	70.6
6 weeks	43	1.10 ± 0.06	0.80 ± 0.07	0.30 ± 0.01	72.7
7 weeks	47	1.25 ± 0.13	0.95 ± 0.13	0.29 ± 0.002	76.5
8 weeks	54	1.55 ± 0.12	1.05 ± 0.07	0.50 ± 0.005	68.0

Table 5.2. Cells in solution and viability during the 9-week experimental period.

5.2.6 Role of attached and free-living cells in denitrification

It may be postulated that both planktonic and attached cells were metabolically active for the following reasons: (1) most of the cells remained planktonic, (2) the number of attached cells increased throughout the experiment, and (3) the number of viable cells in solution was kept almost constant over time. Cell-mineral contact, for at least a small number of cells, was necessary for *T. denitrificans* to oxidize pyrite. The planktonic cells stayed alive and active over time, probably at the expense of the products released from pyrite dissolution.

Despite the need for further research into the metabolism by which *T. denitrificans* cells use pyrite as the electron donor, it may be assumed that ferric ion is the pyrite-attacking agent. This has been suggested for pyrite oxidation by acidophilic bacteria and for chemical pyrite oxidation by oxygen or ferric ion even at neutral pH (Moses et al., 1987). This assumption is supported by the fact that *T. denitrificans* are also ferrous ion-oxidizing bacteria (Straub et al., 1996). Thus, these bacteria would contribute to the ferrous ion oxidation with nitrate as oxidant, regenerating the attacking agent. Cells that attach to the mineral surface could oxidize pyrite by an indirect contact mechanism,

whereas planktonic cells could oxidize ferrous ions dissolved from the mineral (indirect non-contact mechanism).

Although nitrate reduction was not corroborated by chemical analyses, bacteria probably were metabolically active and reduced nitrate using pyrite as the electron donor for two reasons: (1) colonization and direct growth of bacteria on the surface was observed, and (2) the number of planktonic cells remained almost constant. Nitrate reduction was not detected because of the small surface area of the pyrite slabs (blocks of approx. 30 mm^2 and 0.2-0.4 mg, which correspond to approx. 0.075 to 0.150 $m^2\ g^{-1}$).

Additional experiments were performed adding crushed pyrite in order to provide sufficient surface area and roughness for reactions to be detected. In these experiments, in addition to the three pyrite slabs, 1 g of 50-100 μm sterilized powdered pyrite (Navajún pyrite, 0.4259±0.0156 $m^2\ g^{-1}$, see chapter 3) was added to each bottle. The results show that after 45 d, approximately 12% of the initial nitrate was reduced concurrently with the release of sulfate (Fig. 5.4). Efficiency in nitrate removal was in agreement with the results of the experiments of chapter 3 using the same 50-100 μm pyrite. Accordingly, efficiency decreases by increasing initial nitrate concentration (Fig. 5.5).

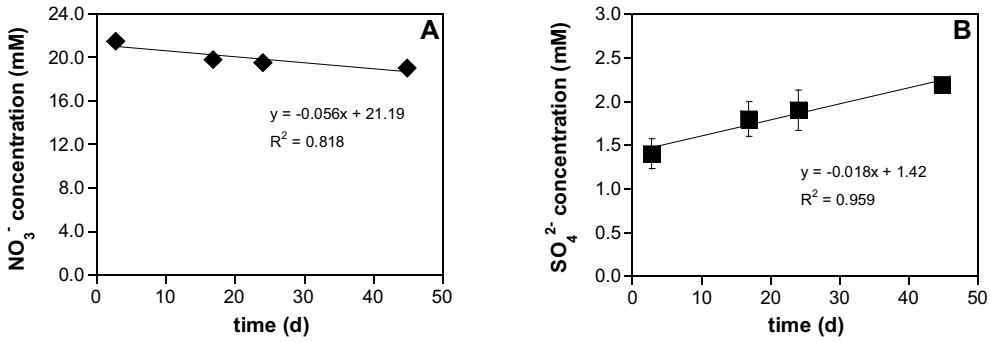

Figure 5.4. Variation of nitrate concentration (a) and sulfate concentration (b) over time in the additional experiments with powdered pyrite. In these experiments, three pyrite blocks and 1 g of 50-100 μm pyrite were added to 48 mL of the modified medium solution and 2 mL of the *T. denitrificans* culture (2×10^8 cells mL^{-1}).

It should be noted that the solid:liquid ratio used in the present experiments (1 g:50 mL) was one order of magnitude lower than the ratio in the experiments of chapter 3 (5 g:25 mL). Pyrite mass-normalized rates in the present experiments were approximately 7-15 times higher than those in the experiments of chapter 3 (data not shown). This discrepancy was probably due to the high cell concentration employed in the present experiments (1×10^{10} cells) compared with the concentration of 5×10^{9} cells used in the experiments of chapter 3.

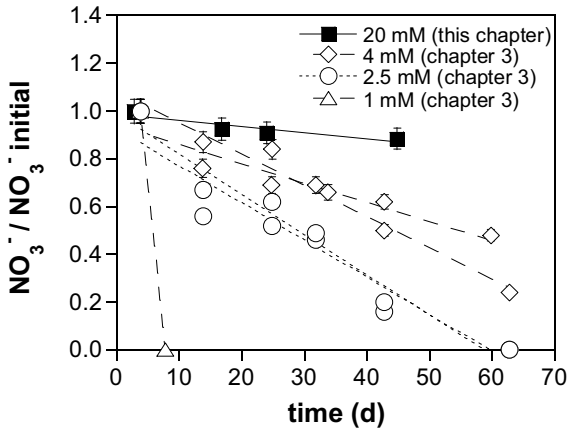

Figure 5.5. Nitrate removal in the additional experiments with powdered pyrite compared with experiments of chapter 3. The relative nitrate concentrations as function of time ($NO_3^-/NO_{3\,initial}^-$) are represented, where NO_3^- is the measured concentration and $NO_{3\,initial}^-$ is the initial nitrate concentration.

5.2.7 Comparison with published data

Given that pyrite colonization by *T. denitrificans* or other denitrifying bacteria has not been studied before, the results were compared with the findings reported for inoculated acidophilic iron-oxidizing bacteria (*Acidithiobacillus ferrooxidans*) adhering to pyrite, and for inoculated iron-reducing bacteria (*Shewanella oneidensis and Shewanella putrefaciens*) colonizing iron (oxy)(hydr)oxides. Table 5.3 shows colonization rates, area covered by bacteria and the proportion of cells attached to mineral surfaces reported in the aforementioned studies.

The discrepancy in the published data may be due to the use of different strains and to the differences in the experimental conditions (inoculum, duration, pH, mineral surface area, etc.) and methodology. Two approaches have been adopted in the literature to determine the number of attached cells on mineral surfaces: direct and indirect methods. The direct counting method consists in determining the number of attached cells by direct microscopic observations with transmitted light microscopy, scanning electron microscopy, fluorescence microscopy, or confocal laser scanning microscopy as performed in the present experiments. Counting is carried out by on-line image analysis or by obtaining pictures of the random fields and then subjecting the pictures to image analysis. By contrast, the indirect methods consist in counting the number of non-adhering bacteria after contact between the mineral and the bacterial suspension and in calculating the amount of attached cells by subtracting the planktonic cell number from the initial cell number.

Some problems are associated with the measurement of attached vs. planktonic bacteria abundance, especially when indirect counting methods are used. Cell multiplication and exchange between adhered and free-living populations can occur over time.

Colonization rates of *T. denitrificans* on pyrite surfaces are approximately 2-3 orders of magnitude lower than those published (or estimated from published data) for attachment of *A. ferrooxidans* onto pyrite (Solari et al., 1992; Edwards et al., 1998; Dziurla et al., 1998; Mielke et al., 2003; Pisapia et al., 2008) and attachment of *S. oneidensis* onto iron(oxy)(hydr)oxides (Neal et al., 2003; Zhang et al., 2010) (Table 5.3). These authors, who also used direct counting methods to determine the number of attached cells, reported low mineral coverage areas (<10%) and percentages of attached cells (<1%) in accordance with the results of the *T. denitrificans* colonization experiments (Table 5.3).

Table 5.3. Comparison of the characterization of attachment of *T. denitrificans* onto pyrite surfaces with published data for attachment of acidophilic iron-oxidizing bacteria onto pyrite surfaces and iron-reducing bacteria onto iron (oxy)(hydr)oxide surfaces.

Reference	Mineral, surface area	Culture	pH	Initial bacterial conc.	Time	Surface cell density at saturation	Colonization rate [1]		% attached cells respect to total cells	Coverage area (% respect to total area)	Comments
				cells mL^{-1}	h		cells mm^{-2} h^{-1}	cells g^{-1} h^{-1}			
Direct counting methods											
this study	py slabs, 30 mm^2	*T. den.*	6.9	2.1×10^7	524	one cell every 50 μm^2	34.9±18	-	0.3	2.0	Calculations were performed during the first 3 weeks [1]
Edwards et al. (1998)	py slabs, 320 mm^2	natural mixed	1	$\sim 1\times 10^8$	144	one cell every 10 μm^2	$\sim 2\times 10^3$	-	0.2 [2]	5.0 [2]	After 6 d adhesion become saturated
Dziurla et al. (1998)	crushed py, 200 cm^2 g^{-1}	*A. ferroox.*	1.8	$\sim 1\times 10^7$	24		$0.7\text{-}1.7\times 10^3$	$1.2\text{-}3.8\times 10^7$	-	0.8-2.2	
Pisapia et al. (2008)	py grains, 50-80 μm	*A. ferroox.*	1-2	$\sim 1\times 10^7$	3		4.6×10^3	7.4×10^7	-	1.3	
				$\sim 1\times 10^8$			1.2×10^4	1.8×10^8	-	3.2	
Mielke et al. (2003)	py cubes, 10 cm^2	*A. ferroox.*	6.5	$\sim 1\times 10^7$	24		5.4×10^3	-	90	6.5 [2]	
			6.8	-	720	one cell every 0.3 μm^2	$\sim 2\times 10^2$	-	>90 [2]	>50 [2]	After 30 d adhesion become saturated
Zhang et al. (2010)	iron oxide, 0.79 cm^2	*S. oneid.*	7.5	8.4×10^8	24	one cell every 13 μm^2	3.2×10^3	-	0.8 [2]	10 [2]	At 8.4×10^8 cells mL^{-1} adhesion become saturated
Neal et al. (2003)	ht crystal, 0.62 cm^2	*S. oneid.*	7	-	100	one cell every 1500 μm^2	6.4	-	-	<1 [2]	After 100 h adhesion become saturated
	mgt crystal (111), 0.68 cm^2			-	25	one cell every 2500 μm^2	16.2	-	-	<1 [2]	After 25 h adhesion become saturated
	mgt crystal (100), 0.71 cm^2			-	25	one cell every 2900 μm^2	13.8	-	-	<1 [2]	After 25 h adhesion become saturated
Indirect counting methods											
Harneit et al. (2006)	crushed py, 50-100 μm	*A. ferroox.*	acid	$\sim 1\times 10^9$	0.16		-	$\sim 1\times 10^{10}$	~80	-	After 10 min adhesion become saturated
Ruiz et al. (2008)	crushed py, 50-100 μm	*A. ferroox.*	acid	$\sim 1\times 10^8$	8		-	-	50	-	
Solari et al. (1992)	crushed py, 250 cm^2 g^{-1}	*A. ferroox.*	2.3	$\sim 1\times 10^9$	3	one cell every 2.5 μm^2	$\sim 8\times 10^4$	$\sim 2\times 10^9$	-	20	After 3 h adhesion become saturated
Ohmura et al. (1993)	crushed py, 60-70 μm	*A. ferroox.*	2	$\sim 4\times 10^8$	0.25		-	$\sim 4\times 10^{10}$	~29 [2]	~23 [2]	
				$\sim 8\times 10^8$			-	$\sim 5\times 10^{10}$	~20 [2]	~30 [2]	
				1×10^9		one cell every 1.1 μm^2	-	7.1×10^{10}	~23 [2]	45	At 1×10^9 cells mL^{-1} adhesion become saturated
Roberts et al. (2006)	crushed mgt, 3.1 m^2 g^{-1}	*S. putref.*	3-5.5	$\sim 1\times 10^9$	2	-	-	-	70-80	-	

(1) After 3 weeks, three-dimensional microcolonies were observed and thus, the number of attached cells calculated from CLSM images was underestimated. Observations of DAPI-stained pyrite slabs with light microscopy suggested that the density of attached cells and the coverage area kept on almost constant values after 3 weeks (see text)

(2) values were inferred from the available data in the published work

py = pyrite

ht = hematite

mgt = magnetite

In the case of colonization of pyrite by *A. ferrooxidans* under circumneutral pH, a larger coverage area (50%) and a percentage of attached cells (90%) were reported (Mielke et al., 2003). The authors showed that the number of viable cells in solution clearly decreased over time, indicating that cells must attach to the pyrite surface in order to survive at pH 7. They postulated that colonization was facilitated by the development of an acidic microenvironment between the cells and the pyrite surface.

Bacteria using only a small fraction of the available area have also been found in studies measuring the attachment of indigenous bacteria to aquifer and marine sediments. Griebler et al. (2002) showed that bacteria colonize only a small proportion (<3%) of the available surface area in *in situ* aquifer sediment microcosms exposed to groundwater. Similarly, Yamamoto and Lopez (1985) and Weise and Rheinheimer (1977) found that less than 5% of the total grain surface was populated by bacteria in marine sands. Therefore, factors other than surface availability such as the mineralogy and particle size must limit microbial colonization of sediments.

However, in laboratory experiments using indirect methods to quantify cell attachment, larger coverage areas (20-45%) and higher percentages of attached cells (20-80%) were reported for *A. ferrooxidans* and *S. putrefaciens* adhesion to crushed pyrite and magnetite, respectively (Solari et al., 1992; Ohmura et al., 1993; Harneit et al., 2006; Roberts et al., 2006; Ruiz et al., 2008) (Table 5.3). These differences could be due to the use of powdered minerals instead of slabs or crystals. The surface area and roughness of these mineral particles were greater, promoting bacterial adhesion. Similarly, Harvey et al. (1984), Bekins et al. (1999) and Griebler et al. (2002) estimated high percentages of attached bacteria (50-99%) for subsurface natural environments. Similar observations were made in laboratory microcosm studies with crushed basalt particles (Lehman et al., 2001). In these studies, the attached bacteria were counted in solution after removal from the particulate sediments by washing, shaking and sonicating or by blending and centrifugation.

5.2.8 Implications

The results of the present study using a pure culture of a denitrifying bacterium and polished and small-area pyrite samples could be qualitatively applied to the natural environment to better understand pyrite-driven denitrification in aquifers and to optimize bioremediation. However, it is uncertain whether the required attachment to pyrite surfaces of at least some cells is specific to this strain or whether it is a common behavior of denitrifying bacteria. Furthermore, the relative roles of attached and planktonic cells probably depend on the composition of the bacterial community, on the geochemical conditions (e.g. pH, redox potential, ionic strength, nutrient availability, dissolved solutes), and on the mineralogy, surface area, heterogeneity and availability of the solid phase to be colonized. In the natural environment, pyrite surfaces with a higher surface area and greater roughness than the ones used in the present experiments will probably promote bacteria attachment.

Further *in situ* colonization experiments are therefore warranted to apply these results to the natural environment of nitrate-contaminated aquifers. The *in situ* colonization experiments consist in placing the mineral into the native contaminated groundwater and in leaving it undisturbed to interact with groundwater and native microorganisms. In groundwater, *in situ* colonization experiments have been used to study bacterial attachment onto natural sediments (Hirsch and Rades-Rohkoh, 1990; Griebler et al., 2002; Herrmann et al., 2008). Other *in situ* microcosms have been employed to evaluate microbial colonization, biofilm development and the diversity of bacterial communities colonizing artificial substrates such as glass beads or polymers (Claret, 1998; Dang and Lovell, 2000; Peacock et al., 2004; Iribar, 2007). The utilization of *in situ* microcosms seems to be the most suitable method for sidestepping the uncertainty of the results obtained exclusively from laboratory studies and could help us to better understand aquifer microbiology.

Given that attached cells have a number of advantages over free cells, the use of immobilization biosystems for bioremediation purposes has been evaluated in order to

optimize biotechnological processes (Cassidy et al. 1996; Singh et al., 2006). Two approaches have been adopted (Cohen, 2001): (1) the addition of a bedding material to enhance self-attachment of indigenous bacteria, which is a biostimulation strategy; and (2) the addition of desired microbial species entrapped in a bedding material, which is a bioaugmentation strategy. Immobilized cells could improve bioremediation processes by preventing bacteria from leaving the system and by protecting them against unfavorable environments. However, most of the research has been performed at laboratory level, and applications of encapsulated cells for *in situ* bioremediation are still in the early developmental stage (Singh et al., 2006). As regards nitrate contamination, few laboratory studies have assessed nitrate removal by immobilized denitrifying bacteria. Tal et al. (1997; 1999; 2003) and Liu et al. (2003) evaluated the use of heterotrophic denitrifying bacteria entrapped within alginate beads with starch and tartrate, respectively. Moreno-Castilla et al. (2003) used *Escherichia coli* cells immobilized on activated carbons to assess ethanol-driven nitrate reduction. Zhang et al. (2009b) assessed polyvinyl alcohol (PVA) beads with attached cells of *T. denitrificans* to remove nitrate using thiosulfate as the electron donor.

As for pyrite-driven denitrification, the results of the present study using *T. denitrificans* suggest that a small number of cells must adhere to the pyrite surface, and that both attached and free-living cells seem to contribute to pyrite-driven denitrification. Therefore, bioremediation strategies based on denitrification with pyrite can be improved by creating optimal growth conditions for the autotrophic denitrifying bacteria in bioreactors, e.g. promoting attachment. For example, immobilized cells could be of considerable use under low hydraulic retention times (i.e. high flow rate and/or small bioreactor size) and could reduce the start-up period.

5.3 Conclusions

Growth and attachment of the autotrophic denitrifying bacterium *Thiobacillus denitrificans* onto pyrite surfaces was studied by means of 9-week colonization experiments using polished pyrite slabs.

A small number of cells were attached to the pyrite surface and direct growth and division onto surface was observed. Single cells attached to the pyrite surface were first detected and after 3 weeks, microcolonies were observed. The microcolonies were observed as islands and only less than 2% of the available pyrite surface was estimated to be covered by cells. The rate of colonization of the pyrite surface was around 35 cells mm^{-2} h^{-1} during the 3-week period. In 4-week old samples, the cells were found to be surrounded by an organic film. After 9 weeks, organic films covered larger areas of the pyrite surface. About 0.3% of total cells were estimated to be attached to the pyrite surface. Planktonic cells survived during the course of the runs and new attachments of free-living cells were observed over time.

The results suggest that at least a small number of *T. denitrificans* cells must attach to pyrite in order to achieve nitrate reduction coupled to pyrite oxidation. However, both attached and free-living cells probably contributed to denitrification. Nevertheless, the relative roles of the two phases and the specific mechanisms remain unresolved.

These results may be applied to the natural environment to predict the spatial distribution of denitrifying bacteria in subsurface environments in an attempt to better understand pyrite-driven denitrification in aquifers. However, further *in situ* colonization experiments are warranted to assess interaction between indigenous bacteria and pyrite in nitrate-contaminated aquifers where mixed natural microbial populations and pyrite surfaces with a larger reactive area, greater roughness and more microtopographic features exist. Furthermore, the results could prove useful in optimizing bioremediation strategies based on the stimulation of pyrite-driven denitrification, e.g. promoting the attachment of denitrifying cells to pyrite in bioreactors.

Chapter 6

General conclusions

This chapter summarizes the main contributions of this thesis.

The **first part of this thesis** deals with the characterization of the denitrification processes occurring in the Osona aquifer and their spatial and temporal variations. Multi-isotopic methods are applied and integrated with classical hydrogeological methods to assess the fate of nitrate in groundwater.

The results confirm that nitrate pollution in the Osona area is mainly derived from the application of pig manure as organic fertilizer. More than 80% of the studied wells have nitrate contents higher than the drinking water threshold of 50 mg L^{-1}. Natural attenuation occurs in the Zone 3, where the main crop fields are located, and in the Zone 1 that corresponds to the Northern recharge area. In the Zone 2 (Southeastern recharge area), however, denitrification is limited to two samples. The denitrification processes are linked to pyrite oxidation, as demonstrated by coupling nitrate with sulfate isotopic data. The relative role of the organic matter to the overall denitrification cannot be determined due to the carbonated lithology of the aquifer.

Due to the fact that sampled waters are a mix between different aquifer levels, as a result of the lack of well casing, and that sampled wells do not coincide with specific groundwater flow directions, the N and O isotopic enrichment factors are estimated using temporal variations of the nitrate concentration and the isotopic composition of a few wells, in which denitrification dominates during the entire studied period. Using the estimated enrichment factors, an approximation to the extent of natural attenuation taking place in the Osona aquifer is calculated, showing a median value between 25% and 33%.

The **second part of this thesis** is devoted to evaluate the feasibility of a bioremediation strategy based on pyrite addition to stimulate native denitrifying bacteria. This part is divided in two sections according to the nature of the experiments.

The first section is dedicated to clarify the role of pyrite as electron donor for denitrification by means of batch and flow-through experiments. Nitrate consumption in the inoculated batch experiments demonstrates that *Thiobacillus denitrificans* is able to reduce nitrate using pyrite as the electron donor. The efficiency in nitrate removal and the nitrate reduction rate depend on the initial nitrate concentration, pH and pyrite grain size. 100% nitrate removal efficiency is attained in long-term inoculated experiments under laboratory conditions similar to those found in slow-moving, nitrate-contaminated groundwater.

Under non-sterilized, non-inoculated conditions, nitrate reduction also takes place but nitrate removal efficiencies are lower, and unpredictable denitrification stages are observed. Although the bacterial community present in these non-inoculated experiments is not native to a nitrate contaminated aquifer, it is able to adapt to the new conditions and reduce nitrate. This bacterial community is probably a mixture of autotrophic and heterotrophic bacteria, both contributing to the overall denitrification. It seems that dead and lysed cells of the autotrophic bacteria act as the carbon source for the heterotrophic bacteria.

The N and O enrichment factors associated with pyrite-driven denitrification by *T. denitrificans* are calculated. The estimated values give an idea of the magnitude of the isotopic fractionation that could be expected at field sites dominated by autotrophic denitrification based on pyrite oxidation.

The second section discusses the capacity of the indigenous bacteria of sediments and groundwater from the Osona aquifer to reduce nitrate using pyrite. Batch experiments show that the addition of pyrite stimulates the activity of the indigenous microbial community and enhances the nitrate removal. The results of the biostimulated and the biostimulated/bioaugmented experiments demonstrate that bioaugmentation with *T. denitrificans* is not necessary, although it slightly accelerates the nitrate removal rate. In the batch experiments, nitrate is removed concurrently with the release of sulfate, confirming that nitrate reduction is related to pyrite oxidation. At least 60% of the reduced nitrate is attributed to denitrification coupled to pyrite oxidation, the residual fraction being ascribed to heterotrophic denitrification. Accordingly, sequencing of selected bands of the *16S rRNA* gene-based DGGE profile demonstrates that not only autotrophic but also heterotrophic denitrifying bacteria are stimulated through pyrite addition. Bacterial populations closely related to *Xanthomonadaceae* might probably be the dominant autotrophic denitrifiers that use pyrite as the electron donor in the experiments. The addition of pyrite results in an increment in the proportion of denitrifying bacteria (increase in the ratio *nosZ/16S rRNA*), which is higher in the sediment-attached population than in the planktonic population. Therefore, molecular analyses demonstrate to be useful to understand the dynamics of the microbial community and should be taken into account for enhancing the performance of bioremediation strategies.

The N and O isotopic enrichment factors are computed and used to recalculate the extent of natural attenuation of nitrate in the Osona aquifer. The median percentage of denitrification is around 10%, instead of 30% that has been overestimated in the first part

of this thesis using enrichment factors roughly estimated in the field. This refinement becomes useful to predict the evolution of nitrate contamination in the aquifer, and it should be taken into account for potential implementation of induced remediation techniques. The isotopic approach proves to be an excellent tool to identify natural denitrification processes in the field, to quantify these attenuation processes and to monitor the efficacy of bioremediation strategies in the laboratory, as well as to assess the efficacy of induced attenuation in future *in situ* tests at field scale.

Nitrate reduction in the flow-through experiments demonstrates the long-term capacity of naturally occurring denitrifying bacteria and the bacterial consortium previously enriched in the batch experiments. Therefore, controlled addition of pyrite to stimulate the activity of indigenous denitrifying bacteria could be considered to remediate nitrate contamination in groundwater in future water management strategies. Further field-scale studies are needed to ascertain whether the results from the laboratory sediment incubations can be extrapolated to *in situ* bioremediation implementations in the contaminated aquifer. The persistence of the proposed biostimulation effect should be considered and monitored over time to establish the longevity of the enhanced denitrification.

The **last part of this thesis** addresses the contribution of attached and free-phase denitrifying bacteria to pyrite-driven denitrification in aquifers. Colonization experiments using polished pyrite slabs are carried out to determine the ability of *T. denitrificans* to grow and colonize pyrite surfaces.

A small number of cells attach to pyrite surfaces, being direct growth and division onto surfaces observed. The rate of colonization of pyrite surface is around 35 cells mm^{-2} h^{-1} under the study conditions and during a 3-week period. At the beginning of the experiments, attachment of single cells of *T. denitrificans* onto the pyrite surface is observed. After 3 weeks, microcolonies are detected isolated ones to others; after 4 weeks, only less than 2% of the available pyrite surface is covered by the cells, and after 9 weeks,

larger areas of pyrite surface are covered by organic films. About 0.3% of total cells are estimated to be attached to the pyrite surface and planktonic cells survive during the course of the runs.

Attachment to pyrite surface is required for at lest a small portion of the cells in order to accomplish pyrite-driven denitrification. Nevertheless, both attached and free-living cells probably contribute to denitrification. The details of the relative roles of the two phases and the specific mechanisms remain unresolved. Further *in situ* colonization experiments are warranted to apply these results to the natural environment of nitrate-contaminated aquifers and to better understand the mechanisms of pyrite-driven natural denitrification.

Hence, bioremediation strategies based on denitrification with pyrite can be improved by creating optimal growth conditions for autotrophic denitrifying bacteria in bioreactors and pilot plants, as for example using immobilized cells to allow bioreactors to succeed under low hydraulic retention times (i.e. high flow rate and/or small bioreactor size) and to reduce the start-up period.

In conclusion, addition of pyrite to stimulate the activity of indigenous denitrifying bacteria could be considered in future water management strategies of nitrate remediation in groundwater, although further research is needed, especially at field scale. However, a significant limitation of this bioremediation strategy could be the release of toxic metals from pyrite oxidation, e.g. As and Ni could be present in minor amounts in the pyrite structure. Thus care should be taken with the source and characterization of the pyrite for its use as amendment. This bioremediation strategy could be optimized, promoting long-term activity, growth and survival of denitrifying bacteria and determining the optimum operational parameters (e.g. hydraulic retention time, nitrate loading rate, etc.) to achieve high efficiency in nitrate removal. Furthermore, more extensive understanding of denitrifying microorganisms and the environmental parameters controlling their activity is required.

Bibliography

Akob, D.M., Mills, H.J., and Kostka, J.E. (2007) Metabolically active microbial communities in uranium-contaminated subsurface sediments. *FEMS Microbiol Ecol* **59**: 95-107.

Altschul, S.F., Gish, W., Miller, W., Myers, E.W., and Lipman, D.J. (1990) Basic local alignment search tool. *J Mol Biol* **215**: 403-410.

Andersson, K.K., and Hooper, A.B. (1983) O_2 and H_2O are each the source of one O in NO_2^- produced from NH_3 by *Nitrosomonas*: ^{15}N-NMR evidence. *FEBS Lett* **164**: 236-240.

Aravena, R., and Robertson, W.D. (1998) Use of multiple isotope tracers to evaluate denitrification in ground water: Study of nitrate from a large-flux septic system plume. *Ground Water* **36**: 975-981.

Aravena, R., Evans, M.L., and Cherry, J.A. (1993) Stable isotopes of oxygen and nitrogen in source identification of nitrate from septic systems. *Ground Water* **31**: 180-186.

Batchelor, B., and Lawrence, A.W. (1978) Autotrophic denitrification using elemental sulfur. *J Water Pollut Con F* **50**: 1986-2001.

Balci, N., Shanks Iii, W.C., Mayer, B., and Mandernack, K.W. (2007) Oxygen and sulfur isotope systematics of sulfate produced by bacterial and abiotic oxidation of pyrite. *Geochim Cosmochim Acta* **71**: 3796-3811.

Barford, C.C., Montoya, J.P., Altabet, M.A., and Mitchell, R. (1999) Steady-state nitrogen isotope effects of N_2 and N_2O production in *Paracoccus denitrificans*. *Appl Environ Microbiol* **65**: 989-994.

Bates, H.K., and Spalding, R.F. (1998) Aquifer denitrification as interpreted from in situ microcosm experiments. *J Environ Qual* **27**: 174-182.

Bates, H.K., Martin, G.E., and Spalding, R.F. (1998) Kinetic isotope effects in production of nitrite-nitrogen and dinitrogen gas during in situ denitrification. *J Environ Qual* **27**: 183-191.

Bekins, B.A., Godsy, E.M., and Warren, E. (1999) Distribution of microbial physiologic types in an aquifer contaminated by crude oil. *Microb Ecol* **37**: 263-275.

Beller, H.R. (2005) Anaerobic, nitrate-dependent oxidation of U(IV) oxide minerals by the chemolithoautotrophic bacterium *Thiobacillus denitrificans*. *Appl Environ Microbiol* **71**: 2170-2174.

Beller, H.R., Madrid, V., Hudson, G.B., McNab, W.W., and Carlsen, T. (2004) Biogeochemistry and natural attenuation of nitrate in groundwater at an explosives test facility. *Appl Geochem* **19**: 1483-1494.

Beller, H.R., Chain, P.S.G., Letain, T.E., Chakicherla, A., Larimer, F.W., Richardson, P.M., Coleman, M.A., Wood, A.P., and Kelly, D.P. (2006) The genome sequence of the obligately chemolithoautotrophic, facultatively anaerobic bacterium *Thiobacillus denitrificans*. *J Bacteriol* **188**: 1473-1488.

Benz, M., Brune, A., and Schink, B. (1998) Anaerobic and aerobic oxidation of ferrous iron at neutral pH by chemoheterotrophic nitrate-reducing bacteria. *Arch Microbiol* **169**: 159-165.

Betlach, M.R., and Tiedje, J.M. (1981) Kinetic explanation for accumulation of nitrite, nitric oxide, and nitrous oxide during bacterial denitrification. *Appl Environ Microbiol* **42**: 1074-1084.

Blaszczyk, M. (1993) Effect of medium composition on the denitrification of nitrate by *Paracoccus denitrificans*. *Appl Environ Microbiol* **59**: 3951-3953.

Böttcher, J., Strebel, O., Voerkelius, S., and Schmidt, H.L. (1990) Using isotope fractionation of nitrate nitrogen and nitrate oxygen for evaluation of microbial denitrification in a sandy aquifer. *J Hydrol* **114**: 413-424.

Bru, D., Sarr, A., and Philippot, L. (2007) Relative abundances of proteobacterial membrane-bound and periplasmic nitrate reductases in selected environments. *Appl Environ Microbiol* **73**: 5971-5974.

Brunauer, S., Emmett, P.H., and Teller, E. (1938) Adsorption of gases in multimolecular layers. *J Am Chem Soc* **60**: 309-319.

Bryan, B.A., Shearer, G., Skeeters, J.L., and Kohl, D.H. (1983) Variable expression of the nitrogen isotope effect associated with denitrification of nitrite. *J Biol Chem* **258**: 8613-8617.

Cardenas, E., Wu, W.M., Leigh, M.B., Carley, J., Carroll, S., Gentry, T. et al. (2008) Microbial communities in contaminated sediments, associated with bioremediation of uranium to submicromolar levels. *Appl Environ Microbiol* **74**: 3718-3729.

Casciotti, K.L., Sigman, D.M., Hastings, M.G., Bohlke, J.K., and Hilkert, A. (2002) Measurement of the oxygen isotopic composition of nitrate in seawater and freshwater using the denitrifier method. *Anal Chem* **74**: 4905-4912.

Cassidy, M.B., Lee, H., and Trevors, J.T. (1996) Environmental applications of immobilized microbial cells: A review. *J Ind Microbiol* **16**: 79-101.

Cey, E.E., Rudolph, D.L., Aravena, R., and Parkin, G. (1999) Role of the riparian zone in controlling the distribution and fate of agricultural nitrogen near a small stream in southern Ontario. *J Contam Hydrol* **37**: 45-67.

Choe, S.H., Ljestrand, H.M., and Khim, J. (2004) Nitrate reduction by zero-valent iron under different pH regimes. *Appl Geochem* **19**: 335-342.

Chon, K., Chang, J.S., Lee, E., Lee, J., Ryu, J., and Cho, J. (2010) Abundance of denitrifying genes coding for nitrate (narG), nitrite (nirS), and nitrous oxide (nosZ) reductases in estuarine versus wastewater effluent-fed constructed wetlands. *Ecol Eng* **In Press, Corrected Proof**.

Claret, C. (1998) A method based on artificial substrates to monitor hyporheic biofilm development. *Int Rev Hydrobiol* **83**: 135-143.

Clark, I.D., and Fritz, P. (1997) *Environmental isotopes in hydrogeology*. New York: Lewis Publishers, 328 p.

Claus, G., and Kutzner, H.J. (1985) Physiology and kinetics of autotrophic denitrification by *Thiobacillus denitrificans*. *Appl Microbiol Biotechnol* **22**: 283-288.

Clément, J.C., Holmes, R.M., Peterson, B.J., and Pinay, G. (2003) Isotopic investigation of denitrification in a riparian ecosystem in western France. *J Appl Ecol* **40**: 1035-1048.

Cohen, Y. (2001) Biofiltration - The treatment of fluids by microorganisms immobilized into the filter bedding material: a review. *Bioresour Technol* **77**: 257-274.

Comly, H.H. (1945) Cyanosis in infants caused by nitrates in well water. *J Amer Med Assoc* **129**: 112-116.

Costerton, J.W., Lewandowski, Z., Caldwell, D.E., Korber, D.R., and Lappin-Scott, H.M. (1995) Microbial biofilms. *Annu Rev Microbiol* **49**: 711-745.

Cravotta, C.A. (1997) Use of stable isotopes of carbon, nitrogen, and sulfur to identify sources of nitrogen in surface waters in the Lower Susquehanna River Basin, Pennsylvania. In *US Geological Survey Water-Supply Paper*. Washinghton (DC): US Geogical Survey, p. 104.

Cravotta, C.A. (1998) Effect of sewage sludge on formation of acidic ground water at a reclaimed coal mine. *Ground Water* **36**: 9-19.

Crundwell, F.K. (1996) The formation of biofilms of iron-oxidising bacteria on pyrite. *Miner Eng* **9**: 1081-1089.

Crundwell, F.K. (2003) How do bacteria interact with minerals? *Hydrometallurgy* **71**: 75-81.

Dandie, C.E., Burton, D.L., Zebarth, B.J., Henderson, S.L., Trevors, J.T., and Goyer, C. (2008) Changes in bacterial denitrifier community abundance over time in an agricultural field and their relationship with denitrification activity. *Appl Environ Microbiol* **74**: 5997-6005.

Dang, H., and Lovell, C.R. (2000) Bacterial primary colonization and early succession on surfaces in marine waters as determined by amplified rRNA gene restriction analysis and sequence analysis of 16S rRNA genes. *Appl Environ Microbiol* **66**: 467-475.

Delwiche, C.C., and Steyn, P.L. (1970) Nitrogen isotope fractionation in soils and microbial reactions. *Environ Sci Technol* **4**: 929-935.

Della Rocca, C., Belgiorno, V., and Meriç, S. (2006) An heterotrophic/autotrophic denitrification (HAD) approach for nitrate removal from drinking water. *Process Biochem* **41**: 1022-1028.

Della Rocca, C., Belgiorno, V., and Meriç, S. (2007) Overview of in-situ applicable nitrate removal processes. *Desalination* **204**: 46-62.

Devito, K.J., Fitzgerald, D., Hill, A.R., and Aravena, R. (2000) Nitrate dynamics in relation to lithology and hydrologic flow path in a river riparian zone. *J Environ Qual* **29**: 1075-1084.

Devlin, J.F., Eedy, R., and Butler, B.J. (2000) The effects of electron donor and granular iron on nitrate transformation rates in sediments from a municipal water supply aquifer. *J Contam Hydrol* **46**: 81-97.

Djigal, D., Baudoin, E., Philippot, L., Brauman, A., and Villenave, C. (2010) Shifts in size, genetic structure and activity of the soil denitrifier community by nematode grazing. *European Journal of Soil Biology* **46**: 112-118.

Dunne Jr, W.M. (2002) Bacterial adhesion: Seen any good biofilms lately? *Clin Microbiol Rev* **15**: 155-166.

Dziurla, M.-A., Achouak, W., Lam, B.-T., Heulin, T., and Berthelin, J. (1998) Enzyme-linked immunofiltration assay to estimate attachment of *Thiobacilli* to pyrite. *Appl Environ Microbiol* **64**: 2937-2942.

Edwards, K.J., Bond, P.L., and Banfield, J.F. (2000) Characteristics of attachment and growth of *Thiobacillus caldus* on sulphide minerals: a chemotactic response to sulphur minerals? *Environ Microbiol* **2**: 324-332.

Edwards, K.J., Schrenk, M.O., Hamers, R., and Banfield, J.F. (1998) Microbial oxidation of pyrite: Experiments using microorganisms from an extreme acidic environment. *Am Mineral* **83**: 1444-1453.

Engesgaard, P., and Kipp, K.L. (1992) A geochemical transport model for redox-controlled movement of mineral fronts in groundwater flow systems: a case of nitrate removal by oxidation of pyrite. *Water Resour Res* **28**: 2829-2843.

Fernández, N., Sierra-Alvarez, R., Field, J.A., Amils, R., and Sanz, J.L. (2008) Microbial community dynamics in a chemolithotrophic denitrification reactor inoculated with methanogenic granular sludge. *Chemosphere* **70**: 462-474.

Finkmann, W., Altendorf, K., Stackebrandt, E., and Lipski, A. (2000) Characterization of N_2O-producing *Xanthomonas*-like isolates from biofilters as *Stenotrophomonas nitritireducens* sp. nov., *Luteimonas mephitis* gen. nov., sp. nov. and *Pseudoxanthomonas broegbernensis* gen. nov., sp. nov. *Int J Syst Evol Microbiol* **50**: 273-282.

Flores, A., Nisola, G.M., Cho, E., Gwon, E.M., Kim, H., Lee, C. et al. (2007) Bioaugmented sulfur-oxidizing denitrification system with *Alcaligenes defragrans* B21 for high nitrate containing wastewater treatment. *Bioprocess Biosystems Eng* **30**: 197-205.

Fowler, T.A., Holmes, P.R., and Crundwell, F.K. (2001) On the kinetics and mechanism of the dissolution of pyrite in the presence of *Thiobacillus ferrooxidans*. *Hydrometallurgy* **59**: 257-270.

Fritz, P., and Fontes, J.C. (1980) Introduction. In *Handbook of environmental isotope geochemistry, Vol 1, The terrestrial environment*. Fritz, P., and Fontes, J.C. (eds). Amsterdam: Elsevier, pp. 1-19.

Fukada, T., Hiscock, K.M., Dennis, P.F., and Grischek, T. (2003) A dual isotope approach to identify denitrification in groundwater at a river-bank infiltration site. *Water Res* **37**: 3070-3078.

Fogel, G.B., Collins, C.R., Li, J., and Brunk, C.F. (1999) Prokaryotic genome size and SSU rDNA copy number: Estimation of microbial relative abundance from a mixed population. *Microb Ecol* **38**: 93-113.

Fustec, E., Mariotti, A., Grillo, X., and Sajus, J. (1991) Nitrate removal by denitrification in alluvial ground water: Role of a former channel. *J Hydrol* **123**: 337-354.

Geets, J., De Cooman, M., Wittebolle, L., Heylen, K., Vanparys, B., De Vos, P. et al. (2007) Real-time PCR assay for the simultaneous quantification of nitrifying and denitrifying bacteria in activated sludge. *Appl Microbiol Biotechnol* **75**: 211-221.

Ginige, M.P., Hugenholtz, P., Daims, H., Wagner, M., Keller, J., and Blackall, L.L. (2004) Use of Stable-Isotope Probing, full-cycle rRNA analysis, and Fluorescence In Situ Hybridization-Microautoradiography to study a methanol-fed denitrifying microbial community. *Appl Environ Microbiol* **70**: 588-596.

Goldstein, R.M., Mallory, L.M., and Alexander, M. (1985) Reasons for possible failure of inoculation to enhance biodegradation. *Appl Environ Microbiol* **50**: 977-983.

Gorby, Y.A., Yanina, S., McLean, J.S., Rosso, K.M., Moyles, D., Dohnalkova, A. et al. (2006) Electrically conductive bacterial nanowires produced by *Shewanella oneidensis* strain MR-1 and other microorganisms. *P Natl Acad Sci USA* **103**: 11358-11363.

Griebler, C., Mindl, B., Slezak, D., and Geiger-Kaiser, M. (2002) Distribution patterns of attached and suspended bacteria in pristine and contaminated shallow aquifers studied with an in situ sediment exposure microcosm. *Aquat Microb Ecol* **28**: 117-129.

Grischek, T., Hiscock, K.M., Metschies, T., and Dennis, P.F. (1998) Factors affecting denitrification during infiltration of river water into a sand and gravel aquifer in Saxony, Germany. *Water Res* **32**: 450-460.

Grüntzig, V., Nold, S.C., Zhou, J., and Tiedje, J.M. (2001) *Pseudomonas stutzeri* nitrite reductase gene abundance in environmental samples measured by real-time PCR. *Appl Environ Microbiol* **67**: 760-768.

Haaijer, S.C.M., Lamers, L.P.M., Smolders, A.J.P., Jetten, M.S.M., and Op de Camp, H.J.M. (2007) Iron sulfide and pyrite as potential electron donors for microbial nitrate reduction in freshwater wetlands. *Geomicrobiol J* **24**: 391-401.

Hall, T.A. (1999) BioEdit: A user-friendly biological sequence alignment editor and analysis program for Windows 95/98/NT. *Nucleic Acids Symp Ser* **41**: 95-98.

Hansen, H.C.B., Guldberg, S., Erbs, M., and Koch, C.B. (2001) Kinetics of nitrate reduction by green rusts - effects of interlayer anion and Fe(II): Fe(III) ratio. *Appl Clay Sci* **18**: 81-91.

Harneit, K., Göksel, A., Kock, D., Klock, J.H., Gehrke, T., and Sand, W. (2006) Adhesion to metal sulfide surfaces by cells of *Acidithiobacillus ferrooxidans*, *Acidithiobacillus thiooxidans* and *Leptospirillum ferrooxidans*. *Hydrometallurgy* **83**: 245-254.

Harvey, R.W., Smith, R.L., and George, L. (1984) Effect of organic contamination upon microbial distributions and heterotrophic uptake in a Cape Cod, Mass., aquifer. *Appl Environ Microbiol* **48**: 1197-1202.

Hashimoto, S., Furukawa, K., and Shioyama, M. (1987) Autotrophic denitrification using elemental sulfur. *J Ferment Technol* **65**: 683-692.

Heaton, T.H.E. (1986) Isotopic studies of nitrogen pollution in the hydrosphere and atmosphere - A review. *Chem Geol* **59**: 87-102.

Henry, S., Baudoin, E., López-Gutiérrez, J.C., Martin-Laurent, F., Brauman, A., and Philippot, L. (2004) Quantification of denitrifying bacteria in soils by nirK gene targeted real-time PCR. *J Microbiol Methods* **59**: 327-335.

Henry, S., Bru, D., Stres, B., Hallet, S., and Philippot, L. (2006) Quantitative detection of the nosZ gene, encoding nitrous oxide reductase, and comparison of the abundances of 16S rRNA, narG, nirK, and nosZ genes in soils. *Appl Environ Microbiol* **72**: 5181-5189.

Henry, S., Texier, S., Hallet, S., Bru, D., Dambreville, C., Chèneby, D. et al. (2008) Disentangling the rhizosphere effect on nitrate reducers and denitrifiers: Insight into the role of root exudates. *Environ Microbiol* **10**: 3082-3092.

Herrmann, S., Kleinsteuber, S., Neu, T.R., Richnow, H.H., and Vogt, C. (2008) Enrichment of anaerobic benzene-degrading microorganisms by *in situ* microcosms. *FEMS Microbiol Ecol* **63**: 94-106.

Hirsch, P., and Rades-Rohkohl, E. (1990) Microbial colonization of aquifer sediment exposed in a groundwater well in Northern Germany. *Appl Environ Microbiol* **56**: 2963-2966.

Hollocher, T.C. (1984) Source of the oxygen-atoms of nitrate in the oxidation of nitrite by *Nitrobacter agilis* and evidence against a P-O-N anhydride mechanism in oxidative-phosphorylation. *Arch Biochem Biophys* **233**: 721-727.

Horibe, Y., Shigehara, K., and Takakuwa, Y. (1973) Isotope separation factor of carbon dioxide–water system and isotopic composition of atmospheric oxygen. *J Geophys Res* **78**: 2625-2629.

Iribar, A. (2007) Composition des communautés bactériennes dénitrifiantes au sein d'un aquifère alluvial et facteurs contrôlant leur structuration: relation entre structure des communautés et dénitrification. PhD Thesis. Université Toulouse III − Paul Sabatier.

Iribar, A., Sánchez-Pérez, J.M., Lyautey, E., and Garabétian, F. (2008) Differentiated free-living and sediment-attached bacterial community structure inside and outside denitrification hotspots in the river-groundwater interface. *Hydrobiologia* **598**: 109-121.

Jones, C.M., Stres, B., Rosenquist, M., and Hallin, S. (2008) Phylogenetic analysis of nitrite, nitric oxide, and nitrous oxide respiratory enzymes reveal a complex evolutionary history for denitrification. *Mol Biol Evol* **25**: 1955-1966.

Jorgensen, C.J., Jacobsen, O.S., Elberling, B., and Aamand, J. (2009) Microbial oxidation of pyrite coupled to nitrate reduction in anoxic groundwater sediment. *Environ Sci Technol* **43**: 4851-4857.

Kandeler, E., Deiglmayr, K., Tscherko, D., Bru, D., and Philippot, L. (2006) Abundance of narG, nirS, nirK, and nosZ genes of denitrifying bacteria during primary successions of a glacier foreland. *Appl Environ Microbiol* **72**: 5957-5962.

Kappler, A., and Newman, D.K. (2004) Formation of Fe(III)-minerals by Fe(II)-oxidizing photoautotrophic bacteria. *Geochim Cosmochim Acta* **68**: 1217-1226.

Kawanishi, T., Hayashi, Y., Kmou, N., Yoneyama, T., and Ozaki, Y. (1993) Dispersion effect on the apparent nitrogen isotope fractionation factor associated with denitrification in soil; Evaluation by a mathematical model. *Soil Biol Biochem* **25**: 349-354.

Kelly, D.P., and Harrison, A.H. (1989) Genus *Thiobacillus*. In *Bergey's manual of systematic bacteriology*. Staley, J.T., Bryant, M.P., Pfennig, N., and Holt, J.G. (eds). Baltimore: Williams & Wilkins, Co, pp. 1842-1858.

Kloos, K., Mergel, A., Rösch, C., and Bothe, H. (2001) Denitrification within the genus *Azospirillum* and other associative bacteria. *Funct Plant Biol* **28**: 991-998.

Knowles, R. (1982) Denitrification. *Microbiol Rev* **46**: 43-70.

Koba, K., Tokuchi, N., Wada, E., Nakajima, T., and Iwatsubo, G. (1997) Intermittent denitrification: The application of a ^{15}N natural abundance method to a forested ecosystem. *Geochim Cosmochim Acta* **61**: 5043-5050.

Koenig, A., Zhang, T., Liu, L., and Fang, H. (2005) Microbial community and biochemistry process in autosulfurotrophic denitrifying biofilm. *Chemosphere* **58**: 1041-1047.

Kölle, W., Werner, P., Strebel, O., and Böttcher, J. (1983) Denitrification by pyrite in a reducing aquifer. *Vom Wasser* **61**: 125-147.

Korom, S.F. (1992) Natural denitrification in the saturated zone - A review. *Water Resour Res* **28**: 1657-1668.

Kroopnick, P., and Craig, H. (1972) Atmospheric oxygen: isotopic composition and solubility fractionation. *Science* **175**: 54-55.

Lane, D.J. (1991) 16S/23S rRNA sequencing. In *Nucleic Acid Techniques in Bacterial Systematics*. Stackebrandt, E., and Goodfellow, M. (eds). New York: Wiley, pp. 115-175.

Lasaga, A.C. (1998) *Kinetic Theory in the Earth Sciences*. Princeton, New Jersey: Princeton University Press, 728 p.

Le Bideau, L., and Dudoignon, P. (1996) Evidence of natural denitrification mechanism at Beuxes (Vienne, France). *C.R. Acad. Sci., Ser. IIa: Sci. Terre Planets* **322**: 555-562.

Leang, C., Coppi, M.V., and Lovley, D.R. (2003) OmcB, a c-type polyheme cytochrome, involved in Fe(III) reduction in *Geobacter sulfurreducens*. *J Bacteriol* **185**: 2096-2103.

Lehman, R.M., Colwell, F.S., and Bala, G.A. (2001) Attached and unattached microbial communities in a simulated basalt aquifer under fracture- and porous-flow conditions. *Appl Environ Microbiol* **67**: 2799-2809.

Lehmann, M.F., Reichert, P., Bernasconi, S.M., Barbieri, A., and McKenzie, J.A. (2003) Modelling nitrogen and oxygen isotope fractionation during denitrification in a lacustrine redox-transition zone. *Geochim Cosmochim Acta* **67**: 2529-2542.

Liu, S.X., Hermanowicz, S.W., and Peng, M. (2003) Nitrate removal from drinking water through the use of encapsulated microorganisms in alginate beads. *Environ Technol* **24**: 1129-1134.

López-Gutiérrez, J.C., Henry, S., Hallet, S., Martin-Laurent, F., Catroux, G., and Philippot, L. (2004) Quantification of a novel group of nitrate-reducing bacteria in the environment by real-time PCR. *J Microbiol Methods* **57**: 399-407.

Lovley, D.R., Holmes, D.E., and Nevin, K.P. (2004) Dissimilatory Fe(III) and Mn(IV) Reduction. *Adv Microb Physiol* **49**: 219-286.

Magee, P.N., and Barnes, J.M. (1956) The production of malignant primary hepatic tumors in the rat by feeding dimethylnitrosamine. *Br J Cancer* **10**: 114-122.

Maidak, B.L., Cole, J.R., Lilburn, T.G., Parker Jr, C.T., Saxman, P.R., Stredwick, J.M. et al. (2000) The RDP (Ribosomal Database Project) continues. *Nucleic Acids Res* **28**: 173-174.

Manconi, I., Carucci, A., Lens, P., and Rossetti, S. (2006) Simultaneous biological removal of sulphide and nitrate by autotrophic denitrification in an activated sludge system. *Water Sci Technol* **53**: 91-99.

Mariotti, A., Landreau, A., and Simon, B. (1988) ^{15}N isotope biogeochemistry and natural denitrification process in groundwater: application to the chalk aquifer of northern France. *Geochim Cosmochim Acta* **52**: 1869-1878.

Mariotti, A., Germon, J.C., Hubert, P., Kaiser, P., Létolle, R., Tardieux, A., and Tardieux, P. (1981) Experimental determination of nitrogen kinetic isotope fractionation - Some principles - Illustration for the denitrification and nitrification processes. *Plant Soil* **62**: 413-430.

Marshall, K.C., and Goodman, A.E. (1994) Effects of adhesion on microbial cell physiology. *Colloids Surf B Biointerfaces* **2**: 1-7.

Mateju, V., Cizinska, S., Krejci, J., and Janoch, T. (1992) Biological water denitrification - A review. *Enzyme Microb Technol* **14**: 170-183.

McClure, N.C., Fry, J.C., and Weightman, A.J. (1991) Survival and catabolic activity of natural and genetically engineered bacteria in a laboratory-scale activated-sludge unit. *Appl Environ Microbiol* **57**: 366-373.

McPherson, M.J., and Møller, S.G. (2000) *PCR*. Oxford: Scientific Publishers, 288 p.

Menció, A., Mas-Pla, J., Otero, N., and Soler, A. (2010) Nitrate as a tracer of groundwater flow in a fractured multilayered aquifer. *Hydrolog Sci J* **submitted for publication**.

Mengis, M., Walther, U., Bernasconi, S.M., and Wehrli, B. (2001) Limitations of using $\delta^{18}O$ for the source identification of nitrate in agricultural soils. *Environ Sci Technol* **35**: 1840-1844.

Mengis, M., Schif, S.L., Harris, M., English, M.C., Aravena, R., Elgood, R.J., and MacLean, A. (1999) Multiple geochemical and isotopic approaches for assessing ground water NO_3 elimination in a riparian zone. *Ground Water* **37**: 448-457.

Mielke, R.E., Pace, D.L., Porter, T., and Southam, G. (2003) A critical stage in the formation of acid mine drainage: Colonization of pyrite by *Acidithiobacillus ferrooxidans* under pH-neutral conditions. *Geobiology* **1**: 81-90.

Miot, J., Benzerara, K., Morin, G., Kappler, A., Bernard, S., Obst, M. et al. (2009) Iron biomineralization by anaerobic neutrophilic iron-oxidizing bacteria. *Geochim Cosmochim Acta* **73**: 696-711.

Moncaster, S.J., Bottrell, S.H., Tellam, J.H., Lloyd, J.W., and Konhauser, K.O. (2000) Migration and attenuation of agrochemical pollutants: insights from isotopic analysis of groundwater sulphate. *J Contam Hydrol* **43**: 147-163.

Moon, H., Shin, D., Nam, K., and Kim, J. (2008) A long-term performance test on an autotrophic denitrification column for application as a permeable reactive barrier. *Chemosphere* **73**: 723-728.

Moreno-Castilla, C., Bautista-Toledo, I., Ferro-García, M.A., and Rivera-Utrilla, J. (2003) Influence of support surface properties on activity of bacteria immobilised on activated carbons for water denitrification. *Carbon* **41**: 1743-1749.

Moses, C.O., Nordstrom, D.K., Herman, J.S., and Mills, A.L. (1987) Aqueous pyrite oxidation by dissolved-oxygen and by ferric iron. *Geochim Cosmochim Acta* **51**: 1561-1571.

Murray, A.E., Hollibaugh, J.T., and Orrego, C. (1996) Phylogenetic compositions of bacterioplankton from two California estuaries compared by denaturing gradient gel electrophoresis of 16S rDNA fragments. *Appl Environ Microbiol* **62**: 2676-2680.

Muyzer, G., and Smalla, K. (1998) Application of denaturing gradient gel electrophoresis (DGGE) and temperature gradient gel electrophoresis (TGGE) in microbial ecology. *Anton Leeuw Int J G* **73**: 127-141.

Muyzer, G., De Waal, E.C., and Uitterlinden, A.G. (1993) Profiling of complex microbial populations by denaturing gradient gel electrophoresis analysis of polymerase chain reaction-amplified genes coding for 16S rRNA. *Appl Environ Microbiol* **59**: 695-700.

Neal, A.L., Rosso, K.M., Geesey, G.G., Gorby, Y.A., and Little, B.J. (2003) Surface structure effects on direct reduction of iron oxides by *Shewanella oneidensis*. *Geochim Cosmochim Acta* **67**: 4489-4503.

Nielsen, J.L., and Nielsen, P.H. (1998) Microbial nitrate-dependent oxidation of ferrous iron in activated sludge. *Environ Sci Technol* **32**: 3556-3561.

North, N.N., Dollhopf, S.L., Petrie, L., Istok, J.D., Balkwill, D.L., and Kostka, J.E. (2004) Change in bacterial community structure during in situ biostimulation of subsurface sediment cocontaminated with uranium and nitrate. *Appl Environ Microbiol* **70**: 4911-4920.

Nübel, U., Engelen, B., Felsre, A., Snaidr, J., Wieshuber, A., Amann, R.I. et al. (1996) Sequence heterogeneities of genes encoding 16S rRNAs in *Paenibacillus polymyxa* detected by temperature gradient gel electrophoresis. *J Bacteriol* **178**: 5636-5643.

Ohmura, N., Kitamura, K., and Saiki, H. (1993) Selective adhesion of *Thiobacillus ferrooxidans* to pyrite. *Appl Environ Microbiol* **59**: 4044-4050.

Osaka, T., Yoshie, S., Tsuneda, S., Hirata, A., Iwami, N., and Inamori, Y. (2006) Identification of acetate- or methanol-assimilating bacteria under nitrate-reducing conditions by stable-isotope probing. *Microb Ecol* **52**: 253-266.

Otero, N., Canals, À., and Soler, A. (2007) Using dual-isotope data to trace the origin and processes of dissolved sulphate: a case study in Calders stream (Llobregat basin, Spain). *Aquat Geochem* **13**: 109-126.

Paerl, H.W. (1985) Influence of attachment on microbial metabolism and growth in aquatic ecosystems. In *Bacterial adhesion*. Savage, D.C., and Fletcher, M. (eds). New York: Plenum Publishing Corp., pp. 363-400.

Park, J.Y., and Yoo, Y.J. (2009) Biological nitrate removal in industrial wastewater treatment: Which electron donor we can choose. *Appl Microbiol Biotechnol* **82**: 415-429.

Parkhurst, D.L. (1995) *User's guide to PHREEQC--A computer program for speciation, reaction-path, advective-transport, and inverse geochemical calculations*: U.S. Geological Survey Water-Resources Investigations Report 95-4227, 143 p.

Pauwels, H., Foucher, J.C., and Kloppmann, W. (2000) Denitrification and mixing in a schist aquifer: influence on water chemistry and isotopes. *Chem Geol* **168**: 307-324.

Pauwels, H., Ayraud-Vergnaud, V., Aquilina, L., and Molénat, J. (2010) The fate of nitrogen and sulfur in hard-rock aquifers as shown by sulfate-isotope tracing. *Appl Geochem* **25**: 105-115.

Pauwels, H., Kloppmann, W., Foucher, J.C., Martelat, A., and Fritsche, V. (1998) Field tracer test for denitrification in a pyrite-bearing schist aquifer. *Appl Geochem* **13**: 767-778.

Peacock, A.D., Chang, Y.J., Istok, J.D., Krumholz, L., Geyer, R., Kinsall, B. et al. (2004) Utilization of microbial biofilms as monitors of bioremediation. *Microb Ecol* **47**: 284-292.

Philippot, L. (2002) Denitrifying genes in bacterial and Archaeal genomes. *Biochim Biophys Acta Gene Struct Expression* **1577**: 355-376.

Philippot, L. (2005) Tracking nitrate reducers and denitrifiers in the environment. *Biochem Soc Trans* **33**: 200-204.

Philippot, L. (2006) Use of functional genes to quantify denitrifiers in the environment. *Biochem Soc Trans* **34**: 101-103.

Pierre, C., Taberner, C., Urquiola, M.M., and Pueyo, J.J. (1994) Sulphur and oxygen isotope composition of sulphates in hypersaline environments, as markers of redox depositional versus diagenetic changes. *Mineral Mag* **58**: 724-725.

Pisapia, C., Humbert, B., Chaussidon, M., and Mustin, C. (2008) Perforative corrosion of pyrite enhanced by direct attachment of *Acidithiobacillus ferrooxidans. Geomicrobiol J* **25**: 261-273.

Postma, D. (1990) Kinetics of nitrate reduction by detrital Fe(II)-silicates. *Geochim Cosmochim Acta* **54**: 903-908.

Postma, D., Boesen, C., Kristiansen, H., and Larsen, F. (1991) Nitrate reduction in an unconfined sandy aquifer - Water chemistry, reduction processes and geochemical modeling. *Water Resour Res* **27**: 2027-2045.

Rabalais, N.N. (2009) Nitrogen in aquatic ecosystems. *AMBIO* **31**: 102-112.

Reyna, L., Wunderlin, D.A., and Genti-Raimondi, S. (2010) Identification and quantification of a novel nitrate-reducing community in sediments of Suquía River basin along a nitrate gradient. *Environ Pollut* **158**: 1608-1614.

Rivett, M.O., Buss, S.R., Morgan, P., Smith, J.W.N., and Bemment, C.D. (2008) Nitrate attenuation in groundwater: A review of biogeochemical controlling processes. *Water Res* **42**: 4215-4232.

Roberts, J.A., Fowle, D.A., Hughes, B.T., and Kulczycki, E. (2006) Attachment behavior of *Shewanella putrefaciens* onto magnetite under aerobic and anaerobic conditions. *Geomicrobiol J* **23**: 631-640.

Robertson, W.D., Russell, B.M., and Cherry, J.A. (1996) Attenuation of nitrate in aquitard sediments of southern Ontario. *J Hydrol* **180**: 267-281.

Rodríguez-Maroto, J.M., García-Herruzo, F., García-Rubio, A., Gómez-Lahoz, C., and Vereda-Alonso, C. (2009) Kinetics of the chemical reduction of nitrate by zero-valent iron. *Chemosphere* **74**: 804-809.

Ruiz, L.M., Valenzuela, S., Castro, M., Gonzalez, A., Frezza, M., Soulère et al. (2008) AHL communication is a widespread phenomenon in biomining bacteria and seems to be involved in mineral-adhesion efficiency. *Hydrometallurgy* **94**: 133-137.

Sahu, A.K., Conneely, T., Nüsslein, K., and Ergas, S.J. (2009) Hydrogenotrophic denitrification and perchlorate reduction in ion exchange brines using membrane biofilm reactors. *Biotechnol Bioeng* **104**: 483-491.

Sánchez, I., Fernández, N., Amils, R., and Sanz, J.L. (2008) Assessment of the addition of *Thiobacillus denitrificans* and *Thiomicrospira denitrificans* to chemolithoautotrophic denitrifying bioreactors. *Int Microbiol* **11**: 179-184.

Sand, W., and Gehrke, T. (2006) Extracellular polymeric substances mediate bioleaching/biocorrosion via interfacial processes involving iron(III) ions and acidophilic bacteria. *Res Microbiol* **157**: 49-56.

Sand, W., Gehrke, T., Jozsa, P.-G., and Schippers, A. (2001) (Bio)chemistry of bacterial leaching - direct vs. indirect bioleaching. *Hydrometallurgy* **59**: 159-175.

Schippers, A., and Sand, W. (1999) Bacterial leaching of metal sulfides proceeds by two indirect mechanisms via thiosulfate or via polysulfides and sulfur. *Appl Environ Microbiol* **65**: 319-321.

Schippers, A., and Jorgensen, B.B. (2002) Biogeochemistry of pyrite and iron sulfide oxidation in marine sediments. *Geochim Cosmochim Acta* **66**: 85-92.

Schwientek, M., Einsiedl, F., Stichler, W., Stögbauer, A., Strauss, H., and Maloszewski, P. (2008) Evidence for denitrification regulated by pyrite oxidation in a heterogeneous porous groundwater system. *Chem Geol* **255**: 60-67.

Sebilo, M., Billen, G., Grably, M., and Mariotti, A. (2003) Isotopic composition of nitrate-nitrogen as a marker of riparian and benthic denitrification at the scale of the whole Seine River system. *Biogeochemistry* **63**: 35-51.

Shearer, G., and Kohl, D.H. (1988) Nitrogen isotopic fractionation and ^{18}O exchange in relation to the mechanism of denitrification of nitrite by *Pseudomonas stutzeri*. *J Biol Chem* **263**: 13231-13245.

Sierra-Alvarez, R., Beristain-Cardoso, R., Salazar, M., Gómez, J., Razo-Flores, E., and Field, J.A. (2007) Chemolithotrophic denitrification with elemental sulfur for groundwater treatment. *Water Res* **41**: 1253-1262.

Sigman, D.M., Casciotti, K.L., Andreani, M., Barford, C., Galanter, M., and Bohlke, J.K. (2001) A bacterial method for the nitrogen isotopic analysis of nitrate in seawater and freshwater. *Anal Chem* **73**: 4145-4153.

Silva, S.R., Kendall, C., Wilkison, D.H., Ziegler, A.C., Chang, C.C.Y., and Avanzino, R.J. (2000) A new method for collection of nitrate from fresh water and the analysis of nitrogen and oxygen isotope ratios. *J Hydrol* **228**: 22-36.

Silverman, M.P. (1967) Mechanism of bacterial pyrite oxidation. *J Bacteriol* **94**: 1046-1051.

Silverman, M.P., and Ehrlich, H.L. (1964) Microbial formation and degradation of minerals. *Adv Appl Microbiol* **6**: 153-206.

Singh, R., Paul, D., and Jain, R.K. (2006) Biofilms: implications in bioremediation. *Trends Microbiol* **14**: 389-397.

Singleton, M.J., Esser, B.K., Moran, J.E., Hudson, G.B., McNab, W.W., and Harter, T. (2007) Saturated zone denitrification: Potential for natural attenuation of nitrate contamination in shallow groundwater under dairy operations. *Environ Sci Technol* **41**: 759-765.

Smith, C.J., Nedwell, D.B., Dong, L.F., and Osborn, A.M. (2007) Diversity and abundance of nitrate reductase genes (narG and napA), nitrite reductase genes (nirS and nrfA), and their transcripts in estuarine sediments. *Appl Environ Microbiol* **73**: 3612-3622.

Smith, R.L., Howes, B.L., and Duff, J.H. (1991) Denitrification in nitrate-contaminated groundwater - Occurrence in steep vertical geochemical gradients. *Geochim Cosmochim Acta* **55**: 1815-1825.

Smith, R.L., Ceazan, M.L., and Brooks, M.H. (1994) Autotrophic, hydrogen-oxidizing, denitrifying bacteria in groundwater, potential agents for bioremediation of nitrate contamination. *Appl Environ Microbiol* **60**: 1949-1955.

Soares, M.I.M. (2000) Biological denitrification of groundwater. *Water, Air, Soil Pollut* **123**: 183-193.

Soares, M.I.M. (2002) Denitrification of groundwater with elemental sulfur. *Water Res* **36**: 1392-1395.

Solari, J.A., Huerta, G., Escobar, B., Vargas, T., Badilla-Ohlbaum, R., and Rubio, J. (1992) Interfacial phenomena affecting the adhesion of *Thiobacillus ferrooxidans* to sulphide mineral surface. *Colloids and Surfaces* **69**: 159-166.

Spalding, R.F., and Exner, M.E. (1993) Occurrence of nitrate in groundwater - A review. *J Environ Qual* **22**: 392-402.

Spalding, R.F., and Parrott, J.D. (1994) Shallow groundwater denitrification. *Sci Total Environ* **141**: 17-25.

Stephenson, D., and Stephenson, T. (1992) Bioaugmentation for enhancing biological wastewater treatment. *Biotechnol Adv* **10**: 549-559.

Stewart, P.S. (1994) Biofilm accumulation model that predicts antibiotic resistance of *Pseudomonas aeruginosa* biofilms. *Antimicrob Agents Chemother* **38**: 1052-1058.

Straub, K.L., and Buchholz-Cleven, B.E.E. (1998) Enumeration and detection of anaerobic ferrous iron-oxidizing, nitrate-reducing bacteria from diverse European sediments. *Appl Environ Microbiol* **64**: 4846-4856.

Straub, K.L., Benz, M., Schink, B., and Widdel, F. (1996) Anaerobic, nitrate-dependent microbial oxidation of ferrous iron. *Appl Environ Microbiol* **62**: 1458-1460.

Sun, W., Sierra-Alvarez, R., Milner, L., Oremland, R., and Field, J.A. (2009) Arsenite and ferrous iron oxidation linked to chemolithotrophic denitrification for the immobilization of arsenic in anoxic environments. *Environ Sci Technol* **43**: 6585-6591.

Sutka, R.L., Ostrom, N.E., Ostrom, P.H., Breznak, J.A., Gandhi, H., Pitt, A.J., and Li, F. (2006) Distinguishing nitrous oxide production from nitrification and denitrification on the basis of isotopomer abundances. *Appl Environ Microbiol* **72**: 638-644.

Tal, Y., van Rijn, J., and Nussinovitch, A. (1997) Improvement of structural and mechanical properties of denitrifying alginate beads by freeze-drying. *Biotechnol Prog* **13**: 788-793.

Tal, Y., Van Rijn, J., and Nussinovitch, A. (1999) Improvement of mechanical and biological properties of freeze-dried denitrifying alginate beads by using starch as a filler and carbon source. *Appl Microbiol Biotechnol* **51**: 773-779.

Tal, Y., Nussinovitch, A., and Van Rijn, J. (2003) Nitrate removal in aquariums by immobilized *Pseudomonas*. *Biotechnol Prog* **19**: 1019-1021.

Teitzel, G.M., and Parsek, M.R. (2003) Heavy metal resistance of biofilm and planktonic *Pseudomonas aeruginosa*. *Appl Environ Microbiol* **69**: 2313-2320.

Teixeira, P., and Oliveira, R. (2002) Metabolism of *Alcaligenes denitrificans* in biofilm vs. planktonic cells. *J Appl Microbiol* **92**: 256-260.

Thomsen, J.K., Geest, T., and Cox, R.P. (1994) Mass spectrometric studies of the effect of pH on the accumulation of intermediates in denitrification by *Paracoccus denitrificans*. *Appl Environ Microbiol* **60**: 536-541.

Throbäck, I.N., Enwall, K., Jarvis, A., and Hallin, S. (2004) Reassessing PCR primers targeting nirS, nirK and nosZ genes for community surveys of denitrifying bacteria with DGGE. *FEMS Microbiol Ecol* **49**: 401-417.

Toyoda, S., Mutobe, H., Yamagishi, H., Yoshida, N., and Tanji, Y. (2005) Fractionation of N_2O isotopomers during production by denitrifier. *Soil Biol Biochem* **37**: 1535-1545.

Tsushima, K., Ueda, S., and Ogura, N. (2002) Nitrate loss for denitrification during high frequency research in floodplain groundwater of the Tama River. *Water, Air, Soil Pollut* **137**: 167-178.

Tsushima, K., Ueda, S., Ohno, H., Ogura, N., Katase, T., and Watanabe, K. (2006) Nitrate decrease with isotopic fractionation in riverside sediment column during infiltration experiment. *Water, Air, Soil Pollut* **174**: 47-61.

Urquiola, M.M. (1994) Aplicación de indicadores geoquímicos al estudio de las facies anóxicas del Eoceno Superior de la cuenca de antepaís surpirenaica (sector oriental). PhD Thesis. University of Barcelona.

Utrilla, R., Pierre, C., Orti, F., and Pueyo, J.J. (1992) Oxygen and sulphur isotope compositions as indicators of the origin of Mesozoic and Cenozoic evaporites from Spain. *Chem Geol Isot Geosci* **102**: 229-244.

Van Loosdrecht, M.C.M., Lyklema, J., Norde, W., and Zehnder, A.J.B. (1990) Influence of interfaces on microbial activity. *Microbiol Rev* **54**: 75-87.

Van Rijn, J., Tal, Y., and Barak, Y. (1996) Influence of volatile fatty acids on nitrite accumulation by a *Pseudomonas stutzeri* strain isolated from a denitrifying fluidized bed reactor. *Appl Environ Microbiol* **62**: 2615-2620.

Van Stempvoort, D.R., and Krouse, H.R. (1994) Controls of $\delta^{18}O$ in sulphate. In *Environmental Geochemistry of Sulphide Oxidation*. Alpers, C.N., and Blowes, D.W. (eds). Washington: American Chemical Society, p. 446–480.

Vitòria, L., Grandia, F., and Soler, A. (2004a) Evolution of the chemical (NH_4) and isotopic ($\delta^{15}N$-NH_4) composition of pig manure stored in an experimental pit. In *Isotope Hydrology and Integrated Water Resources Management*. Viena: International Atomic Energy Agency, pp. 260-261.

Vitòria, L., Otero, N., Soler, A., and Canals, A. (2004b) Fertilizer characterization: Isotopic data (N, S, O, C, and Sr). *Environ Sci Technol* **38**: 3254-3262.

Vitòria, L., Soler, A., Canals, A., and Otero, N. (2008) Environmental isotopes (N, S, C, O, D) to determine natural attenuation processes in nitrate contaminated waters: Example of Osona (NE Spain). *Appl Geochem* **23**: 3597-3611.

Vogel, J.C., and Ehhalt, D.H. (1963) The use of carbon isotopes in groundwater studies. In *Radioisotopes in Hydrology*. Vienna: International Atomic Energy Agency, pp. 383-396.

Vogel, J.C., Talma, A.S., and Heaton, T.H.E. (1981) Gaseous nitrogen as evidence for denitrification in groundwater. *J Hydrol* **50**: 191-200.

Vogel, T.M. (1996) Bioaugmentation as a soil bioremediation approach. *Curr Opin Biotechnol* **7**: 311-316.

Volkmer, B.G., Ernst, B., Simon, J., Kuefer, R., Bartsch Jr, G., Bach, D., and Gschwend, J.E. (2005) Influence of nitrate levels in drinking water on urological malignancies: A community-based cohort study. *Br J Urol Int* **95**: 972-976.

Wagner, C.D. (1983) Sensitivity factors for XPS analysis of surface atoms. *J Electron Spectrosc Relat Phenom* **32**: 99-102.

Wang, Q., Garrity, G.M., Tiedje, J.M., and Cole, J.R. (2007) Naïve Bayesian classifier for rapid assignment of rRNA sequences into the new bacterial taxonomy. *Appl Environ Microbiol* **73**: 5261-526.

Ward, M.H., deKok, T.M., Levallois, P., Brender, J., Gulis, G., Nolan, B.T., and VanDerslice, J. (2005) Workgroup report: Drinking-water nitrate and health-recent findings and research needs. *Environ Health Perspect* **113**: 1607-1614.

Weber, K.A., Picardal, F.W., and Roden, E.E. (2001) Microbially catalyzed nitrate-dependent oxidation of biogenic solid-phase Fe(II) compounds. *Environ Sci Technol* **35**: 1644-1650.

Weber, K.A., Pollock, J., Cole, K.A., O'Connor, S.M., Achenbach, L.A., and Coates, J.D. (2006) Anaerobic nitrate-dependent iron(II) bio-oxidation by a novel lithoautotrophic betaproteobacterium, strain 2002. *Appl Environ Microbiol* **72**: 686-694.

Weise, W., and Rheinheimer, G. (1977) Scanning electron microscopy and epifluorescence investigation of bacterial colonization of marine sand sediments. *Microb Ecol* **4**: 175-188.

Wellman, R.P., Cook, F.D., and Krouse, H.R. (1968) Nitrogen-15: Microbiological alteration of abundance. *Science* **161**: 269-270.

Widdel, F., and Bak, F. (1992) Gram-negative mesophilic sulfate-reducing bacteria. In *The Prokaryotes*. A. Balows, H.G.T., M. Dworkin, W. Harper and K.-H. Schleifer (ed). New York: Springer Verlag, pp. 3352-3378.

Widory, D., Petelet-Giraud, E., Négrel, P., and Ladouche, B. (2005) Tracking the sources of nitrate in groundwater using coupled nitrogen and boron isotopes: A synthesis. *Environ Sci Technol* **39**: 539-548.

Widory, D., Kloppmann, W., Chery, L., Bonnin, J., Rochdi, H., and Guinamant, J.L. (2004) Nitrate in groundwater: An isotopic multi-tracer approach. *J Contam Hydrol* **72**: 165-188.

Yamamoto, N., and Lopez, G. (1985) Bacterial abundance in relation to surface area and organic content of marine sediments. *J Exp Mar Biol Ecol* **90**: 209-220.

Yoshida, M., Ishii, S., Otsuka, S., and Senoo, K. (2009) Temporal shifts in diversity and quantity of nirS and nirK in a rice paddy field soil. *Soil Biol Biochem* **41**: 2044-2051.

Young, R.A. (1993) *The Rietveld Method*. International Union of Crystallography, Oxford University Press, 298 p.

Yu, Z., and Morrison, M. (2004) Comparisons of different hypervariable regions of rrs genes for use in fingerprinting of microbial communities by PCR-denaturing gradient gel electrophoresis. *Appl Environ Microbiol* **70**: 4800-4806.

Zhang, M., Ginn, B.R., DiChristina, T.J., and Stack, A.G. (2010) Adhesion of *Shewanella oneidensis* MR-1 to iron (oxy)(hydr)oxides: Microcolony formation and isotherm. *Environ Sci Technol* **44**: 1602-1609.

Zhang, T., and Fang, H.H.P. (2006) Applications of real-time polymerase chain reaction for quantification of microorganisms in environmental samples. *Appl Microbiol Biotechnol* **70**: 281-289.

Zhang, T.C., and Lampe, D.G. (1999) Sulfur:limestone autotrophic denitrification processes for treatment of nitrate-contaminated water: Batch experiments. *Water Res* **33**: 599-608.

Zhang, Y.-C., Slomp, C.P., Broers, H.P., Passier, H.F., and Cappellen, P.V. (2009a) Denitrification coupled to pyrite oxidation and changes in groundwater quality in a shallow sandy aquifer. *Geochim Cosmochim Acta* **73**: 6716-6726.

Zhang, Z., Lei, Z., He, X., Zhang, Z., Yang, Y., and Sugiura, N. (2009b) Nitrate removal by *Thiobacillus denitrificans* immobilized on poly(vinyl alcohol) carriers. *J Hazard Mater* **163**: 1090-1095.

Zumft, W.G. (1997) Cell biology and molecular basis of denitrification. *Microbiol Mol Biol Rev* **61**: 533-616.

Appendix A:

Laboratory methods

In this appendix the main laboratory methods and protocols used in the experimental work are briefly described. Most of the analyses of the solid and aqueous samples were carried out according to conventional methodologies described elsewhere. The microbiology procedures are described with more detail to facilitate the comprehension of the experimental conditions.

1 Field/laboratory sampling and preservation of samples

1.1 Groundwater

Groundwater samples were collected from production wells using the pumps installed in the wells. Physicochemical parameters such as pH, temperature, conductivity, dissolved O_2 and Eh, were measured *in situ*, using a flow cell to avoid contact with the atmosphere. pH was measured by a pH-meter and combined electrode with temperature compensation, which was calibrated regularly with standard buffer solutions. The estimated measurement error for pH was ≤0.05 pH units. Eh was measured using a Pt combination electrode that was calibrated with standard buffer solutions of 220 and 468 mV. Measurements were corrected to the Standard Hydrogen Electrode and the measurement error was ≤5 mV. Electrical conductivity was performed with a Pt cell calibrated with standard KCl solutions. The measurement error for conductivity was ±1%. The concentration of dissolved oxygen was determined by a portable luminescent dissolved oxygen meter with compensation of temperature, salinity and altitude and with an accuracy of 5%.

Groundwater samples were collected from continuously pumped water from the wells when Eh values stabilized. Most of the water samples were collected in plastic bottles. Samples for ammonium analysis and those for experiments of chapter 4 were collected in glass bottles. All bottles were totally filled with water to avoid air in the bottle headspace that may oxidize reduced chemical species or inhibit strict anaerobes. Thereafter, samples were stored at 4°C prior to analyses and/or utilization in the

experiments, except those bottles with samples for $\delta^{13}C_{DIC}$ analyses, which were stored at ambient temperature.

1.2 Core

A core hole was drilled up to a depth of 12 m, about 3 m below the groundwater table, in April 2008 near the city of Roda de Ter, 8 km northeast of Vic in the Osona region. The saturated material was sampled with a core barrel. After removing the core from the barrel, core fragments of approximately 1200 cm^3 were immediately preserved at 4°C in autoclaved glass flasks with a CO_2 atmosphere generated by a BBL® disposable gas generator envelope (GasPak Anaerobic System, BBL, Cockeysville, MD, USA).

In the laboratory, the core fragments were aseptically processed under anaerobic conditions in a sterilized glove box. The core fragments were broken using a sterilized hammer to obtain unaltered fragments of size of about 100 cm^3. Therefore, these fragments were further crushed to centimetric fragments using the sterilized hammer and the portions were placed in sterilized containers under an anaerobic atmosphere until used in the experiments.

1.3 Aqueous and solid samples from laboratory experiments

Aqueous samples from batch experiments were obtained at appropriate intervals using sterile syringes. Output solutions of the flow-through experiments were sampled periodically.

Aliquots of aqueous samples were filtered through 0.22 μm syringe filters to measure pH, concentrations of cations, anions and, in some samples, isotopic composition. For the measurement of cation concentration, samples were preserved in nitric acid. For bacterial count, molecular analysis and measurement of alkalinity, samples were not filtered.

Solid samples were retrieved at the end of the batch and flow-through experiments using sterilized filters and filter devices. In the colonization experiments (chapter 5) the pyrite blocks were taken out of the solution with sterilized forceps and rinsed with pH 7.1 sterile phosphate buffer.

2 Analytical methods

2.1 Microbiology protocols

2.1.1. Sterilization

Most of the laboratory material (flasks, reactors, tubing, pipettes, tubes, output bottles, etc.), the solutions used in the experiments and the glass bottles used to collect groundwater and core samples from the aquifer were sterilized by autoclaving. Before placing them into the autoclave, openings of flasks or beakers and utensils were covered by aluminum foil. The autoclave is a sealed device that allows the entrance of steam under pressure. The use of moist heat facilitates killing of all microorganisms, including heat-resistant endospores. The usual procedure is to heat at 1.1 kg cm^{-2} steam pressure, which yields a temperature of 121 °C. At this temperature, autoclaving time to achieve sterilization is generally considered to be 10-15 min. Pyrite powder and pyrite slabs were also sterilized by autoclaving at 121°C for 15 min previously to be used in the experiments.

Some solutions were sterilized by filtration through membrane filters capable of retaining microorganisms (0.2-0.45 μm pore dimension sterilized filters). During filtration, microorganisms are retained in part by the small size of the filter pores and in part by adsorption on the pore walls during their passage through the filter. The filter is appropriately mounted, and the mounting is inserted into receiving flasks. The assembly is sterilized by autoclaving prior to use. After the solution has been poured onto the filter, its passage is accelerated by suction.

To maintain aseptic conditions inside the anaerobic glove box, UV radiation was used. A germicidal lamp was utilized to kill micro-organisms in the air and on surfaces. The UV radiation has low penetration power, so the organisms to be killed must be directly exposed to the rays. For example, organisms covered with paper, glass and textiles are not affected. Furthermore, the effectiveness of UV radiation may decrease as the distance from radiation source increases. It should be noted that UV radiation may damage the eye retina and prolonged exposure to UV light can cause burns and skin cancer. Hence, while working with UV radiation, protection is necessary. Moreover, work surfaces in the glove box were washed and wiped with 70% ethanol solution and the inlet gas was filtered through 0.22 μm sterilized membrane filter (Millipore Corp., Bedford, MA, USA) before entering the glove box.

In order to prevent contamination during handling and manipulation of cultures, aseptic techniques were used. All the material was sterilized immediately before using in culture transfers by autoclaving or by dipping in ethanol and passing through a flame to ignite the ethanol. The flame was also used on the lips of media bottles before and after pipetting from them.

2.1.2. Culture preparation

Thiobacillus denitrificans (strain 12475 from German Collection of Microorganisms and Cell Cultures, DSMZ, German; origin from a domestic sewage lagoon in the Sheffield Sewage Work, UK) was cultured with thiosulfate in an anaerobic (pH 6.8) nutrient medium specially designed for *T. denitrificans*, following Beller (2005).

The medium consists of a mixed solution of $Na_2S_2O_3 \cdot 5H_2O$ (20 mM), NH_4Cl (18.7 mM), KNO_3 (20 mM), KH_2PO_4 (14.7 mM), $NaHCO_3$ (30 mM), $MgSO_4 \cdot 7H_2O$ (3.25 mM), $FeSO_4 \cdot 7H2O$ (0.08 mM), $CaCl_2 \cdot 2H_2O$ (0.05 mM) and sterile vitamin, trace element and selenate-tungstate solutions (stock solutions 1, 4, 6, 7 and 8 of Widdel and Bak, 1992). The Table A1 shows the composition of the solutions used to prepare the medium. Solution A, double distilled water and stock solutions 1 and 4 were sterilized separately by

autoclaving at 121 °C for 15 min. Solutions B and C and stock solutions 6, 7 and 8 were sterilized by filtration. After sterilization, all solutions were combined and distributed as required (500 mL of solution A, 30 mL of solution B, 8 mL of solution C, 1 mL of each stock solution and 457 mL of double distilled water).

The cultures were preserved under anaerobic conditions at 30°C and unshaken. They were maintained by 5-weekly sub-culturing, transferring 1 mL of the previous stock culture to inoculate 20 mL of fresh media. Thereafter, the cultures were harvested by centrifugation, washed, and re-suspended in a sterile saline solution (Ringer 1/4 solution) immediately before the start of the experiments.

Solution A	
	g L^{-1}
$Na_2S_2O_3 \cdot 5H_2O$	9.9280
NH_4Cl	1.9991
KNO_3	4.0440
KH_2PO_4	4.0013
$MgSO_4 \cdot 7H_2O$	1.6016
$CaCl_2 \cdot 2H_2O$	0.0147

Solution B	
$NaHCO_3$ (1 M)	84 g L^{-1}

Solution C	
$FeSO_4 \cdot 7H_2O$ (0.01 M)	2.779 g L^{-1}

Stock solution 1 (100 mL)	
DDW	98.7 mL
HCl (25%)	1.25 mL
$FeSO_4 \cdot 7H_2O$	0.21 g
H_3BO_3	3. mg
$MnCl_2 \cdot 4H_2O$	10 mg
$CoCl_2 \cdot 6H_2O$	19 mg
$NiCl_2 \cdot 6H_2O$	2.4 mg
$CuCl_2 \cdot 2H_2O$	0.2 mg
$ZnSO_4 \cdot 7H_2O$	14.4 mg
$Na_2MoO_4 \cdot 2H_2O$	3.6 mg

Stock solution 4 (100 mL)	
DDW	100 mL
NaOH	0.04 g
$Na_2SeO_3 \cdot 5H_2O$	0.6 mg
$Na_2WO_4 \cdot 2H_2O$	0.8 mg

Stock solution 6 (100 mL)	
phosphate buffer 10 mM pH 7.1	100 mL
4-aminobenzonic acid	4 mg
D+ biotin	1 mg
nicotinic acid	10 mg
calcium D+ panthothenate	5 mg
pyridoxine	15 mg

Stock solution 7 (100 mL)	
thiamine	10 mg
phosphate buffer 25 mM pH 3.4	100 mL

Stock solution 8 (100 mL)	
DDW	100 mL
Cyanocobalamine (vit B12)	5 mg

Table A1. Formulations for the solutions used to prepare the medium solution specially designed for *T. denitrificans*. The 10 mM pH 7.1 phosphate buffer consists of 0.4554 g L^{-1} of $NaH_2PO_4 \cdot H_2O$ and 1.7956 g L^{-1} of $Na_2HPO_4 \cdot 7H_2O$.

2.1.3. Bacterial counts and viability

Bacterial enumeration was performed by epifluorescent direct counting. First, the Irgalan black-stained polycarbonate membrane filter (Isopore filters, 0.2-µm pore size; Millipore) was placed on the filter tower apparatus support, which was pre-wetted with one drop of sterile double distilled water. Thereafter, the sample was added to the filter device and diluted with 0.2-µm-pore-size filtered double distilled water to achieve a final volume of 10 mL to be filtered. Afterwards, 100 µL of a 10 µg mL^{-1} DAPI (49-6-diamidino-2-phenylindole dihydrochloride, Sigma-Aldrich Corp., St. Louis, MO, USA) solution were added to the sample in the filter apparatus and the sample and the stain were allowed to stand for 5 min. Thereafter, the stained sample was filtered at a vacuum of less than 200 mbar to avoid cell breakage, lysis, and penetration. The membrane filter was then removed with forceps and was placed in a microslide with a small drop of immersion oil. Finally, the filter was covered with a coverglass. The total number of cells was enumerated by direct counts of DAPI-stained cells using epifluorescent illumination on a light microscope. The number of cells was counted within squares of an ocular grid at ×1000. Counts were obtained from randomly located fields covering a wide area of the filter and a minimum number of 200 cells were counted per filter. Bacterial density in the original sample was calculated from the number of cells counted, the area of the filter and the counting grid, the volume of diluted sample filtered and the dilution factor.

The LIVE/DEAD® BacLight™ bacterial viability kits (Molecular Probes Europe BV, Leiden, The Netherlands) were used to discriminate between viable cells and dead cells. The BacLight™ bacterial viability kits contain green-fluorescent nucleic acid stain SYTO® 9 and red-fluorescent nucleic acid stain Propidium Iodide (PI). When used alone, the SYTO® 9 stain generally labels all bacteria that have both intact membranes and damaged membranes. In contrast, PI stain penetrates only those bacteria with damaged membranes, causing a reduction in the SYTO® 9 stain fluorescence when both dyes are present. For this reason, bacteria with intact cell membranes (viable cells) stain green fluorescence, whereas bacteria with damaged membranes (dead cells) stain red

fluorescence. Samples were stained with the LIVE/DEAD® BacLight™ bacterial viability fluorescent dye and observed with a fluorescence microscope using suitable optical filters. The numbers of live and dead bacteria were counted as described above.

2.1.4. Molecular analysis

16S rRNA gene-based denaturing gradient gel electrophoresis (DGGE) has been used as a useful and rapid routine analysis to determine bacterial diversity and population changes in microbial communities (Muyzer et al., 1993). The general strategy for genetic fingerprinting of microbial communities consists of, first, the extraction of DNA, second, the amplification of genes encoding the *16S rRNA* and, third, the analysis of polymerase chain reaction (PCR) products by DGGE. Separation of the DNA fragments in DGGE is based on the decreased electrophoretic mobility of partially melted double-stranded DNA molecules in polyacrylamide gels containing a linear gradient of DNA denaturals (a mixture of urea and formamide). Molecules with different sequences may have different melting behavior, and will, therefore stop mitigating at different positions in the gel. Each individual discrete band represents a unique variant of the gene, and therefore a unique member of the community. Furthermore, it is possible to identify community members by sequencing excised bands.

The number of bands observed in DGGE profiles provides an estimation of the community diversity (species richness) and the relative intensity of each band provides a rough estimate of the relative abundance (evenness) of each species. It should be noted that PCR-DGGE cannot reflect minor species in the environment. Several different studies revealed that only bacterial populations that make up 1% or more of the total community can be detected by DGGE (Muyzer et al., 1993; Murray et al., 1996). Furthermore, care should be taken with interpretation of DGGE results, as major bands in the gels could not represent major populations in the original environment due to bias in DNA extraction and PCR amplification (Muyzer and Smalla, 1998). In addition, one organism may produce more than one band because of multiple, heterogeneous rRNA operons (Nübel et al., 1996), which might lead to an overestimation of the number of

bacteria within natural communities. Despite these limitations, molecular methods can reveal the presence of microorganisms that cannot be detected by classical cultivation techniques.

Because of the wide phylogenetic diversity of denitrifying bacteria (Zumf, 1997), the commonly targeted rRNA genes are impractical for examining denitrifying communities (Philippot, 2005). Therefore, most studies of denitrifiers in natural habitats have targeted the functional genes that code for enzymes involved in denitrification: narG, nirK, nirS, nosZ, norB, etc (e.g. Throbäck et al., 2004). Of the known molecular markers for denitrifiers, the *nosZ* gene has been shown to have the greatest level of congruence with *16S rRNA*-based taxonomic classification (Jones et al., 2008). However, the database of these genes of pure cultures is not complete, and therefore, the analyses on denitrifying functional genes are hard to correlate with phylogenetic information.

Therefore, both *16S rRNA* and *nosZ* gene-based DGGE were used in this thesis to determine microbial community changes associated with the biostimulation treatments (chapter 4). Furthermore, quantitative PCR (qPCR) was also performed to quantify the proportion of denitrifying bacteria (*nosZ* gene copies) to the total bacteria (*16S rRNA* gene copies). The ratio of the number of copies of the *nosZ* gene to the copies of the *16S rRNA* gene was determined to evaluate the relative abundance of denitrifying bacteria compared to total bacteria.

qPCR is a method based on the use of fluorogenic probes to quantify the copy number of target DNA in a sample. This technique records the fluorescent signal generated during the PCR amplification. The signal is generated by the binding of the fluorophore SybrGreen to double-stranded DNA. When SybrGreen bound to DNA, a fluorescent signal is emitted following light excitation. As amplicon numbers accumulate after each PCR cycle, there is a corresponding increase in fluorescence. The cycle number Ct is defined as the cycle in which the fluorescence signal crosses a certain threshold (in correlation to the background fluorescence of the assay). This Ct value is proportional to the logarithm of the target concentration in the assay. From dilution series of a standard

with known concentration of target sequences, running in parallel assays, a calibration curve is created (Ct versus logarithm of the starting concentration). The Ct values obtained for each sample are compared with a standard curve to determine the initial copy number of the target gene. The precision of microbial quantification using qPCR relies on the assumption that the environmental sample and the standard solutions share the same PCR efficiency. It is thus crucial to check the PCR efficiency in the analysis of both standard solutions and environmental samples. The amplification efficiency (E) is estimated using the slope of the standard curve through the following formula:

$$E = [(10^{-1/slope}) - 1] \times 100$$

The efficiency of the PCR should be between 90% and 110% (McPherson and Moller, 2000). In practice, a reliable standard curve should have a R^2 value of more than 0.95 and a slope between -3.0 and -3.9 corresponding to PCR efficiencies of 80-115%.

This technology has been successfully applied to quantify functional genes as markers for bacteria in the environment (Zhang and Fang, 2006). In the case of denitrifying functional genes (narG, nirS, nirK, nosZ, etc.), qPCR has been used to evaluate the relative abundance of denitrifying bacteria compared to total bacteria in different environmental samples (Grüntzig et al., 2001; Henry et al., 2004; 2006; 2008; López-Gutiérrez et al., 2004; Kandeler et al., 2006; Philippot, 2006; 2009; Bru et al., 2007; Geets et al., 2007; Smith et al., 2007; Dandie et al., 2008; Chon et al., 2010.; Yoshida et al., 2009; Djigal et al., 2010; Reyna et al., 2010). It should be noted that *16S rRNA* gene numbers from environmental samples cannot be converted to cell numbers as the exact number of copies of the *16S rRNA* gene in any given bacterial species varies, ranging from 1 to 13 (Fogel et al., 1999). In contrast to *16S rRNA*, only single copies per genome have been found to date for the denitrifying genes (Philippot, 2002). An exception is the narG gene, which can be present in up to three copies (Philippot, 2002). Therefore, the number of denitrifying genes per organism is expected to be close to the gene copy number obtained by quantitative PCR.

Molecular analyses of initial and final samples of the pyrite-amended batch experiments (chapter 4) were performed at the GIRO Technological Centre, using the following protocol:

2.1.4.1. Biomass concentration

To extract total DNA from initial groundwater samples and from aqueous samples retrieved at the end of the batch experiments, the samples were concentrated by filtering through 0.22-μm cellulose acetate filters (200 mL of groundwater samples or 50 mL of aqueous samples). Sediment (0.25 g approximately) was collected from the aquifer and at the end of the batch experiments (after 100 d of incubation) for subsequent DNA extraction. Both the filters and the solid samples were stored at -20°C prior to analysis.

2.1.4.2. DNA extraction

Total DNA from the frozen solid samples and from the frozen filters was extracted in duplicate following a bead beating protocol by means of the commercial PowerSoil™ DNA Isolation Kit (MoBio Laboratories, Inc., Carlsbad, CA, USA), following the manufacturer's instructions. No further purification was required to prevent PCR inhibition. The isolated DNA was stored at -20°C for further molecular analyses.

2.1.4.3. Amplification by PCR

For DGGE, the extracted DNA was amplified by polymerase chain reaction (PCR). The V3-V5 variable regions of the *16S rRNA* gene were amplified using the 16F341-GC and 16R907 primers (Yu and Morrison, 2004). The F341-GC primer included a GC clamp at the 5′ end (5′-CGCCCGCCGCGCCCCGCGCCCGTCCCGCCGCCCCCGCCCG-3′). Fragments of the *nosZ* gene were amplified using the primers *NosZ*-F (Kloos et al., 2001) and *NosZ*1622R-GC (Throbäck et al., 2004). The 22R-GC primer included a GC clamp at the 5′ end (5′-GGCGGCGCGCCGCCCGCCCCGCCCCCGTCGCCC-3′). All PCRs were performed with a mastercycler gradient (Eppendorff, Hamburg, Germany). Each PCR mixture (50 μL) contained 1.25 U of Takara Ex Taq DNA polymerase (Takara Bio Inc., Otsu, Shiga, Japan), 25 mM TAPS (pH 9.3), 50 mM KCl, 2 mM $MgCl_2$, 200 μM each deoxynucleoside triphosphate (dNTPS), 0.5 μM each primer and 100 ng of template DNA

quantified using a Low DNA Mass Ladder (Gibco BRL, Rockville, MD, USA) and a ND-1000 spectrophotometer (Nanodrop Technologies, Wilmington, DE, USA). The PCR profile consisted in an initial denaturation at 94°C for 5 min followed by 30 cycles of the following steps: one denaturation step at 94°C for 1 min, one annealing step at 55°C /53°C (*16S rRNA*/*nosZ*, respectively) for 1 min and one elongation step at 72°C for 45 s. The last step involved an extension at 72°C for 10 min. Amplicons were purified prior to the DGGE analysis using the DNA purification system Wizard® Plus SV (Promega Corporation). PCR reactions were done in duplicate.

2.1.4.4. DGGE

The DGGE protocol was similar to that described by Muyzer et al. (1993). Approximately 800 ng of purified PCR products quantified using Nanodrop (ND-1000, Nanodrop Technologies) were loaded onto 8% (w/v) polyacrylamide gels (0.75 mm thick- to obtain a better resolution), with a denaturing chemical gradients ranging from 30% to 70% (100% denaturant stock solution contains 7 mM urea and 40% (w/v) formamide). DGGE were performed in 1×TAE buffer solution (40 mM Tris, 20 mM sodium acetate, 1 mM EDTA; pH 7.4) using a DGGE-4001 system (CBS Scientific, Del Mar, CA, USA) at 100 V and 60°C for 16 h.

2.1.4.5. Analysis of DGGE images

The DGGE gels were stained for 45 min in a 1×TAE buffer solution containing SybrGold (Molecular Probes, Inc., Eugene, OR, USA), and then scanned under blue light by means of a Blue-converter plate (UVP, Upland, CA, USA) and a transilluminator (GeneFlash Synoptics Ltd, Cambridge, UK). The obtained DGGE profiles were processed by means of the Gene Tools software v. 4.0 (SynGene Synoptics, Cambridge, UK) and corrected manually. After normalization of the gels, bands with relative peak area intensity above 2% were set aside for further analyses.

2.1.4.6. Sequencing and phylogenetic analysis of DGGE bands

Selected DGGE bands were removed with a sterile razor blade resuspended in 50 µl sterilized MilliQ water and stored at 4°C overnight. A 1:100 dilution of supernatant was

used to reamplify the *16S rRNA* DGGE bands with primers 16F341-GC and 16R907 to ascertain their DGGE mobility in the same conditions. The 25-µl PCR reaction mixture contained 0.625 U of Takara Ex Taq Hot Start DNA polymerase (Takara Bio Inc.), 25 mM TAPS (pH 9.3), 0.5 mL of Ex Taq buffer (2 mM $MgCl_2$), 200 µM each deoxynucleoside triphosphate (dNTPS), 0.5 µM of each primer and 1 µL of template DNA. Reamplification conditions consisted in 30 cycles of the following steps: one denaturation step at 94°C for 30 s, one annealing step at 55°C for 30 s and one elongation step at 72°C for 45 s. The last step involved an extension at 72°C for 5 min.

Finally, band amplicons were sequenced using the primer 16R907 without GC-clamp. Sequencing conditions consisted in an initial denaturation step at 96°C for 1 min, followed by 25 cycles of one denaturation step at 96°C for 10 s, one annealing step at 55°C for 5 s and one elongation step at 60°C for 4 min. Sequencing was accomplished using the ABI Prism Big Dye Terminator cycle-sequencing reaction kit v. 3.1 (Perkin-Elmer Applied Biosystems, Foster City, CA, USA) and an ABI 3700 DNA sequencer (PE Applied Biosystems) following the manufacturer's instructions. The sequences were edited and assembled using the BioEdit software package v. 7.0.9 (http://www.mbio.ncsu.edu/BioEdit/bioedit.html) (Ibis Biosciences, Carlsbad, CA, USA) (Hall, 1999), and were inspected for the presence of ambiguous base assignments. Thereafter, the sequences were subjected to the Check Chimera program of the Ribosomal Database Project (http://rdp.cme.msu.edu) (Maidak et al., 2000). The sequences were then aligned against GenBank database by using the alignment tool comparison software BLASTn (http://www.ncbi.nlm.nih.gov/BLAST) and RDP search (Altschul et al., 1990; Maidak et al., 2000). Sequences were matched to phylogenetic groups by using the RDP Naive Bayesian Classifier (Wang et al., 2007).

The *16S rRNA* gene nucleotide sequences determined in the present study were deposited into the GenBank database under accession numbers HM765437-HM765449.

2.1.4.7. Quantitative PCR assays

16S rRNA and *nosZ* gene copy numbers were quantified by quantitative PCR assays via comparison to standard curves. Two independent real-time qPCR reactions were performed for each gene (*16S rRNA* and *nosZ*), for each duplicate genomic DNA extraction. qPCR assays were run on a MX3000P Real Time PCR equipment (Stratagene, La Jolla, CA, USA) using a reaction mixture of 25 μl containing the SYBR® Green I qPCR Master Mix (Stratagene), the primers, and the DNA-diluted template. An additional fluorescent dye, 6-carboxy-Xrhodamine (ROX), was added to serve as an internal passive reference. Amplification of products was obtained by using the primers 519F/907R each of them at 200nM for *16S rRNA* gene (Lane, 1991) and *nosZ*1F/*nosZ*1R each of them at 200 nM for *nosZ* gene (Kandeler et al., 2006).

Thermal cycling conditions for the *nosZ*1 primers were as follows: an initial cycle at 95°C for 10 min followed by 40 cycles of 95°C for 30 s, 62°C for 1 min and 80°C for 15 s (fluorescence acquisition step). The thermocycling steps of the qPCR for *16S rRNA* amplification included an initial cycle at 95°C for 10 min and 40 cycles of 95°C for 30 s, 50°C for 30 s, 72°C for 45 s and 80°C for 15 s (fluorescence acquisition step). Product size and purity were confirmed by both melting-curve analysis (Mx3000P real-time PCR instrument software, version 4.0) and gel electrophoresis. Serial dilutions of total DNA extracts from sediment/water samples were quantified and compared to check for the potential presence of PCR inhibitors.

To perform calibration curves, standards were prepared with serial dilutions of a given amount of clone-plasmids containing PCR amplicons of the *16S rRNA* or the *nosZ* genes (recombinant TOPO-TA and pGEM-T Easy Vector plasmids containing *16S rRNA* and *nosZ* inserts, from the GIRO CT collection). Standard curves obtained from both genes showed a linear range between 10^1 and 10^8 gene copies reaction^{-1}, with slopes ranging from -3.3 to -3.5. The calculated PCR efficiencies for *16S rRNA* and *nosZ* assays were 96 and 97%, respectively.

2.2 Chemical analyses

2.2.1. pH and alkalinity

pH was measured at room temperature (22±2 °C) using a Crison pH Meter with temperature compensation and calibrated with standard buffer solutions. The pH error was 0.02 pH units.

Alkalinity in unfiltered samples was measured by titration using an Aquamerck® alkalinity test kit (Merck, Darmstadt, Germany), with a detection limit of 0.1 meq L^{-1}.

2.2.2. Anion concentration

Anion concentrations (nitrate, nitrite, chloride, and sulfate) were determined by High Performance Liquid Chromatography (HPLC), using a Waters IC-Pack™ Anion column and borate/gluconate eluent with 12% of HPLC grade acetonitrile. The error associated with the measurements was estimated to be 5% for nitrate, chloride and sulfate and 10% for nitrite. Blank and duplicates were analyzed with each batch of samples.

Samples for ammonium analysis were preserved acidified to pH<2 with H_2SO_4. Ammonium concentrations were measured using an Orion ammonium ion selective electrode with an analytical uncertainty of 10% and a detection limit of 0.01 mM.

2.2.3. Cation concentration

Total Fe, total S, Mg, Ca, Na, P, and K were measured by inductively coupled plasma-atomic emission spectrometry (ICP-AES) using a Thermo Jarrel-Ash with CID detector and a Perkin-Elmer® Optima 3200 RL. The detection limits of Mg, Ca, Na, S, Fe, P and K were 2.06, 2.50, 4.35, 3.12, 0.36, 3.23 and 2.56 μmol L^{-1}, respectively. Calibration with sets of standards was performed and the regression coefficients exceeded 0.999. To check the accuracy of the results, three laboratory standards were analyzed every 15 samples. Blanks and duplicates were also analyzed with each batch of samples. ICP analyses were performed at the Scientific-Technical Services of Barcelona University.

2.3 Isotopic analyses

Stable isotopes are measured as the ratio between the desired isotope and the most-abundant one. Because measuring such a small difference cannot be feasibly done in an absolute way, these ratios are almost always established with respect to international standards. As a result, measures are usually expressed in terms of δ per mil relative to the international standards: V-SMOW (Vienna Standard Mean Oceanic Water) for $\delta^{18}O$, AIR (Atmospheric N_2) for $\delta^{15}N$, V-CDT (Vienna Canyon Diablo Troillite) for $\delta^{34}S$ and V-PDB (Vienna Peedee Belemnite) for $\delta^{13}C$.

The isotope ratios were calculated using international and internal laboratory standards. Reproducibility (≡1σ) of the samples was determined as follows: ±0.3‰ for $\delta^{15}N_{NO3}$; ±0.2‰ for $\delta^{34}S$; ±0.5‰ for both $\delta^{18}O_{NO3}$, and $\delta^{18}O_{SO4}$; and ±0.2‰ for $\delta^{13}C_{DIC}$.

Isotopic analyses were prepared at the laboratory of the Applied Mineralogy and Environment Research Group and analyzed at the Scientific-Technical Services of Barcelona University, except for the isotopic composition of dissolved nitrates of most samples, which was analyzed by the denitrifier method at the Woods Hole Oceanographic Institution (Woods Hole, MA, US).

2.3.1. $\delta^{18}O$ and $\delta^{15}N$ of dissolved nitrate

Samples for N and O isotopes of nitrate were preserved in KOH (pH 11) solution and frozen prior to analysis. In most of the samples, the $\delta^{15}N$ and $\delta^{18}O$ of dissolved nitrate were obtained at the Woods Hole Oceanographic Institution, following the denitrifier method (Sigman et al., 2001; Casciotti et al., 2002). Briefly, denitrifiers were cultured in standard medium amended with nitrate, in stoppered glass bottles. Cells in the stationary phase were concentrated by centrifugation, resuspended in fresh, nitrate-free medium, and dispensed in stoppered glass vials, which were then purged with an inert gas. Thereafter, samples of dissolved nitrate (10-20 nmol) were added to the sample vials and were incubated overnight to allow for complete conversion of nitrate to N_2O before the addition of 0.1 mL of 10 N NaOH to stop bacterial activity and scavenge CO_2. The N_2O

analyte was then purged and trapped from each vial and the isotopic composition of N_2O was then analyzed by Gas Chromatography coupled to Isotope Ratio Mass Spectrometry (GC/IRMS).

For the groundwater samples of the May 2006 campaign (chapter 2), nitrate analyses were performed using the anion exchange method (Silva et al., 2000). Preparation of samples is described in Vitòria et al. (2008). Briefly, dissolved nitrates were concentrated using anion-exchange columns Bio Rad® AG1-X8 100-200 mesh anion exchange resin, after extracting the sulfates and phosphates by precipitation with $BaCl_2$ and filtration. Thereafter, dissolved nitrates were eluted with HCl and converted to $AgNO_3$ by adding silver oxide. The $AgNO_3$ solution was then freeze dried to purify the $AgNO_3$ for analysis. The $\delta^{15}N_{NO3}$ was analyzed in a Carlo Erba Elemental Analyzer (EA) coupled in continuous flow with a Finnigan Delta C Isotope Ratio Mass Spectrometer (IRMS). The $\delta^{18}O_{NO3}$ was analyzed in duplicate with a ThermoQuest TC/EA (high temperature conversion-elemental analyzer) unit coupled with a Finnigan Matt Delta C IRMS.

2.3.2. $\delta^{18}O$ and $\delta^{34}S$ of dissolved sulfate

The dissolved sulfate was precipitated as $BaSO_4$ by adding $BaCl_2 \cdot 2H_2O$ after acidifying the sample with HCl and boiling it in order to prevent $BaCO_3$ precipitation. The precipitate was dried in an oven at < 50 °C. One part of the dried precipitate was used for $\delta^{18}O_{SO4}$ analysis, which was performed in duplicate with a ThermoQuest TC/EA (high temperature conversion-elemental analyzer) unit coupled with a Finnigan Matt Delta C IRMS. The rest of the precipitate was further dried at 110 °C and the $\delta^{34}S_{SO4}$ was analyzed in an EA (Carlo Erba) coupled with an IRMS (Delta C Finnigan Mat.).

2.3.3. $\delta^{13}C$ of dissolved inorganic carbon

Unfiltered samples were treated with NaOH-$BaCl_2$ solution to precipitate carbonates together with sulfates and phosphates. Later, samples were filtered at 3 μm and the precipitates were dried in an oven at <50 °C. The precipitate was scraped off the

filter paper and stored in a desiccator until analysis. The $\delta^{13}C$ of the total dissolved inorganic C, mainly HCO_3^-, was analyzed in a Carlo Erba EA coupled with a Finnigan Delta C IRMS.

2.4 Solids characterization

2.4.1. Preparation of pyrite for experiments

Pyrite samples were crushed and sieved to obtain two particle sizes, one ranging from 25 to 50 μm and the other from 50 to 100 μm. Thereafter, pyrite powder was sterilized by autoclaving at 121°C for 15 min previously to use in the experiments.

To prepare thin polished pyrite slabs of 1 mm thickness, single whole crystals of pyrite were used. The thin polished slabs were prepared by Spectrum Petrographics, Inc (Vancouver, Canada). Thereafter, a slow-speed saw was used to cut 3 mm length and width blocks from the glued slabs. This procedure allowed the individual blocks to be removed from the glass slide (approximately 3 × 3 × 1 mm blocks). The blocks were thereafter washed individually with ethanol (Edwards et al., 2000). Finally, the blocks were sterilized by autoclaving at 121°C for 15 min before the beginning of the experiments.

2.4.2. X-ray diffraction (XRD)

The bulk mineralogical composition of the solid phases was determined by X-ray diffraction (XRD) using a Bruker D5005 diffractometer with Cu Kα radiation over a 2θ range from 0 to 60 degrees, with a scan speed of 0.025°/18 s. Structure refinement was performed according to the Rietveld method (Young, 1993) to perform quantitative phase analyses.

2.4.3. Surface area

Specific surface areas were determined by the Brunauer-Emmett-Teller (BET) gas adsorption method (Brunauer et al., 1938). The BET areas were measured with a

Micromeritics ASAP 2000 surface area analyzer using 5-point N_2 adsorption isotherms at -196 °C. Prior to analysis the samples were degassed under vacuum for several hours. The error associated with the measurements of the BET surface area was around 15%.

2.4.4. X-ray Photoelectron Spectra (XPS)

X-ray Photoelectron spectra (XPS) of initial and reacted samples were recorded with a Physical Electronics (PHI) 5500 spectrometer using a monochromatic X-ray source with an Al Kα line of 1486.6 eV and operated at 350 W. All these measurements were made in an ultra high vacuum (UHV) chamber (pressure between 6.6×10^{-11} and 6.6×10^{-12} atm). The analyzer pass energy was 23 eV. The energy scale was calibrated using the $3d_{5/2}$ line for Ag with a width of 0.8 eV and a binding energy of 368.3 eV. All binding energies were corrected by adjusting the C1s peak (corresponding to contamination from hydrocarbons) to a binding energy of 284.6 eV. Atomic concentrations of iron and sulfur were determined from the XPS areas subsequent to the Shirley background subtraction divided by atomic sensitivity factors (Wagner, 1983). Due to the lack of sample cooling while acquiring the measurements, loss of potentially present elemental sulfur could occur. XPS analyses were performed at the Scientific-Technical Services of Barcelona University.

2.4.5. Electron microprobe analysis (EMPA)

The chemical composition of pyrite samples was determined by electron microprobe analysis (EMPA) using a Cameca SX-50 electron microprobe analyzer with wave-length dispersive X-ray spectrometers (WDS). This technique is based on the measurement of characteristic X-ray intensities emitted by the elements present in the sample when the latter is bombarded with a focused electron beam. For each element, the ratio of the characteristic X-ray intensity emitted from the sample to that emitted from a standard of known composition is measured.

Before the analyses, the samples were embedded in epoxy resin, cut and polished. Elements and X-ray lines used for the analysis were Fe (Kα), S (Kα), As (Lα), Pb (Mα), Zn

(Kα), Cu (Kα), Ni (Kα), Co (Kα), and Si (Kα). Operating conditions included an accelerating voltage of 20 kV, a beam current of 20 nA and a measurement spot size of about 5 μm. In order to improve the statistics of the count rates, acquisition times for both peak and background were 30 s for Fe, S and Si, and 60 s for As, Pb, Zn, Cu, Ni and Co. Standard specimens used for calibration were pure samples of the considered elements. A total of 20 EMPA analyses were performed in each sample at positions randomly selected, and the average value was calculated. The detection limits for Fe, S, As, Pb, Zn, Cu, Ni, Co and Si were 0.078±0.003, 0.047±0.002, 0.020±0.001, 0.186±0.001, 0.029±0.000, 0.025±0.000, 0.027±0.000, 0.020±0.000 and 0.006±0.001 at.%, respectively. EMPA analyses were performed at the Scientific-Technical Services of Barcelona University.

2.4.6. Scanning Electron Microscopy (SEM)

Samples were fixed with 2.5% glutaraldehyde (Merck) in a pH 7.1 phosphate buffer solution (4°C, overnight) to maintain the cell structure and to secure attached cells to the pyrite surface. Thereafter, samples were washed with the phosphate buffer solution and afterward, samples were dehydrated sequentially in graded ethanol solutions (25, 50, 75, 100 and 100% EtOH) for 10 min each. After dehydration, samples were chemically dried using hexamethyldisilazane (HMDS, TedPella Inc., Redding, CA, USA) (2 times, 5 min each), and then air dried in a fume hood for 2 h. Finally, samples were mounted on stubs and sputter coated with C or gold palladium alloy before examination. Samples were examined with a Hitachi H-4100FE microscopy or a Leica Stereoscan S360 Cambridge Electron Microscopy with energy-dispersive microanalysis (EDS; INCA Energy 200), using a beam potential of 15 kV. SEM analyses were performed at the Scientific-Technical Services of Barcelona University.

2.4.7. Confocal Laser Scanning Microscopy (CLSM)

The pyrite slabs were fixed in 3% paraformaldehyde (Merck) in the pH 7.1 phosphate buffer solution, at 4°C overnight. Thereafter, the slabs were stained with DAPI. After staining, the slides were mounted and examined with a Leica TCS SPE laser scanning confocal microscope. Images were captured with LAS AF software and

analyzed using ImageJ software. CLSM analyses were performed at the Department of Biological Sciences of the University of Southern California.

Appendix B:

Chemical and isotopic data of Osona groundwater

Table B1. Values of conductivity, temperature, pH, DO and Eh for Osona groundwater samples of Zone 1.

well	well depth	Cond.	Tª	pH	DO	Eh
	m	µs/cm	ºC		mg L^{-1}	mV
ZONE 1						
April 2005						
LMR-011	160	1580	15.2	7.0	4.9	383
LMV-005	51	1089	n.d.	7.1	4.8	n.d.
LMV-009	33	1265	n.d.	6.9	7.7	n.d.
MNL-018	14	1246	9.7	7.0	16.3	388
MNL-019	60	1664	8.7	7.5	4.5	345
MNL-027	5	1492	n.d.	6.9	8.3	n.d.
ORI-001	n.d.	918	10.9	7.0	1.4	319
SMC-001	110	1140	10.3	7.4	4.6	387
SMC-002	115	1162	7.7	6.9	2.7	363
SMC-010	120	1006	7.7	7.1	4.5	357
SMC-024	28	852	7.9	7.3	7.3	344
SMC-025	80	827	12.5	7.2	7.7	364
SMC-037	67	892	14.3	7.3	8.6	351
SPT-001	100	907	13.5	7.0	2.7	355
SPT-010	200	751	9.0	7.0	3.1	357
SVT-004	20	1491	11.4	6.8	5.6	341
TOR-002	3	1138	11.0	7.1	5.0	461
TOR-004	47	735	11.1	7.4	4.5	409
TOR-009	65	1190	8.0	7.3	1.6	404
TOR-013	70	1080	12.9	6.9	3.3	361
October 2005						
LMR-011	160	1994	16.1	6.8	n.d.	420
LMV-005	51	1036	16.3	7.4	n.d.	459
LMV-009	33	1109	14.6	7.1	n.d.	419
MNL-018	14	1153	15.0	7.0	n.d.	405
MNL-019	60	1106	16.2	7.1	n.d.	352
MNL-027	5	1262	17.5	6.9	n.d.	356
ORI-001	n.d.	960	16.3	7.1	n.d.	301
SMC-001	110	840	n.d.	7.3	n.d.	n.d.
SMC-002	115	936	n.d.	6.9	n.d.	n.d.
SMC-010	120	907	n.d.	7.0	n.d.	n.d.
SMC-024	28	747	n.d.	6.8	n.d.	n.d.
SMC-025	80	892	n.d.	6.7	n.d.	n.d.
SMC-037	67	780	16.1	7.0	n.d.	341
SPT-001	100	807	16.9	7.0	n.d.	365
SVT-004	20	1247	15.1	6.8	n.d.	378
TOR-002	3	1049	15.0	7.0	n.d.	404
TOR-004	47	554	15.2	7.4	n.d.	375
TOR-009	65	1166	18.0	6.9	n.d.	427
TOR-013	70	948	15.3	6.9	n.d.	381
May 2006						
LMV 009	33	1337	15.2	6.9	7.6	420
MAN 019	60	1275	16.0	7.1	1.7	310
SMC 002	115	914	16.2	6.8	0.8	343
SMC 010	120	880	16.4	7.0	1.1	357
SMC 025	28	634	18.4	7.1	6.8	426
SMC 024	80	741	15.6	7.1	5.7	441
SMC 037	67	697	17.7	6.9	1.0	356
SVT 004	20	1489	14.4	6.7	4.0	417
TOR 002	3	1214	15.9	7.0	5.8	441

n.d. = not determined

Table B2. Chemical data for Osona groundwater samples of Zone 1.

well	NO_2^-	NH_4^+	NO_3^-	HCO_3^-	Cl^-	SO_4^{2-}	Na^+	Ca^{2+}	Mg^+	K^+	Fe	Mn
	mg L^{-1}											
ZONE 1												
April 2005												
LMR-011	0.00	<0.02	139.0	434.8	72.0	177	44	219	50	23	n.d.	n.d.
LMV-005	0.07	0.22	116.0	397.2	73.0	96	58	141	36	5	n.d.	n.d.
LMV-009	0.00	<0.02	223.0	416.8	71.0	118	34	188	47	10	n.d.	n.d.
MNL-018	0.00	<0.02	120.0	388.4	90.9	188	36	181	42	13	n.d.	n.d.
MNL-019	1.98	<0.02	102.0	426.5	101.0	397	180	118	52	8	n.d.	n.d.
MNL-027	0.00	<0.02	157.8	477.3	121.2	239	33	227	60	14	n.d.	n.d.
ORI-001	0.43	0.22	63.0	443.1	25.4	110	24	144	32	16	n.d.	n.d.
SMC-001	0.00	0.31	149.0	409.9	53.0	120	25	174	43	3	n.d.	n.d.
SMC-002	0.00	<0.02	126.0	444.1	56.0	82	26	178	32	4	n.d.	n.d.
SMC-010	0.04	<0.02	101.0	343.1	55.0	117	28	153	32	8	n.d.	n.d.
SMC-024	0.00	<0.02	50.9	345.5	40.4	93	20	135	26	6	n.d.	n.d.
SMC-025	0.03	<0.02	21.6	396.3	18.3	95	19	125	30	6	n.d.	n.d.
SMC-037	0.00	0.02	30.6	419.7	29.2	100	25	131	34	3	n.d.	n.d.
SPT-001	0.14	<0.02	38.1	409.9	53.0	120	18	142	37	5	n.d.	n.d.
SPT-010	0.03	<0.02	14.1	474.3	10.0	67	24	132	27	2	n.d.	n.d.
SVT-004	0.05	0.12	208.0	557.8	118.5	91	28	292	20	5	n.d.	n.d.
TOR-002	0.00	<0.02	68.5	438.2	36.2	332	23	185	45	5	n.d.	n.d.
TOR-004	0.00	<0.02	22.6	240.6	25.8	78	16	101	14	3	n.d.	n.d.
TOR-009	0.03	<0.02	154.0	449.0	60.0	144	23	202	41	6	n.d.	n.d.
TOR-013	0.00	<0.02	84.0	386.0	32.3	148	17	161	39	3	n.d.	n.d.
October 2005												
LMR-011	0.04	<0.02	267.6	419.7	120	201	37	239	49	31	0.074	< 0.02
LMV-005	0.10	<0.02	77.7	424.6	76	106	74	123	32	5	0.074	< 0.02
LMV-009	0.03	<0.02	181.0	408.9	61	108	32	169	42	9	0.063	< 0.02
MNL-018	0.04	0.02	220.0	360.1	68	188	32	191	43	11	0.103	< 0.02
MNL-019	0.34	<0.02	82.3	422.1	67	284	92	125	52	8	0.166	< 0.02
MNL-027	0.02	<0.02	155.9	488.0	86	244	33	219	59	15	0.104	< 0.02
ORI-001	0.10	<0.02	50.0	450.4	24	144	24	133	30	23	0.131	< 0.02
SMC-001	<0,01	<0.02	78.3	405.0	38	109	27	125	40	2	0.145	< 0.02
SMC-002	<0,01	<0.02	135.9	439.2	53	84	23	181	32	3	0.132	< 0.02
SMC-010	<0,01	<0.02	143.1	390.4	56	114	26	174	32	8	0.109	< 0.02
SMC-024	<0,01	<0.02	56.4	400.2	40	103	19	122	31	6	0.095	< 0.02
SMC-025	<0,01	<0.02	25.5	475.8	23	111	29	161	32	8	0.076	< 0.02
SMC-037	<0,01	<0.02	35.2	419.7	30	105	24	127	34	2	0.068	< 0.02
SPT-001	0.09	<0.02	33.3	405.0	20	132	16	131	34	4	0.102	< 0.02
SVT-004	0.07	<0.02	191.7	536.8	83	98	28	261	20	5	0.083	< 0.02
TOR-002	0.06	<0.02	68.6	430.4	25	248	23	179	44	6	0.114	< 0.02
TOR-004	0.02	<0.02	36.0	234.2	43	118	14	82	11	2	0.290	< 0.02
TOR-009	0.02	<0.02	161.1	450.9	72	151	26	204	42	6	0.078	< 0.02
TOR-013	0.02	<0.02	80.9	383.1	33	165	16	157	38	3	0.080	< 0.02
May 2006												
LMV 009	n.d.	n.d.	252.5	412.4	73	117	32	210	53	9	< 0.02	< 0.02
MAN 019	n.d.	n.d.	240.8	429.4	86	332	191	123	57	8	0.122	< 0.02
SMC 002	n.d.	n.d.	125.6	439.2	52	81	25	194	36	4	< 0.02	< 0.02
SMC 010	n.d.	n.d.	151.7	341.6	48	116	30	178	39	6	0.049	< 0.02
SMC 025	n.d.	n.d.	17.0	390.4	18	92	21	125	35	4	< 0.02	< 0.02
SMC 024	n.d.	n.d.	44.1	392.8	28	81	17	151	29	6	< 0.02	< 0.02
SMC 037	n.d.	n.d.	31.6	424.6	30	103	25	145	38	2	< 0.02	< 0.02
SVT 004	n.d.	n.d.	223.2	558.8	118	83	29	309	23	4	0.078	< 0.02
TOR 002	n.d.	n.d.	87.6	427.0	28	242	25	210	53	5	< 0.02	< 0.02

n.d. = not determined

Table B3. Isotopic data for Osona groundwater samples of Zone 1.

well	$\delta^{13}C_{HCO3}$	$\delta^{34}S_{SO4}$	$\delta^{18}O_{SO4}$	$\delta^{15}N_{NO3}$	$\delta^{18}O_{NO3}$	$\delta^{18}O_{H2O}$
	(‰)	(‰)	(‰)	(‰)	(‰)	(‰)
ZONE 1						
April 2005						
LMR-011	-13.5	-7.7	4.2	14.7	4.3	-6.7
LMV-005	-12.2	-7.2	4.3	21.6	8.5	-6.3
LMV-009	-12.4	2.2	5.1	13.0	2.5	-7.0
MNL-018	-12.6	-3.7	4.6	13.4	4.1	-6.9
MNL-019	-10.8	-16.6	2.3	35.3	17.6	-6.3
MNL-027	-12.6	-12.4	3.2	15.1	4.2	-6.6
ORI-001	-13.7	-3.7	3.2	13.4	3.6	-5.5
SMC-001	-12.5	-6.6	3.2	13.5	4.8	-6.7
SMC-002	-13.7	-3.7	3.6	12.9	5.0	-6.7
SMC-010	-12.3	-10.9	4.0	16.8	6.7	-6.1
SMC-024	-11.3	-9.9	4.3	15.8	4.6	-6.4
SMC-025	-12.6	-13.1	4.5	17.0	9.8	-7.1
SMC-037	-12.3	-12.7	4.7	18.2	8.4	-6.7
SPT-001	-12.5	-18.2	2.6	19.3	9.3	-6.8
SPT-010	-14.1	-8.6	4.5	5.3	3.2	-7.4
SVT-004	-6.9	2.1	4.9	14.0	3.0	-6.1
TOR-002	-14.0	-15.1	3.4	9.5	4.1	-7.0
TOR-004	-12.1	7.3	9.0	13.7	3.1	-8.1
TOR-009	-12.9	-5.2	3.4	11.3	4.4	-6.6
TOR-013	-11.8	-8.5	2.9	11.4	3.7	-6.7
October 2005						
LMR-011	-14.1	-3.6	4.7	13.7	4.0	-6.6
LMV-005	-12.3	-7.7	4.6	24.4	11.4	-6.1
LMV-009	-11.4	3.4	6.2	12.9	2.5	-6.5
MNL-018	-12.3	-2.7	4.2	11.6	3.7	-6.3
MNL-019	-9.3	-15.7	3.5	20.8	10.2	-6.6
MNL-027	-11.5	-12.6	3.3	14.9	4.2	-6.1
ORI-001	-12.7	-3.7	4.7	17.0	5.6	-6.7
SMC-001	-10.2	-9.3	3.8	14.1	5.5	-6.7
SMC-002	-13.4	-3.1	3.6	12.7	4.7	-6.9
SMC-010	-13.1	-9.4	3.1	13.7	5.0	-6.7
SMC-024	-13.0	-10.1	4.7	17.0	5.7	-6.6
SMC-025	-12.2	-11.0	4.9	17.5	11.4	-6.5
SMC-037	-11.4	-13.8	4.8	18.8	8.0	-7.3
SPT-001	-11.2	-18.4	2.0	19.3	10.0	-6.4
SVT-004	-7.4	1.6	5.1	13.2	3.0	-6.1
TOR-002	-13.4	-15.9	2.9	9.6	2.9	-6.5
TOR-004	-11.3	7.1	8.8	12.5	3.8	-8.0
TOR-009	-12.7	-7.7	4.2	12.5	4.9	-6.3
TOR-013	-12.7	-11.4	3.5	12.4	5.2	-6.5
May 2006						
LMV 009	-12.5	0.9	4.9	13.2	5.9	-6.9
MAN 019	-11.4	-14.9	3.1	20.1	11.2	-6.4
SMC 002	-12.3	-3.7	3.7	12.7	6.2	-6.4
SMC 010	-11.8	-11.0	3.3	14.5	6.2	-6.2
SMC 025	-11.2	-13.4	4.3	16.0	11.7	-7.1
SMC 024	-9.2	-9.0	6.0	17.4	5.9	-6.4
SMC 037	-12.1	-14.7	6.0	17.5	9.3	-6.5
SVT 004	-11.6	1.0	5.4	14.8	4.7	-6.4
TOR 002	-14.3	-9.0	3.7	9.6	3.5	-6.8

n.d. = not determined

Table B4. Values of conductivity, temperature, pH, DO and Eh for Osona groundwater samples of Zone 2.

well	well depth	Cond.	T[a]	pH	DO	Eh
	m	µs/cm	ºC		mg L^{-1}	mV
ZONE 2						
April 2005						
CDT-004	60	919	14.0	7.1	1.6	359
CDT-009	70	976	10.3	7.2	4.5	411
CDT-011	90	804	14.0	7.0	2.8	455
FLG-006	45	1091	6.8	7.0	6.0	365
FLG-016	15	863	6.9	7.5	5.7	390
SEB-015	100	1364	10.6	6.9	1.9	249
SJV-004	35	870	11.0	6.8	5.3	400
TAR-004	23	738	6.9	n.d.	5.6	n.d.
TVR-006	180	620	9.0	7.4	5.6	355
TVR-008	30	856	n.d.	7.1	5.9	404
October 2005						
CDT-004	60	876	n.d.	6.8	n.d.	n.d.
CDT-009	70	936	n.d.	6.7	n.d.	n.d.
CDT-011	90	715	n.d.	6.8	n.d.	n.d.
FLG-006	45	1039	n.d.	6.7	n.d.	n.d.
FLG-016	15	848	n.d.	6.9	n.d.	n.d.
SEB-015	100	1419	n.d.	7.5	n.d.	n.d.
SEB-018	60	1400	n.d.	7.0	n.d.	n.d.
SJV-004	35	781	n.d.	6.6	n.d.	n.d.
TAR-004	23	674	15.8	6.8	n.d.	322
TVR-006	180	598	n.d.	7.1	n.d.	n.d.
TVR-008	30	713	n.d.	6.8	n.d.	n.d.
May 2006						
CDT 011	90	700	16.8	6.9	3.8	451
FLG 006	45	983	17.1	6.9	6.1	402
FLG 016	15	810	17.6	7.3	6.9	382
SEB 015	100	1121	17.6	6.9	4.8	378
SJV 004	35	705	15.7	6.8	8.6	471
TAR 004	23	625	15.3	6.5	7.9	469
TAV 008	30	683	13.8	7.0	6.6	390

n.d. = not determined

Table B5. Chemical data for Osona groundwater samples of Zone 2.

well	NO_2^-	NH_4^+	NO_3^-	HCO_3^-	Cl^-	SO_4^{2-}	Na^+	Ca^{2+}	Mg^+	K^+	Fe	Mn
	mg L^{-1}											
ZONE 2												
April 2005												
CDT-004	0.1	<0.02	150.7	344.0	67	68	17	157	29	2	n.d.	n.d.
CDT-009	0.0	<0.02	129.3	369.9	68	67	18	172	22	3	n.d.	n.d.
CDT-011	0.0	<0.02	43.9	413.3	33	67	14	148	22	1	n.d.	n.d.
FLG-006	0.0	<0.02	129.2	368.9	55	66	21	192	22	5	n.d.	n.d.
FLG-016	0.0	<0.02	81.5	368.9	46	98	14	145	34	4	n.d.	n.d.
SEB-015	0.0	0.12	178.4	426.5	124	165	57	191	49	9	n.d.	n.d.
SJV-004	0.0	<0.02	51.8	442.6	51	60	10	194	11	1	n.d.	n.d.
TAR-004	0.0	<0.02	109.0	233.3	42	54	17	129	9	1	n.d.	n.d.
TVR-006	0.0	<0.02	21.1	315.8	18	68	13	115	16	2	n.d.	n.d.
TVR-008	0.0	0.02	80.0	390.9	27	57	14	155	21	2	n.d.	n.d.
October 2005												
CDT-004	<0,01	<0.02	144.4	361.1	50	72	15	150	29	2	0.245	< 0.02
CDT-009	<0,01	<0.02	138.2	380.6	60	74	19	171	23	3	0.081	< 0.02
CDT-011	<0,01	<0.02	35.7	405.0	22	67	14	127	22	1	0.087	< 0.02
FLG-006	<0,01	<0.02	227.9	373.3	64	90	19	199	24	7	0.108	< 0.02
FLG-016	0.03	<0.02	92.0	380.6	46	103	14	146	33	3	0.123	< 0.02
SEB-015	3.89	<0.02	58.5	575.8	127	234	310	59	16	5	0.423	0.027
SEB-018	1.56	0.40	10.4	502.2	138	277	296	53	21	4	0.121	< 0.02
SJV-004	0.02	<0.02	45.1	451.4	29	51	8	174	10	< 1	0.083	< 0.02
TAR-004	0.00	0.02	104.2	256.2	33	54	15	126	9	1	0.214	< 0.02
TVR-006	<0,01	0.02	24.6	307.4	13	87	14	110	16	1	0.154	< 0.02
TVR-008	<0,01	0.02	62.2	376.2	22	53	18	130	19	2	0.101	< 0.02
May 2006												
CDT 011	n.d.	n.d.	42.1	414.8	26	69	14	153	28	1	< 0.02	< 0.02
FLG 006	n.d.	n.d.	253.7	356.2	57	91	19	229	28	5	0.031	< 0.02
FLG 016	n.d.	n.d.	148.4	336.7	33	84	14	168	37	3	< 0.02	< 0.02
SEB 015	n.d.	n.d.	267.4	427.0	98	172	90	215	55	5	< 0.02	< 0.02
SJV 004	n.d.	n.d.	57.9	461.2	32	65	11	212	13	< 1	< 0.02	< 0.02
TAR 004	n.d.	n.d.	106.7	231.8	27	50	16	133	10	< 1	0.082	< 0.02
TAV 008	n.d.	n.d.	102.1	390.0	28	57	12	171	23	2	0.030	< 0.02

n.d. = not determined

Table B6. Isotopic data for Osona groundwater samples of Zone 2.

well	$\delta^{13}C_{HCO3}$	$\delta^{34}S_{SO4}$	$\delta^{18}O_{SO4}$	$\delta^{15}N_{NO3}$	$\delta^{18}O_{NO3}$	$\delta^{18}O_{H2O}$
	(‰)	(‰)	(‰)	(‰)	(‰)	(‰)
ZONE 2						
April 2005						
CDT-004	-13.1	-4.9	2.4	12.0	3.3	-6.6
CDT-009	-13.4	-0.4	4.4	12.5	3.4	-6.9
CDT-011	-13.7	-4.8	4.6	12.3	3.6	-7.2
FLG-006	-13.9	3.2	4.8	11.5	2.7	-6.8
FLG-016	-11.8	1.7	3.8	10.0	2.3	-6.9
SEB-015	-12.7	-8.4	3.4	13.9	3.9	-6.9
SJV-004	-15.3	2.7	6.0	11.2	5.4	-7.2
TAR-004	-15.5	6.5	6.3	9.2	0.7	-7.0
TVR-006	-12.4	-13.1	7.2	8.9	1.6	-7.0
TVR-008	-13.0	0.0	4.9	11.8	3.5	-6.9
October 2005						
CDT-004	-12.5	-5.0	2.1	12.1	3.1	-6.8
CDT-009	-12.4	-0.8	3.8	12.3	3.4	-6.7
CDT-011	-12.0	-4.9	4.1	12.5	3.6	-7.2
FLG-006	-13.8	3.3	4.5	10.9	3.0	-6.8
FLG-016	-13.1	1.6	3.1	10.2	1.5	-6.5
SEB-015	-11.6	-4.4	1.0	18.8	6.0	-7.0
SEB-018	-11.9	-19.4	1.4	17.1	4.0	-6.6
SJV-004	-11.0	1.8	5.6	10.4	4.1	-6.3
TAR-004	-13.4	6.2	5.8	9.5	0.7	-6.9
TVR-006	-11.4	-16.0	7.3	9.8	3.7	-7.0
TVR-008	-10.8	-1.0	5.1	11.5	3.4	-6.8
May 2006						
CDT 011	-13.7	-4.7	5.9	13.3	5.5	-7.3
FLG 006	-14.3	3.8	4.6	11.0	4.2	-6.8
FLG 016	-12.5	3.0	4.1	9.2	1.4	-7.1
SEB 015	-10.1	-7.8	2.9	13.6	6.4	-6.6
SJV 004	-13.7	2.9	7.5	11.5	7.0	-7.2
TAR 004	-14.3	6.8	8.1	10.0	2.9	-7.3
TAV 008	-11.7	-13.5	4.4	11.7	4.6	-6.9

n.d. = not determined

Table B7. Values of conductivity, temperature, pH, DO and Eh for Osona groundwater samples of Zone 3.

well	well depth	Cond.	Tª	pH	DO	Eh
	m	µs/cm	ºC		mg L^{-1}	mV
ZONE 3						
April 2005						
BAL-001	n.d.	1015	14.8	7.1	5.7	392
BAL-005	30	1034	13.6	6.9	9.3	408
FLG-019	20	1351	12.4	6.9	4.3	362
GRB-007	60	1150	10.7	7.1	3.2	376
GRB-101	17	1318	12.9	7.0	8.0	383
GRB-106	70	1022	13.6	7.3	8.9	344
GRB-111	50	1733	9.6	6.8	5.5	218
GRB-112	14	1387	11.4	7.2	5.3	347
GRB-113	11	1652	10.2	7.0	3.6	321
GRB-115	6	1313	9.4	7.2	7.8	396
GRB-117	8	1580	12.8	6.9	12.0	361
GRB-118	52	1615	13.0	7.1	4.0	364
GRB-119	11	1412	10.4	6.8	6.9	388
MAL-001	12	1850	13.0	7.3	1.6	372
MAL-003	7	1560	7.2	7.0	3.5	360
SCV-003	5	1300	11.9	6.9	6.7	415
SEB-017	9	1345	10.9	6.9	2.4	370
TAR-003	45	1427	8.8	7.4	7.5	361
TON-001	35	2370	11.6	7.1	2.9	370
TON-002	n.d.	841	12.9	7.4	6.2	415
TON-006	n.d.	2930	13.2	6.9	2.1	378
TON-007	16	2330	13.6	6.9	2.8	359
TON-008	32	2240	13.1	7.0	3.2	176
TVR-003	75	1133	9.1	7.1	6.8	386
VIC-004	70	2290	8.4	7.3	2.7	251
VIC-007	30	1396	10.8	7.1	6.4	393
VIC-019	140	1133	9.2	7.4	1.1	348
VIC-100	40	1103	11.5	7.0	3.6	383
VIC-103	12	1760	8.9	6.9	2.4	270

Table B7. (continued)

well	well depth	Cond.	T[a]	pH	DO	Eh
	m	µs/cm	ºC		mg L^{-1}	mV
ZONE 3						
October 2005						
BAL-001	n.d.	883	14.4	7.0	n.d.	359
BAL-005	30	1010	15.4	7.0	n.d.	402
FLG-019	20	1119	n.d.	6.6	n.d.	n.d.
GRB-007	60	n.d.	15.1	7.0	n.d.	439
GRB-101	17	1367	16.6	6.9	n.d.	347
GRB-106	70	1137	15.5	7.0	n.d.	397
GRB-111	50	1685	18.0	7.1	n.d.	467
GRB-112	14	1224	13.6	7.1	n.d.	335
GRB-113	11	1367	14.6	7.1	n.d.	364
GRB-115	6	1132	15.0	7.0	n.d.	375
GRB-117	8	n.d.	15.2	6.8	n.d.	460
GRB-118	52	n.d.	14.9	6.9	n.d.	399
GRB-119	11	1840	14.4	6.9	n.d.	430
MAL-001	12	1558	14.1	6.9	n.d.	321
MAL-003	7	1267	16.2	7.0	n.d.	378
SCV-003	5	1138	13.9	6.9	n.d.	436
SEB-017	9	1300	n.d.	7.0	n.d.	n.d.
TAR-003	45	1336	16.0	7.2	n.d.	398
TON-001	35	1683	14.5	7.0	n.d.	335
TON-006	n.d.	2700	15.4	7.1	n.d.	364
TON-007	16	2630	14.9	7.0	n.d.	299
TON-008	32	1487	13.9	6.7	n.d.	183
TVR-003	75	1040	n.d.	6.7	n.d.	n.d.
VIC-004	70	2030	15.1	7.0	n.d.	229
VIC-007	30	1027	n.d.	7.0	n.d.	n.d.
VIC-019	140	1130	n.d.	6.7	n.d.	n.d.
VIC-100	40	1103	n.d.	6.7	n.d.	n.d.
VIC-103	12	1449	n.d.	6.1	n.d.	n.d.
May 2006						
BAL 005	n.d.	1060	15.3	7.2	8.6	422
GRB 106	70	1330	15.5	6.9	5.2	450
GRB 111	50	1554	15.0	6.9	4.9	490
GRB 117	8	1604	14.7	6.9	6.1	388
GRB 118	52	1676	14.9	6.9	5.0	448
GRB 119	11	1746	14.7	6.9	6.7	427
MAL 003	7	1280	17.0	6.9	5.2	433
TAR 003	45	1272	19.5	7.2	n.d.	416
TON 001	35	1890	16.6	6.9	0.9	395
TON 006	n.d.	2380	17.0	6.8	5.3	399
TON 008	32	1780	14.8	6.8	1.9	116
TAV 003	75	1019	14.6	6.9	4.5	414
VIC 004	70	2480	16.0	7.0	4.6	317
VIC 007	30	1371	13.9	6.8	1.1	223
VIC 019	140	891	16.6	6.9	1.3	369
VIC 103	12	1395	16.2	6.9	4.0	252

n.d. = not determined

Table B8. Chemical data for Osona groundwater samples of Zone 3.

well	NO_2^-	NH_4^+	NO_3^-	HCO_3^-	Cl^-	SO_4^{2-}	Na^+	Ca^{2+}	Mg^+	K^+	Fe	Mn
	mg L^{-1}											
ZONE 3												
April 2005												
BAL-001	0.0	0.02	180.0	388.4	87	44	20	166	38	0	n.d.	n.d.
BAL-005	0.0	<0.02	101.9	418.2	101	145	32	168	49	3	n.d.	n.d.
FLG-019	0.0	0.02	141.2	461.6	138	141	64	216	25	10	n.d.	n.d.
GRB-007	0.0	0.02	160.0	373.3	79	116	48	175	31	8	n.d.	n.d.
GRB-101	0.0	<0.02	191.8	370.4	137	224	44	206	58	4	n.d.	n.d.
GRB-106	0.2	<0.02	127.2	378.2	74	162	44	137	43	23	n.d.	n.d.
GRB-111	0.0	<0.02	124.0	444.1	136	274	53	221	67	11	n.d.	n.d.
GRB-112	0.0	<0.02	202.7	409.4	80	212	36	209	48	24	n.d.	n.d.
GRB-113	0.0	0.12	396.0	360.1	111	169	39	238	67	15	n.d.	n.d.
GRB-115	0.0	<0.02	142.3	402.6	108	240	41	188	62	5	n.d.	n.d.
GRB-117	0.1	0.02	302.0	407.5	145	180	40	242	49	5	n.d.	n.d.
GRB-118	0.0	0.02	299.0	422.1	99	197	70	228	49	10	n.d.	n.d.
GRB-119	0.0	0.02	321.3	394.3	145	186	40	244	52	7	n.d.	n.d.
MAL-001	0.0	<0.02	118.4	462.6	152	462	85	213	105	11	n.d.	n.d.
MAL-003	0.0	<0.02	127.0	464.1	139	321	60	219	73	11	n.d.	n.d.
SCV-003	0.0	0.12	144.1	450.4	71	208	26	202	54	3	n.d.	n.d.
SEB-017	0.0	<0.02	156.2	445.5	89	216	32	231	46	3	n.d.	n.d.
TAR-003	0.0	<0.02	100.1	424.6	93	276	106	146	56	4	n.d.	n.d.
TON-001	0.1	0.60	18.2	339.2	171	968	119	314	110	15	n.d.	n.d.
TON-002	0.0	0.02	124.2	327.0	35	52	16	125	30	2	n.d.	n.d.
TON-006	0.0	<0.02	102.4	537.3	574	491	228	270	124	7	n.d.	n.d.
TON-007	0.1	<0.02	166.6	454.3	378	495	135	272	131	11	n.d.	n.d.
TON-008	0.0	0.12	76.0	436.8	269	586	159	244	93	18	n.d.	n.d.
TVR-003	0.0	<0.02	159.0	374.8	51	76	25	191	32	4	n.d.	n.d.
VIC-004	0.2	0.02	260.5	405.5	429	316	226	206	74	8	n.d.	n.d.
VIC-007	0.0	0.02	100.1	478.7	105	309	52	209	70	10	n.d.	n.d.
VIC-019	0.0	<0.02	98.1	389.4	118	167	52	161	53	4	n.d.	n.d.
VIC-100	0.0	<0.02	127.4	357.7	87	121	32	171	31	7	n.d.	n.d.
VIC-103	0.0	0.12	16.8	551.0	214	345	102	220	76	4	n.d.	n.d.

Table B8. (continued)

well	NO_2^-	NH_4^+	NO_3^-	HCO_3^-	Cl^-	SO_4^{2-}	Na^+	Ca^{2+}	Mg^+	K^+	Fe	Mn
	mg L^{-1}											
ZONE 3												
October 2005												
BAL-001	<0,01	0.02	169.6	380.6	56	41	17	150	35	< 1	0.076	< 0.02
BAL-005	0.02	<0.02	64.2	361.1	72	237	38	157	47	3	0.076	< 0.02
FLG-019	<0,01	<0.02	149.7	407.5	143	179	62	193	23	8	0.078	< 0.02
GRB-007	0.05	<0.02	204.2	378.2	160	163	94	184	32	10	0.073	< 0.02
GRB-101	0.03	<0.02	197.7	378.2	114	270	50	217	62	5	0.053	< 0.02
GRB-106	0.06	<0.02	174.5	397.7	61	189	43	163	48	14	0.062	< 0.02
GRB-111	1.79	0.02	211.9	461.2	407	211	137	270	68	8	0.327	0.100
GRB-112	0.03	<0.02	169.7	414.8	63	227	38	189	49	20	0.071	< 0.02
GRB-113	0.03	<0.02	522.2	286.0	74	98	30	212	52	11	0.073	< 0.02
GRB-115	0.11	0.02	153.0	395.3	74	233	35	181	59	5	0.077	< 0.02
GRB-117	0.03	<0.02	322.9	400.2	111	165	36	241	49	6	0.110	< 0.02
GRB-118	0.05	<0.02	286.0	405.0	106	178	40	233	47	9	0.111	< 0.02
GRB-119	0.07	<0.02	303.2	366.0	111	141	32	225	47	5	0.088	< 0.02
MAL-001	0.04	<0.02	46.0	507.5	162	524	118	205	102	9	0.077	< 0.02
MAL-003	0.00	<0.02	151.0	451.4	102	263	55	198	65	7	0.079	< 0.02
SCV-003	0.03	<0.02	114.8	446.5	55	211	24	206	51	3	1.48	0.042
SEB-017	0.02	<0.02	64.4	500.7	167	239	192	148	31	4	0.068	< 0.02
TAR-003	0.01	<0.02	278.0	383.1	97	248	88	172	64	5	0.106	< 0.02
TON-001	<0,01	<0.02	34.9	317.2	149	832	129	249	98	8	0.083	< 0.02
TON-006	0.05	0.07	72.2	524.6	626	445	285	255	115	8	0.080	< 0.02
TON-007	0.29	1.17	123.3	517.3	464	650	220	274	149	16	0.070	< 0.02
TON-008	0.01	0.12	87.5	435.3	168	482	116	211	81	15	0.076	< 0.02
TVR-003	<0,01	<0.02	203.5	378.2	67	101	27	189	31	4	0.080	< 0.02
VIC-004	0.14	<0.02	332.8	391.4	315	304	179	225	69	5	0.096	< 0.02
VIC-007	0.01	<0.02	98.1	389.4	85	157	49	138	47	4	0.080	< 0.02
VIC-019	0.03	<0.02	183.9	414.8	74	168	35	197	38	7	0.082	< 0.02
VIC-100	<0,01	<0.02	190.5	388.9	70	153	35	189	35	7	0.118	< 0.02
VIC-103	<0,01	0.07	34.7	546.6	175	332	106	195	68	4	1.42	0.048
May 2006												
BAL 005	n.d.	n.d.	152.5	424.6	85	151	32	189	57	3	< 0.02	< 0.02
GRB 106	n.d.	n.d.	188.8	392.8	74	184	41	191	54	17	0.091	< 0.02
GRB 111	n.d.	n.d.	225.7	370.9	156	192	58	234	63	8	0.067	< 0.02
GRB 117	n.d.	n.d.	390.4	370.9	107	163	38	282	59	5	< 0.02	< 0.02
GRB 118	n.d.	n.d.	375.2	409.9	143	186	46	281	58	13	< 0.02	< 0.02
GRB 119	n.d.	n.d.	528.9	329.4	137	170	39	302	63	4	< 0.02	< 0.02
MAL 003	n.d.	n.d.	163.6	441.6	98	305	55	234	79	9	< 0.02	< 0.02
TAR 003	n.d.	n.d.	207.8	402.6	94	244	104	176	66	4	0.021	< 0.02
TON 001	n.d.	n.d.	29.6	341.6	150	997	131	354	120	14	0.023	< 0.02
TON 006	n.d.	n.d.	99.4	536.8	455	488	227	287	130	9	< 0.02	< 0.02
TON 008	n.d.	n.d.	89.1	453.8	196	580	157	273	108	20	< 0.02	< 0.02
TAV 003	n.d.	n.d.	256.4	366.0	67	100	28	219	37	4	< 0.02	< 0.02
VIC 004	n.d.	n.d.	529.4	351.4	495	304	252	282	91	6	0.038	< 0.02
VIC 007	n.d.	n.d.	132.1	468.5	73	388	56	248	88	11	0.513	0.049
VIC 019	n.d.	n.d.	117.0	395.3	80	162	47	168	56	4	< 0.02	< 0.02
VIC 103	n.d.	n.d.	39.2	n.d.	175	344	99	225	78	4	0.572	0.057

n.d. = not determined

Table B9. Isotopic data for Osona groundwater samples of Zone 3.

well	$\delta^{13}C_{HCO3}$	$\delta^{34}S_{SO4}$	$\delta^{18}O_{SO4}$	$\delta^{15}N_{NO3}$	$\delta^{18}O_{NO3}$	$\delta^{18}O_{H2O}$
	(‰)	(‰)	(‰)	(‰)	(‰)	(‰)
ZONE 3						
April 2005						
BAL-001	-12.8	3.8	4.5	10.1	1.8	-6.8
BAL-005	-14.1	-8.8	3.3	10.8	3.7	-7.1
FLG-019	-14.3	-0.1	7.6	13.8	3.0	-6.9
GRB-007	-12.9	-2.1	5.1	13.4	3.8	-6.7
GRB-101	-12.5	-1.6	2.9	13.0	2.6	-6.8
GRB-106	-12.3	-1.1	4.0	18.2	4.2	-6.4
GRB-111	-12.3	-6.8	1.6	13.4	3.7	-6.8
GRB-112	-13.3	-5.8	3.9	12.5	5.6	-6.7
GRB-113	-12.1	-5.7	3.5	11.9	2.6	-5.4
GRB-115	-12.6	-2.0	4.7	13.3	5.3	-6.5
GRB-117	-12.5	-2.7	3.6	13.5	4.0	-6.5
GRB-118	-12.3	-4.3	3.3	14.6	5.2	-6.6
GRB-119	-12.8	-2.2	4.1	13.1	4.1	-6.6
MAL-001	-12.9	-5.4	3.1	14.8	6.3	-6.9
MAL-003	-13.9	-6.4	4.2	13.6	3.8	-6.8
SCV-003	-12.9	-3.7	1.7	13.3	4.3	-6.7
SEB-017	-12.9	-14.8	2.0	13.2	4.5	-5.1
TAR-003	-11.5	-11.6	1.9	12.5	4.2	-6.9
TON-001	-11.4	7.5	8.3	28.3	9.2	-6.6
TON-002	-11.9	3.3	5.0	9.0	0.4	-6.8
TON-006	-13.7	-8.6	3.1	15.6	6.0	-6.7
TON-007	-13.2	-8.1	2.8	14.4	5.2	-6.7
TON-008	-13.0	1.1	5.5	18.3	5.2	-7.0
TVR-003	-12.8	1.5	4.1	12.1	2.8	-6.7
VIC-004	-11.0	-1.0	4.0	19.1	7.3	-6.8
VIC-007	-13.0	-2.8	4.2	17.9	6.4	-6.8
VIC-019	-12.4	-10.4	3.7	14.9	5.0	-6.8
VIC-100	-12.9	-0.5	4.9	14.7	5.0	-6.9
VIC-103	-12.3	-3.6	6.4	22.2	9.8	-6.4

Table B9. (continued)

well	$\delta^{13}C_{HCO3}$	$\delta^{34}S_{SO4}$	$\delta^{18}O_{SO4}$	$\delta^{15}N_{NO3}$	$\delta^{18}O_{NO3}$	$\delta^{18}O_{H2O}$
	(‰)	(‰)	(‰)	(‰)	(‰)	(‰)
ZONE 3						
October 2005						
BAL-001	-11.3	4.0	3.7	9.6	1.1	-6.8
BAL-005	-11.9	-19.5	n.d.	9.8	4.5	-6.7
FLG-019	-13.6	-0.2	5.9	13.2	3.4	-6.2
GRB-007	-13.9	-0.2	4.3	13.3	3.8	-6.5
GRB-101	-13.2	-5.9	n.d.	13.7	3.5	-7.0
GRB-106	-12.9	-2.1	2.5	9.2	1.9	-6.8
GRB-111	-13.4	-6.8	1.7	12.7	3.7	-6.5
GRB-112	-13.5	-8.1	3.4	14.4	6.8	-7.0
GRB-113	-11.8	-4.4	3.0	11.4	1.8	-6.8
GRB-115	-12.4	-1.9	4.1	13.1	4.9	-6.5
GRB-117	-11.9	-1.3	3.8	13.8	3.9	-6.8
GRB-118	-12.5	-2.5	3.7	14.1	4.4	-6.6
GRB-119	-12.6	-0.7	3.6	12.6	3.7	-6.2
MAL-001	-12.8	-6.9	5.2	21.1	10.7	-6.4
MAL-003	-14.1	-5.8	3.8	15.1	5.1	-6.4
SCV-003	-11.5	-14.5	6.9	13.6	4.5	-6.7
SEB-017	-10.8	-17.9	1.3	20.0	8.5	-6.4
TAR-003	-10.7	-10.3	0.4	12.2	3.1	-6.9
TON-001	-10.4	-3.0	2.6	10.4	3.0	-6.1
TON-006	-12.4	-9.3	2.7	15.4	6.0	-6.7
TON-007	-13.2	-6.0	4.2	16.6	7.9	-5.4
TON-008	-12.2	-0.2	4.3	14.9	3.9	-6.9
TVR-003	-12.2	0.9	4.8	12.0	2.8	-6.7
VIC-004	-11.3	-1.7	3.8	17.7	6.5	-6.5
VIC-007	n.d.	n.d.	n.d.	n.d.	n.d.	n.d.
VIC-019	-12.4	-11.5	4.2	14.0	3.8	-6.5
VIC-100	-12.5	-1.4	6.0	13.6	3.6	-6.6
VIC-103	-11.2	-4.4	6.2	18.1	7.1	-6.4
May 2006						
BAL 005	-13.8	-8.8	2.6	11.2	5.2	-7.1
GRB 106	-12.8	-1.3	2.5	10.4	3.6	-6.6
GRB 111	-12.1	-4.3	1.3	12.6	6.2	-7.1
GRB 117	-13.2	-1.1	2.6	13.6	5.4	-6.3
GRB 118	-7.6	-1.5	3.7	14.7	6.5	-6.5
GRB 119	-12.8	-0.2	3.7	12.4	5.5	-6.6
MAL 003	-13.1	-5.0	3.2	13.5	4.5	-6.7
TAR 003	-10.0	-10.4	1.4	12.4	5.0	-7.1
TON 001	-10.9	1.1	8.9	n.d.	n.d.	-6.3
TON 006	-13.0	-0.6	3.6	16.0	7.9	-6.8
TON 008	-12.0	9.3	4.8	16.0	6.2	-7.1
TAV 003	-12.3	-2.1	-1.1	12.3	4.5	-6.7
VIC 004	-10.3	-0.3	-1.1	16.7	7.1	-6.7
VIC 007	-12.2	-6.1	3.0	14.7	5.8	-7.0
VIC 019	-11.3	-12.6	4.0	14.6	5.9	-6.9
VIC 103	-11.6	-5.3	7.1	17.4	9.4	-6.7

n.d. = not determined

Appendix C:

Experimental data from the batch and flow-through experiments of chapter 3

Table C1. Experimental data from the pyrite-amended batch experiments inoculated with *T. denitrificans* presented in chapter 3 of this thesis (n.d.: not determined; b.d.l.: below detection limit).

Sample	Time	pH	NO_3^-	NO_2^-	NH_4^+	SO_4^{2-}	Fe	Mg	Ca	Na	P	K
	d		mM									
TD-1a-initial	0.0	6.8	4.26	0.07	16.8	0.00	b.d.l.	1.38	0.09	28.48	13.24	18.62
TD-1a-pre	1.1	6.5	4.22	0.06	16.3	9.37	0.51	3.39	1.17	27.33	10.82	17.68
TD-1a-initial	1.3	6.8	4.26	0.07	16.8	0.00	b.d.l.	1.38	0.09	28.48	13.24	18.62
TD-1a-0	3.8	6.8	3.89	0.24	16.7	3.70	0.02	3.23	0.78	27.69	12.85	18.01
TD-1a-1	13.8	6.9	2.20	0.28	16.4	5.69	b.d.l.	3.01	1.00	33.91	11.50	18.57
TD-1a-2	24.9	7.4	2.00	0.27	17.2	6.98	b.d.l.	3.00	1.02	34.27	10.56	18.65
TD-1a-3	31.8	7.1	1.87	0.36	19.7	7.32	b.d.l.	2.97	1.01	33.88	10.20	18.45
TD-1a-4	42.8	7.1	1.66	0.52	15.9	7.72	b.d.l.	1.28	0.66	34.43	8.46	18.73
TD-1a-5	62.8	6.9	1.26	0.41	n.d.	8.27	0.01	3.09	1.04	37.08	10.15	20.14
TD-1b-initial	0.0	6.8	4.26	0.07	16.8	0.00	b.d.l.	1.38	0.09	28.48	13.24	18.62
TD-1b-pre	1.1	6.3	4.33	0.05	16.5	11.93	0.60	3.35	1.24	28.61	8.79	18.39
TD-1b-initial	1.3	6.8	4.26	0.07	16.8	0.00	b.d.l.	1.38	0.09	28.48	13.24	18.62
TD-1b-0	3.8	6.7	4.27	0.05	17.6	2.79	0.02	2.71	0.56	27.64	13.28	18.01
TD-1b-1	13.8	7.0	3.39	0.11	17.3	2.94	b.d.l.	2.18	0.66	31.76	12.37	17.87
TD-1b-2	24.9	7.3	3.20	0.21	17.2	3.17	b.d.l.	2.03	0.63	31.67	12.08	17.85
TD-1b-3	31.8	7.1	3.05	0.33	19.2	3.17	b.d.l.	2.03	0.58	32.49	11.78	18.24
TD-1b-4	42.8	7.2	2.58	0.69	15.4	3.19	b.d.l.	1.14	0.28	33.20	10.97	18.59
TD-1b-5	62.8	7.0	1.49	0.84	n.d.	3.38	b.d.l.	1.89	0.64	34.19	12.14	19.03
TD-1c-initial	0.0	6.8	4.26	0.07	16.8	0.00	b.d.l.	1.38	0.09	28.48	13.24	18.62
TD-1c-pre	1.1	6.7	4.32	0.03	16.1	8.07	0.42	3.14	0.69	27.94	11.29	18.10
TD-1c-initial	1.3	6.8	4.26	0.07	16.8	0.00	b.d.l.	1.38	0.09	28.48	13.24	18.62
TD-1c-0	3.8	6.6	3.76	0.20	16.1	2.92	0.01	2.28	0.62	27.95	12.86	18.22
TD-1c-1	13.8	6.9	3.26	0.12	15.4	3.56	0.01	1.86	0.68	33.13	11.75	17.80
TD-1c-2	24.9	7.5	3.16	0.18	17.4	3.71	0.01	1.93	0.54	33.89	11.63	18.18
TD-1c-3	31.8	6.9	2.59	0.60	18.4	4.01	b.d.l.	2.12	0.48	33.61	11.70	17.98
TD-1c-4	42.8	7.2	1.86	1.12	15.8	4.22	b.d.l.	1.34	0.23	35.08	10.68	18.34
TD-1c-5	62.8	7.0	0.90	0.71	n.d.	4.94	b.d.l.	2.28	0.84	37.94	12.10	19.84
TD-2a-initial	0.0	6.8	2.51	0.05	19.3	0.00	0.02	2.09	0.24	27.23	14.54	17.46
TD-2a-pre	1.1	6.4	2.59	0.04	17.1	12.77	0.58	3.28	1.53	27.39	8.83	17.30
TD-2a-initial	1.3	6.8	2.51	0.05	19.3	0.00	0.02	2.09	0.24	27.23	14.54	17.46
TD-2a-0	3.8	6.9	2.51	0.07	17.9	4.21	0.02	2.71	0.85	27.24	13.03	17.38
TD-2a-1	13.8	6.6	1.63	0.17	18.3	4.50	b.d.l.	2.33	0.91	30.83	11.25	16.30
TD-2a-2	24.9	n.d.	n.d.	n.d.	n.d.	n.d.	b.d.l.	2.35	0.75	31.90	10.88	16.82
TD-2a-3	31.8	7.3	1.14	0.37	19.2	5.04	b.d.l.	2.42	0.74	31.93	10.66	16.75
TD-2a-4	42.8	7.2	0.64	0.67	14.7	5.03	b.d.l.	0.88	0.47	32.23	9.16	16.83
TD-2a-5	62.8	6.9	0.00	0.18	n.d.	5.41	b.d.l.	2.41	0.75	34.35	10.93	17.85
TD-2b-initial	0.0	6.8	2.51	0.05	19.3	0.00	0.02	2.09	0.24	27.23	14.54	17.46
TD-2b-pre	1.1	6.3	2.55	0.05	16.3	13.04	0.68	3.21	1.14	27.60	8.60	17.42
TD-2b-initial	1.3	6.8	2.51	0.05	19.3	0.00	0.02	2.09	0.24	27.23	14.54	17.46
TD-2b-0	3.8	6.9	2.48	0.07	17.1	4.17	0.02	2.65	0.82	27.51	12.74	17.55
TD-2b-1	13.8	7.0	1.38	0.16	16.3	4.62	0.03	2.25	0.79	31.68	11.06	16.41
TD-2b-2	24.9	7.5	1.29	0.14	16.56	4.99	0.02	2.04	0.64	32.40	10.75	16.71
TD-2b-3	31.8	7.1	1.22	0.22	18.4	5.01	0.01	2.13	0.64	32.98	10.92	16.99
TD-2b-4	42.8	7.3	0.50	0.88	15.1	5.07	0.01	1.17	0.58	33.29	10.12	17.16
TD-2b-5	62.8	6.9	0.00	0.17	n.d.	5.17	b.d.l.	2.27	0.72	35.46	11.52	17.99

Table C1. (continued).

Sample	Time	pH	NO_3^-	NO_2^-	NH_4^+	SO_4^{2-}	Fe	Mg	Ca	Na	P	K
	d		mM									
TD-2c-initial	0.0	6.8	2.51	0.05	19.3	0.00	0.02	2.09	0.24	27.23	14.54	17.46
TD-2c-pre	1.1	6.4	2.59	0.04	17.0	14.10	0.47	3.10	1.28	26.71	8.21	16.88
TD-2c-initial	1.3	6.8	2.51	0.05	19.3	0.00	0.02	2.09	0.24	27.23	14.54	17.46
TD-2c-0	3.8	7.0	2.19	0.27	15.8	2.96	0.01	2.58	0.71	26.52	13.49	17.05
TD-2c-1	13.8	6.8	1.46	0.13	15.5	3.80	b.d.l.	2.59	0.81	30.83	12.31	16.46
TD-2c-2	24.9	7.0	1.35	0.20	17.11	4.11	b.d.l.	2.29	0.69	31.53	11.91	16.78
TD-2c-3	31.8	7.0	1.01	0.44	18.2	4.17	b.d.l.	2.29	0.67	31.41	11.81	16.66
TD-2c-4	42.8	7.1	0.36	0.95	14.7	4.25	b.d.l.	0.90	0.42	32.00	10.28	16.88
TD-2c-5	62.8	6.9	0.00	0.25	n.d.	4.51	b.d.l.	2.19	0.65	34.34	11.97	17.95
TD-3a-initial	0.0	6.8	0.80	0.02	18.2	0.00	0.01	2.50	0.12	25.76	14.68	15.71
TD-3a-pre	1.1	6.3	0.79	0.03	18.4	11.54	0.31	3.26	1.25	26.32	9.03	15.90
TD-3a-initial	1.3	6.8	0.80	0.02	18.2	0.00	0.01	2.50	0.12	25.76	14.68	15.71
TD-3a-0	3.8	7.0	0.94	0.05	16.0	3.06	b.d.l.	2.91	0.72	26.31	13.61	16.07
TD-3a-1	13.8	6.6	0.00	0.02	16.2	4.44	0.02	2.31	0.84	24.51	9.95	12.38
TD-3a-2	24.9	7.1	0.00	0.02	17.11	5.17	b.d.l.	2.89	0.94	30.92	12.02	15.66
TD-3a-3	31.8	7.2	0.00	0.02	18.9	5.50	b.d.l.	2.88	1.03	30.95	11.66	15.64
TD-3a-4	42.8	7.1	0.00	0.02	15.9	5.79	b.d.l.	1.44	0.59	30.98	10.21	15.61
TD-3a-5	62.8	6.8	0.00	0.02	n.d.	6.04	b.d.l.	3.04	0.90	34.52	12.01	17.37
TD-3b-initial	0.0	6.8	0.80	0.02	18.2	0.00	0.01	2.50	0.12	25.76	14.68	15.71
TD-3b-pre	1.1	6.6	0.90	0.03	19.2	9.23	0.21	3.09	0.64	26.33	11.00	15.98
TD-3b-initial	1.3	6.8	0.80	0.02	18.2	0.00	0.01	2.50	0.12	25.76	14.68	15.71
TD-3b-0	3.8	6.9	0.80	0.02	15.3	4.05	0.01	3.28	0.82	26.86	13.60	16.40
TD-3b-1	13.8	6.8	0.00	0.02	16.2	6.79	0.01	2.85	1.11	30.97	11.77	15.48
TD-3b-2	24.9	7.4	0.00	0.02	17.22	8.37	b.d.l.	2.82	1.05	35.41	10.70	15.68
TD-3b-3	31.8	6.9	0.00	0.02	18.4	8.71	b.d.l.	2.82	1.06	31.73	10.37	15.81
TD-3b-4	42.8	7.0	0.00	0.02	16.0	9.04	b.d.l.	1.55	0.72	32.34	8.97	16.11
TD-3b-5	62.8	6.8	0.00	0.02	n.d.	10.73	b.d.l.	2.91	1.00	34.26	10.48	16.95
TD-3c-initial	0.0	6.8	0.80	0.02	18.2	0.00	0.01	2.50	0.12	25.76	14.68	15.71
TD-3c-pre	1.1	6.3	0.84	0.04	18.9	13.52	0.31	3.23	1.20	25.91	8.41	15.67
TD-3c-initial	1.3	6.8	0.80	0.02	18.2	0.00	0.01	2.50	0.12	25.76	14.68	15.71
TD-3c-0	3.8	6.7	0.90	0.04	16.5	3.22	0.01	3.20	0.76	27.00	13.94	16.39
TD-3c-1	13.8	6.9	0.00	0.03	16.6	4.26	b.d.l.	2.89	1.07	31.52	13.01	15.60
TD-3c-2	24.9	7.1	0.00	0.02	17.44	5.28	b.d.l.	2.75	0.93	31.19	11.65	15.33
TD-3c-3	31.8	7.0	0.00	0.01	18.7	5.71	b.d.l.	2.84	0.97	32.55	11.70	16.09
TD-3c-4	42.8	7.2	0.00	0.01	14.1	6.11	b.d.l.	1.47	0.64	32.63	10.10	16.21
TD-3c-5	62.8	6.8	0.00	0.02	n.d.	6.35	b.d.l.	2.80	0.97	35.54	11.68	17.50
TD-3d-initial	0.0	6.8	0.80	0.02	18.2	0.00	0.01	2.50	0.12	25.76	14.68	15.71
TD-3d-pre	1.1	6.5	0.87	0.04	18.8	9.30	0.26	3.13	0.85	24.61	9.95	14.98
TD-3d-initial	1.3	6.8	0.80	0.02	18.2	0.00	0.01	2.50	0.12	25.76	14.68	15.71
TD-3d-0	3.8	6.8	0.69	0.27	20.7	4.11	0.01	3.27	0.79	26.29	13.27	16.03
TD-3d-1	13.8	6.9	0.00	0.09	16.2	5.96	0.01	2.89	1.05	29.63	11.52	15.23
TD-3d-2	24.9	7.1	0.00	0.01	16.89	7.01	b.d.l.	2.91	1.00	31.56	10.63	15.96
TD-3d-3	31.8	7.1	0.00	0.01	19.1	7.42	b.d.l.	2.93	1.02	31.34	10.35	16.03
TD-3d-4	42.8	7.1	0.00	0.01	15.9	7.61	b.d.l.	1.60	0.66	31.17	8.88	15.98
TD-3d-5	62.8	6.8	0.00	0.01	n.d.	7.81	0.07	2.97	0.97	32.84	10.33	16.81

Table C1. (continued).

Sample	Time	pH	NO_3^-	NO_2^-	NH_4^+	SO_4^{2-}	Fe	Mg	Ca	Na	P	K
	d		mM									
TD-4-initial	0.0	7.1	4.06	0.00	n.d.	0.00	0.00	3.08	0.11	32.31	13.52	20.00
TD-4-pre	1.8	5.8	4.11	0.00	n.d.	66.64	22.99	4.06	13.88	39.97	0.13	18.83
TD-4-initial	1.9	7.1	4.06	0.00	n.d.	0.00	0.00	3.08	0.11	32.31	13.52	20.00
TD-4-0	3.8	6.9	4.38	0.00	n.d.	20.09	0.11	2.78	3.14	34.52	4.88	19.40
TD-4-1	13.8	6.5	2.30	0.00	n.d.	20.24	0.02	2.39	1.92	34.84	3.24	17.96
TD-4-2	24.8	n.d.	1.17	0.00	n.d.	21.98	n.d.	n.d.	n.d.	n.d.	n.d.	n.d.
TD-5-initial	0.0	7.1	4.06	0.00	n.d.	0.00	0.02	3.08	0.11	32.31	13.52	20.00
TD-5-pre	1.8	5.2	4.09	0.00	n.d.	44.37	13.21	4.05	9.27	30.21	2.64	19.96
TD-5-initial	1.9	7.1	4.06	0.00	n.d.	0.00	0.02	3.08	0.11	32.31	13.52	20.00
TD-5-0	3.8	6.9	3.82	0.00	n.d.	14.74	0.05	2.53	2.34	31.30	7.07	19.22
TD-5-1	13.8	6.7	3.34	0.00	n.d.	14.90	0.01	2.02	1.27	32.69	5.79	18.60
TD-5-2	24.8	6.7	n.d.	n.d.	n.d.	n.d.	0.00	2.05	1.03	34.13	5.55	19.44
TD-5-3	33.8	6.7	2.89	0.00	n.d.	15.24	0.01	2.15	1.00	34.66	5.43	19.45
TD-5-4	42.8	6.7	2.66	0.00	n.d.	15.69	b.d.l.	1.85	0.94	31.56	4.81	17.42
TD-5-5	59.8	6.9	2.50	0.00	n.d.	17.43	b.d.l.	2.34	1.15	38.24	5.16	20.89
TD-6-initial	0.0	7.1	0.95	0.00	n.d.	0.00	0.00	n.d.	n.d.	n.d.	8.71	n.d.
TD-6-pre	1.8	4.9	0.99	0.00	n.d.	49.65	22.50	3.57	2.41	30.67	5.52	15.01
TD-6-initial	1.9	7.1	0.95	0.00	n.d.	0.00	0.00	n.d.	n.d.	n.d.	8.71	n.d.
TD-6-0	3.8	6.9	1.06	0.00	n.d.	9.87	0.05	1.85	0.22	30.43	8.56	14.75
TD-6-1	7.8	6.9	0.06	0.02	n.d.	10.15	0.01	1.55	0.16	30.61	7.94	14.13
TD-6-2	9.8	6.8	0.00	0.00	n.d.	10.45	0.01	1.57	0.16	31.12	8.10	14.34
TD-6-3	11.8	7.0	0.00	0.00	n.d.	10.22	0.02	1.54	0.15	31.07	8.08	14.36
TD-6-4	13.8	6.8	0.00	0.00	n.d.	10.38	0.01	1.55	0.14	32.03	8.17	14.66
TD-6-5	15.7	7.0	0.00	0.00	n.d.	10.51	0.02	1.55	0.13	32.40	8.11	14.93
TD-7-initial	0.0	7.1	0.95	0.00	n.d.	0.00	0.00	n.d.	n.d.	n.d.	8.71	n.d.
TD-7-pre	1.8	5.3	1.04	0.00	n.d.	37.09	12.41	3.39	1.70	30.58	4.31	14.62
TD-7-initial	1.9	7.1	0.95	0.00	n.d.	0.00	0.00	n.d.	n.d.	n.d.	8.71	n.d.
TD-7-0	3.8	6.9	0.66	0.00	n.d.	7.56	0.04	1.62	0.14	30.55	8.85	14.63
TD-7-1	7.8	6.9	0.00	0.02	n.d.	7.90	0.01	1.21	0.10	31.18	8.09	14.21
TD-7-2	9.8	6.9	0.00	0.00	n.d.	8.06	0.01	1.20	0.08	31.89	8.16	14.40
TD-7-3	11.8	7.0	0.00	0.00	n.d.	8.13	0.03	1.15	0.08	31.14	8.08	14.04
TD-7-4	13.8	6.9	0.00	0.00	n.d.	8.17	0.02	1.18	0.09	32.32	8.36	14.72
TD-7-5	15.7	7.0	0.00	0.00	n.d.	8.33	0.02	1.15	0.07	32.12	8.26	14.54
TD-8-initial	0.0	7.1	4.06	0.00	n.d.	0.00	0.02	3.08	0.11	32.31	13.52	20.00
TD-8-pre	1.8	5.0	4.04	0.00	n.d.	60.36	23.53	4.26	11.64	29.66	2.44	19.27
TD-8-initial	1.9	7.1	4.06	0.00	n.d.	0.00	0.02	3.08	0.11	32.31	13.52	20.00
TD-8-0	3.8	6.9	4.45	0.00	n.d.	17.88	0.09	2.71	2.89	30.89	6.28	19.24
TD-8-1	13.8	6.6	4.01	0.00	n.d.	16.65	0.01	2.25	1.81	32.61	5.04	18.70
TD-8-2	24.8	6.6	3.93	0.00	n.d.	16.76	0.01	2.26	1.87	32.85	4.71	18.56
TD-8-3	33.8	6.5	4.19	0.00	n.d.	16.93	0.01	2.36	1.42	33.99	4.62	19.17
TD-8-4	42.8	6.5	3.64	0.00	n.d.	16.93	0.03	2.35	1.22	34.24	4.34	19.13
TD-8-5	59.8	n.d.	n.d.	n.d.	n.d.	n.d.	n.d.	n.d.	n.d.	n.d.	n.d.	n.d.

Table C1. (continued).

Sample	Time	pH	NO_3^-	NO_2^-	NH_4^+	SO_4^{2-}	Fe	Mg	Ca	Na	P	K
	d		mM									
TD-9-initial	0.0	7.1	4.06	0.00	n.d.	0.00	0.02	3.08	0.11	32.31	13.52	20.00
TD-9-pre	1.8	4.7	4.08	0.00	n.d.	67.78	29.52	4.44	12.94	30.63	2.76	19.90
TD-9-initial	1.9	7.1	4.06	0.00	n.d.	0.00	0.02	3.08	0.11	32.31	13.52	20.00
TD-9-0	3.8	6.5	3.71	0.00	n.d.	27.13	0.39	3.08	6.85	30.86	4.29	19.07
TD-9-1	13.8	6.1	2.53	0.00	n.d.	27.52	0.12	2.89	5.64	32.36	2.85	18.40
TD-9-2	24.8	6.1	2.11	0.00	n.d.	28.35	0.17	2.99	5.39	33.15	2.40	18.68
TD-9-3	33.8	6.0	2.13	0.00	n.d.	28.49	0.23	3.13	5.54	33.83	2.29	19.18
TD-9-4	42.8	5.8	2.16	0.00	n.d.	30.15	0.21	3.18	5.16	34.15	1.98	19.31
TD-9-5	59.8	6.2	2.09	0.00	n.d.	31.69	0.28	3.50	5.99	35.93	1.66	19.63
TD-10-initial	0.0	6.8	4.26	0.01	16.8	0.00	0.00	1.38	0.09	28.48	13.24	18.62
TD-10-pre	1.1	6.2	4.35	0.02	17.2	45.80	7.37	3.59	5.95	41.27	0.13	17.18
TD-10-initial	1.3	6.8	4.26	0.01	16.8	0.00	0.00	1.38	0.09	28.48	13.24	18.62
TD-10-0	3.8	6.8	4.76	0.02	16.3	18.11	0.02	2.82	2.43	32.81	5.54	18.17
TD-10-1	13.8	6.6	0.22	0.02	16.4	18.48	0.01	2.56	1.82	38.44	4.11	17.97
TD-10-2	15.7	6.8	0.00	0.01	17.2	18.68	0.01	2.66	1.25	38.20	3.96	17.49
TD-11-initial	0.0	6.8	2.51	0.02	19.3	0.00	0.02	2.09	0.24	27.23	14.54	17.46
TD-11-pre	1.1	5.0	2.78	0.02	17.1	63.02	20.50	3.89	6.52	28.10	2.79	17.63
TD-11-initial	1.3	6.8	2.51	0.02	19.3	0.00	0.02	2.09	0.24	27.23	14.54	17.46
TD-11-0	3.8	6.6	2.85	0.02	18.0	15.86	0.05	2.85	2.90	26.96	7.24	17.18
TD-11-1	13.8	6.4	0.00	0.00	16.8	19.57	0.03	2.55	2.84	30.81	5.65	16.08
TD-11-2	15.7	6.7	0.00	0.00	16.3	19.76	0.02	2.60	2.72	31.92	5.40	16.66
TD-12-initial	0.0	7.1	4.10	0.00	n.d.	0.00	0.00	3.16	0.12	34.29	13.71	21.26
TD-12-pre	1.8	5.0	4.20	0.00	n.d.	48.31	20.20	5.01	11.21	32.13	3.03	20.58
TD-12-initial	1.9	7.1	4.10	0.00	n.d.	0.00	0.00	3.16	0.12	34.29	13.71	21.26
TD-12-0	3.8	6.9	4.29	0.00	n.d.	12.52	0.06	2.66	1.54	33.29	5.98	20.36
TD-12-1	5.8	6.7	3.67	0.00	n.d.	12.09	0.04	2.51	1.39	36.09	5.76	20.22
TD-12-2	7.8	6.6	3.19	0.00	n.d.	12.51	0.02	2.55	1.28	34.37	5.16	19.02
TD-12-3	9.8	6.1	2.98	0.00	n.d.	12.66	0.01	2.00	0.92	26.58	3.87	14.75
TD-12-4	11.7	6.7	2.37	0.00	n.d.	12.93	0.01	2.53	1.13	34.37	4.75	18.93
TD-12-5	13.8	6.7	2.15	0.00	n.d.	13.10	0.02	2.56	1.17	33.93	4.76	18.54
TD-13-initial	0.0	7.1	5.31	0.00	n.d.	0.00	0.00	3.45	0.14	33.87	13.85	21.87
TD-13-pre	1.8	5.2	5.70	0.00	n.d.	34.83	15.17	4.42	0.21	32.79	4.72	20.75
TD-13-initial	1.9	7.1	5.31	0.00	n.d.	0.00	0.00	3.45	0.14	33.87	13.85	21.87
TD-13-0	3.8	6.3	3.72	0.00	n.d.	18.39	1.14	3.62	0.13	32.93	4.45	20.39
TD-13-1	5.8	6.1	3.38	0.00	n.d.	17.02	0.42	3.63	0.13	37.00	4.02	21.09
TD-13-2	7.8	6.0	3.02	0.00	n.d.	17.28	0.30	3.28	0.13	33.98	3.54	19.45
TD-13-3	9.8	5.9	2.18	0.00	n.d.	17.55	0.31	3.29	0.11	34.21	3.38	19.30
TD-13-4	11.7	5.7	1.88	0.00	n.d.	19.40	0.34	3.31	0.09	33.90	3.20	18.97
TD-13-5	13.8	5.7	0.88	0.00	n.d.	19.88	0.44	3.45	0.08	35.39	3.02	19.76

Table C1. (continued).

Sample	Time	pH	NO_3^-	NO_2^-	NH_4^+	SO_4^{2-}	Fe	Mg	Ca	Na	P	K
	d		mM									
TD-14-initial	0.0	7.1	5.31	0.00	n.d.	0.00	0.00	3.45	0.14	33.87	13.85	21.87
TD-14-pre	1.8	5.1	4.58	0.00	n.d.	36.85	20.98	5.26	0.52	32.98	2.05	20.96
TD-14-initial	1.9	7.1	5.31	0.00	n.d.	0.00	0.00	3.45	0.14	33.87	13.85	21.87
TD-14-0	3.8	6.5	3.32	0.00	n.d.	19.44	0.71	3.57	0.15	32.20	4.73	19.86
TD-14-1	5.8	6.3	2.64	0.00	n.d.	18.97	0.43	3.47	0.14	36.29	4.44	20.82
TD-14-2	7.8	6.1	1.28	0.00	n.d.	20.21	0.33	3.23	0.15	34.15	3.89	19.38
TD-14-3	9.8	6.0	0.44	0.00	n.d.	22.26	0.28	3.20	0.12	32.93	3.55	18.41
TD-14-4	11.7	n.d.	0.00	0.00	n.d.	23.57	0.40	3.61	0.12	37.54	3.91	21.04
TD-14-5	13.8	5.9	0.00	0.00	n.d.	23.59	0.38	3.38	0.11	34.10	3.59	19.19
TD-15-initial	0.0	7.1	4.10	0.00	n.d.	0.00	0.00	3.16	0.12	34.29	13.71	21.26
TD-15-pre	1.8	4.6	4.66	0.00	n.d.	70.99	37.36	5.01	11.21	32.13	3.03	20.58
TD-15-initial	1.9	7.1	4.10	0.00	n.d.	0.00	0.00	3.16	0.12	34.29	13.71	21.26
TD-15-0	3.8	6.8	3.94	0.00	n.d.	15.16	0.11	2.66	1.54	33.29	5.98	20.36
TD-15-1	5.8	6.5	2.47	0.00	n.d.	15.42	0.05	2.51	1.39	36.09	5.76	20.22
TD-15-2	7.8	6.4	0.24	0.04	n.d.	17.40	0.04	2.55	1.28	34.37	5.16	19.02
TD-15-3	9.8	6.3	0.00	0.00	n.d.	17.92	0.03	2.00	0.92	26.58	3.87	14.75
TD-15-4	11.7	6.4	0.00	0.00	n.d.	18.34	0.07	2.53	1.13	34.37	4.75	18.93
TD-15-5	13.8	6.3	0.00	0.00	n.d.	18.37	0.06	2.56	1.17	33.93	4.76	18.54
TD-16-initial	0.0	7.1	2.64	0.00	n.d.	0.00	0.00	3.22	0.36	30.65	13.55	17.94
TD-16-pre	1.8	5.9	3.07	0.00	n.d.	28.43	2.94	3.25	4.03	30.83	2.74	17.78
TD-16-initial	1.9	7.1	2.64	0.00	n.d.	0.00	0.00	3.22	0.36	30.65	13.55	17.94
TD-16-0	3.8	7.0	2.79	0.00	n.d.	6.19	0.02	2.24	0.56	29.77	10.07	17.05
TD-16-1	7.8	6.9	0.24	0.00	n.d.	7.86	0.01	1.88	0.35	31.45	9.09	16.71
TD-16-2	9.8	6.9	0.00	0.17	n.d.	8.07	b.d.l.	1.88	0.32	31.74	9.08	16.92
TD-16-3	11.8	6.9	0.00	0.00	n.d.	8.05	0.01	1.83	0.64	30.61	9.04	16.30
TD-16-4	13.8	6.9	0.00	0.00	n.d.	7.88	0.01	1.83	0.64	30.62	9.23	16.31
TD-16-5	15.7	7.1	0.00	0.00	n.d.	8.23	0.01	1.88	0.58	31.93	9.31	17.05
TD-17-initial	0.0	7.1	4.10	0.00	n.d.	0.00	0.00	3.16	0.12	34.29	13.71	21.26
TD-17-pre	1.8	5.0	4.66	0.00	n.d.	54.99	24.63	4.35	9.25	33.06	1.74	20.17
TD-17-initial	1.9	7.1	4.10	0.00	n.d.	0.00	0.00	3.16	0.12	34.29	13.71	21.26
TD-17-0	3.8	6.7	3.79	0.00	n.d.	16.91	0.17	2.95	2.72	33.57	5.06	20.12
TD-17-1	5.8	6.5	3.51	0.00	n.d.	15.74	0.08	2.71	2.32	36.19	4.51	20.20
TD-17-2	7.8	6.5	3.39	0.00	n.d.	16.00	0.06	2.48	1.99	34.59	4.08	19.23
TD-17-3	9.8	6.3	2.64	0.00	n.d.	16.56	0.04	2.48	1.90	34.64	3.87	19.11
TD-17-4	11.7	6.4	1.18	0.00	n.d.	18.35	0.02	2.68	1.82	37.24	3.59	20.26
TD-17-5	13.8	6.3	0.55	0.00	n.d.	18.89	0.03	2.76	1.79	36.38	3.14	19.51
TD-18-initial	0.0	7.1	4.10	0.00	n.d.	0.00	0.00	3.16	0.12	34.29	13.71	21.26
TD-18-pre	1.8	5.1	4.47	0.00	n.d.	56.87	24.80	4.35	11.41	32.28	2.02	20.12
TD-18-initial	1.9	7.1	4.10	0.00	n.d.	0.00	0.00	3.16	0.12	34.29	13.71	21.26
TD-18-0	3.8	6.9	3.52	0.00	n.d.	12.55	0.06	2.38	1.76	32.79	6.93	19.80
TD-18-1	5.8	6.7	3.37	0.00	n.d.	11.78	0.03	2.15	1.48	35.41	6.68	19.96
TD-18-2	7.8	6.7	3.26	0.00	n.d.	11.96	0.02	1.92	1.19	34.11	6.12	19.21
TD-18-3	9.8	6.6	1.76	0.00	n.d.	12.80	0.02	1.94	1.13	34.26	6.01	19.19
TD-18-4	11.7	6.6	0.14	0.00	n.d.	15.18	0.02	2.09	1.04	34.95	5.80	19.34
TD-18-5	13.8	6.6	0.00	0.00	n.d.	15.48	0.01	2.14	0.99	35.50	5.74	19.50

Table C2. Experimental data from the pyrite-amended batch experiments inoculated with *T. denitrificans* focusing in calculate isotopic fractionation presented in chapter 3 of this thesis (n.d.: not determined; b.d.l.: below detection limit).

Sample	Time	pH	NO_3^-	NO_2^-	NH_4^+	SO_4^{2-}	Fe	Mg	Ca	Na	P	K	$\delta^{15}N_{NO3}$		$\delta^{18}O_{NO3}$	
	d		mM										‰	sd	‰	sd
TD-20-initial	0.0	7.0	4.54	0.00	n.d.	0.00	0.00	3.03	0.12	28.58	12.94	18.89	n.d.	n.d.	n.d.	n.d.
TD-20-pre	1.8	6.2	5.38	0.00	n.d.	22.69	1.65	3.35	4.47	28.31	4.86	18.61	n.d.	n.d.	n.d.	n.d.
TD-20-initial	1.9	7.0	4.54	0.00	n.d.	0.00	0.00	3.03	0.12	28.58	12.94	18.89	n.d.	n.d.	n.d.	n.d.
TD-20-0	3.8	6.9	4.61	0.00	n.d.	10.84	0.07	2.60	1.43	27.68	7.82	18.02	-2.3	0.0	25.2	0.1
TD-20-1	13.8	6.9	3.51	0.00	n.d.	11.11	0.01	2.30	1.01	29.51	6.59	17.59	2.4	0.2	28.8	0.1
TD-20-2	24.8	6.9	3.19	0.00	n.d.	11.18	0.00	2.24	0.89	29.54	6.42	17.59	4.2	0.2	30.6	0.1
TD-20-3	33.8	6.7	3.03	0.00	n.d.	11.20	0.00	2.24	0.95	28.82	6.53	17.03	5.7	0.0	31.8	0.0
TD-20-4	42.8	6.8	2.84	0.00	n.d.	11.27	0.01	2.23	1.24	29.29	6.65	17.20	6.6	0.2	32.7	0.1
TD-20-5	59.8	6.9	2.20	0.00	n.d.	11.49	0.00	2.20	1.35	28.88	6.63	16.77	8.4	0.1	34.9	0.2
TD-21-initial	0.0	7.1	2.64	0.00	n.d.	0.00	0.00	3.22	0.36	30.65	13.55	17.94	n.d.	n.d.	n.d.	n.d.
TD-21-pre	1.8	6.4	2.81	0.00	n.d.	22.00	28.25	3.96	5.96	28.40	6.40	16.53	n.d.	n.d.	n.d.	n.d.
TD-21-initial	1.9	7.1	2.64	0.00	n.d.	0.00	0.00	3.22	0.36	30.65	13.55	17.94	n.d.	n.d.	n.d.	n.d.
TD-21-0	3.8	7.0	2.71	0.00	n.d.	10.36	4.56	3.32	2.59	30.36	3.87	16.85	-2.3	0.0	25.1	0.1
TD-21-1	7.8	7.0	2.36	0.00	n.d.	13.84	3.93	3.22	2.66	31.03	3.39	16.11	n.d.	n.d.	n.d.	n.d.
TD-21-2	9.8	6.8	2.39	0.00	n.d.	17.29	3.98	3.25	2.65	31.15	3.37	16.04	-0.2	0.1	26.5	0.1
TD-21-3	11.8	7.0	2.33	0.00	n.d.	18.10	4.11	3.30	3.21	32.28	3.34	16.71	n.d.	n.d.	n.d.	n.d.
TD-21-4	13.8	7.1	2.26	0.00	n.d.	19.49	3.99	3.31	2.39	32.18	3.29	16.71	1.3	0.0	28.0	0.1
TD-21-5	15.7	7.0	2.22	0.00	n.d.	21.43	4.41	3.55	2.98	34.17	3.53	17.81	2.6	0.0	29.2	0.0

Table C3. Experimental data from the blank and inoculated flow-through experiments presented in chapter 3 of this thesis (i: input; o: output; n.d.: not determined; b.d.l.: below detection limit).

Sample	Time	Flow rate	Nitrate (i)	Nitrate (o)	Nitrite (o)	Fe (o)	S (o)	pH (o)
	d	mL min^{-1}	mM	mM	mM	μM	μM	
BLANK-PYR-1-1	0.0	0.009	0.43	0.42	0.00	111.87	1210.00	4.5
BLANK-PYR-1-2	2.2	0.011	0.43	0.44	0.00	46.02	433.54	4.8
BLANK-PYR-1-3	9.1	0.005	0.43	0.42	0.02	1.67	39.52	5.3
BLANK-PYR-1-4	23.1	0.002	0.43	0.45	0.01	1.12	23.60	6.6
BLANK-PYR-1-5	32.1	0.011	0.39	0.41	0.01	0.95	18.80	5.8
BLANK-PYR-1-6	37.4	0.012	0.39	0.39	0.01	b.d.l.	7.08	6.4
BLANK-PYR-1-7	44.1	0.012	0.39	0.40	0.01	b.d.l.	5.18	6.2
BLANK-PYR-1-8	51.1	0.008	0.39	0.40	0.01	b.d.l.	5.09	6.7
BLANK-PYR-1-9	58.1	0.012	0.45	0.43	0.01	b.d.l.	4.12	7.2
BLANK-PYR-1-10	65.5	0.010	0.48	0.44	0.00	b.d.l.	4.18	7.4
BLANK-PYR-1-11	73.1	0.000	0.48	0.52	0.00	b.d.l.	3.59	7.3
IN-PYR-1-1	0.0	0.003	2.04	1.97	0.13	3.59	222.81	7.0
IN-PYR-1-2	4.0	0.002	2.04	1.68	0.20	3.03	255.23	7.0
IN-PYR-1-3	12.0	0.002	2.46	1.33	0.37	1.44	271.36	7.2
IN-PYR-1-4	21.0	0.002	2.46	1.37	0.51	32.31	182.39	8.6
IN-PYR-1-5	37.3	0.002	2.46	1.11	0.56	2.03	189.62	7.1
IN-PYR-1-6	48.9	0.002	2.57	1.50	0.46	1.76	165.74	7.1
IN-PYR-1-7	59.3	0.005	2.57	1.73	0.36	1.77	99.44	7.1
IN-PYR-1-8	66.0	0.005	2.49	0.90	0.60	2.33	35.11	7.0
IN-PYR-1-9	73.1	0.001	2.49	0.00	0.00	2.36	103.35	7.1
IN-PYR-1-10	90.0	0.002	2.49	0.00	0.00	1.52	133.47	8.5
IN-PYR-1-11	105.0	0.001	2.49	0.00	0.00	27.67	40.05	6.9
IN-PYR-1-12	116.0	0.003	2.49	0.00	0.00	7.07	60.69	7.0
IN-PYR-1-13	126.0	0.004	2.49	0.00	0.00	n.d.	n.d.	7.0
IN-PYR-1-14	135.0	0.002	2.49	0.00	0.03	6.62	0.00	7.2
IN-PYR-1-15	147.0	0.003	2.49	0.00	0.01	4.93	36.25	6.9
IN-PYR-1-16	156.0	0.003	2.49	0.00	0.01	3.79	0.00	6.7
IN-PYR-1-17	168.0	0.003	2.49	0.00	0.02	4.61	0.00	7.1
IN-PYR-1-18	177.0	0.003	2.49	0.00	0.00	4.86	91.79	7.0
IN-PYR-1-19	186.0	0.004	1.95	0.00	0.00	6.17	8.71	7.1
IN-PYR-1-20	198.0	0.003	1.95	0.00	0.00	5.36	0.00	7.3

Table C4. Experimental data from the non-inoculated flow-through experiments presented in chapter 3 of this thesis (i: input; o: output; n.d.: not determined; b.d.l.: below detection limit).

Sample	Time	Flow rate	Nitrate (i)	Nitrate (o)	Nitrite (o)	Fe (o)	S (o)	pH (o)
	d	mL min^{-1}	mM	mM	mM	μM	μM	
NON-PYR-1-1	0.0	0.009	0.42	0.52	0.03	440.11	1292.96	4.0
NON-PYR-1-2	7.0	0.011	0.42	0.39	0.00	29.81	270.01	4.5
NON-PYR-1-3	14.0	0.011	0.42	0.28	0.06	0.27	59.53	5.1
NON-PYR-1-4	21.0	0.011	0.42	0.35	0.01	7.76	11.52	4.8
NON-PYR-1-5	28.1	0.011	0.42	0.34	0.01	8.62	7.28	4.7
NON-PYR-1-6	35.0	0.011	0.42	0.35	0.01	6.52	6.99	4.7
NON-PYR-1-7	42.1	0.011	0.42	0.34	n.d.	4.86	8.20	4.9
NON-PYR-1-8	49.0	0.011	0.42	0.33	0.00	3.30	5.33	4.6
NON-PYR-1-9	56.0	0.011	0.42	0.35	0.00	7.36	2.04	4.5
NON-PYR-1-10	63.1	0.011	0.42	0.35	0.00	4.42	4.68	4.6
NON-PYR-1-11	70.0	0.011	0.42	0.41	0.00	2.40	2.31	4.5
NON-PYR-1-12	77.0	0.011	0.42	0.41	0.00	b.d.l.	2.70	6.6

Table C4. (continued).

Sample	Time	Flow rate	Nitrate (i)	Nitrate (o)	Nitrite (o)	Fe (o)	S (o)	pH (o)
	d	mL min^{-1}	mM	mM	mM	µM	µM	
NON-PYR-2-1	0.0	0.008	0.28	0.27	0.00	38.50	364.86	4.5
NON-PYR-2-2	6.9	0.012	0.28	0.21	0.04	1.54	29.24	5.1
NON-PYR-2-3	13.9	0.012	0.28	0.18	0.13	b.d.l.	12.52	6.2
NON-PYR-2-4	20.9	0.012	0.28	0.19	0.11	b.d.l.	4.19	6.6
NON-PYR-2-5	27.9	0.012	0.30	0.20	0.09	b.d.l.	2.31	6.9
NON-PYR-2-6	34.9	0.012	0.30	0.22	0.06	b.d.l.	0.80	7.0
NON-PYR-2-7	42.2	0.012	0.26	0.19	0.06	b.d.l.	0.05	6.7
NON-PYR-2-8	48.9	0.012	0.26	0.17	0.08	b.d.l.	1.40	7.1
NON-PYR-2-9	55.9	0.013	0.26	0.15	0.10	b.d.l.	0.50	6.8
NON-PYR-2-10	62.9	0.010	0.26	0.14	0.10	b.d.l.	1.93	7.3
NON-PYR-2-11	70.0	0.012	0.26	0.16	0.09	b.d.l.	6.45	7.4
NON-PYR-2-12	76.9	0.012	0.26	0.16	0.09	b.d.l.	1.33	6.9
NON-PYR-2-13	83.9	0.012	0.25	0.13	0.09	b.d.l.	0.57	7.4
NON-PYR-2-14	90.9	0.018	0.25	0.20	0.05	0.95	40.54	7.3
NON-PYR-2-15	96.0	0.012	0.26	0.17	0.06	0.87	6.61	7.7
NON-PYR-2-16	99.9	0.011	0.26	0.17	0.05	0.39	6.25	7.1
NON-PYR-2-17	105.2	0.011	0.26	0.18	0.03	b.d.l.	5.70	7.3
NON-PYR-2-18	111.9	0.011	0.26	0.18	0.03	b.d.l.	6.52	6.9
NON-PYR-2-19	118.9	0.011	0.26	0.16	0.04	b.d.l.	5.85	7.5
NON-PYR-2-20	125.9	0.012	0.31	0.18	0.05	b.d.l.	6.02	7.4
NON-PYR-2-21	133.3	0.012	0.31	0.16	0.06	b.d.l.	6.07	7.4
NON-PYR-2-22	140.9	0.012	0.31	0.15	0.06	b.d.l.	7.18	7.8
NON-PYR-2-23	147.9	0.012	0.31	0.14	0.06	b.d.l.	6.08	8.0
NON-PYR-2-24	152.1	0.012	0.31	0.15	0.05	b.d.l.	6.90	7.0
NON-PYR-2-25	163.1	0.011	0.31	0.08	0.07	b.d.l.	6.42	7.1
NON-PYR-2-26	176.2	0.012	0.31	0.07	0.08	b.d.l.	6.02	6.9
NON-PYR-2-27	187.9	0.012	0.31	0.07	0.00	b.d.l.	7.29	6.6
NON-PYR-2-28	197.3	0.012	0.31	0.08	0.00	b.d.l.	6.08	7.0
NON-PYR-2-29	210.2	0.013	0.31	0.14	0.01	b.d.l.	24.15	6.3
NON-PYR-2-30	217.9	0.013	0.45	0.36	0.00	b.d.l.	2.30	6.8
NON-PYR-2-31	223.9	0.013	0.45	0.40	0.00	b.d.l.	2.80	7.0
NON-PYR-2-32	230.9	0.013	0.45	0.42	0.00	b.d.l.	3.11	7.1
NON-PYR-2-33	236.9	0.013	0.45	0.40	0.00	b.d.l.	2.49	7.1
NON-PYR-2-34	244.9	0.013	0.45	0.39	0.00	b.d.l.	0.30	6.5
NON-PYR-2-35	251.9	0.013	0.45	0.36	0.00	b.d.l.	0.25	7.2
NON-PYR-2-36	258.9	0.013	0.45	0.36	0.00	b.d.l.	0.31	7.2
NON-PYR-2-37	265.9	0.013	0.41	0.28	0.01	b.d.l.	0.32	6.3
NON-PYR-2-38	272.9	0.011	0.41	0.25	0.01	b.d.l.	0.23	7.5
NON-PYR-2-39	279.9	0.011	0.41	0.26	0.01	b.d.l.	0.29	7.5
NON-PYR-2-40	286.9	0.012	0.41	0.16	0.01	b.d.l.	0.36	7.0
NON-PYR-2-41	293.9	0.012	0.41	0.10	0.01	b.d.l.	0.46	7.1
NON-PYR-2-42	300.9	0.011	0.47	0.13	0.01	b.d.l.	0.33	6.7
NON-PYR-2-43	307.9	0.012	0.47	0.12	0.01	b.d.l.	0.18	6.7
NON-PYR-2-44	313.9	0.012	0.47	0.12	0.01	b.d.l.	0.15	6.8
NON-PYR-2-45	319.9	0.012	0.48	0.14	0.01	b.d.l.	0.35	7.5
NON-PYR-2-46	323.9	0.012	0.48	0.15	0.01	b.d.l.	0.20	7.0
NON-PYR-2-47	327.9	0.012	0.48	0.15	0.01	b.d.l.	0.30	7.3
NON-PYR-2-48	334.9	0.012	0.48	0.14	0.01	b.d.l.	0.28	7.5
NON-PYR-2-49	344.9	0.012	0.48	0.13	0.01	b.d.l.	0.34	7.5
NON-PYR-2-50	350.8	0.012	0.48	0.09	0.01	b.d.l.	0.33	7.5
NON-PYR-2-51	356.9	0.011	0.50	0.06	0.01	b.d.l.	0.43	7.1
NON-PYR-2-52	362.9	0.008	0.51	0.04	0.00	b.d.l.	0.43	6.7
NON-PYR-2-53	368.9	0.011	0.51	0.03	0.00	b.d.l.	0.48	7.1
NON-PYR-2-54	372.9	0.011	0.51	0.09	0.00	b.d.l.	0.44	7.1

Table C4. (continued).

Sample	Time	Flow rate	Nitrate (i)	Nitrate (o)	Nitrite (o)	Fe (o)	S (o)	pH (o)
	d	mL min^{-1}	mM	mM	mM	μM	μM	
NON-PYR-3a-1	0.0	0.003	0.42	0.27	0.01	50.42	370.05	4.1
NON-PYR-3a-2	14.0	0.007	0.42	0.43	0.01	11.44	140.05	4.3
NON-PYR-3a-3	21.0	0.008	0.42	0.20	0.04	b.d.l.	61.03	4.9
NON-PYR-3a-4	28.0	0.009	0.42	0.10	0.06	b.d.l.	31.31	5.6
NON-PYR-3a-5	35.1	0.008	0.42	0.10	0.17	b.d.l.	18.09	5.8
NON-PYR-3a-6	42.0	0.008	0.42	0.11	0.17	b.d.l.	15.15	6.3
NON-PYR-3a-7	49.0	0.005	0.42	0.15	0.16	b.d.l.	14.94	5.6
NON-PYR-3a-8	56.1	0.007	0.42	0.17	0.14	b.d.l.	22.93	5.2
NON-PYR-3a-9	63.0	0.009	0.42	0.18	0.19	b.d.l.	11.40	5.4
NON-PYR-3a-10	70.0	0.009	0.42	0.18	0.22	b.d.l.	9.54	7.2
NON-PYR-3a-11	77.3	0.009	0.42	0.16	0.25	b.d.l.	6.85	7.2
NON-PYR-3a-12	84.0	0.009	0.42	0.18	0.25	b.d.l.	5.38	7.2
NON-PYR-3a-13	91.0	0.008	0.42	0.22	0.19	b.d.l.	5.40	7.0
NON-PYR-3a-14	98.3	0.003	0.38	0.23	0.17	b.d.l.	5.92	7.7
NON-PYR-3a-15	105.3	0.009	0.38	0.25	0.15	b.d.l.	9.36	7.6
NON-PYR-3a-16	112.3	0.011	0.38	0.27	0.08	b.d.l.	6.99	5.2
NON-PYR-3a-17	118.3	0.011	0.49	0.33	0.07	b.d.l.	5.30	7.4
NON-PYR-3a-18	125.3	0.011	0.49	0.39	0.03	b.d.l.	5.30	6.9
NON-PYR-3a-19	132.3	0.011	0.49	0.39	0.05	b.d.l.	6.64	7.3
NON-PYR-3a-20	139.1	0.011	0.49	0.42	0.07	b.d.l.	8.31	3.7
NON-PYR-3a-21	146.1	0.010	0.49	0.43	0.06	b.d.l.	6.05	7.0
NON-PYR-3a-22	155.0	0.011	0.49	0.42	0.04	b.d.l.	4.19	7.1
NON-PYR-3a-23	162.3	0.011	0.49	0.42	0.06	b.d.l.	4.75	7.5
NON-PYR-3a-24	170.1	0.011	0.48	0.42	0.04	b.d.l.	4.41	7.5
NON-PYR-3a-25	176.3	0.010	0.48	0.41	0.03	b.d.l.	4.14	6.7
NON-PYR-3a-26	182.0	0.011	0.49	0.41	0.03	b.d.l.	3.37	7.1
NON-PYR-3a-27	189.0	0.011	0.49	0.44	0.00	b.d.l.	3.79	7.4
NON-PYR-3a-28	196.3	0.011	0.49	0.43	0.01	b.d.l.	2.27	7.1
NON-PYR-3a-29	204.1	0.011	0.58	0.47	0.01	b.d.l.	2.84	7.4
NON-PYR-3a-30	211.1	0.011	0.53	0.47	0.00	b.d.l.	2.06	6.8
NON-PYR-3a-31	217.1	0.011	0.53	0.47	0.00	b.d.l.	2.53	7.5
NON-PYR-3a-32	224.3	0.011	0.53	0.46	0.00	b.d.l.	2.06	6.9
NON-PYR-3a-33	231.0	0.012	0.57	0.52	0.00	b.d.l.	2.04	4.9
NON-PYR-3a-34	238.3	0.012	0.57	0.48	0.00	b.d.l.	2.19	6.9
NON-PYR-3a-35	245.0	0.012	0.57	0.48	0.00	b.d.l.	2.04	7.8

Table C4. (continued).

Sample	Time	Flow rate	Nitrate (i)	Nitrate (o)	Nitrite (o)	Fe (o)	S (o)	pH (o)
	d	mL min^{-1}	mM	mM	mM	μM	μM	
NON-PYR-3b-1	0.0	0.006	0.43	0.43	0.00	148.27	1045.97	4.7
NON-PYR-3b-2	7.0	0.009	0.43	0.42	0.02	34.79	414.15	4.9
NON-PYR-3b-3	14.0	0.009	0.43	0.29	0.03	b.d.l.	135.78	5.3
NON-PYR-3b-4	21.0	0.009	0.43	0.18	0.06	b.d.l.	58.13	6.5
NON-PYR-3b-5	28.1	0.009	0.43	0.14	0.07	b.d.l.	27.64	6.7
NON-PYR-3b-6	35.0	0.008	0.43	0.14	0.06	b.d.l.	18.34	7.1
NON-PYR-3b-7	42.1	0.005	0.43	0.11	0.19	b.d.l.	14.11	7.1
NON-PYR-3b-8	49.0	0.009	0.43	0.14	0.18	b.d.l.	12.07	7.0
NON-PYR-3b-9	56.0	0.009	0.43	0.23	0.14	b.d.l.	10.68	7.1
NON-PYR-3b-10	63.1	0.009	0.43	0.28	0.12	b.d.l.	8.68	7.0
NON-PYR-3b-11	70.0	0.009	0.43	0.25	0.17	b.d.l.	6.88	7.0
NON-PYR-3b-12	77.0	0.009	0.43	0.22	0.21	b.d.l.	6.26	7.6
NON-PYR-3b-13	84.3	0.010	0.43	0.18	0.24	b.d.l.	5.11	7.8
NON-PYR-3b-14	91.0	0.010	0.43	0.23	0.18	b.d.l.	3.63	7.6
NON-PYR-3b-15	98.0	0.010	0.43	0.33	0.05	b.d.l.	3.85	7.1
NON-PYR-3b-16	105.3	0.010	0.39	0.35	0.03	b.d.l.	4.49	7.8
NON-PYR-3b-17	112.3	0.009	0.39	0.38	0.03	b.d.l.	4.21	7.7
NON-PYR-3b-18	119.3	0.010	0.39	0.43	0.00	b.d.l.	3.65	5.2
NON-PYR-3b-19	125.3	0.010	0.37	0.40	0.02	b.d.l.	7.06	7.3
NON-PYR-3b-20	132.3	0.010	0.49	0.47	0.00	b.d.l.	7.57	7.2
NON-PYR-3b-21	139.3	0.010	0.49	0.47	0.01	b.d.l.	9.43	7.2
NON-PYR-3b-22	146.1	0.009	0.49	0.47	0.01	b.d.l.	9.59	7.1
NON-PYR-3b-23	153.1	0.009	0.49	0.47	0.01	b.d.l.	7.68	7.3
NON-PYR-3b-24	162.0	0.010	0.49	0.47	0.01	b.d.l.	4.65	7.3
NON-PYR-3b-25	169.3	0.011	0.49	0.46	0.01	b.d.l.	3.68	7.5
NON-PYR-3b-26	177.1	0.011	0.49	0.46	0.01	b.d.l.	4.78	7.6
NON-PYR-3b-27	183.3	0.010	0.49	0.45	0.01	b.d.l.	5.20	7.0
NON-PYR-3b-28	189.0	0.010	0.37	0.39	0.00	b.d.l.	4.20	7.9
NON-PYR-3b-29	196.0	0.009	0.37	0.35	0.01	b.d.l.	5.36	7.1
NON-PYR-3b-30	203.3	0.010	0.37	0.35	0.01	b.d.l.	4.65	7.6

Table C4. (continued).

Sample	Time	Flow rate	Nitrate (i)	Nitrate (o)	Nitrite (o)	Fe (o)	S (o)	pH (o)
	d	mL min^{-1}	mM	mM	mM	μM	μM	
NON-PYR-3c-1	0.0	0.009	0.42	0.56	0.01	384.96	1282.36	4.4
NON-PYR-3c-2	7.0	0.009	0.42	0.39	0.01	46.77	413.52	4.3
NON-PYR-3c-3	14.0	0.010	0.42	0.19	0.07	b.d.l.	118.57	4.9
NON-PYR-3c-4	21.0	0.010	0.42	0.17	0.05	b.d.l.	41.54	6.2
NON-PYR-3c-5	28.1	0.010	0.42	0.18	0.05	b.d.l.	22.53	6.2
NON-PYR-3c-6	35.0	0.010	0.42	0.17	0.05	b.d.l.	17.65	6.7
NON-PYR-3c-7	42.1	0.010	0.42	0.13	0.17	0.50	16.96	6.2
NON-PYR-3c-8	49.0	0.010	n.d.	n.d.	n.d.	b.d.l.	14.44	6.4
NON-PYR-3c-9	56.0	0.010	0.42	0.26	0.08	b.d.l.	11.96	6.3
NON-PYR-3c-10	63.1	0.010	0.42	0.28	0.06	b.d.l.	10.58	6.4
NON-PYR-3c-11	70.0	0.010	0.42	0.31	0.05	b.d.l.	7.87	6.4
NON-PYR-3c-12	77.0	0.010	0.42	0.31	0.05	b.d.l.	6.51	7.2
NON-PYR-3c-13	84.3	0.010	0.42	0.27	0.12	b.d.l.	5.41	7.2
NON-PYR-3c-14	91.0	0.010	0.42	0.24	0.14	b.d.l.	4.31	6.9
NON-PYR-3c-15	98.0	0.010	0.42	0.27	0.12	b.d.l.	3.53	6.9
NON-PYR-3c-16	105.3	0.010	0.37	0.28	0.10	b.d.l.	3.24	7.5
NON-PYR-3c-17	112.3	0.008	0.37	0.28	0.09	b.d.l.	4.65	7.6
NON-PYR-3c-18	119.3	0.010	0.37	0.32	0.07	b.d.l.	4.17	5.3
NON-PYR-3c-19	125.3	0.010	0.38	0.32	0.04	b.d.l.	6.54	7.4
NON-PYR-3c-20	132.3	0.010	0.48	0.43	0.02	b.d.l.	4.80	7.1
NON-PYR-3c-21	139.3	0.010	0.48	0.46	0.02	b.d.l.	5.13	6.8
NON-PYR-3c-22	146.1	0.009	0.48	0.46	0.01	b.d.l.	6.38	6.7
NON-PYR-3c-23	153.1	0.009	0.48	0.44	0.04	b.d.l.	5.15	8.5
NON-PYR-3c-24	162.0	0.010	0.48	0.42	0.05	b.d.l.	3.85	7.2
NON-PYR-3c-25	169.3	0.010	0.48	0.41	0.05	b.d.l.	3.19	7.3
NON-PYR-3c-26	177.1	0.010	0.47	0.40	0.01	b.d.l.	2.69	7.6
NON-PYR-3c-27	183.3	0.009	0.47	0.38	0.02	b.d.l.	3.30	7.4
NON-PYR-3c-28	189.0	0.010	0.49	0.40	0.01	b.d.l.	2.89	7.8
NON-PYR-3c-29	196.0	0.010	0.49	0.43	0.00	b.d.l.	2.90	7.1
NON-PYR-3c-30	203.3	0.010	0.49	0.43	0.00	b.d.l.	2.90	7.4
NON-PYR-3c-31	211.1	0.01	0.49	0.42	0.01	b.d.l.	2.10	7.3
NON-PYR-3c-32	218.1	0.01	0.46	0.36	0.00	b.d.l.	3.32	7.3
NON-PYR-3c-33	224.1	0.01	0.46	0.35	0.00	b.d.l.	3.20	7.3
NON-PYR-3c-34	231.3	0.01	0.46	0.34	0.00	b.d.l.	3.09	7.1
NON-PYR-3c-35	238.0	0.01	0.47	0.29	0.03	b.d.l.	2.80	5.4
NON-PYR-3c-36	245.3	0.01	0.47	0.24	0.01	b.d.l.	3.18	7.1
NON-PYR-3c-37	252.0	0.01	0.47	0.20	0.03	b.d.l.	1.93	8.0

Table C4. (continued).

Sample	Time	Flow rate	Nitrate (i)	Nitrate (o)	Nitrite (o)	Fe (o)	S (o)	pH (o)
	d	mL min^{-1}	mM	mM	mM	μM	μM	
NON-PYR-3d-1	0.0	0.005	0.43	0.65	0.01	548.61	1843.70	4.2
NON-PYR-3d-2	7.0	0.008	0.43	0.43	0.00	24.97	652.40	5.6
NON-PYR-3d-3	14.0	0.009	0.43	0.24	0.08	b.d.l.	65.83	6.3
NON-PYR-3d-4	21.0	0.009	0.43	0.22	0.05	b.d.l.	21.32	6.7
NON-PYR-3d-5	28.1	0.009	0.43	0.27	0.04	b.d.l.	12.02	6.7
NON-PYR-3d-6	35.0	0.009	0.43	0.28	0.04	b.d.l.	9.40	6.9
NON-PYR-3d-7	42.1	0.009	0.43	0.28	0.08	b.d.l.	8.70	6.9
NON-PYR-3d-8	49.0	0.007	0.43	0.28	0.09	b.d.l.	9.52	6.9
NON-PYR-3d-9	56.0	0.009	0.43	0.29	0.07	b.d.l.	7.96	6.9
NON-PYR-3d-10	63.1	0.009	0.43	0.30	0.07	b.d.l.	8.04	7.0
NON-PYR-3d-11	70.0	0.009	0.39	0.36	0.05	b.d.l.	7.01	6.9
NON-PYR-3d-12	77.0	0.009	0.39	0.41	0.01	b.d.l.	5.95	7.3
NON-PYR-3d-13	84.3	0.009	0.37	0.37	0.01	b.d.l.	6.09	7.3
NON-PYR-3d-14	91.0	0.009	0.37	0.31	0.02	b.d.l.	4.78	7.1
NON-PYR-3d-15	98.0	0.009	0.37	0.31	0.04	b.d.l.	4.42	7.1
NON-PYR-3d-16	105.3	0.009	0.38	0.30	0.04	b.d.l.	4.26	7.9
NON-PYR-3d-17	112.3	0.008	0.38	0.29	0.02	b.d.l.	4.60	7.9
NON-PYR-3d-18	119.3	0.009	0.38	0.34	0.00	b.d.l.	6.17	5.5
NON-PYR-3d-19	125.3	0.009	0.38	0.33	0.01	b.d.l.	5.27	6.6
NON-PYR-3d-20	132.3	0.009	0.38	0.32	0.02	b.d.l.	4.07	7.4
NON-PYR-3d-21	139.3	0.009	0.49	0.33	0.07	b.d.l.	3.64	7.5
NON-PYR-3d-22	146.1	0.009	0.49	0.33	0.06	b.d.l.	3.11	7.5
NON-PYR-3d-23	153.1	0.009	0.49	0.32	0.07	b.d.l.	2.72	7.4
NON-PYR-3d-24	162.0	0.009	0.49	0.36	0.05	b.d.l.	2.12	8.3
NON-PYR-3d-25	169.3	0.009	0.49	0.33	0.04	b.d.l.	1.91	7.6
NON-PYR-3d-26	177.1	0.008	0.49	0.37	0.02	b.d.l.	2.35	7.9
NON-PYR-3d-27	183.3	0.008	0.49	0.34	0.03	b.d.l.	2.14	7.2
NON-PYR-3d-28	189.0	0.008	0.49	0.34	0.03	b.d.l.	2.96	7.7
NON-PYR-3d-29	196.0	0.008	0.49	0.34	0.05	b.d.l.	2.90	7.4
NON-PYR-3d-30	203.3	0.009	0.49	0.31	0.04	b.d.l.	2.36	7.7
NON-PYR-3d-31	211.1	0.01	0.49	0.30	0.04	b.d.l.	0.92	7.8
NON-PYR-3d-32	218.1	0.01	0.43	0.20	0.06	b.d.l.	1.67	7.5
NON-PYR-3d-33	224.1	0.01	0.43	0.27	0.02	b.d.l.	1.46	7.7
NON-PYR-3d-34	231.3	0.01	0.43	0.18	0.06	b.d.l.	2.33	7.5
NON-PYR-3d-35	238.0	0.01	0.46	0.18	0.06	b.d.l.	2.03	5.6

Table C4. (continued).

Sample	Time	Flow rate	Nitrate (i)	Nitrate (o)	Nitrite (o)	Fe (o)	S (o)	pH (o)
	d	mL min^{-1}	mM	mM	mM	µM	µM	
Initial stage of 48 d with 1.1 mM NO_3^- solution as input								
NON-PYR-3e-1	48.0	0.054	0.41	n.d.	n.d.	b.d.l.	3.11	7.0
NON-PYR-3e-2	49.3	0.016	0.37	0.44	0.03	b.d.l.	2.90	7.1
NON-PYR-3e-3	55.0	0.011	0.37	0.38	0.03	b.d.l.	2.96	6.7
NON-PYR-3e-4	63.1	0.013	0.37	0.36	0.04	b.d.l.	3.11	6.7
NON-PYR-3e-5	70.0	0.015	0.37	0.33	0.06	b.d.l.	3.61	6.5
NON-PYR-3e-6	77.1	0.013	0.37	0.29	0.09	b.d.l.	2.96	6.9
NON-PYR-3e-7	84.0	0.010	0.44	0.26	0.09	b.d.l.	2.90	6.9
NON-PYR-3e-8	91.2	0.014	0.44	0.33	0.07	b.d.l.	5.36	6.9
NON-PYR-3e-9	98.1	0.015	0.44	0.33	0.06	b.d.l.	3.12	6.8
NON-PYR-3e-10	105.1	0.015	0.44	0.37	0.05	b.d.l.	10.85	6.7
NON-PYR-3e-11	112.1	0.015	0.44	0.42	0.02	b.d.l.	4.12	6.2
NON-PYR-3e-12	119.2	0.015	0.44	0.44	0.01	b.d.l.	19.87	5.2
NON-PYR-3e-13	126.1	0.010	0.44	0.45	0.01	b.d.l.	12.33	5.2
NON-PYR-3e-14	135.3	0.008	0.44	0.43	0.01	0.89	55.07	4.2
NON-PYR-3e-15	141.3	0.015	0.42	0.40	0.01	b.d.l.	35.36	4.6
NON-PYR-3e-16	148.2	0.013	0.42	0.40	0.01	b.d.l.	24.49	5.0
NON-PYR-3e-17	155.2	0.010	0.42	0.41	0.01	0.66	19.11	5.7
NON-PYR-3e-18	162.0	0.015	0.42	0.41	0.01	0.76	40.04	4.4
NON-PYR-3e-19	168.1	0.013	0.42	0.41	0.01	0.78	17.80	5.5
NON-PYR-3e-20	175.0	0.020	0.42	0.41	n.d.	0.44	14.40	6.2

Table C4. (continued).

Sample	Time	Flow rate	Nitrate (i)	Nitrate (o)	Nitrite (o)	Fe (o)	S (o)	pH (o)
	d	mL min^{-1}	mM	mM	mM	µM	µM	
Initial stage of 70 d with pH 3 HCl solution as input								
NON-PYR-3f-1	70.0	0.010	0.44	0.38	0.03	1.27	7.38	3.3
NON-PYR-3f-2	77.1	0.011	0.44	0.38	0.04	b.d.l.	5.95	5.6
NON-PYR-3f-3	84.0	0.011	0.44	0.39	0.03	b.d.l.	4.64	6.4
NON-PYR-3f-4	90.9	0.011	0.41	0.37	0.02	b.d.l.	2.73	7.3
NON-PYR-3f-5	98.0	0.013	0.41	0.39	0.02	b.d.l.	8.79	7.0
NON-PYR-3f-6	103.1	0.009	0.41	0.38	0.02	b.d.l.	27.92	7.0
NON-PYR-3f-7	107.0	0.012	0.41	0.37	0.01	b.d.l.	4.79	7.0
NON-PYR-3f-8	112.3	0.012	0.42	0.37	0.01	b.d.l.	2.20	7.0
NON-PYR-3f-9	119.0	0.013	0.42	0.34	0.02	b.d.l.	2.33	6.9
NON-PYR-3f-10	126.0	0.013	0.50	0.39	0.03	b.d.l.	1.78	n.d.
NON-PYR-3f-11	133.0	0.012	0.50	0.38	0.03	b.d.l.	2.47	7.1
NON-PYR-3f-12	140.3	0.012	0.50	0.35	0.04	b.d.l.	1.53	7.1
NON-PYR-3f-13	147.9	0.012	0.50	0.36	0.04	b.d.l.	1.88	7.2
NON-PYR-3f-14	155.0	0.014	0.50	0.36	0.04	b.d.l.	0.53	7.2
NON-PYR-3f-15	159.2	0.014	0.50	0.36	0.04	b.d.l.	1.41	6.8
NON-PYR-3f-16	170.2	0.014	0.50	0.26	0.07	b.d.l.	0.00	5.9
NON-PYR-3f-17	183.2	0.014	0.50	0.28	0.05	b.d.l.	0.00	6.1
NON-PYR-3f-18	195.0	0.020	0.50	0.22	0.06	b.d.l.	0.00	7.1
NON-PYR-3f-19	204.4	0.010	0.51	0.36	0.01	b.d.l.	2.11	7.1
NON-PYR-3f-20	217.2	0.013	0.51	0.37	0.01	b.d.l.	1.58	7.0
NON-PYR-3f-21	225.0	0.004	0.51	0.42	0.01	b.d.l.	31.87	6.9
NON-PYR-3f-22	231.0	0.013	0.50	0.41	0.01	b.d.l.	6.41	7.1
NON-PYR-3f-23	237.9	0.014	0.50	0.39	0.01	b.d.l.	3.49	7.1
NON-PYR-3f-24	243.9	0.014	0.50	0.37	0.01	b.d.l.	2.23	7.3
NON-PYR-3f-25	251.9	0.013	0.50	0.36	0.01	b.d.l.	1.05	7.3
NON-PYR-3f-26	258.9	0.013	0.49	0.83	0.03	b.d.l.	1.45	7.4
NON-PYR-3f-27	266.0	0.013	0.49	0.33	0.02	b.d.l.	1.40	7.6
NON-PYR-3f-28	273.0	0.013	0.43	0.29	0.02	4.82	20.13	7.6
NON-PYR-3f-29	280.0	0.013	0.43	0.30	n.d.	b.d.l.	2.43	7.3
NON-PYR-3f-30	287.0	0.014	0.43	0.31	0.01	b.d.l.	3.80	7.4
NON-PYR-3f-31	294.0	0.013	0.43	0.28	0.01	b.d.l.	1.17	7.2
NON-PYR-3f-32	301.0	0.013	0.41	0.28	0.01	3.06	5.67	7.5
NON-PYR-3f-33	308.0	0.013	0.47	0.33	0.02	b.d.l.	0.69	7.4
NON-PYR-3f-34	315.0	0.014	0.47	0.32	0.02	b.d.l.	1.73	7.1
NON-PYR-3f-35	321.0	0.014	0.47	0.32	0.02	b.d.l.	1.45	7.3
NON-PYR-3f-36	326.9	0.014	0.47	0.31	0.02	b.d.l.	1.56	7.8
NON-PYR-3f-37	331.0	0.014	0.51	0.34	0.02	b.d.l.	0.79	7.7
NON-PYR-3f-38	334.9	0.014	0.51	0.36	0.02	b.d.l.	1.53	7.6
NON-PYR-3f-39	342.0	0.014	0.51	0.35	0.02	b.d.l.	0.92	7.6
NON-PYR-3f-40	352.0	0.015	0.51	0.33	0.02	b.d.l.	1.89	7.6
NON-PYR-3f-41	357.9	0.014	0.51	0.26	0.02	b.d.l.	1.06	7.6
NON-PYR-3f-42	364.0	0.013	0.52	0.19	0.02	b.d.l.	1.00	7.4
NON-PYR-3f-43	370.0	0.010	0.51	0.20	0.01	b.d.l.	2.66	7.7
NON-PYR-3f-44	375.9	0.015	0.51	0.26	0.00	b.d.l.	1.06	5.7
NON-PYR-3f-45	380.0	0.013	0.51	0.31	0.00	b.d.l.	2.35	6.9

Table C4. (continued).

Sample	Time	Flow rate	Nitrate (i)	Nitrate (o)	Nitrite (o)	Fe (o)	S (o)	pH (o)
	d	mL min^{-1}	mM	mM	mM	μM	μM	
NON-PYR-4a-1	0.0	0.008	0.48	0.49	0.00	10.28	267.66	5.3
NON-PYR-4a-2	7.0	0.011	0.48	0.43	0.00	b.d.l.	46.96	6.5
NON-PYR-4a-3	14.3	0.013	0.45	0.41	0.01	b.d.l.	12.02	6.9
NON-PYR-4a-4	21.0	0.011	0.45	0.41	0.01	b.d.l.	6.52	7.0
NON-PYR-4a-5	28.0	0.012	0.45	0.40	0.01	b.d.l.	4.46	7.0
NON-PYR-4a-6	35.0	0.009	0.42	0.39	0.00	b.d.l.	3.12	7.3
NON-PYR-4a-7	42.1	0.010	0.42	0.39	0.01	b.d.l.	2.40	7.0
NON-PYR-4a-8	49.0	0.011	0.42	0.40	0.01	b.d.l.	2.83	6.9
NON-PYR-4a-9	56.0	0.011	0.42	0.38	0.01	b.d.l.	2.48	7.5
NON-PYR-4a-10	63.0	0.017	0.42	0.40	0.01	b.d.l.	4.89	7.2
NON-PYR-4a-11	68.1	0.008	0.41	0.41	0.01	b.d.l.	3.17	7.5
NON-PYR-4a-12	72.0	0.010	0.41	0.39	0.01	b.d.l.	1.06	7.2
NON-PYR-4a-13	77.3	0.010	0.42	0.39	0.01	b.d.l.	1.20	7.3
NON-PYR-4a-14	84.0	0.010	0.42	0.37	0.01	b.d.l.	1.24	7.0
NON-PYR-4a-15	91.0	0.010	0.50	0.38	0.05	b.d.l.	2.43	7.3
NON-PYR-4a-16	98.0	0.010	0.50	0.37	0.05	b.d.l.	2.97	7.3
NON-PYR-4a-17	105.4	0.010	0.50	0.36	0.04	b.d.l.	2.36	7.2
NON-PYR-4a-18	113.0	0.010	0.50	0.35	0.04	b.d.l.	1.81	7.7
NON-PYR-4a-19	120.0	0.011	0.50	0.39	0.02	b.d.l.	1.02	7.6
NON-PYR-4a-20	124.2	0.010	0.50	0.38	0.03	b.d.l.	0.97	7.0
NON-PYR-4a-21	135.2	0.010	0.50	0.31	0.03	b.d.l.	1.71	6.2
NON-PYR-4a-22	148.3	0.010	0.50	0.30	0.03	b.d.l.	0.07	6.3
NON-PYR-4a-23	160.0	0.009	0.50	0.25	0.03	b.d.l.	1.41	7.0
NON-PYR-4a-24	169.4	0.004	0.51	0.25	0.02	b.d.l.	3.03	7.0
NON-PYR-4a-25	190.0	0.003	0.51	0.34	0.01	b.d.l.	6.42	7.0
NON-PYR-4a-26	196.0	0.002	0.50	0.28	0.03	b.d.l.	8.26	7.3
NON-PYR-4a-27	203.0	0.011	0.50	0.34	0.01	b.d.l.	5.48	7.1
NON-PYR-4a-28	208.9	0.011	0.50	0.35	0.02	b.d.l.	1.44	7.4
NON-PYR-4a-29	217.0	0.011	0.50	0.33	0.02	n.d.	n.d.	7.3
NON-PYR-4a-30	224.0	0.011	0.49	0.28	0.04	n.d.	n.d.	7.4
NON-PYR-4a-31	231.0	0.011	0.49	0.29	0.05	n.d.	n.d.	7.8
NON-PYR-4a-32	238.0	0.012	0.43	0.25	0.05	n.d.	n.d.	7.6
NON-PYR-4a-33	245.0	0.002	0.43	0.24	0.05	n.d.	n.d.	n.d.
NON-PYR-4a-34	252.0	0.011	0.43	0.29	0.03	n.d.	n.d.	7.8
NON-PYR-4a-35	259.0	0.008	0.43	0.29	0.03	n.d.	n.d.	7.3
NON-PYR-4a-36	266.0	0.011	0.41	0.27	0.05	n.d.	n.d.	7.1

Table C4. (continued).

Sample	Time	Flow rate	Nitrate (i)	Nitrate (o)	Nitrite (o)	Fe (o)	S (o)	pH (o)
	d	mL min^{-1}	mM	mM	mM	μM	μM	
Initial stage of 200 d with 1.0 mM NO_3^- solution as input								
NON-PYR-4b-1	204.4	0.013	0.54	0.54	0.00	b.d.l.	0.90	6.1
NON-PYR-4b-2	217.2	0.013	0.54	0.55	0.00	b.d.l.	0.07	6.1
NON-PYR-4b-3	225.0	0.013	0.54	0.56	0.00	b.d.l.	1.03	7.2
NON-PYR-4b-4	231.0	0.013	0.54	0.56	0.00	b.d.l.	0.00	6.6
NON-PYR-4b-5	237.9	0.013	0.52	0.46	0.00	b.d.l.	2.72	6.5
NON-PYR-4b-6	243.9	0.013	0.52	0.39	0.00	b.d.l.	2.21	6.9
NON-PYR-4b-7	251.9	0.013	0.52	0.39	0.00	b.d.l.	1.00	7.2
NON-PYR-4b-8	258.9	0.013	0.52	0.38	0.00	b.d.l.	0.74	6.7
NON-PYR-4b-9	266.0	0.013	0.52	0.38	0.00	b.d.l.	0.79	6.7
NON-PYR-4b-10	273.0	0.013	0.43	0.29	0.00	b.d.l.	1.21	6.1
NON-PYR-4b-11	280.0	0.012	0.43	0.26	0.01	b.d.l.	1.20	7.4
NON-PYR-4b-12	287.0	0.014	0.43	0.26	0.01	b.d.l.	0.00	6.8
NON-PYR-4b-13	294.0	0.013	0.43	0.24	0.01	b.d.l.	1.24	7.3
NON-PYR-4b-14	301.0	0.013	0.43	0.23	0.02	b.d.l.	0.62	7.3
NON-PYR-4b-15	308.0	0.002	0.48	0.25	0.01	b.d.l.	0.00	7.4
NON-PYR-4b-16	315.0	0.008	0.48	0.24	0.01	b.d.l.	0.00	7.0
NON-PYR-4b-17	321.0	0.012	0.48	0.22	0.01	b.d.l.	1.58	7.1
NON-PYR-4b-18	326.9	0.012	0.48	0.21	0.02	b.d.l.	1.37	7.8
NON-PYR-4b-19	331.0	0.006	0.48	0.24	0.01	b.d.l.	0.00	7.8
NON-PYR-4b-20	334.9	0.006	0.47	0.33	0.01	b.d.l.	2.37	7.3
NON-PYR-4b-21	352.0	0.010	0.47	0.34	0.01	b.d.l.	2.44	7.2
NON-PYR-4b-22	357.9	0.008	0.47	0.30	0.02	b.d.l.	0.00	7.4
NON-PYR-4b-23	364.0	0.010	0.48	0.15	0.01	b.d.l.	0.00	7.4
NON-PYR-4b-24	370.0	0.007	0.51	0.00	0.01	b.d.l.	0.00	7.7
NON-PYR-4b-25	375.9	0.010	0.51	0.07	0.01	b.d.l.	0.00	5.9
NON-PYR-4b-26	380.0	0.010	0.51	0.00	0.01	b.d.l.	2.66	7.1

Table C4. (continued).

Sample	Time	Flow rate	Nitrate (i)	Nitrate (o)	Nitrite (o)	Fe (o)	S (o)	pH (o)
	d	mL min^{-1}	mM	mM	mM	μM	μM	
NON-PYR-4c-1	0.0	0.008	0.53	0.56	0.00	849.19	1994.67	5.2
NON-PYR-4c-2	7.0	0.002	0.53	0.56	0.00	333.28	954.61	4.3
NON-PYR-4c-3	14.3	0.004	0.53	0.49	0.00	155.24	257.81	4.6
NON-PYR-4c-4	35.0	0.008	0.53	0.47	0.01	b.d.l.	67.11	6.1
NON-PYR-4c-5	42.1	0.012	0.53	0.50	0.01	b.d.l.	13.90	6.9
NON-PYR-4c-6	49.0	0.013	0.53	0.50	0.01	b.d.l.	7.68	6.8
NON-PYR-4c-7	56.0	0.013	0.42	0.38	0.02	b.d.l.	3.04	7.1
NON-PYR-4c-8	63.0	0.012	0.42	0.38	0.02	b.d.l.	1.67	7.0
NON-PYR-4c-9	68.1	0.010	0.41	0.38	0.02	b.d.l.	15.80	7.4
NON-PYR-4c-10	72.0	0.012	0.41	0.35	0.03	b.d.l.	5.51	7.0
NON-PYR-4c-11	77.3	0.013	0.42	0.33	0.05	b.d.l.	2.05	7.3
NON-PYR-4c-12	84.0	0.009	0.42	0.30	0.07	b.d.l.	3.48	7.1
NON-PYR-4c-13	91.0	0.012	0.48	0.34	0.09	b.d.l.	3.48	7.4
NON-PYR-4c-14	98.0	0.012	0.48	0.30	0.10	b.d.l.	2.16	7.3
NON-PYR-4c-15	105.4	0.010	0.48	0.26	0.13	b.d.l.	2.44	7.4
NON-PYR-4c-16	113.0	0.011	0.49	0.27	0.11	b.d.l.	4.14	7.7
NON-PYR-4c-17	120.0	0.013	0.49	0.30	0.09	b.d.l.	1.23	7.5
NON-PYR-4c-18	124.2	0.009	0.49	0.27	0.10	b.d.l.	1.38	7.1
NON-PYR-4c-19	135.2	0.012	0.49	0.16	0.14	b.d.l.	2.97	6.3
NON-PYR-4c-20	148.3	0.012	0.49	0.12	0.15	b.d.l.	1.97	6.3
NON-PYR-4c-21	160.0	0.010	0.49	0.09	0.14	b.d.l.	2.16	7.3
NON-PYR-4c-22	169.4	0.004	0.48	0.21	0.04	b.d.l.	19.76	7.0
NON-PYR-4c-23	190.0	0.004	n.d.	n.d.	n.d.	b.d.l.	20.84	7.1
NON-PYR-4c-24	196.0	0.012	0.49	0.35	0.02	b.d.l.	8.52	7.3
NON-PYR-4c-25	203.0	0.012	0.49	0.35	0.01	b.d.l.	2.73	7.0
NON-PYR-4c-26	208.9	0.012	0.49	0.36	0.02	b.d.l.	1.28	7.4
NON-PYR-4c-27	217.0	0.012	0.49	0.36	0.02	b.d.l.	1.69	7.3
NON-PYR-4c-28	224.0	0.012	0.48	0.32	0.03	b.d.l.	1.72	7.4
NON-PYR-4c-29	231.0	0.011	0.48	0.30	0.04	b.d.l.	0.00	7.7
NON-PYR-4c-30	238.0	0.012	0.43	0.26	0.04	b.d.l.	2.23	7.8
NON-PYR-4c-31	245.0	0.012	0.43	0.29	0.03	b.d.l.	2.61	7.5
NON-PYR-4c-32	252.0	0.012	0.43	0.32	0.01	b.d.l.	0.00	7.5
NON-PYR-4c-33	259.0	0.002	0.43	0.31	0.01	b.d.l.	0.00	7.6
NON-PYR-4c-34	266.0	0.013	0.41	0.29	0.02	b.d.l.	3.68	7.6
NON-PYR-4c-35	273.0	0.013	0.47	0.29	0.03	b.d.l.	1.11	7.5
NON-PYR-4c-36	280.0	0.007	0.47	0.26	0.05	b.d.l.	1.47	7.1
NON-PYR-4c-37	286.0	0.011	0.47	0.28	0.04	b.d.l.	1.96	7.3
NON-PYR-4c-38	292.0	0.011	0.47	0.28	0.04	b.d.l.	1.34	7.9
NON-PYR-4c-39	296.0	0.012	0.47	0.32	0.04	b.d.l.	0.00	7.7
NON-PYR-4c-40	300.0	0.012	0.51	0.35	0.03	b.d.l.	1.41	8.1
NON-PYR-4c-41	307.0	0.012	0.51	0.35	0.03	b.d.l.	1.20	7.9
NON-PYR-4c-42	317.0	0.012	0.51	0.35	0.03	1.07	4.60	7.8
NON-PYR-4c-43	322.9	0.012	0.51	0.29	0.03	b.d.l.	1.14	7.8
NON-PYR-4c-44	329.0	0.011	0.52	0.23	0.02	b.d.l.	0.00	7.5
NON-PYR-4c-45	335.0	0.008	0.51	0.17	0.02	b.d.l.	0.00	7.7
NON-PYR-4c-46	341.0	0.012	0.51	0.24	0.00	b.d.l.	0.00	5.7
NON-PYR-4c-47	345.0	0.012	0.51	0.31	0.00	b.d.l.	2.81	7.1

Table C4. (continued).

Sample	Time	Flow rate	Nitrate (i)	Nitrate (o)	Nitrite (o)	Fe (o)	S (o)	pH (o)
	d	mL min^{-1}	mM	mM	mM	µM	µM	
Initial stage of 65 d with 1.0 mM NO_3^- solution as input								
NON-PYR-4d-1	68.2	0.012	0.44	0.40	0.00	b.d.l.	0.00	6.9
NON-PYR-4d-2	76.0	0.012	0.47	0.41	0.00	b.d.l.	0.66	7.3
NON-PYR-4d-3	82.9	0.012	0.47	0.42	0.00	b.d.l.	1.41	7.5
NON-PYR-4d-4	89.9	0.012	0.60	0.47	0.00	b.d.l.	0.29	7.4
NON-PYR-4d-5	96.8	0.012	0.60	0.50	0.00	b.d.l.	0.22	7.4
NON-PYR-4d-6	103.9	0.010	0.59	0.50	0.00	b.d.l.	0.41	7.5
NON-PYR-4d-7	110.9	0.010	0.59	0.47	0.01	b.d.l.	1.35	7.5
NON-PYR-4d-8	118.2	0.011	0.43	0.35	0.01	b.d.l.	1.48	7.2
NON-PYR-4d-9	124.9	0.011	0.43	0.34	0.01	b.d.l.	0.60	7.2
NON-PYR-4d-10	131.9	0.009	0.43	0.31	0.01	b.d.l.	0.00	7.3
NON-PYR-4d-11	138.8	0.009	0.40	0.29	0.00	b.d.l.	0.60	7.5
NON-PYR-4d-12	146.0	0.011	0.44	0.33	0.01	b.d.l.	0.10	7.2
NON-PYR-4d-13	152.8	0.011	0.44	0.33	0.00	b.d.l.	1.60	6.7
NON-PYR-4d-14	159.8	0.011	0.41	0.30	0.01	1.12	2.01	7.4
NON-PYR-4d-15	166.9	0.011	0.41	0.34	0.01	b.d.l.	1.33	7.2
NON-PYR-4d-16	172.0	0.005	0.41	0.35	0.01	b.d.l.	3.43	7.9
NON-PYR-4d-17	175.9	0.007	0.42	0.33	0.01	b.d.l.	7.22	7.4
NON-PYR-4d-18	187.9	0.011	0.42	0.28	0.01	b.d.l.	3.96	7.1
NON-PYR-4d-19	194.9	0.012	0.50	0.33	0.01	b.d.l.	2.79	7.8
NON-PYR-4d-20	201.9	0.012	0.50	0.31	0.01	b.d.l.	1.64	7.8
NON-PYR-4d-21	209.2	0.005	0.50	0.26	0.01	b.d.l.	2.97	7.6
NON-PYR-4d-22	216.8	0.009	0.50	0.28	0.02	b.d.l.	4.47	8.2
NON-PYR-4d-23	223.9	0.011	0.50	0.27	0.01	b.d.l.	2.32	8.2
NON-PYR-4d-24	228.1	0.007	0.50	0.21	0.02	b.d.l.	1.50	7.2
NON-PYR-4d-25	239.1	0.008	0.50	0.09	0.02	b.d.l.	2.62	7.6

Table C4. (continued).

Sample	Time	Flow rate	Nitrate (i)	Nitrate (o)	Nitrite (o)	Fe (o)	S (o)	pH (o)
	d	mL min^{-1}	mM	mM	mM	μM	μM	
NON-PYR-4e-1	0.0	0.011	0.53	0.73	0.00	178.76	1630.82	4.1
NON-PYR-4e-2	7.3	0.011	0.53	0.23	0.02	b.d.l.	145.45	7.0
NON-PYR-4e-3	13.9	0.011	0.53	0.24	0.11	b.d.l.	23.73	7.6
NON-PYR-4e-4	20.9	0.002	0.53	0.30	0.00	b.d.l.	985.16	4.9
NON-PYR-4e-5	27.9	0.009	0.53	0.41	0.00	b.d.l.	209.35	6.5
NON-PYR-4e-6	35.0	0.010	0.53	0.36	0.03	b.d.l.	13.16	7.7
NON-PYR-4e-7	41.9	0.011	0.53	0.44	0.03	b.d.l.	52.64	7.4
NON-PYR-4e-8	48.9	0.009	0.42	0.35	0.04	b.d.l.	7.98	7.3
NON-PYR-4e-9	55.9	0.013	0.42	0.39	0.02	b.d.l.	57.04	6.9
NON-PYR-4e-10	61.0	0.008	0.41	0.36	0.00	60.16	301.72	4.6
NON-PYR-4e-11	64.9	0.012	0.41	0.34	0.01	b.d.l.	35.61	7.0
NON-PYR-4e-12	70.2	0.012	0.42	0.32	0.03	b.d.l.	15.86	7.6
NON-PYR-4e-13	77.0	0.011	0.42	0.34	0.02	b.d.l.	9.58	7.3
NON-PYR-4e-14	83.9	0.011	0.48	0.37	0.03	b.d.l.	22.91	7.5
NON-PYR-4e-15	90.9	0.012	0.48	0.39	0.02	b.d.l.	4.04	7.7
NON-PYR-4e-16	98.3	0.012	0.48	0.40	0.02	b.d.l.	2.95	7.5
NON-PYR-4e-17	105.9	0.013	0.49	0.35	0.03	b.d.l.	7.28	7.9
NON-PYR-4e-18	112.9	0.014	0.49	0.35	0.05	b.d.l.	2.54	7.7
NON-PYR-4e-19	117.1	0.013	0.49	0.29	0.04	b.d.l.	2.20	7.3
NON-PYR-4e-20	128.1	0.013	0.49	0.17	0.05	b.d.l.	3.13	7.5
NON-PYR-4e-21	141.2	0.013	0.49	0.26	0.05	b.d.l.	1.88	7.2
NON-PYR-4e-22	152.9	0.014	0.49	0.21	0.05	b.d.l.	1.94	7.4
NON-PYR-4e-23	162.3	0.010	0.48	0.29	0.05	b.d.l.	2.13	7.2
NON-PYR-4e-24	175.2	0.013	0.48	0.24	0.07	b.d.l.	2.43	7.4
NON-PYR-4e-25	182.9	0.004	0.48	0.27	0.00	5.12	625.90	6.7
NON-PYR-4e-26	188.9	0.010	0.49	0.33	0.02	0.79	26.87	7.2
NON-PYR-4e-27	197.9	0.014	0.49	0.28	0.03	b.d.l.	4.80	7.9
NON-PYR-4e-28	209.9	0.013	0.49	0.34	0.03	b.d.l.	3.16	7.6
NON-PYR-4e-29	216.9	0.013	0.48	0.32	0.05	b.d.l.	2.13	7.4
NON-PYR-4e-30	223.9	0.013	0.48	0.33	0.04	b.d.l.	2.15	7.6
NON-PYR-4e-31	230.9	0.013	0.43	0.20	0.07	b.d.l.	0.51	8.9
NON-PYR-4e-32	237.9	0.013	0.43	0.27	0.05	b.d.l.	0.30	7.5
NON-PYR-4e-33	244.9	0.015	0.43	0.22	0.08	b.d.l.	0.36	7.4
NON-PYR-4e-34	251.9	0.013	0.43	0.19	0.09	b.d.l.	0.37	8.8
NON-PYR-4e-35	258.9	0.013	0.41	0.19	0.08	b.d.l.	0.27	8.6
NON-PYR-4e-36	266.0	0.012	0.47	n.d.	n.d.	b.d.l.	0.26	8.2
NON-PYR-4e-37	273.5	0.012	0.47	n.d.	n.d.	b.d.l.	0.19	7.3
NON-PYR-4e-38	278.9	0.007	0.47	n.d.	n.d.	b.d.l.	0.36	7.7
NON-PYR-4e-39	284.9	0.011	0.47	0.14	0.10	b.d.l.	0.32	8.3
NON-PYR-4e-40	288.9	0.014	0.47	0.29	0.06	b.d.l.	0.09	7.9
NON-PYR-4e-41	292.9	0.015	0.51	0.30	0.07	b.d.l.	0.10	7.8
NON-PYR-4e-42	299.9	0.002	0.51	0.10	0.06	b.d.l.	26.60	7.9
NON-PYR-4e-43	309.9	0.010	0.51	0.24	0.04	b.d.l.	7.04	7.7
NON-PYR-4e-44	315.8	0.010	0.51	0.05	0.06	b.d.l.	4.51	8.7
NON-PYR-4e-45	321.9	0.010	0.52	0.00	0.02	b.d.l.	1.92	7.1
NON-PYR-4e-46	327.9	0.006	0.51	0.03	0.02	b.d.l.	1.83	8.3
NON-PYR-4e-47	333.9	0.010	0.51	0.01	0.01	b.d.l.	0.53	6.3
NON-PYR-4e-48	337.9	0.010	0.51	0.02	0.01	b.d.l.	0.71	7.7

Table C4. (continued).

Sample	Time	Flow rate	Nitrate (i)	Nitrate (o)	Nitrite (o)	Fe (o)	S (o)	pH (o)
	d	mL min^{-1}	mM	mM	mM	µM	µM	
NON-PYR-5a-1	0.0	0.007	0.95	0.93	0.00	86.94	1055.53	5.4
NON-PYR-5a-2	7.1	0.011	0.95	0.93	0.00	b.d.l.	154.45	5.2
NON-PYR-5a-3	14.0	0.011	0.95	0.86	0.02	b.d.l.	24.27	6.7
NON-PYR-5a-4	21.0	0.011	0.95	0.85	0.04	b.d.l.	9.55	7.2
NON-PYR-5a-5	27.9	0.012	0.95	0.87	0.03	b.d.l.	4.90	7.2
NON-PYR-5a-6	35.0	0.011	1.00	0.88	0.04	b.d.l.	3.40	7.2
NON-PYR-5a-7	42.0	0.012	1.00	0.87	0.04	b.d.l.	3.35	7.4
NON-PYR-5a-8	49.3	0.011	0.79	0.78	0.03	b.d.l.	3.99	7.1
NON-PYR-5a-9	56.0	0.011	0.79	0.78	0.01	b.d.l.	0.69	7.3
NON-PYR-5a-10	63.0	0.012	0.79	0.76	0.01	b.d.l.	0.59	7.0
NON-PYR-5a-11	70.0	0.010	0.79	0.75	0.02	b.d.l.	0.00	7.3
NON-PYR-5a-12	77.1	0.012	0.79	0.74	0.03	b.d.l.	1.98	7.4
NON-PYR-5a-13	84.0	0.012	0.79	0.73	0.04	b.d.l.	5.64	6.8
NON-PYR-5a-14	90.9	0.011	0.76	0.67	0.05	b.d.l.	0.59	7.3
NON-PYR-5a-15	98.0	0.011	0.76	0.68	0.06	1.09	12.78	7.2
NON-PYR-5a-16	103.1	0.010	0.82	0.70	0.06	0.44	13.36	7.5
NON-PYR-5a-17	107.0	0.012	0.82	0.70	0.08	b.d.l.	6.48	7.0
NON-PYR-5a-18	112.3	0.012	0.83	0.71	0.08	b.d.l.	4.04	7.2
NON-PYR-5a-19	119.0	0.012	0.83	0.69	0.09	b.d.l.	4.07	7.1
NON-PYR-5a-20	126.0	0.012	0.83	0.67	0.10	b.d.l.	4.29	7.5
NON-PYR-5a-21	133.0	0.012	0.98	0.78	0.11	b.d.l.	3.70	7.4
NON-PYR-5a-22	140.3	0.012	0.98	0.76	0.13	b.d.l.	3.95	7.5
NON-PYR-5a-23	147.9	0.012	0.98	0.73	0.14	b.d.l.	5.21	7.9
NON-PYR-5a-24	155.0	0.012	0.99	0.72	0.14	b.d.l.	2.98	8.0
NON-PYR-5a-25	159.2	0.012	0.99	0.76	0.12	b.d.l.	2.91	7.2
NON-PYR-5a-26	170.2	0.012	0.99	0.72	0.12	b.d.l.	4.33	6.7
NON-PYR-5a-27	183.2	0.012	0.99	0.70	0.13	b.d.l.	4.07	6.6
NON-PYR-5a-28	195.0	0.012	0.99	0.51	0.22	b.d.l.	6.13	7.1
NON-PYR-5a-29	204.4	0.012	0.96	0.60	0.15	b.d.l.	4.47	7.0
NON-PYR-5a-30	217.2	0.011	0.96	0.74	0.06	b.d.l.	2.12	7.0
NON-PYR-5a-31	225.0	0.011	0.96	0.78	0.05	b.d.l.	2.03	7.2
NON-PYR-5a-32	231.0	0.011	0.96	0.76	0.04	b.d.l.	1.82	7.2
NON-PYR-5a-33	237.9	0.011	0.96	0.78	0.04	b.d.l.	1.16	7.3
NON-PYR-5a-34	243.9	0.011	0.96	0.79	0.04	b.d.l.	2.04	7.5
NON-PYR-5a-35	251.9	0.006	0.96	0.78	0.03	b.d.l.	0.46	7.3
NON-PYR-5a-36	258.9	0.012	0.93	0.79	0.04	b.d.l.	0.53	7.5
NON-PYR-5a-37	266.0	0.012	0.86	0.66	0.04	b.d.l.	0.33	6.1
NON-PYR-5a-38	273.0	0.012	0.86	0.64	0.04	b.d.l.	0.16	7.9
NON-PYR-5a-39	280.0	0.012	0.86	0.63	0.06	b.d.l.	0.00	7.7
NON-PYR-5a-40	287.0	0.013	0.86	0.65	0.05	b.d.l.	0.00	7.1
NON-PYR-5a-41	294.0	0.013	0.86	0.62	0.06	b.d.l.	0.00	7.4
NON-PYR-5a-42	301.0	0.013	0.86	0.63	0.07	b.d.l.	0.00	7.3
NON-PYR-5a-43	308.0	0.012	1.00	0.76	0.06	b.d.l.	0.48	7.6
NON-PYR-5a-44	315.0	0.013	0.95	0.79	0.05	b.d.l.	0.50	6.9
NON-PYR-5a-45	321.0	0.013	0.95	0.80	0.04	b.d.l.	0.52	7.1
NON-PYR-5a-46	326.9	0.013	0.95	0.80	0.04	b.d.l.	0.59	7.6
NON-PYR-5a-47	331.0	0.013	0.95	0.81	0.04	b.d.l.	0.57	7.6
NON-PYR-5a-48	334.9	0.013	0.95	0.81	0.03	b.d.l.	0.00	7.8
NON-PYR-5a-49	342.0	0.014	0.95	0.80	0.03	b.d.l.	0.00	7.7
NON-PYR-5a-50	352.0	0.014	0.95	0.80	0.02	b.d.l.	0.45	8.0
NON-PYR-5a-51	357.9	0.013	0.95	0.72	0.03	b.d.l.	0.86	7.6
NON-PYR-5a-52	364.0	0.014	0.98	0.63	0.09	b.d.l.	2.30	6.0
NON-PYR-5a-53	370.0	0.009	1.09	0.82	0.05	b.d.l.	0.00	6.4
NON-PYR-5a-54	375.9	0.014	1.09	0.91	0.01	b.d.l.	0.00	4.5
NON-PYR-5a-55	380.0	0.013	1.09	0.95	0.00	b.d.l.	2.92	5.9

Table C4. (continued).

Sample	Time	Flow rate	Nitrate (i)	Nitrate (o)	Nitrite (o)	Fe (o)	S (o)	pH (o)
	d	mL min^{-1}	mM	mM	mM	μM	μM	
NON-PYR-5b-1	0.0	0.007	0.95	0.95	0.00	88.84	1014.00	5.8
NON-PYR-5b-2	7.1	0.011	0.95	0.94	0.00	2.86	226.92	5.9
NON-PYR-5b-3	14.0	0.011	0.95	0.85	0.02	b.d.l.	27.51	7.2
NON-PYR-5b-4	21.0	0.012	0.95	0.84	0.03	b.d.l.	8.23	7.3
NON-PYR-5b-5	27.9	0.012	0.95	0.85	0.03	b.d.l.	4.68	7.2
NON-PYR-5b-6	35.0	0.012	1.00	0.86	0.04	b.d.l.	3.39	7.3
NON-PYR-5b-7	42.0	0.011	1.00	0.86	0.05	b.d.l.	3.08	7.3
NON-PYR-5b-8	49.3	0.011	0.79	0.77	0.03	b.d.l.	2.13	7.0
NON-PYR-5b-9	56.0	0.013	0.79	0.78	0.01	b.d.l.	1.67	7.0
NON-PYR-5b-10	63.0	0.013	0.79	0.77	0.01	b.d.l.	0.00	6.8
NON-PYR-5b-11	70.0	0.010	0.79	0.77	0.01	b.d.l.	0.00	7.3
NON-PYR-5b-12	77.1	0.012	0.79	0.76	0.02	b.d.l.	0.00	7.3
NON-PYR-5b-13	84.0	0.013	0.79	0.73	0.04	b.d.l.	1.46	7.0
NON-PYR-5b-14	90.9	0.012	0.76	0.71	0.03	b.d.l.	0.12	7.4
NON-PYR-5b-15	98.0	0.018	0.76	0.72	0.03	1.97	5.65	7.1
NON-PYR-5b-16	103.1	0.010	0.82	0.73	0.04	0.82	16.46	7.4
NON-PYR-5b-17	107.0	0.012	0.82	0.74	0.04	b.d.l.	6.79	6.8
NON-PYR-5b-18	112.3	0.012	0.83	0.76	0.03	b.d.l.	4.03	7.1
NON-PYR-5b-19	119.0	0.012	0.83	0.75	0.03	b.d.l.	3.80	7.1
NON-PYR-5b-20	126.2	0.013	0.83	0.74	0.03	b.d.l.	3.08	7.4
NON-PYR-5b-21	133.0	0.012	1.04	0.93	0.03	b.d.l.	3.46	7.4
NON-PYR-5b-22	140.3	0.012	1.04	0.90	0.05	b.d.l.	3.93	7.4
NON-PYR-5b-23	147.9	0.013	1.04	0.85	0.06	b.d.l.	3.75	7.7
NON-PYR-5b-24	155.0	0.014	1.06	0.84	0.08	b.d.l.	3.26	8.0
NON-PYR-5b-25	159.2	0.014	1.06	0.87	0.05	b.d.l.	3.14	7.5
NON-PYR-5b-26	170.2	0.014	1.06	0.83	0.05	b.d.l.	3.08	6.6
NON-PYR-5b-27	183.2	0.014	1.06	0.83	0.07	b.d.l.	2.95	6.6
NON-PYR-5b-28	195.0	0.015	1.06	0.63	0.15	b.d.l.	5.54	6.9
NON-PYR-5b-29	204.4	0.014	1.02	0.76	0.07	b.d.l.	3.92	7.0
NON-PYR-5b-30	217.2	0.015	1.02	0.84	0.02	b.d.l.	1.90	7.0
NON-PYR-5b-31	225.0	0.014	1.02	0.86	0.02	b.d.l.	0.82	7.2
NON-PYR-5b-32	231.0	0.013	1.02	0.86	0.02	b.d.l.	2.29	7.2
NON-PYR-5b-33	237.9	0.015	1.02	0.86	0.02	b.d.l.	5.11	7.2
NON-PYR-5b-34	243.9	0.015	1.02	0.87	0.01	b.d.l.	1.02	7.4
NON-PYR-5b-35	251.9	0.008	1.02	0.85	0.02	b.d.l.	0.51	7.5
NON-PYR-5b-36	258.9	0.013	n.d.	n.d.	n.d.	b.d.l.	0.00	7.4
NON-PYR-5b-37	266.0	0.013	0.86	0.68	0.03	b.d.l.	0.61	7.7
NON-PYR-5b-38	273.0	0.013	0.86	0.66	0.04	b.d.l.	0.63	6.8
NON-PYR-5b-39	280.0	0.011	0.86	0.61	0.06	b.d.l.	0.00	7.8
NON-PYR-5b-40	287.0	0.010	0.86	0.60	0.06	b.d.l.	0.00	8.0
NON-PYR-5b-41	294.0	0.011	0.86	0.58	0.06	b.d.l.	0.75	7.8
NON-PYR-5b-42	301.0	0.009	0.86	0.58	0.07	b.d.l.	0.38	7.8
NON-PYR-5b-43	308.0	0.009	1.00	0.65	0.08	b.d.l.	0.35	7.8
NON-PYR-5b-44	315.0	0.011	0.95	0.74	0.07	b.d.l.	0.69	7.1
NON-PYR-5b-45	321.0	0.008	0.95	0.74	0.06	b.d.l.	0.00	7.2
NON-PYR-5b-46	326.9	0.012	0.95	0.75	0.07	b.d.l.	0.86	7.7
NON-PYR-5b-47	331.0	0.011	0.95	0.78	0.06	b.d.l.	0.87	7.7
NON-PYR-5b-48	334.9	0.010	0.95	0.77	0.05	b.d.l.	0.65	6.9
NON-PYR-5b-49	342.0	0.011	0.95	0.76	0.06	b.d.l.	0.00	7.8
NON-PYR-5b-50	352.0	0.011	0.95	0.76	0.05	b.d.l.	1.19	7.7
NON-PYR-5b-51	357.9	0.011	0.95	0.66	0.07	b.d.l.	0.85	7.7
NON-PYR-5b-52	364.0	0.011	0.98	0.53	0.13	b.d.l.	2.02	6.5
NON-PYR-5b-53	370.0	0.004	1.09	0.64	0.11	b.d.l.	0.00	6.3
NON-PYR-5b-54	375.9	0.010	1.09	0.82	0.04	0.47	5.27	4.5
NON-PYR-5b-55	380.0	0.010	1.09	0.94	0.00	b.d.l.	3.32	5.5

Table C4. (continued).

Sample	Time	Flow rate	Nitrate (i)	Nitrate (o)	Nitrite (o)	Fe (o)	S (o)	pH (o)
	d	mL min^{-1}	mM	mM	mM	µM	µM	
NON-PYR-6a-1	0.0	0.008	1.29	1.65	0.01	362.40	1277.99	4.5
NON-PYR-6a-2	7.0	0.008	1.29	1.36	0.01	101.93	550.74	4.7
NON-PYR-6a-3	14.0	0.003	1.29	1.28	0.01	10.32	250.55	4.4
NON-PYR-6a-4	21.0	0.002	1.29	1.05	0.05	b.d.l.	34.46	6.6
NON-PYR-6a-5	35.0	0.009	1.29	1.06	0.05	b.d.l.	22.11	7.1
NON-PYR-6a-6	42.1	0.009	1.29	1.04	0.13	0.75	15.04	6.6
NON-PYR-6a-7	49.0	0.009	1.29	1.02	0.14	b.d.l.	11.15	6.8
NON-PYR-6a-8	56.0	0.009	1.31	1.07	0.11	b.d.l.	10.36	6.8
NON-PYR-6a-9	63.1	0.009	1.31	1.13	0.09	b.d.l.	10.24	7.0
NON-PYR-6a-10	70.0	0.009	1.31	1.19	0.12	b.d.l.	6.82	7.0
NON-PYR-6a-11	77.0	0.009	1.31	1.17	0.14	b.d.l.	7.32	7.3
NON-PYR-6a-12	84.3	0.009	1.31	1.04	0.20	b.d.l.	5.64	7.4
NON-PYR-6a-13	91.0	0.010	1.31	0.93	0.23	b.d.l.	4.37	7.0
NON-PYR-6a-14	98.0	0.010	1.31	0.96	0.18	b.d.l.	4.16	7.1
NON-PYR-6a-15	105.3	0.010	1.38	1.02	0.14	b.d.l.	4.16	7.7
NON-PYR-6a-16	112.3	0.008	1.38	1.07	0.11	b.d.l.	3.90	7.6
NON-PYR-6a-17	119.3	0.010	1.38	1.16	0.09	b.d.l.	3.31	5.2
NON-PYR-6a-18	125.3	0.010	1.29	1.15	0.13	0.69	4.48	7.5
NON-PYR-6a-19	132.3	0.010	1.29	1.11	0.18	b.d.l.	5.54	7.7
NON-PYR-6a-20	139.3	0.010	1.61	1.24	0.12	b.d.l.	4.83	7.7
NON-PYR-6a-21	146.1	0.003	1.61	1.30	0.04	b.d.l.	8.31	7.3
NON-PYR-6a-22	153.1	0.009	1.61	1.56	0.00	b.d.l.	8.99	7.7
NON-PYR-6a-23	162.0	0.010	1.61	1.74	0.00	b.d.l.	4.37	7.2
NON-PYR-6a-24	169.3	0.010	1.61	1.59	0.00	b.d.l.	3.35	7.4
NON-PYR-6a-25	177.1	0.011	1.33	1.31	0.01	b.d.l.	2.67	7.7
NON-PYR-6a-26	183.3	0.011	1.33	1.29	0.00	b.d.l.	1.93	7.1
NON-PYR-6a-27	189.0	0.011	1.44	1.36	0.01	b.d.l.	2.65	7.7
NON-PYR-6a-28	196.0	0.010	1.44	1.41	0.00	b.d.l.	1.84	7.0
NON-PYR-6a-29	203.3	0.008	1.44	n.d.	n.d.	b.d.l.	1.48	7.6

Table C4. (continued).

Sample	Time	Flow rate	Nitrate (i)	Nitrate (o)	Nitrite (o)	Fe (o)	S (o)	pH (o)
	d	mL min^{-1}	mM	mM	mM	μM	μM	
NON-PYR-6b-1	0.0	0.003	1.30	n.d.	n.d.	68.68	346.29	4.3
NON-PYR-6b-2	14.0	0.002	1.30	1.21	0.00	16.99	136.37	4.4
NON-PYR-6b-3	35.1	0.005	1.30	1.31	0.00	81.88	142.74	4.2
NON-PYR-6b-4	42.0	0.009	1.30	1.26	0.00	33.39	66.08	4.2
NON-PYR-6b-5	49.0	0.009	1.30	1.26	0.00	4.08	27.54	4.4
NON-PYR-6b-6	56.1	0.009	1.30	1.24	0.00	1.31	16.78	4.7
NON-PYR-6b-7	63.0	0.009	1.30	1.33	0.01	b.d.l.	12.03	4.1
NON-PYR-6b-8	70.0	0.007	1.30	1.29	0.05	b.d.l.	10.22	6.5
NON-PYR-6b-9	77.3	0.009	1.30	1.11	0.14	b.d.l.	7.76	7.0
NON-PYR-6b-10	84.0	0.011	1.30	0.98	0.18	b.d.l.	7.34	6.8
NON-PYR-6b-11	91.0	0.009	1.30	1.07	0.11	b.d.l.	5.79	7.0
NON-PYR-6b-12	98.3	0.009	1.13	1.08	0.08	b.d.l.	4.52	7.7
NON-PYR-6b-13	105.3	0.007	1.13	1.10	0.06	b.d.l.	4.78	7.7
NON-PYR-6b-14	112.3	0.009	1.13	1.23	0.00	b.d.l.	3.71	5.2
NON-PYR-6b-15	118.3	0.009	1.79	1.69	0.02	b.d.l.	2.96	7.4
NON-PYR-6b-16	125.3	0.009	1.79	1.67	0.00	b.d.l.	3.13	7.1
NON-PYR-6b-17	132.3	0.009	1.79	1.67	0.00	b.d.l.	2.49	6.9
NON-PYR-6b-18	139.1	0.009	1.79	1.70	0.00	b.d.l.	3.55	5.8
NON-PYR-6b-19	146.1	0.008	1.79	1.68	0.00	b.d.l.	2.98	6.9
NON-PYR-6b-20	155.0	0.009	1.79	1.67	0.00	b.d.l.	2.47	7.0
NON-PYR-6b-21	162.3	0.009	1.79	1.71	0.00	b.d.l.	3.28	7.8
NON-PYR-6b-22	170.1	0.009	1.44	1.41	0.00	b.d.l.	2.02	7.4
NON-PYR-6b-23	176.3	0.009	1.44	1.42	0.00	b.d.l.	3.94	6.8
NON-PYR-6b-24	182.0	0.009	1.45	1.39	0.00	b.d.l.	2.82	7.6
NON-PYR-6b-25	189.0	0.009	1.45	1.41	0.00	b.d.l.	1.90	6.8
NON-PYR-6b-26	196.3	0.009	1.45	1.40	0.00	b.d.l.	2.84	7.3

Table C4. (continued).

Sample	Time	Flow rate	Nitrate (i)	Nitrate (o)	Nitrite (o)	Fe (o)	S (o)	pH (o)
	d	mL min^{-1}	mM	mM	mM	μM	μM	
NON-PYR-7-1	0.0	0.001	1.72	n.d.	n.d.	902.06	2532.28	4.3
NON-PYR-7-2	7.0	0.009	1.72	1.88	0.01	280.18	1152.62	4.5
NON-PYR-7-3	14.0	0.010	1.72	1.69	0.01	22.69	233.52	4.5
NON-PYR-7-4	21.0	0.010	1.72	1.68	0.02	2.04	57.54	5.3
NON-PYR-7-5	28.1	0.010	1.73	1.69	0.02	0.56	20.62	5.6
NON-PYR-7-6	35.0	0.010	1.73	1.69	0.02	b.d.l.	11.12	6.0
NON-PYR-7-7	42.1	0.010	1.73	1.65	0.01	b.d.l.	7.90	6.0
NON-PYR-7-8	49.0	0.010	1.73	1.63	0.02	b.d.l.	8.50	6.0
NON-PYR-7-9	56.0	0.009	1.73	1.64	0.01	b.d.l.	9.62	6.3
NON-PYR-7-10	63.1	0.010	1.73	1.65	0.01	b.d.l.	9.96	6.3
NON-PYR-7-11	70.0	0.010	1.73	1.79	0.00	b.d.l.	8.19	6.2
NON-PYR-7-12	77.0	0.010	1.73	1.80	0.00	b.d.l.	6.41	7.1
NON-PYR-7-13	84.3	0.010	1.73	1.62	n.d.	b.d.l.	6.23	7.3
NON-PYR-7-14	91.0	0.010	1.73	1.42	0.09	b.d.l.	5.50	7.4
NON-PYR-7-15	98.0	0.010	1.73	1.43	0.08	b.d.l.	5.79	6.9
NON-PYR-7-16	105.3	0.010	1.56	1.47	0.08	b.d.l.	6.46	7.5
NON-PYR-7-17	112.3	0.008	1.56	1.52	0.05	b.d.l.	7.23	7.6
NON-PYR-7-18	119.3	0.010	1.56	1.61	0.04	b.d.l.	5.33	5.2
NON-PYR-7-19	125.3	0.010	1.80	1.63	0.02	b.d.l.	6.08	7.2
NON-PYR-7-20	132.3	0.010	1.91	1.83	0.03	b.d.l.	6.05	7.1
NON-PYR-7-21	139.3	0.010	1.91	1.85	0.04	b.d.l.	5.34	7.1
NON-PYR-7-22	146.1	0.010	1.91	1.81	0.04	b.d.l.	5.46	6.9
NON-PYR-7-23	153.1	0.009	1.91	1.82	0.05	b.d.l.	4.73	7.0
NON-PYR-7-24	162.0	0.010	1.91	1.83	0.04	b.d.l.	4.28	7.1
NON-PYR-7-25	169.3	0.010	1.91	1.84	0.02	b.d.l.	4.31	7.3
NON-PYR-7-26	177.1	0.010	1.91	1.84	0.02	b.d.l.	3.29	7.5
NON-PYR-7-27	183.3	0.010	1.93	1.82	0.03	b.d.l.	3.74	6.9
NON-PYR-7-28	189.0	0.010	1.93	1.85	0.02	b.d.l.	3.84	7.3
NON-PYR-7-29	196.0	0.010	1.93	1.90	0.00	b.d.l.	2.71	6.8
NON-PYR-7-30	203.3	0.010	1.93	1.93	0.01	b.d.l.	3.20	7.2

Appendix D:

Experimental data from the batch and flow-through experiments of chapter 4

Table D1. Experimental data from the blank and control batch experiments presented in chapter 4 of this thesis (n.d.: not determined; b.d.l.: below detection limit).

Time	NO_3^-	NO_2^-	SO_4^{2-}	pH	Alkalinity	Fe	Mg	Ca	Na	P	K
d		mM			meq L-1				mM		
Blank experiment (OS-13)											
0	2.18	0.00	1.30	6.84	n.d.	b.d.l.	1.34	3.39	0.92	0.02	1.11
5	2.11	0.04	6.42	6.01	n.d.	1.34	1.49	5.43	1.02	0.01	1.34
15	2.10	0.03	6.63	6.21	n.d.	0.89	1.56	8.15	0.86	0.02	1.11
29	2.07	0.02	6.40	6.57	n.d.	0.29	1.52	8.66	0.57	0.05	1.13
46	2.07	0.06	6.12	6.65	n.d.	b.d.l.	1.47	8.59	0.93	0.01	1.10
70	1.96	0.06	6.29	6.65	n.d.	b.d.l.	1.58	9.25	0.49	0.06	1.11
85	1.93	0.05	6.17	6.81	n.d.	b.d.l.	1.60	8.83	0.97	0.02	1.12
104	1.97	0.03	6.47	6.87	n.d.	b.d.l.	1.72	9.16	0.96	0.07	1.25
Pyrite-free experiments (OS-1 and OS-2)											
0	1.75	0.02 ± 0.00	1.37	6.84	7.00	b.d.l.	6.84	4.15	1.09	0.03	1.11
4	1.81 ± 0.03	0.02 ± 0.00	1.42 ± 0.01	6.75 ± 0.03	8.10 ± 0.85	b.d.l.	1.58 ± 0.16	4.42 ± 0.22	1.33 ± 0.18	0.06 ± 0.00	1.12 ± 0.02
14	1.82 ± 0.01	0.00 ± 0.00	1.45 ± 0.06	6.86 ± 0.01	8.70 ± 0.42	b.d.l.	1.47 ± 0.01	4.39 ± 0.01	1.02 ± 0.05	0.07 ± 0.00	1.11 ± 0.01
28	1.75 ± 0.03	0.00 ± 0.00	1.47 ± 0.05	6.79 ± 0.03	8.10 ± 0.14	b.d.l.	1.52 ± 0.03	4.49 ± 0.09	1.15 ± 0.03	0.08 ± 0.02	1.13 ± 0.00
35	1.68 ± 0.01	0.01 ± 0.00	1.47 ± 0.00	7.21 ± 0.02	8.30 ± 0.42	b.d.l.	1.50 ± 0.00	4.40 ± 0.00	1.27 ± 0.19	0.04 ± 0.01	1.10 ± 0.01
49	1.78 ± 0.17	0.00 ± 0.00	1.47 ± 0.01	6.81 ± 0.02	8.00 ± 0.71	b.d.l.	1.53 ± 0.03	4.22 ± 0.22	1.03 ± 0.15	0.04 ± 0.02	1.12 ± 0.04
79	1.67 ± 001	0.02 ± 0.00	1.50 ± 0.02	6.93 ± 0.05	6.90 ± 0.14	b.d.l.	1.48 ± 0.01	4.05 ± 0.01	1.23 ± 0.11	0.03 ± 0.01	1.09 ± 0.01
94	1.64 ± 0.02	0.01 ± 0.00	1.49 ± 0.02	6.85 ± 0.01	7.85 ± 0.49	b.d.l.	1.51 ± 0.02	4.23 ± 0.03	1.09 ± 0.10	0.02 ± 0.02	1.07 ± 0.01
Pyrite-free experiments, autoclaved material (OS-11 and OS-12)											
0	1.75	0.02 ± 0.00	1.37	6.84	7.00	b.d.l.	6.84	4.15	1.09	0.03	1.11
4	1.83 ± 0.02	0.00 ± 0.00	1.49 ± 0.11	6.62 ± 0.10	6.10 ± 1.41	b.d.l.	1.45 ± 0.05	3.57 ± 0.60	1.10 ± 0.31	0.02 ± 0.02	1.19 ± 0.07
14	1.82 ± 0.08	0.01 ± 0.01	1.49 ± 0.05	6.79 ± 0.07	7.15 ± 1.48	b.d.l.	1.50 ± 0.06	4.22 ± 0.60	1.00 ± 0.04	0.05 ± 0.00	1.19 ± 0.06
28	1.84 ± 0.04	0.00 ± 0.00	1.51 ± 0.11	6.77 ± 0.08	7.75 ± 1.06	b.d.l.	1.53 ± 0.06	4.37 ± 0.49	1.15 ± 0.15	0.03 ± 0.01	1.20 ± 0.06
35	1.97 ± 0.10	0.00 ± 0.00	n.d.	7.12 ± 0.01	7.00 ± 0.00	n.d.	1.52 ± 0.00	4.60 ± 0.00	n.d.	n.d.	n.d.
49	1.86 ± 0.03	0.00 ± 0.00	1.55 ± 0.12	6.98 ± 0.12	7.95 ± 1.20	b.d.l.	1.54 ± 0.09	4.35 ± 0.55	1.21 ± 0.01	0.02 ± 0.01	1.19 ± 0.06
79	1.68 ± 0.09	0.01 ± 0.01	1.50 ± 0.13	7.05 ± 0.05	5.65 ± 2.47	b.d.l.	1.51 ± 0.06	3.89 ± 0.44	1.17 ± 0.22	0.03 ± 0.00	1.17 ± 0.06
94	1.65 ± 0.10	0.01 ± 0.01	1.51 ± 0.08	6.80 ± 0.03	8.75 ± 0.35	b.d.l.	1.53 ± 0.05	4.39 ± 0.22	0.86 ± 0.11	0.04 ± 0.02	1.19 ± 0.04

Table D2. Experimental data from the pyrite-amended batch experiments presented in chapter 4 of this thesis (n.d.: not determined; b.d.l.: below detection limit). Isotopic data are from the biostimulated experiment OS-4 and the biostimulated/bioaugmented experiment OS-10. Standard deviation of the replicate isotopic analyses is shown.

Time	NO_3^-	NO_2^-	SO_4^{2-}	pH	Alkalinity	Fe	Mg	Ca	Na	P	K	$\delta^{15}N_{NO3}$	$\delta^{18}O_{NO3}$
d		mM			meq L-1				mM			‰	
Biostimulated experiments (OS-3, OS-4, OS-7 and OS-8)													
0	1.75	0.02 ± 0.00	1.37	6.84	7.00	b.d.l.	1.41	4.15	1.09	0.03	1.11	14.9 ± 0.0	5.7 ± 0.3
4	1.73 ± 0.03	0.03 ± 0.01	3.35 ± 0.27	6.62 ± 0.03	6.73 ± 0.25	0.43 ± 0.08	1.52 ± 0.04	4.91 ± 0.11	1.18 ± 0.16	0.04 ± 0.03	1.13 ± 0.06	n.d.	n.d.
14	1.42 ± 0.03	0.00 ± 0.01	3.53 ± 0.30	6.78 ± 0.03	7.70 ± 0.41	b.d.l.	1.58 ± 0.11	5.83 ± 0.36	1.11 ± 0.19	0.04 ± 0.02	1.13 ± 0.11	20.8 ± 0.1	10.9 ± 0.1
28	1.32 ± 0.05	0.00 ± 0.00	3.61 ± 0.36	6.78 ± 0.05	7.50 ± 0.27	b.d.l.	1.60 ± 0.14	5.85 ± 0.46	1.13 ± 0.22	0.05 ± 0.03	1.16 ± 0.14	n.d.	n.d.
35	1.21 ± 0.04	0.00 ± 0.00	3.74 ± 0.47	7.15 ± 0.04	7.03 ± 0.33	b.d.l.	1.61 ± 0.12	5.83 ± 0.41	1.10 ± 0.08	0.04 ± 0.02	1.20 ± 0.11	n.d.	n.d.
49	1.04 ± 0.03	0.00 ± 0.00	3.84 ± 0.45	6.85 ± 0.07	7.35 ± 0.45	b.d.l.	1.68 ± 0.13	6.02 ± 0.52	1.37 ± 0.09	0.05 ± 0.02	1.23 ± 0.12	28.7 ± 0.1	17.0 ± 0.2
79	0.66 ± 0.08	0.02 ± 0.01	4.00 ± 0.40	6.99 ± 0.05	6.20 ± 1.21	b.d.l.	1.67 ± 0.15	5.55 ± 0.78	1.22 ± 0.13	0.03 ± 0.00	1.21 ± 0.12	43.0 ± 0.1	28.2 ± 0.1
94	0.40 ± 0.12	0.02 ± 0.01	4.19 ± 0.43	6.78 ± 0.02	7.53 ± 0.31	b.d.l.	1.72 ± 0.13	6.45 ± 0.50	1.28 ± 0.26	0.04 ± 0.00	1.21 ± 0.13	62.1 ± 0.0	42.1 ± 0.0
Biostimulated/bioaugmented experiments (OS-9 and OS-10)													
0	1.75	0.02 ± 0.00	1.37	6.84	7.00	b.d.l.	1.41	4.15	1.09	0.03	1.11	14.9 ± 0.0	5.7 ± 0.3
4	1.66 ± 0.01	0.03 ± 0.00	3.26 ± 0.02	6.60 ± 0.00	6.65 ± 0.21	0.50 ± 0.01	1.49 ± 0.00	4.84 ± 0.02	2.10 ± 0.11	0.02 ± 0.01	1.14 ± 0.01	n.d.	n.d.
14	1.33 ± 0.01	0.00 ± 0.01	3.38 ± 0.01	6.76 ± 0.06	7.65 ± 0.49	b.d.l.	1.48 ± 0.02	5.64 ± 0.18	1.88 ± 0.09	0.03 ± 0.01	1.13 ± 0.01	22.0 ± 0.2	11.8 ± 0.2
28	1.16 ± 0.01	0.00 ± 0.00	3.46 ± 0.02	6.82 ± 0.01	7.50 ± 0.28	b.d.l.	1.50 ± 0.02	5.63 ± 0.07	2.08 ± 0.05	0.03 ± 0.01	1.13 ± 0.04	n.d.	n.d.
35	1.05 ± 0.03	0.00 ± 0.00	3.52 ± 0.01	7.08 ± 0.02	7.55 ± 0.07	b.d.l.	1.53 ± 0.01	5.59 ± 0.04	2.08 ± 0.27	0.04 ± 0.01	1.13 ± 0.01	n.d.	n.d.
49	0.94 ± 0.09	0.00 ± 0.00	3.69 ± 0.14	6.88 ± 0.06	7.80 ± 0.42	b.d.l.	1.58 ± 0.05	5.77 ± 0.18	2.05 ± 0.22	0.02 ± 0.01	1.15 ± 0.02	31.7 ± 0.1	19.0 ± 0.0
79	0.50 ± 0.12	0.02 ± 0.00	3.98 ± 0.12	7.00 ± 0.02	4.25 ± 0.35	b.d.l.	1.59 ± 0.08	5.06 ± 0.99	2.12 ± 0.22	0.03 ± 0.03	1.15 ± 0.05	51.7 ± 0.1	34.8 ± 0.2
94	0.21 ± 0.16	0.02 ± 0.01	4.16 ± 0.14	6.78 ± 0.00	7.75 ± 0.07	b.d.l.	1.64 ± 0.05	6.06 ± 0.14	2.19 ± 0.38	0.05 ± 0.00	1.15 ± 0.04	87.1 ± 0.1	62.1 ± 0.1
***T. denitrificans* experiments (OS-15 and OS-16)**													
0	2.18	0.00 ± 0.00	1.3	6.84	n.d.	b.d.l.	1.34	3.39	0.92	0.02	1.11	n.d.	n.d.
5	1.92 ± 0.06	0.08 ± 0.06	5.17 ± 1.07	6.41 ± 0.16	n.d.	0.67 ± 0.75	1.43 ± 0.08	5.20 ± 0.56	2.53 ± 0.69	0.03 ± 0.04	1.18 ± 0.01	n.d.	n.d.
15	1.28 ± 0.22	0.12 ± 0.06	5.48 ± 1.17	6.26 ± 0.08	n.d.	0.20 ± 0.24	1.43 ± 0.11	7.12 ± 1.04	2.71 ± 0.88	0.03 ± 0.01	1.14 ± 0.02	n.d.	n.d.
29	1.03 ± 0.49	0.15 ± 0.07	5.53 ± 1.28	6.64 ± 0.03	n.d.	b.d.l.	1.50 ± 0.11	8.27 ± 1.65	2.65 ± 0.62	0.03 ± 0.04	1.19 ± 0.05	n.d.	n.d.
46	1.03 ± 0.50	0.12 ± 0.09	5.25 ± 1.09	6.63 ± 0.02	n.d.	b.d.l.	1.46 ± 0.06	7.59 ± 1.15	2.80 ± 0.44	0.02 ± 0.02	1.14 ± 0.04	n.d.	n.d.
70	1.01 ± 0.51	0.02 ± 0.03	5.49 ± 1.16	6.68 ± 0.02	n.d.	b.d.l.	1.61 ± 0.12	8.16 ± 1.38	2.73 ± 0.97	0.00 ± 0.00	1.17 ± 0.04	n.d.	n.d.
85	1.02 ± 0.48	0.00 ± 0.00	5.49 ± 0.86	6.77 ± 0.03	n.d.	b.d.l.	1.64 ± 0.02	7.87 ± 0.67	2.88 ± 0.51	0.03 ± 0.00	1.19 ± 0.10	n.d.	n.d.
104	0.95 ± 0.48	0.00 ± 0.00	5.78 ± 0.88	6.82 ± 0.03	n.d.	b.d.l.	1.75 ± 0.03	8.40 ± 0.86	2.68 ± 0.54	0.01 ± 0.02	1.20 ± 0.04	n.d.	n.d.

Table D3. Experimental data from the flow-through experiments presented in chapter 4 of this thesis (i: input; o: output; n.d.: not determined; b.d.l.: below detection limit).

Sample	Time	Flow rate	Nitrate (i)	Nitrate (o)	Nitrite (o)	Fe (o)	S (i)	S (o)	pH (o)
	d	mL min^{-1}	mM	mM	mM	μM	μM	μM	
OS-31-1	7.1	0.0025	1.71	0.48	0.27	3.47	1656.3	2113.02	6.7
OS-31-2	14.0	0.0039	1.71	0.00	0.05	12.33	1656.3	1838.07	6.6
OS-31-3	24.0	0.0032	1.71	0.00	0.06	110.32	1656.3	1413.50	6.8
OS-31-4	32.1	0.0031	1.71	0.00	0.08	3.76	1656.3	505.02	8.3
OS-31-5	39.0	0.0028	1.71	0.01	0.04	1.86	1656.3	159.42	8.3
OS-31-6	50.0	0.0029	1.94	0.00	0.03	11.30	1656.3	18.59	6.7
OS-31-7	60.0	0.0028	1.99	0.00	0.06	14.15	1656.3	55.73	6.8
OS-31-8	69.1	0.0027	1.99	0.00	0.05	10.21	1656.3	79.51	6.9
OS-31-9	81.0	0.0027	1.97	0.00	0.03	9.72	1656.3	74.83	6.8
OS-31-10	90.0	0.0027	1.97	0.00	0.02	8.19	1656.3	47.05	6.9
OS-31-11	102.0	0.0027	1.97	0.00	0.02	4.40	1656.3	103.35	6.7
OS-31-12	111.0	0.0027	1.97	0.00	0.01	3.99	1656.3	88.45	6.1
OS-31-13	120.0	0.0027	1.97	0.00	0.00	5.28	1656.3	110.07	7.0
OS-31-14	132.0	0.0026	1.97	0.00	0.00	4.82	1656.3	38.79	7.0
OS-31-15	139.0	0.0024	1.97	0.00	0.00	10.26	1656.3	62.90	7.3
OS-31-16	145.9	0.0026	1.97	0.00	0.00	7.21	1656.3	19.02	7.1
OS-31-17	159.0	0.0025	1.97	0.00	0.00	3.38	1656.3	53.58	6.9
OS-31-18	168.0	0.0024	1.97	0.00	0.00	1.06	1656.3	2.00	6.9
OS-31-19	180.0	0.0024	1.97	0.00	0.00	12.76	1656.3	86.13	7.9
OS-31-20	182.0	0.0023	1.97	0.00	0.00	5.85	1656.3	100.34	6.8
OS-41-1	7.1	0.0026	2.54	0.45	0.01	2.27	0.00	702.64	7.0
OS-41-2	14.0	0.0020	2.54	0.00	0.00	1.17	0.00	576.37	7.2
OS-41-3	24.0	0.0031	2.54	0.00	0.00	4.44	0.00	345.41	7.1
OS-41-4	39.0	0.0016	2.54	0.00	0.02	1.11	0.00	155.08	8.6
OS-41-5	50.0	0.0033	2.54	0.00	0.00	13.27	0.00	2.00	6.9
OS-41-6	60.0	0.0033	2.44	0.00	0.00	13.53	0.00	55.60	7.0
OS-41-7	69.1	0.0032	2.44	0.00	0.00	16.09	0.00	2.00	7.1
OS-41-8	81.0	0.0032	2.44	0.00	0.01	11.95	0.00	31.72	7.1
OS-41-9	90.0	0.0033	2.44	0.00	0.01	12.59	0.00	2.00	7.0
OS-41-10	102.0	0.0016	2.44	0.00	0.01	2.63	0.00	2.00	6.9
OS-41-11	111.0	0.0014	2.44	0.00	0.01	10.12	0.00	2.00	6.8
OS-41-12	120.0	0.0015	2.44	0.00	0.01	2.05	0.00	2.00	7.1
OS-41-13	132.0	0.0029	2.12	0.00	0.00	6.20	0.00	2.00	7.1
OS-41-14	139.0	0.0032	2.12	0.00	0.00	8.71	0.00	1.98	7.5
OS-41-15	145.9	0.0032	2.12	0.00	0.00	8.16	0.00	2.00	7.4
OS-41-16	159.0	0.0031	2.12	0.00	0.00	8.44	0.00	9.95	7.2
OS-41-17	168.0	0.0025	2.12	0.00	0.00	7.82	0.00	11.58	7.1
OS-41-18	180.0	0.0027	2.12	0.00	0.00	12.48	0.00	35.30	7.5
OS-41-19	182.0	0.0023	2.12	0.00	0.00	20.14	0.00	44.18	7.2

Table D3. (continued).

Sample	Time	Flow rate	Nitrate (i)	Nitrate (o)	Nitrite (o)	Fe (o)	S (i)	S (o)	pH (o)
	d	mL min^{-1}	mM	mM	mM	μM	μM	μM	
OS-71-1	7.1	0.0019	1.71	0.07	0.45	3.47	1656.3	2113.02	6.7
OS-71-2	14.0	0.0028	1.71	0.00	0.06	12.33	1656.3	1838.07	6.6
OS-71-3	24.0	0.0027	1.71	0.00	0.06	110.32	1656.3	1413.50	6.8
OS-71-4	32.1	0.0026	1.71	0.00	0.04	3.76	1656.3	505.02	8.3
OS-71-5	39.0	0.0028	1.71	0.00	0.03	1.86	1656.3	159.42	8.3
OS-71-6	50.0	0.0026	1.94	0.00	0.02	11.30	1656.3	18.59	6.7
OS-71-7	60.0	0.0026	1.99	0.00	0.06	14.15	1656.3	55.73	6.8
OS-71-8	69.1	0.0025	1.99	0.00	0.07	10.21	1656.3	79.51	6.9
OS-71-9	81.0	0.0025	1.97	0.00	0.02	9.72	1656.3	74.83	6.8
OS-71-10	90.0	0.0025	1.97	0.00	0.03	8.19	1656.3	47.05	6.9
OS-71-11	102.0	0.0025	1.97	0.00	0.03	4.40	1656.3	103.35	6.7
OS-71-12	111.0	0.0025	1.97	0.00	0.03	3.99	1656.3	88.45	6.1
OS-71-13	120.0	0.0025	1.97	0.00	0.01	5.28	1656.3	110.07	7.0
OS-71-14	132.0	0.0025	1.97	0.00	0.00	4.82	1656.3	38.79	7.0
OS-71-15	139.0	0.0024	1.97	0.00	0.00	10.26	1656.3	62.90	7.3
OS-71-16	145.9	0.0024	1.97	0.00	0.00	7.21	1656.3	19.02	7.1
OS-71-17	159.0	0.0025	1.97	0.00	0.00	3.38	1656.3	53.58	6.9
OS-71-18	168.0	0.0024	1.97	0.00	0.00	1.06	1656.3	2.00	6.9
OS-71-19	180.0	0.0024	1.97	0.00	0.00	12.76	1656.3	86.13	7.9
OS-71-20	182.0	0.0024	1.97	0.00	0.00	5.85	1656.3	100.34	6.8
OS-81-1	7.1	0.0018	2.55	0.23	0.55	4.16	0.00	294.96	7.1
OS-81-2	14.0	0.0043	2.55	0.00	0.00	1.79	0.00	135.36	7.2
OS-81-3	24.0	0.0042	2.55	0.00	0.00	1.64	0.00	148.14	7.1
OS-81-4	32.1	0.0043	2.55	0.00	0.00	5.05	0.00	76.16	8.4
OS-81-5	50.0	0.0007	2.55	0.00	0.00	2.21	0.00	1.21	6.9
OS-81-6	60.0	0.0026	2.33	0.00	0.00	6.21	0.00	2.00	7.1
OS-81-7	69.1	0.0045	2.33	0.00	0.00	16.20	0.00	0.79	7.1
OS-81-8	81.0	0.0044	2.33	0.00	0.01	13.82	0.00	2.00	7.1
OS-81-9	90.0	0.0045	2.33	0.00	0.01	16.45	0.00	10.73	7.0
OS-81-10	102.0	0.0044	2.33	0.00	0.00	14.58	0.00	2.00	6.9
OS-81-11	111.0	0.0020	2.33	0.00	0.01	6.72	0.00	2.00	6.7
OS-81-12	120.0	0.0043	2.33	0.00	0.02	8.53	0.00	37.15	7.1
OS-81-13	132.0	0.0009	n.d.	n.d.	n.d.	2.50	0.00	5.14	7.2

Table D3. (continued).

Sample	Time	Flow rate	Nitrate (i)	Nitrate (o)	Nitrite (o)	Fe (o)	S (i)	S (o)	pH (o)
	d	mL min^{-1}	mM	mM	mM	μM	μM	μM	
OS-91-1	7.1	0.0025	1.71	0.00	0.19	2.75	1656.3	2153.06	6.7
OS-91-2	14.0	0.0030	1.71	0.00	0.06	23.96	1656.3	1947.29	6.8
OS-91-3	24.0	0.0026	1.71	0.00	0.05	153.84	1656.3	1625.24	6.8
OS-91-4	32.1	0.0026	1.71	0.00	0.03	5.44	1656.3	495.65	8.0
OS-91-5	39.0	0.0029	1.71	0.02	0.03	2.43	1656.3	33.26	8.2
OS-91-6	50.0	0.0025	1.94	0.00	0.00	15.50	1656.3	85.50	6.7
OS-91-7	60.0	0.0026	1.99	0.00	0.06	35.68	1656.3	69.72	6.8
OS-91-8	69.1	0.0025	1.99	0.00	0.06	20.36	1656.3	26.43	6.8
OS-91-9	81.0	0.0025	1.97	0.00	0.06	19.53	1656.3	10.90	6.9
OS-91-10	90.0	0.0026	1.97	0.00	0.06	35.56	1656.3	26.85	6.8
OS-91-11	102.0	0.0025	1.97	0.00	0.06	24.36	1656.3	61.71	6.7
OS-91-12	111.0	0.0025	1.97	0.00	0.05	13.24	1656.3	6.16	6.3
OS-91-13	120.0	0.0025	1.97	0.01	0.05	15.07	1656.3	0.00	6.9
OS-91-14	132.0	0.0025	1.97	0.00	0.00	9.10	1656.3	40.16	6.9
OS-91-15	139.0	0.0027	1.97	0.00	0.00	2.93	1656.3	16.19	7.4
OS-91-16	145.9	0.0029	1.97	0.00	0.00	5.69	1656.3	17.74	7.1
OS-91-17	159.0	0.0028	1.97	0.00	0.00	8.28	1656.3	21.15	6.9
OS-91-18	168.0	0.0026	1.97	0.00	0.00	6.81	1656.3	26.25	7.1
OS-91-19	180.0	0.0026	1.97	0.00	0.00	16.89	1656.3	29.85	7.5
OS-91-20	182.0	0.0026	1.97	0.00	0.00	n.d.	1656.3	n.d.	7.0
OS-101-1	7.1	0.0010	2.47	0.00	0.00	3.84	0.00	515.77	7.1
OS-101-2	14.0	0.0045	2.47	0.00	0.00	0.85	0.00	386.70	7.2
OS-101-3	24.0	0.0044	2.47	0.00	0.00	1.03	0.00	231.46	7.2
OS-101-4	32.1	0.0022	2.47	0.00	0.01	1.57	0.00	136.69	8.5
OS-101-5	39.0	0.0037	2.47	0.00	0.03	1.46	0.00	42.75	8.6
OS-101-6	50.0	0.0044	2.47	0.00	0.00	2.22	0.00	76.49	6.9
OS-101-7	60.0	0.0042	2.31	0.00	0.00	1.59	0.00	50.74	7.0
OS-101-8	69.1	0.0042	2.31	0.00	0.00	1.96	0.00	65.55	7.0
OS-101-9	81.0	0.0041	2.31	0.00	0.00	2.03	0.00	33.04	7.1
OS-101-10	90.0	0.0041	2.31	0.00	0.00	1.79	0.00	35.91	7.0
OS-101-11	102.0	0.0041	2.31	0.00	0.00	1.59	0.00	39.96	6.9
OS-101-12	111.0	0.0040	2.31	0.00	0.01	1.34	0.00	8.30	7.2
OS-101-13	120.0	0.0041	2.31	0.00	0.00	4.92	0.00	16.93	7.1
OS-101-14	132.0	0.0044	2.12	0.00	0.00	6.68	0.00	42.79	7.1
OS-101-15	139.0	0.0091	2.12	0.00	0.00	11.81	0.00	0.00	7.2
OS-101-16	145.9	0.0041	2.12	0.00	0.00	16.45	0.00	0.00	7.3
OS-101-17	159.0	0.0041	2.12	0.00	0.00	16.30	0.00	0.00	7.1
OS-101-18	168.0	0.0022	2.12	0.00	0.00	9.90	0.00	0.00	7.2
OS-101-19	180.0	0.0018	2.12	0.00	0.00	n.d.	0.00	n.d.	7.8
OS-101-20	182.0	0.0023	2.12	0.00	0.00	n.d.	0.00	n.d.	7.1

Table D3. (continued).

Sample	Time	Flow rate	Nitrate (i)	Nitrate (o)	Nitrite (o)	Fe (o)	S (i)	S (o)	pH (o)
	d	mL min^{-1}	mM	mM	mM	µM	µM	µM	
OS-17-1	7.1	0.0026	1.71	0.25	0.48	2194.45	1656.3	10490.13	6.5
OS-17-2	14.0	0.0032	1.71	0.00	0.03	852.78	1656.3	8797.63	6.6
OS-17-3	24.0	0.0028	1.71	0.00	0.03	305.64	1656.3	5850.53	6.7
OS-17-4	32.1	0.0028	1.71	0.00	0.02	7.46	1656.3	2509.79	7.9
OS-17-5	39.0	0.0030	1.71	0.00	0.00	2.61	1656.3	794.83	8.1
OS-17-6	50.0	0.0027	1.94	0.00	0.03	12.47	1656.3	2.00	6.6
OS-17-7	60.0	0.0027	1.99	0.00	0.04	26.98	1656.3	0.00	6.8
OS-17-8	69.1	0.0028	1.99	0.00	0.04	25.91	1656.3	16.14	6.9
OS-17-9	81.0	0.0028	1.97	0.00	0.01	41.69	1656.3	33.62	6.9
OS-17-10	90.0	0.0028	1.97	0.00	0.02	45.21	1656.3	11.36	6.9
OS-17-11	102.0	0.0028	1.97	0.00	0.01	39.93	1656.3	30.17	6.7
OS-17-12	111.0	0.0027	1.97	0.00	0.01	31.20	1656.3	2.00	6.3
OS-17-13	120.0	0.0028	1.97	0.00	0.00	33.49	1656.3	36.82	6.9
OS-17-14	132.0	0.0028	1.97	0.00	0.01	22.69	1656.3	26.40	6.9
OS-17-15	139.0	0.0015	1.97	0.00	0.00	19.39	1656.3	0.00	7.1
OS-17-16	145.9	0.0010	1.97	0.00	0.00	496.10	1656.3	223.44	7.5
OS-18-1	7.1	0.0035	2.51	2.57	0.05	12.25	0.00	10629.86	6.9
OS-18-2	14.0	0.0042	2.51	2.23	0.38	2.04	0.00	5818.10	7.0
OS-18-3	24.0	0.0042	2.51	0.00	0.00	1.70	0.00	2964.96	7.1
OS-18-4	32.1	0.0005	2.51	0.00	0.01	1.83	0.00	1947.57	8.2
OS-18-5	50.0	0.0014	2.51	0.00	0.00	2.60	0.00	965.82	6.9
OS-18-6	60.0	0.0037	2.37	0.00	0.00	5.84	0.00	230.81	7.0
OS-18-7	69.1	0.0041	2.37	0.00	0.00	8.36	0.00	79.37	7.0
OS-18-8	81.0	0.0044	2.37	0.00	0.00	7.66	0.00	2.00	7.2
OS-18-9	90.0	0.0044	2.37	0.00	0.01	8.81	0.00	0.00	7.0
OS-18-10	102.0	0.0043	2.37	0.00	0.01	10.59	0.00	0.00	6.9
OS-18-11	111.0	0.0043	2.37	0.00	0.01	8.84	0.00	0.00	7.2
OS-18-12	120.0	0.0015	2.37	0.00	0.01	11.89	0.00	0.00	7.1
OS-18-13	139.0	0.0004	2.12	0.00	0.00	2.17	0.00	0.00	7.3
OS-18-14	145.9	0.0034	2.12	0.00	0.00	9.20	0.00	0.00	7.3
OS-18-15	159.0	0.0039	2.12	0.00	0.00	5.21	0.00	0.00	7.1
OS-18-16	168.0	0.0027	2.12	0.00	0.00	7.10	0.00	33.02	7.1
OS-18-17	180.0	0.0038	2.12	0.00	0.00	11.28	0.00	2.00	7.6
OS-18-18	182.0	0.0025	2.12	0.00	0.00	17.27	0.00	0.00	7.1